

**ENHANCED PHYSICOCHEMICAL PROCESSES  
FOR THE TREATMENT OF  
PETROLEUM-CONTAMINATED SYSTEMS**

A Thesis

Submitted to the Faculty of Graduate Studies and Research

in Partial Fulfillment of the Requirements

for the Degree of

Doctor of Philosophy

in Environmental Systems Engineering

University of Regina

by

Shan Zhao

Regina, Saskatchewan

September 15, 2015

Copyright 2015: S. Zhao

**UNIVERSITY OF REGINA**  
**FACULTY OF GRADUATE STUDIES AND RESEARCH**  
**SUPERVISORY AND EXAMINING COMMITTEE**

Shan Zhao, candidate for the degree of Doctor of Philosophy in Environmental Systems Engineering, has presented a thesis titled, ***Enhanced Physicochemical Processes for the Treatment of petroleum-Contaminated Systems***, in an oral examination held on August 24, 2015. The following committee members have found the thesis acceptable in form and content, and that the candidate demonstrated satisfactory knowledge of the subject material.

External Examiner:           \*Dr. Lianfa Song, Texas Tech University

Supervisor:                    Dr. Guo H. Huang, Environmental Systems Engineering

Committee Member:         Dr. Tsun Wai Kelvin Ng, Environmental Systems Engineering

Committee Member:         Dr. Chunjiang An, Environmental Systems Engineering

Committee Member:         Dr. Dianliang Deng, Department of Mathematics & Statistics

Chair of Defense:            Dr. Rodney A. Kelln, Department of Chemistry/Biochemistry

\*via teleconference

## ABSTRACT

In Canada, environmental issues caused by petroleum-contaminated sites are becoming a major concern. Therefore, effective physicochemical remediation technologies are desired for produced water treatment and groundwater remediation in oil fields.

In this dissertation research, the feasibility of treating produced water using synthetic polymers combined with natural diatomite was evaluated. Using diatomite as an adsorbent and a coagulant aid, this study provided an economical and enhanced approach for utilizing diatomite in the clean-up of produced water.

A pilot-scale electrocoagulation process was developed for enhanced removal of hardness, chemical oxygen demand, and turbidity to mitigate the scaling and fouling of Reverse Osmosis membranes. Response surface methodology was employed to refine operating parameters and to evaluate individual/interactive effects of parameters on pollutant recovery.

The modification of palygorskite with gemini surfactants enhanced phenanthrene retention in solid particles from aqueous phase. The effects of solution chemistry on phenanthrene sorption to modified palygorskite were systematically studied. The effectiveness of gemini modified palygorskite as the novel remediation material in polycyclic aromatic hydrocarbon contaminated water remediation was revealed and examined.

A multi-level fuzzy-factorial inference approach was proposed to elucidate the sorption behavior of phenanthrene on palygorskite modified with gemini surfactants. Fuzzy vertex analysis discretized the design factors with triangular membership functions

into multiple deterministic levels. Examination of curvature effects of factors revealed the nonlinear complexity inherent in the sorption process. The potential interactions among experimental factors were detected, which was meaningful for providing a deep insight into the sorption mechanisms under the influences of factors at different levels.

The enhancement of soil retention for phenanthrene was investigated through the sorption barriers created by binary mixture of cationic gemini and nonionic surfactants. The research addressed the sorption characteristic and mechanism of gemini surfactant in complex soil system using a developed Two-step Adsorption and Partition Model. The sorption barrier substantially enhanced the soil retention capabilities for phenanthrene, while the sorption of gemini was inhibited by the increasing nonionic surfactant dose.

The interactions among water, soil, surfactant, and contaminant in petroleum-contaminated systems have been revealed. This research can provide reference on the implementation of remediation technologies at petroleum-contaminated sites.

## ACKNOWLEDGMENTS

I would like to express my deepest gratitude to Dr. Gordon Huang, my supervisor, for his extremely helpful guidance, support and encouragement that have nourished this dissertation research from beginning to successful completion. His profound knowledge and integral view on research have made a deep impression on me. I will always remember the precious time I spent under his excellent leadership during my Ph.D. study at Regina. My appreciation must also extend to his family, in particular Ms. Chunling Ke for her continuous and kind help.

I would like to extend thanks to my external examiner (Dr. Lianfa Song) and committee members (Dr. Dianliang Deng, Dr. Kelvin Ng, and Dr. Chunjiang An) for their insightful suggestions that were helpful in improving the dissertation. My further appreciation goes to Drs. Jia Wei, Aili Yang, Hui Yu, Baiyu Zhang, Yurui Fan, Peng Zhang, Yanpeng Cai, Qian Tan, and Wei Sun for their constructive advice and friendship.

I gratefully acknowledge the Faculty of Graduate Studies and Research and the Faculty of Engineering and Applied Science at the University of Regina for providing research scholarships, teaching assistantships, and research awards during the course of my Ph.D. study.

I would also express my thanks to my friends in the Environmental Informatics Laboratory for their assistance in various aspects of my research and for their support with constant friendship. They are Renfei Liao, Yao Yao, Zhong Li, Xiuquan Wang, Guanhui Cheng, Shuo Wang, Jiapei Chen, Xiujuan Chen, Xiaying Xin, Yuanyuan Zhai, Cong Dong, Xiong Zhou, Jian Shen, Jinxin Zhu, Kai Huang, Chen Lu, and many others.

## **DEDICATION**

This dissertation is dedicated to my entire family for their unconditional love, steadfast support and constant encouragement during the course of my Ph.D. study.

I am grateful to my fiance, for his endless love and unconditional support. Thanks are also due to my aunt, Yucui Cao and my grandmother, Huiqin Niu, for their kind understanding and encouragement.

My deepest gratitude must be reserved for my beloved parents, Yuchun Cao and Bin Zhao, for their love, patience, support and sacrifice that have brought about all of my success.

# TABLE OF CONTENTS

<b>ABSTRACT</b> .....	i
<b>ACKNOWLEDGMENTS</b> .....	iii
<b>DEDICATION</b> .....	iv
<b>TABLE OF CONTENTS</b> .....	v
<b>LIST OF TABLES</b> .....	xii
<b>LIST OF FIGURES</b> .....	xiv
<b>LIST OF ABBREVIATIONS</b> .....	xiv
<b>CHAPTER 1 INTRODUCTION</b> .....	1
1.1. BACKGROUND.....	1
1.2. CHALLENGES IN THE TREATMENT OF PRODUCED WATER .....	3
1.3. CHALLENGES IN THE TREATMENT OF PAHS-CONTAMINATED GROUNDWATER.....	6
1.4. CHALLENGES IN GROUNDEATER REMEDIATION .....	8
1.5. OBJECTIVES .....	10
1.6. ORGANIZATION .....	12
<b>CHAPTER 2 LITERATURE REVIEW</b> .....	14
2.1. POLYCYCLIC AROMATIC HYDROCARBONS .....	14
2.2. GEMINI SURFACTANTS .....	17
2.3. PRODUCED WATER TREATMENT TECHNOLOGIES.....	20
2.3.1. Characteristics of Produced Water .....	20
2.3.2. Treatment of Produced Water .....	23
2.3.2.1. <i>Chemical Coagulation</i> .....	23

2.3.2.2. <i>Adsorption</i> .....	25
2.3.2.3. <i>Membrane Filtration</i> .....	27
2.3.2.4. <i>Electrocoagulation</i> .....	33
2.3.2.5. <i>Combined Treatment</i> .....	38
2.4. SORPTION OF ORGANIC COMPOUNDS ON LOW-COST CLAY SORBENTS	
.....	41
2.5. SORPTION THEORY .....	44
2.5.1. Main Types of Sorption Isotherms.....	44
2.5.2. Sorption Isotherm Models .....	47
2.5.2.1. <i>Langmuir Isotherm Model</i> .....	47
2.5.2.2. <i>Freundlich Isotherm Model</i> .....	48
2.5.2.3. <i>Dubinin-Radushkevich Isotherm Model</i> .....	49
2.5.2.4. <i>Temkin Isotherm Model</i> .....	50
2.5.2.5. <i>Flory-Huggins Isotherm Model</i> .....	50
2.5.2.6. <i>Redlich and Peterson Isotherm Model</i> .....	51
2.5.2.7. <i>Sips Isotherm Model</i> .....	52
2.5.2.8. <i>Toth Isotherm Model</i> .....	52
2.6. SURFACTANT SORPTION MODELING .....	53
2.6.1. Mechanisms of Surfactant Sorption at the Solid/Aqueous Interface .....	53
2.6.2. Modeling Studies of Surfactant Sorption .....	54
2.6.3. Two-Step Model.....	57
2.7. SORPTION BARRIERS AT THE CONTAMINATED SITES FOR	
GROUNDWATER REMEDIATION.....	59

2.8. EXPERIMENTAL DESIGN AND MODELING .....	63
2.8.1. Factorial Design .....	63
2.8.1.1. <i>The General Factorial Design</i> .....	66
2.8.1.2. <i>Two-Level Factorial Design</i> .....	68
2.8.1.3. <i>Multi-Level Factorial Design</i> .....	69
2.8.1.4. <i>Applications</i> .....	69
2.8.2. Response Surface Method .....	72
2.9. LITERATURE REVIEW SUMMARY .....	76
<b>CHAPTER 3 ENHANCED COAGULATION/FLOCCULATION BY COMBINING DIATOMITE WITH SYNTHETIC POLYMERS FOR PRODUCED WATER TREATMENT</b> .....	79
3.1. BACKGROUND .....	79
3.2. MATERIALS AND METHODS .....	83
3.2.1. Materials .....	83
3.2.2. Experimental Procedure .....	83
3.2.3. Analytical Methods .....	86
3.3. RESULTS AND DISCUSSION .....	87
3.3.1. Preliminary Experiments .....	87
3.3.2. Combining PAC/PFS/PAM with Diatomite .....	94
3.3.2.1. <i>PAC with Diatomite</i> .....	94
3.3.2.2. <i>PFS with Diatomite</i> .....	99
3.3.2.3. <i>PAM with Diatomite</i> .....	100
3.3.3. Operating Refinements by combining PAC with diatomite .....	102

3.3.3.1. <i>Initial pH</i> .....	102
3.3.3.2. <i>Settling Time</i> .....	106
3.4. SUMMARY .....	109
<b>CHAPTER 4 HARDNESS, COD AND TURBIDITY REMOVALS FROM PRODUCED WATER BY ELECTROCOAGULATION PRETREATMENT PRIOR TO REVERSE OSMOSIS MEMBRANES</b> .....	110
4.1. BACKGROUND.....	110
4.2. MATERIAL AND METHODS .....	114
4.2.1. Materials .....	114
4.2.2. Experimental Devices .....	114
4.2.3. Experimental Design.....	119
4.3. RESULTS AND DISCUSSION .....	124
4.3.1. Preliminary Experiments .....	124
4.3.1.1. <i>Initial pH</i> .....	124
4.3.1.2. <i>Current Density</i> .....	129
4.3.1.3. <i>Electrolysis Time</i> .....	132
4.3.2. CCD Experiments .....	134
4.3.3. Membrane Fouling Studies.....	145
4.4. SUMMARY .....	148
<b>CHAPTER 5 PHENANTHRENE SORPTION ON PALYGORSKITE MODIFIED WITH GEMINI SURFACTANTS: EFFECTS OF AQUEOUS SOLUTION CHEMISTRY</b> .....	149
5.1. BACKGROUND.....	149

5.2. MATERIALS AND METHODS .....	152
5.2.1. Chemicals .....	152
5.2.2. Preparation of Surfactant-Modified Palygorskite .....	153
5.2.3. Sorption Studies .....	156
5.2.4. Effect of Aqueous Solution Parameters .....	156
5.2.5. Analytical Methods .....	157
5.2.6. Data Analysis.....	158
5.3. RESULTS AND DISCUSSION .....	158
5.3.1. Characterization of the Modified PGS.....	158
5.3.2. Modeling of Gemini Sorption at the PGS/Aqueous Interface.....	161
5.3.3. Effect of Initial pH on PHE Sorption.....	165
5.3.4. Effect of Organic Matter on PHE Sorption .....	169
5.3.5. Effect of Ionic Strength on PHE Sorption .....	174
5.3.6. PHE Sorption Isotherms .....	177
5.3.7. Thermodynamic Studies of PHE Sorption .....	181
5.4. SUMMARY .....	184
<b>CHAPTER 6 INSIGHT INTO SORPTION MECHANISM OF PHENANTHRENE ONTO GEMINI MODIFIED PALYGORSKITE THROUGH A MULTI-LEVEL FUZZY-FACTORIAL INFERENCE APPROACH .....</b>	<b>186</b>
6.1. BACKGROUND.....	186
6.2. MATERIALS AND METHODS.....	189
6.2.1. Materials .....	189
6.2.2. Sorption Studies .....	190

6.2.3. Fuzzy Set Theory .....	191
6.2.4. Multi-Level Factorial Analysis .....	193
6.3. RESULTS AND DISCUSSION .....	198
6.3.1. Multivariate Statistical Analysis .....	198
6.3.2. Characterization of Linear and Curvature Effects of Factors.....	204
6.3.3. Detection of Interactions among Factors .....	210
6.3.3.1. <i>Interaction between Initial PHE Concentration and Ionic Strength</i> .....	210
6.3.3.2 <i>Interaction between Ionic Strength and pH</i> .....	213
6.3.3.3. <i>Interaction between Added HA Dose and Ionic Strength</i> .....	214
6.3.3.4 <i>Interaction between Temperature and pH</i> .....	215
6.3.3.5. <i>Interaction between Added HA Dose and pH</i> .....	216
6.4. SUMMARY .....	219
 <b>CHAPTER 7 ENHANCEMENT OF SOIL RETENTION FOR PHENANTHRENE THROUGH BINARY CATIONIC GEMINI AND NONIONIC SURFACTANT MIXTURES.....</b>	
	220
7.1. BACKGROUND.....	220
7.2. MATERIALS AND METHODS .....	222
7.2.1. Chemicals .....	222
7.2.2. Soils.....	223
7.2.3. Sorption Studies .....	223
7.2.4. Analytical Methods .....	224
7.2.5. The Apparent Soil-Water Distribution Coefficient.....	225
7.2.6. Data Analysis.....	226

7.3. RESULTS AND DISCUSSION .....	230
7.3.1. Characterization of the Soil Samples .....	230
7.3.2. Sorption of PHE by Soil with the Addition of Single Cationic 12-2-12 Gemini Surfactant .....	234
7.3.3. Sorption Isotherms of the 12-2-12 Gemini Surfactant at Different Temperatures.....	238
7.3.4. Modeling of the 12-2-12 Gemini Sorption Process at the Soil/Water Interface .....	248
7.3.5. Thermodynamic Studies of the 12-2-12 Gemini Sorption at the Soil/Water Interface.....	253
7.3.6. Sorption of PHE by Soil through the Addition of Single Nonionic C <sub>12</sub> E <sub>10</sub> Surfactant .....	256
7.3.7. Sorption of PHE by Soil with the Addition of Binary Mixtures of Cationic 12- 2-12 Gemini and Nonionic C <sub>12</sub> E <sub>10</sub> Surfactant.....	259
7.3.8. Sorption of Gemini Surfactant by Soil through the Addition of Binary Mixtures of Cationic 12-2-12 Gemini and Nonionic C <sub>12</sub> E <sub>10</sub> Surfactant .....	266
7.4. SUMMARY .....	270
<b>CHAPTER 8 CONCLUSIONS .....</b>	<b>271</b>
8.1. SUMMARY .....	271
8.2. RESEARCH ACHIEVEMENTS.....	274
8.3. RECOMMENDATIONS FOR FUTURE RESEARCH .....	275
<b>REFERENCES .....</b>	<b>277</b>

## LIST OF TABLES

Table 3.1 Characteristics of the produced water .....	85
Table 4.1 Characteristics of the produced water from one oil site, Saskatchewan, Canada .....	116
Table 4.2 Original and coded variables in the CCD design .....	122
Table 4.3 A 2 <sup>3</sup> full factorial CCD design with its experimental and predicted values ....	123
Table 4.4 ANOVA report for the RSM model of COD removal .....	137
Table 4.5 ANOVA report for the RSM model of turbidity removal .....	138
Table 4.6 ANOVA report for the RSM model of hardness removal .....	139
Table 4.7 Validation experiments for the refined operating conditions .....	144
Table 4.8 Characteristics of the product water .....	147
Table 5.1 The structure and physicochemical properties of the selected surfactants and PAHs .....	154
Table 5.2 Properties of the original PGS and gemini modified PGS .....	155
Table 5.3 Parameters of TAPM for 12-2-12 gemini sorptionon PGS .....	164
Table 5.4 Freundlich isotherm parameters for the sorption of PHE on PGS and modified PGS .....	180
Table 5.5 Thermodynamic parameters for PHE sorption on PGS and modified PGS ....	183
Table 6.1 Experimental factors at low, high, and medium level.....	197
Table 6.2 Analysis of Variance Table.....	201
Table 6.3 The main effects of factors .....	205
Table 7.1 The structure and physicochemical properties of the selected surfactants and PAHs .....	227

Table 7.2 Properties of the selected soil sample .....	228
Table 7.3 Elemental analysis of the original soil and the soil samples with the addition of gemi ni surfactants .....	232
Table 7.4 Parameters of TAPM for 12-2-12 gemini sorption on soil .....	252
Table 7.5 Thermodynamic parameters for 12-2-12 gemini sorption on soil.....	255

## LIST OF FIGURES

Figure 2.1 Chemical structures of some commonly studied PAHs .....	16
Figure 2.2 The monomer, micelle, and chemical structure of cationic 12-s-12 gemini surfactants. ....	19
Figure 2.3 The two-step isotherm for cationic surfactants sorbed to silica. (a) The general shape of the sorption isotherm. (b) The proposed sorption model .....	56
Figure 2.4 <i>In situ</i> sorption barriers for groundwater remediation .....	62
Figure 2.5 A factorial experimental (a) without interaction and (b) with interaction .....	65
Figure 3.1 Percentage of COD removed at various dosages of diatomite, PAC and PFS.	90
Figure 3.2 Residual turbidity at various dosages of diatomite, PAC and PFS .....	91
Figure 3.3 Percentage of COD removed at various dosages of PAC, PFS and PAM when combined with diatomite .....	96
Figure 3.4 Residual turbidity at various dosages of PAC, PFS and PAM when combined with diatomite .....	98
Figure 3.5 Percentage of COD removed at different initial pH by combining PAC with diatomite and by single PAC or diatomite .....	104
Figure 3.6 Residual turbidity at different initial pH by combining PAC with diatomite and by single PAC or diatomite .....	105
Figure 3.7 Percentage of COD removed against settling time by combining PAC with diatomite and by single PAC or diatomite .....	107
Figure 3.8 Residual turbidity against settling time by combining PAC with diatomite and by single PAC or diatomite .....	108
Figure 4.1 Schematic diagram of a) the EC reactor, b) the electrode, and c) the pilot-scale	

EC-RO process.....	117
Figure 4.2 Effect of initial pH on COD, turbidity and hardness removals. Current density = 5.56 mA/cm <sup>2</sup> , electrolysis time = 30 min .....	128
Figure 4.3 Effect of current density on COD, turbidity and hardness removals. Initial pH around 7 ~ 8, electrolysis time = 30 min .....	131
Figure 4.4 Effect of electrolysis time on COD, turbidity and hardness removals. Initial pH around 7 ~ 8, current density = 5.56 mA/cm <sup>2</sup> .....	133
Figure 4.5 Effect of initial pH and current density on COD removal; 3D surface graph and contour plots.....	141
Figure 4.6 Effect of initial pH and current density on turbidity removal; 3D surface graph and contour plots.....	142
Figure 4.7 Effect of initial pH and current density on hardness removal; 3D surface graph and contour plots.....	143
Figure 4.8 Permeate flux trends during RO filtration: Comparison between EC pretreated water and raw produced water .....	146
Figure 5.1 FT-IR spectra of untreated PGS and gemini modified PGS. ....	160
Figure 5.2 The sorption isotherms of 12-2-12 gemini surfactant at PGS/aqueous interface .....	163
Figure 5.3 The sorption isotherms of PHE on (a) PGS and (b) modified PGS at different pH levels.....	168
Figure 5.4 The sorption isotherms of PHE on (a) PGS, initial PHE concentration 0.5 mg/L; (b) modified PGS, initial PHE concentration 0.5 mg/L;(c) PGS, initial PHE concentration 0.75 mg/L;(d) modified PGS, initial PHE concentration 0.75 mg/L;	

(e) PGS, initial PHE concentration 1.0 mg/L; and (f) modified PGS, initial PHE concentration 1.0 mg/L with the addition of HA from 0 to 80 mg/L. ....	173
Figure 5.5 The sorption isotherms of PHE on (a) PGS and (b) modified PGS at different ionic strength levels. ....	176
Figure 5.6 The sorption isotherms of PHE on (a) PGS and (b) modified PGS at different temperatures. ....	179
Figure 6.1 Sorption data expressed as fuzzy sets with triangular membership functions. ....	196
Figure 6.2 (a) Normal probability plot of residuals for PHE sorption data; (b) Residuals versus run number.....	200
Figure 6.3 Half-normal plot of factor effects .....	203
Figure 6.4 Plots for main effects of factors .....	206
Figure 6.5 Interaction plots for AC, CE, BC, DE, and BE.....	212
Figure 6.6 The interaction plot matrix of environmental factors at three levels.....	218
Figure 7.1 Coleville site map.....	229
Figure 7.2 FT-IR spectra of the pure gemini powder, the natural soil, and the five soil samples with gemini sorption .....	233
Figure 7.3 The measured apparent sorption coefficients $K_d^*$ of PHE in presence of single 12-2-12 gemini surfactant (PHE at various initial concentration).....	236
Figure 7.4 The sorbed 12-2-12 gemini amount and measured apparent sorption coefficients $K_d^*$ of PHE in the presence of single 12-2-12 gemini surfactant.....	237
Figure 7.5 The sorption isotherms of 12-2-12 gemini surfactant at different temperatures .....	243

Figure 7.6 The schematic sorption process for 12-2-12 gemini surfactant at the soil/aqueous interface .....	245
Figure 7.7 The two-step adsorption and partition isotherm of 12-2-12 gemini surfactant at the soil/water interface. ....	246
Figure 7.8 Schematic diagram of interactions in water, soil, surfactant, and contaminant system .....	247
Figure 7.9 The sorbed C <sub>12</sub> E <sub>10</sub> amount and measured apparent sorption coefficients $K_d^*$ of PHE in presence of individual C <sub>12</sub> E <sub>10</sub> surfactant .....	258
Figure 7.10 The measured apparent sorption coefficients $K_d^*$ of PHE by soil with the addition of 12-2-12 gemini and C <sub>12</sub> E <sub>10</sub> surfactant mixtures.....	263
Figure 7.11 The sorbed 12-2-12 gemini amount and measured apparent sorption coefficients $K_d^*$ of PHE versus the added C <sub>12</sub> E <sub>10</sub> dose at the 12-2-12 gemini dose of 1230 mg/L.....	264
Figure 7.12 The measured $K_d^*$ value of PHE versus the sorbed 12-2-12 gemini amount at the 12-2-12 gemini dose of 1230 mg/L .....	265
Figure 7.13 The sorbed 12-2-12 gemini amount with the added C <sub>12</sub> E <sub>10</sub> dose in presence of 12-2-12 gemini and C <sub>12</sub> E <sub>10</sub> surfactant mixtures .....	269

## LIST OF ABBREVIATIONS

12-2-12	N1-dodecyl-N1,N1,N2,N2-tetramethyl-N2-octylethane-1, 2-diaminium bromide
2,4-D	2, 4-dichlorophenoxyacetic
ANOVA	analysis of variance
BBD	Box-Behnken design
BTEX	benzene, toluene, ethylbenzene, and xylene
C <sub>12</sub> E <sub>10</sub>	decaethylene glycol monododecyl ether
CC	chemical coagulation
CCD	central composite design
CCME	Canadian Council of Ministers of the Environment
CEC	cationic exchange capacity
CFV	cross-flow velocity
CHC	critical hemimicelle concentration
CMC	critical micelle concentration
COD	chemical oxygen demand
CTMAB	cetyltrimethylammonium bromide
DAF	dissolved air flotation
DOM	dissolved organic matter
EC	electrocoagulation
EF	electro-flotation
EO	electro-oxidation
FR	flux recovery
FT-IR	fourier transform infrared spectroscopy
GPGS	geminis modified palygorskite

HA	humic acid
HPLC	high-performance liquid chromatography
J	permeate flux
MF	microfiltration
MMT	montmorillonite
NF	nanofiltration
NOM	natural organic matter
O&G	oil and grease
PAC	polyaluminum chloride
PAC	powdered activated carbon
PAHs	polycyclic aromatic hydrocarbons
PAM	polyacrylamide
PCE	perchloroethylene
PFS	polyferric sulfate
PGS	palygorskite
PHE	phenanthrene
PRB	permeable reactive barriers
PTRC	Petroleum Technology Research Centre
PVDF	polyvinylidene fluoride
PZSS	poly-zinc-silicate-sulfate
R	rejection percentage
RO	reverse osmosis
RR	resistance removal
RSM	response surface methodology
SBBR	spouted bed bioreactor

SDBS	sodium dodecylbenzenesulfonate
SDS	sodium dodecyl sulfonate
SOM	soil organic matter
TAM	two-step adsorption model
TAPM	two-step adsorption and partition model
TMP	transmembrane pressure
TOC	total organic carbon
UF	ultrafiltration
ULPRO	ultra-low pressure reverse osmosis
US EPA	US Environmental Protection Agency

# CHAPTER 1

## INTRODUCTION

### 1.1. BACKGROUND

To date, over hundreds of petroleum-contaminated sites have been identified in urban, rural and remote areas across Canada (CCME, 2008, 2014). Because petroleum products are discharged into subsurface systems due to the leakage of underground storage tanks and pipelines, soil and groundwater contamination has become of major concern in recent years (Zhang, 2007; He, 2008; Yu, 2010). When released to the soil environment, the petroleum contaminants can pose a long-term or immediate threat to human health or the environment, including fire/explosion hazard, human and environmental toxicity, groundwater contamination (Environment Canada), odour, and impairment of soil processes such as water retention and nutrient cycling (CCME, 2008, 2014). The large number of sites and the extent of contamination make this a multibillion dollar problem in Canada. Therefore, proper management of petroleum-contaminated systems is indispensable to clean up subsurface environments, protect human health as well as control costs.

Produced water treatment is one of the biggest issues that need to be addressed at the petroleum-contaminated sites (Dimoglo et al., 2004; Wei, 2007; Bande et al., 2008; Li and Fu, 2009; Younker et al., 2011; Ighilahriz et al., 2014). During oil and gas extraction operations, huge volumes of produced water from the hydrocarbon reservoir are brought to the surface along with the oil or gas. If treated properly, produced water can serve as an alternative supplement for limited freshwater resources, especially in crop irrigation

and livestock watering (Ezechi et al., 2015). Once the wastewater is pumped to water facilities, it can be treated through various physical and chemical processes, including adsorption, coagulation, flocculation, electrocoagulation, dissolved air flotation, and membrane filtration (Zouboulis and Avranas, 2000; Alther, 2002; Larue et al., 2003; Zhong et al., 2003; Ezechi et al., 2005, 2015; Zeng et al., 2007; Cañizares et al., 2008; Abbasi et al., 2010a; Abadi et al., 2011; Younker and Walsh, 2014). Among them, chemical coagulation/flocculation is the most conventional way to clean produced water as well as meet environmental standards at minimal costs (Ahmad et al., 2006; Zeng and Park, 2009). The use of electrochemical technologies for the treatment of produced water has aroused increasing interests in recent years due to its effectiveness in destabilization of oil suspensions (Cañizares et al., 2008; Ezechi et al., 2015,). Membrane filtration is one type of advanced water treatment technique which can provide beneficial reuse of produced water (Murray-Gulde et al., 2003a; Çakmakce et al., 2008; Salahi et al., 2010). There also has been growing interest in using low-cost natural minerals to remove contaminants from produced water (Doyle and Brown, 2000; Alther, 2002; Moazed and Viraraghavan, 2005). The combination of certain these technologies might reach better pollutant removal while retain cost efficiency in produced water treatment process.

Another research area at petroleum-contaminated sites is focused on soil and groundwater remediation (Riser-Roberts, 1998; Chapelle, 1999; Khan et al., 2004). Many oil fields in Canada have suffered from groundwater contamination by complicated mixtures of petroleum hydrocarbons, e.g. polycyclic aromatic hydrocarbons (PAHs), chlorinated solvents, fuels, metals, and/or radioactive materials (Turle et al., 2007). In the past decades, pump and treat has been acknowledged as one of the most widely used *ex*

*situ* treatment methods to clean up groundwater (Mackay and Cherry, 1989; Pankow and Cherry, 1996; Mulligan et al., 2001). Except for pump and treat, the formation of *in situ* reactive barriers is a promising alternative for groundwater remediation (Barrier and Table, 1998; Gavaskar et al., 1998; Thiruvengkatachari et al., 2008). Reactive barriers provide a concept of utilizing reactive media (clay or soil) to immobilize the contaminants and enhance their sorption to the media (Blowes et al., 2000). As the contaminated groundwater flows through the barrier, the pollutants are transformed to nontoxic or immobile products. Compared to traditional pump and treat process, sorption barriers can be used *in situ*, eliminating the cost of extra operating equipment and surface facilities. Previous studies have been reported on the effective contaminant removal from groundwater by these barriers (Barrier and Table, 1998; Wilkin et al., 2005; Thiruvengkatachari et al., 2008; Li and Hong, 2009). In addition, modifying the media (clay/soil) with surfactants can create a hydrophobic environment and substantially increase the sorption of hydrocarbons contaminants (Burriss and Antworth, 1992; Wagner et al., 1994; Juang et al., 2004; Sanchez-Martin et al., 2006; Rodríguez-Cruz et al., 2007a, Rodríguez-Cruz et al., 2007b). The retention of organic contaminants can be largely enhanced with the addition of conventional or novel surfactants. These surfactant modified materials might have the potential to be used as the sorption barriers for petroleum-contaminated groundwater remediation.

## **1.2. CHALLENGES IN THE TREATMENT OF PRODUCED WATER**

Produced water is a term used in the oil industry to describe water that is produced as a byproduct along with the oil and gas. Constituents typically associated with produced

waters from conventional oil and gas production include: dispersed oil, dissolved or soluble organic components, treatment chemicals, produced solids, scales, bacteria, dissolved formation minerals, salinity, and dissolved gases. Oil wells sometimes produce huge volumes of water with the oil, and this has become increasingly unacceptable from both environmental and social concerns. Therefore, operators in oil industries are increasingly focusing on efforts to find efficient and cost-effective treatment methods to remove pollutants from produced waters, including physical, chemical, and biological methods (Zouboulis and Avranas, 2000; Nadarajah et al., 2002; Larue et al., 2003; Zhang et al., 2005; Ahmad et al., 2006; Cañizares et al., 2008; Çakmakce et al., 2008; Zeng and Park, 2009; Abbasi et al., 2010a; Abadi et al., 2011; Zhao et al., 2014; Zhao et al., 2014). Chemical coagulation is the most widely used treatment technique, where ferric and aluminum salts are the most widely used agents for destabilization of oil pollutants (Jiang et al., 2004a; Ahmad et al., 2006; Zeng et al., 2007; Seki et al., 2010; Wu et al., 2011a). However, this technique involves a number of drawbacks such as the large amount of coagulant dose, corrosion issues with reducing pH and sludge problems produced from the coagulation process (Shi et al., 2004; Ahmad et al., 2006; Zeng et al., 2007; Seki et al., 2010; Yan et al., 2012). Therefore, it is necessary to find other efficient methods.

Adsorption is another most conventional technology and it offers one means of cleaning produced water as well as meeting environmental standards at minimal cost. Over recent years there has been increasing interest in using low-cost natural minerals for wastewater treatment (Bailey et al., 1999; Babel and Kurniawan, 2003; Nayak and Singh, 2007; Ahmaruzzaman, 2008; Gupta, 2009; Gupta et al., 2009; Rafatullah et al., 2010; Yagub et al., 2014). Due to the superior properties such as high porosity, high

permeability, small particle size, high surface area, and chemical inertness, diatomite has been widely applied for water treatment containing various types of contaminants (Sari et al., 2010; Caliskan et al., 2011; Hadjar et al., 2011; Sheng et al., 2012; Wang, 2013). Therefore, the combination of polymer coagulants with diatomite may produce some optimal properties because added diatomite may serve as the coagulant aid and enhance the coagulation process. As is reported in the early literature, the enhanced coagulation process of combining diatomite with PAC to remove algae and natural organic matters has been investigated (Wu et al., 2011a). To date, there is less data on the coagulation and flocculation characteristics of polymer coagulants with diatomite in produced water treatment. Moreover, diatomite as both an adsorbent and a coagulant aid to treat oil suspension has not been extensively studied.

In recent years, there has been growing interest in the use of electrochemical technologies for the treatment of produced water (Dimoglo et al., 2004; Wei, 2007; Bande et al., 2008; Li and Fu, 2009; Younker et al., 2011; Ighilahriz et al., 2014). Compared to chemical coagulation, EC has the advantages of short reaction time, compact size, simple operation, low capital and operating costs, and less sludge production. It is a promising technology in removing light and finely dispersed oil particles with high efficiency (Chen et al., 2000a). In addition, because of allowing high rejection rate of salts and colloids, RO is usually combined with other pretreatment techniques for the advanced treatment and beneficial reuse of produced water (Murray-Gulde et al., 2003a; Xu et al., 2008; Al-Zoubi et al., 2009; Fakhru'l-Razi et al., 2009). Because EC is recognized as an effective technique to remove hardness (Malakootian et al., 2010) and destabilize oil suspensions from wastewater, these probably make EC an

efficient RO pretreatment technique to reduce membrane scaling and fouling. However, limited data was reported on the treatment of produced water through EC-RO system.

In addition, operating parameters such as initial oil concentration, pH, current density, coagulation time, electrode distance, and wastewater conductivity are involved in EC process. The statistical refinements of such operating parameters can be applied to maximize the treatment efficiencies. Response surface method is widely used as an experimental design technique to evaluate the relationship between the experimental factors and the measured response and to optimize the experimental process with minimum number of runs (Pey et al., 2006; K rbahti et al., 2007; Saravanathamizhan et al., 2007; Veps l inen et al., 2009; Khayet et al., 2011; Trinh and Kang, 2011; Maher et al., 2014; Schenone et al., 2015). However, there has been no record related to statistical refinement of enhanced hardness removal through EC.

### **1.3. CHALLENGES IN THE TREATMENT OF PAHS-CONTAMINATED GROUNDWATER**

PAHs are aromatic hydrocarbons with two or more fused benzene rings. They are ubiquitously present and have been identified as carcinogenic, mutagenic, and teratogenic. Both natural and anthropogenic sources can cause the release of PAHs to the environment, such as forest fires, volcanic eruptions, vehicular emissions, industrial combustion of fossil fuels, burning of garbage, used lubricating oil and oil filters (Kaushik and Haritash, 2006), municipal solid waste incineration and petroleum spills and discharge. PAHs are recognized as one common pollutant in many petroleum-contaminated sites. They can transport and be accumulated in groundwater and surface

water for a long period of time, and are difficult to biodegrade.

Sorption of PAHs to various sorbents is effective to remove PAHs from aqueous phase, such as fly ash (An and Huang, 2012), clayey soil (Zhang et al., 2011), and petroleum coke-derived porous carbon (Yuan et al., 2010), etc. Recently, there are emerging interests in using clay minerals such as montmorillonite, bentonite, kaolin, and diatomite, for the removal of PAHs. If modified with surfactants, their sorption capacity for PAHs can be largely improved. This is demonstrated by the enhanced PAHs sorption on inorgano–organo-bentonite (Ma and Zhu, 2006), modified sepiolite (Gök et al., 2008), dissolved organic matter-montmorillonite (Wu et al., 2011b), and organo-bentonite (Zhou et al., 2013).

Among the low-cost clay minerals, palygorskite has received growing interest as a potential alternative to the conventional sorbents from both the environmental and the economic points of view. After modifying with a conventional surfactant, the adsorption capacity of palygorskite for hydrophobic contaminants has improved, including dyes (Huang et al., 2007a; Sarkar et al., 2011), pesticides (Sanchez-Martin et al., 2006; Rodríguez-Cruz et al., 2007b), herbicides (Xi et al., 2010), and phenolic compounds (Huang et al., 2007; Chang et al., 2009; Sarkar et al., 2010; Wang et al., 2011a; Sarkar et al., 2012), etc.

Gemini surfactants are a relatively new group of surfactants, which have many unique properties that are superior to the conventional surfactants (Rosen and Tracy, 1998; Menger and Keiper, 2000; Shukla and Tyagi, 2006). Compared to conventional surfactants, modifying clays with gemini surfactants can provide clays with higher sorption capacity for organic contaminants, including dyes (Wang et al., 2013a), 2-

naphthol/4-chlorophenol (Li and Rosen, 2000), catechol/phenol (Liu et al., 2014), and pesticides/phenol (Zhou et al., 2009). In addition, the enhanced solubilization of PAHs by the addition of single gemini surfactant, binary, and ternary gemini surfactant mixtures was investigated by Wei et al. (Wei et al., 2011a; Wei et al., 2011b; Wei et al., 2012; Wei et al., 2013). However, there is limited data regarding the modification of palygorskite with a gemini surfactant for the removal of PAHs from aqueous phase.

In addition, aqueous parameters such as pH, ionic strength, temperature, and dissolved organic matter have been identified as essential factors influencing organic contaminants' sorption behaviors at the solid/aqueous interface (Ko et al., 1998; Zhang et al., 2010a). The overall main factor effects and interactions of different factors can be estimated through the factorial design of experiments (Montgomery et al., 1984; Chegrouche and Bensmaili, 2002; Seki et al., 2006; Ponnusami et al., 2007; Kavak, 2009; Zhao et al., 2009; Gottipati and Mishra, 2010). However, the information regarding the solution chemistry effects on PAHs sorption to palygorskite needs to be clarified. The factorial analysis on the main effects and interactions of aqueous solution parameters on the sorption process is still required.

#### **1.4. CHALLENGES IN GROUNDEATER REMEDIATION**

Groundwater resources in petroleum-contaminated sites are highly vulnerable to contamination from petroleum products. Except for the conventional *ex-situ* pump-and-treat systems, the implementation of *in situ* permeable reactive barriers (PRB) has been proposed for the cleanup of contaminated groundwater (Barrier and Table, 1998; Moon et al., 2003).

These barriers are installed in the path of flowing groundwater, using media which cause chemical or biochemical reactions to transform or immobilize contaminants (Blowes et al., 2000). As the plume moves through these barriers, the contaminants are transformed to nontoxic or immobile products. They can be used *in situ*, eliminating the need for extensive operating equipment and surface facilities as well as continuous input of energy (Thiruvengkatachari et al., 2008). These barriers have been widely applied for groundwater remediation containing heavy metal (Barrier and Table, 1998; Wilkin et al., 2005; Li and Hong, 2009), inorganic anions (Barrier and Table, 1998), and organic compounds (Thiruvengkatachari et al., 2008). *In situ* barriers are especially effective in removing organic contaminants from groundwater flows (Han et al., 2000; Czurda and Haus, 2002; Bowman, 2003; Thiruvengkatachari et al., 2008).

To be effective as a barrier component, the solid phase must be sufficiently reactive to result in the desired contaminant change. Literature has reported the application of certain types of soil or clay minerals with surfactants to immobilize organic contaminants (Burriss and Antworth, 1992; Wagner et al., 1994; Juang et al., 2004; Sanchez-Martin et al., 2006; Rodríguez-Cruz et al., 2007a; Rodríguez-Cruz et al., 2007b). The addition of appropriate surfactant can build a sorption barrier in soil, which can intercept and retard the pollutant plume of organic contaminants. Composed of two long-chain hydrophobic tails, gemini surfactants can markedly modify the soil surface with increasing hydrophobic features. However, the sorption characteristic and mechanism of gemini surfactant at the soil/water interface and the corresponding modeling studies are scarce. The sorption barriers created by gemini surfactants or their binary surfactant mixtures for enhanced soil retention of PAHs are still challenging in many aspects.

## 1.5. OBJECTIVES

In this dissertation research, we will study the enhanced physiochemical processes for the treatment of petroleum-contaminated systems. The specific objectives of this dissertation research include the following aspects:

(1) To investigate the coagulation and flocculation characteristics of PAC, PFS and PAM with diatomite for the produced water treatment. In detail, 1) to evaluate the feasibility of the possible combination of synthetic polymers with diatomite to treat oily wastewater; 2) to explore the mechanisms of synthetic polymers combined with diatomite to promote pollutant removal, using diatomite as an adsorbent and a coagulant aid; and 3) to refine the coagulation/flocculation process by studying the operating variables.

(2) To develop an integrated EC-RO process for enhanced removal of hardness, COD, and turbidity, where combined effectiveness of EC for the pretreatment of produced water prior to RO membranes will be highlighted. First, three important operating variables (initial pH, current density, and electrolysis time) will be investigated to assess the recovery of contaminants. Second, the method of Central Composite Design (CCD) will be employed to obtain desired parameters for higher removal efficiency with a limited number of experiments. Third, practical applicability of the EC-RO process will be demonstrated through analysis of permeate flux and effluent quality in treating produced water from one oil field in Canada.

(3) To reveal the effectiveness of the gemini modified palygorskite as a novel remediation material in removing PAHs from aqueous solution. The sorption of gemini surfactants on palygorskite will be studied and the sorption mechanisms will be

explicated through modeling studies. The effects of aqueous chemistry characteristics on PAHs sorption to palygorskite clay will be explored. The research is also to reveal the distribution of PAHs in a palygorskite-water system and facilitate the potential modification and utilization of palygorskite for enhanced removal of PAHs from contaminated water effluents.

(4) To propose a multi-level fuzzy-factorial inference approach for characterizing the curvature effects of environmental factors and their potential interactions, enhancing our understanding of the sorption behavior of phenanthrene on palygorskite modified with a gemini surfactant. Fuzzy vertex analysis will be employed to discretize design factors with triangular membership functions into multiple deterministic levels based on the  $\alpha$ -cut concept and interval analysis. Multi-level factorial ANOVA will be performed to identify the main effects of factors and their interactions on PAHs sorption to modified PGS. The proposed approach will be used to elucidate the sorption mechanism through detecting the curvature effects of factors and examining their potential interactions in the sorption process.

(5) To investigate the enhanced soil retention of PAHs through the addition of mixed cationic-nonionic surfactants and to assess the effectiveness of sorption barrier created by the binary surfactant mixtures. A systematical investigation on the efficiency and mechanism of PAHs sorption onto soil in the presence of single cationic gemini and binary surfactant mixtures (gemini and nonionic surfactants) will be performed. The sorption of individual gemini surfactant at the soil/water interface will be studied and a two-step adsorption and partition model will be developed to elucidate the corresponding sorption mechanism. Thermodynamic investigation will be conducted to further

characterize the nature of the sorption process. The results obtained from this study will help reveal the interactions among water, soil, surfactant, and contaminant in groundwater remediation processes.

## **1.6. ORGANIZATION**

The dissertation is organized into eight chapters: an introduction, a literature review chapter, five experimental result chapters, and a concluding chapter. In Chapter 2, a comprehensive literature review will be provided covering the previous studies and fundamental theories, including PAHs, gemini surfactants, produced water treatment technologies, clay sorbents, sorption theories, sorption barriers, and experimental design and modeling methods. Chapter 3 will introduce the chemical treatment of produced water through enhanced coagulation/flocculation by combining diatomite with synthetic polymers. Diatomite will be used as both an adsorbent and a coagulant aid to treat oil suspension. In Chapter 4, EC-RO will be combined as the pretreatment and advanced treatment of produced water. EC process will be refined to maximum the pollutant removal using Response Surface Method and single/combined effects of operating variables on pollutant removals will be studied. In Chapter 5, effectiveness of gemini modified palygorskite as a novel remediation material for PAHs-contaminated water will be revealed. The effects of solution parameters on PAH sorption to the modified palygorskite will be investigated. Chapter 6 will propose a multi-level fuzzy-factorial inference approach for characterizing the curvature effects of environmental factors and their potential interactions, providing insight into the sorption behavior of PAH on palygorskite modified with a gemini surfactant. Fuzzy set theory will be used to

determine design factors with membership functions. A multi-level factorial design will examine curvature effects of factors on response. Factorial ANOVA will reveal statistical significance of factors and their interactions at three levels. Chapter 7 will focus on the enhanced retention of PAHs by binary cationic gemini and nonionic surfactant mixtures on soil. The sorption characteristic and mechanism of gemini surfactant in complex soil system will be addressed, and the sorption process will be investigated through model development. The interactions among water, soil, surfactant, and contaminant in groundwater remediation processes will be revealed. Finally, conclusions of this dissertation, as well as recommendations for future research, are drawn toward the end of Chapter 8.

## CHAPTER 2

### LITERATURE REVIEW

#### 2.1. POLYCYCLIC AROMATIC HYDROCARBONS

PAHs are chemical compounds made up of more than two fused aromatic rings in a linear or clustered arrangement. PAHs usually contain only carbon and hydrogen atoms, although nitrogen, sulphur and oxygen atoms may readily substitute in the benzene ring to form heterocyclic aromatic compounds (Gan et al., 2009). They are formed during the thermal decomposition of organic molecules and the subsequent recombination (Haritash and Kaushik, 2009). Both natural and anthropogenic sources can cause the release of PAHs to the environment, such as forest fires, volcanic eruptions, vehicular emissions, industrial combustion of fossil fuels, burning of garbage, used lubricating oil and oil filters (Kaushik and Haritash, 2006), municipal solid waste incineration and petroleum spills and discharge, etc. PAHs are highly toxic, mutagenic and carcinogenic compounds, and are probably recognized as the first environmental carcinogens. In early 1997, US Environmental Protection Agency (EPA) has targeted 16 PAHs as priority pollutants, including naphthalene, acenaphthylene, acenaphthene, fluorene, phenanthrene, anthracene, fluoranthene, pyrene, chrysene, benzo[a]anthracene, benzo[b]fluoranthene, benzo[k]fluoranthene, benzo[a]pyrene, indeno(1,2,3-c,d)pyrene, benzo(g,h,i)perylene, and dibenzo(a,h)anthracene (Mastral and Callen, 2000). With the increasing molecular weight, their solubility decreases, while the hydrophobicity and persistence increase. Once PAHs appear in natural environment, they are resistant to biodegradation under natural conditions. Though PAHs are the principal contaminants in air, soil and water

also serve as the ultimate environmental sinks for these chemicals. The fate of PAHs in environment includes volatilization, photo-oxidation, chemical oxidation, adsorption on soil particles, leaching and microbial degradation (Wild and Jones, 1995). The chemical structures of some commonly studied PAHs are given in Figure 2.1 (Haritash and Kaushik, 2009).

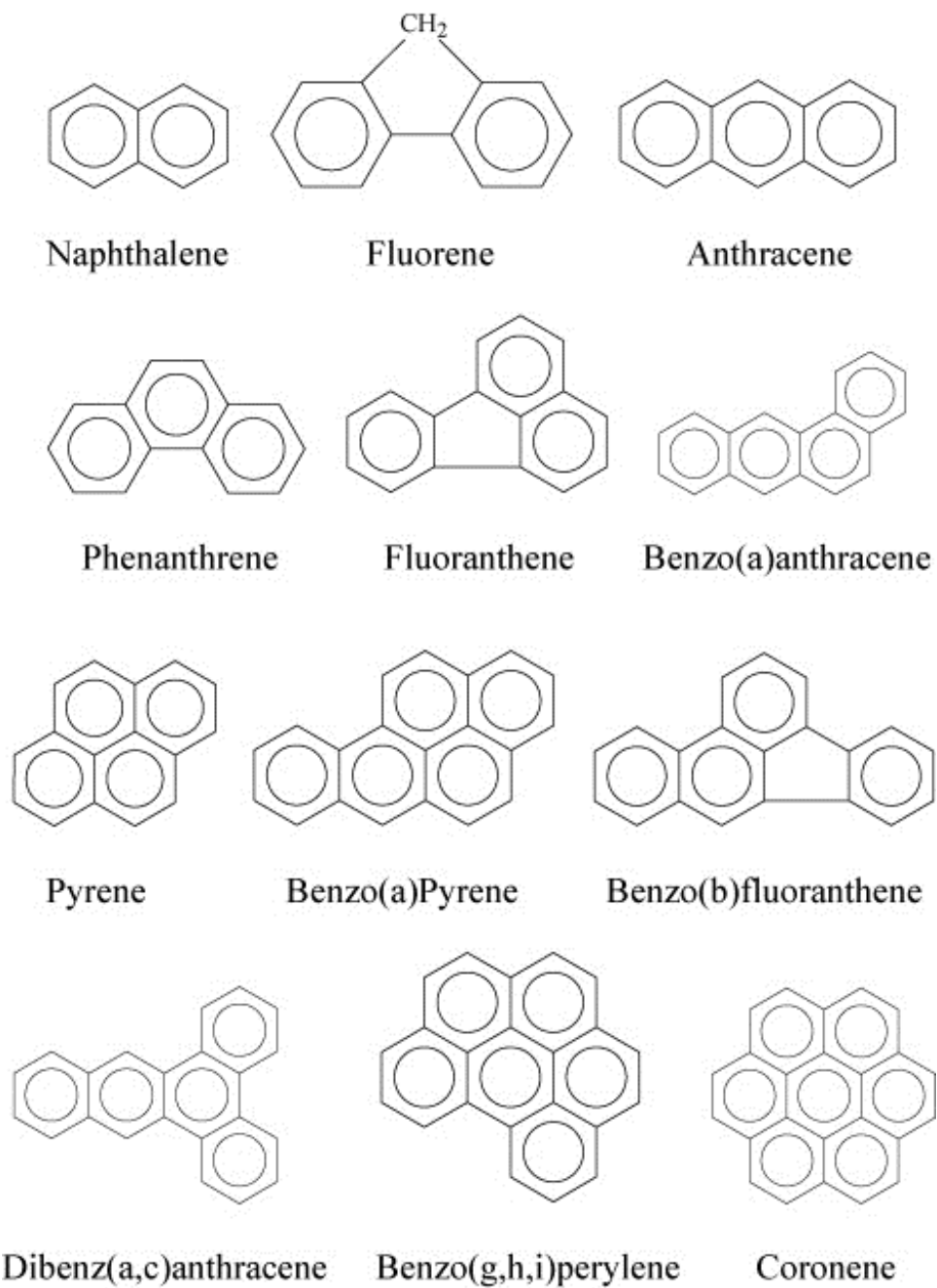


Figure 2.1 Chemical structures of some commonly studied PAHs (Haritash and Kaushik, 2009)

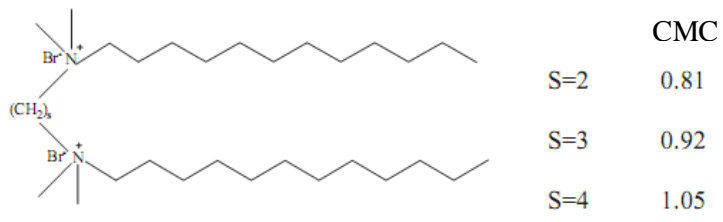
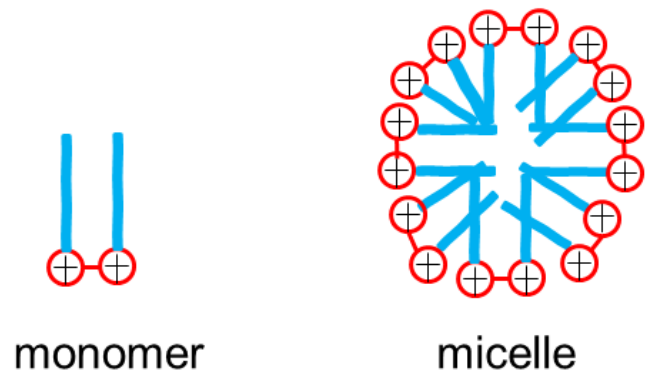
## 2.2. GEMINI SURFACTANTS

Gemini surfactants are composed of two hydrophobic tails and two head groups linked by the spacer group. Though they are a relatively new group of surfactants, the possibilities of using gemini have already been attracting increasing attention. The gemini surfactants have many unique properties that are superior to those of their single-chain counterparts, such as remarkably low critical micelle concentrations (CMCs); much higher efficiency in reducing surface tensions; unusual aggregation morphologies; and better wetting, solubilizing, and foaming properties, which make them potentially useful in many applications. Considerable effort has been exerted to design and synthesize an enormous variety of gemini surfactants with the required properties and to understand the relationship between the structures of gemini surfactants and their various properties in aqueous phase (Wang et al., 2003). Generally, gemini surfactants can be classified into different groups according to the charges of their head groups, including anionic gemini surfactants (Deshpande et al., 2000), cationic gemini surfactants (Atkin et al., 2003a), nonionic gemini surfactants (Castro et al., 2002), and zwitterionic gemini surfactants (Seredyuk et al., 2001). The chemical structures of cationic 12-s-12 gemini surfactants are schematically represented in Figure 2.2.

Due to their extraordinary surface activity, gemini surfactants are regarded as an outstanding new generation of surfactants with excellent properties of solubilization, soil cleanup, and oil recovery (Pérez et al., 1996). Water solubility enhancement of phenanthrene by a cationic gemini surfactant, four cationic and nonionic conventional surfactants as well as their equimolar binary combinations have been studied and compared. Results reveal that gemini/nonionic mixed surfactants with the same chain

length are more appropriate for soil and water remediation (Wei et al., 2011b). The sorption of two cationic gemini surfactants onto some soil solids and the removal of some pollutants by the solid surfaces have been investigated (Li and Rosen, 2000; Rosen and Li, 2001). The increased sorption of the pollutant onto the gemini, compared to that of the conventional surfactant, has shown that the gemini was more effective in removing pollutants from aqueous media. A family of sulfate gemini surfactants has been synthesized and characterized due to the great potential in various industrial applications (Gao and Sharma, 2013). The unique and versatile structure of these surfactants has offered attractive properties for enhanced oil recovery.

Recently, a novel class of gemini biocompatible surfactants derived from arginine has been prepared (Pérez et al., 1996). They are composed of double chain amphiphiles with two hydrophilic chiral head groups from the natural amino acid L-arginine and a polymethylene spacer chain of an adjustable length. These surfactants are biocompatible and less toxic to the environment because they are produced from amino acid sources. Their decomposition products after long-term exposure to the environment are perhaps nontoxic (Pinazo et al., 1999). These surfactants have potential applications in foaming, agrichemical spreading aids, and cleaning processes. For example, bis-quaternary ammonium salts have found broad utilization ranging from industrial to personal care use. Water-soluble ester containing two quaternary ammonium groups are used as bleach activator. Some cationic gemini surfactants are used as hair conditioners and fabric softeners (Menger and Keiper, 2000). As industrial technology and academic research make further progress, demands for high-performance surface active compound with excellent biodegradability are increasing.



**cationic 12-s-12 gemini**

Figure 2.2 The monomer, micelle, and chemical structure of cationic 12-s-12 gemini surfactants (Wei et al., 2013)

## **2.3. PRODUCED WATER TREATMENT TECHNOLOGIES**

### **2.3.1. Characteristics of Produced Water**

Produced water is water trapped in underground formations that is brought to the surface along with oil or gas. Oil and gas reservoirs often have water as well as hydrocarbons, sometimes in a zone that lies under the hydrocarbons, and sometimes in the same zone with the oil and gas. In oil and gas production activities, additional water is injected into the reservoir to sustain the pressure and achieve greater recovery levels. To achieve maximum oil recovery, waterflooding is often implemented, in which water is injected into the reservoirs to help force the oil to the production wells. The injected water eventually reaches the production wells, and so in the later stages of waterflooding, the produced water proportion of the total production increases. It is by far the largest volume byproduct or waste stream associated with oil and gas production.

With respect to the significant matter of environmental concern, many countries have implemented more stringent regulatory standards for discharging produced water (Fakhru'l-Razi et al., 2009). The permitted limits of dispersed fraction of oil and gre (O&G) for treated produced water in Canada are 30 mg/L daily average (Veil et al., 2004). Based on US EPA regulations, the daily maximum limit for O&G is 42 mg/L and the monthly average limit is 29 mg/L (US EPA). The monthly average limits of O&G discharge and COD prescribed by the Peoples Republic of China are 10 and 100mg/L, respectively (Tellez et al., 2002). Based on the Convention for the Protection of the Marine Environment of the North-East Atlantic (OSPAR Convention), the annual average limit for discharge of dispersed oil for produced water into the sea is 40 mg/L (Commission, 2005).

Produced water characteristics depend on the nature of the producing/storage formation from which they are withdrawn, the operational conditions, and chemicals used in process facilities. Some factors such as geological location of the field, its geological formation, lifetime of its reservoirs, and type of hydrocarbon product being produced affect the physical and chemical properties of produced water. Although the composition of produced water from different sources can vary by order of magnitude, produced water composition is qualitatively similar to oil and/or gas production. Constituents typically associated with produced waters from conventional oil and gas production include:

(1) Dispersed oil. Dispersed oil consists of small droplets suspended in the aqueous phase. If the dispersed oil contacts the ocean floor, contamination and accumulation of oil on ocean sediments may occur, which can disturb the benthic community (Veil et al., 2004).

(2) Dissolved or soluble organic components, such as organic acids, PAHs, phenols, and volatiles. These hydrocarbons are likely contributors to produced water toxicity, and their toxicities are additive (Glickman, 1998).

(3) Treatment chemicals, such as biocides, reverse emulsion breakers, and corrosion inhibitors. Some of these treatment chemicals can be lethal at levels as low as 0.1 parts per million (Glickman, 1998). Corrosion inhibitors can make oil/water separation less efficient due to the formation of more stable emulsions.

(4) Produced solids, such as precipitated solids, sand and silt, carbonates, clays, corrosion products, and other suspended solids derived from the producing formation and from well bore operations. The solids can influence produced water fate and effects, and fine-grained solids can reduce the removal efficiency of oil/water separators, leading to

exceedances of oil and grease limits in discharged produced water (Cline, 1998).

(5) Scales, such as calcium carbonate, calcium sulfate, barium sulfate, strontium sulfate, and iron sulfate. Scales can clog flow lines, form oily sludge that must be removed, and form emulsions that are difficult to break (Cline, 1998).

(6) Bacteria. Bacteria can clog equipment and pipelines. They can also form difficult-to-break emulsions and hydrogen sulfide, which can be corrosive.

(7) Dissolved formation minerals, such as cations and anions, heavy metals, naturally occurring radioactive materials, etc. Besides toxicity, these may cause production problems.

(8) Salinity. Environmental effects of produced water salts can occur in all regions where oil and gas have been produced. It is a major contributor of toxicity.

(9) Dissolved gases. CO<sub>2</sub>, O<sub>2</sub>, and H<sub>2</sub>S are common gases included in produced water.

Produced water pollution is mainly manifested in the following aspects (Yu et al.):

(1) affecting drinking water and groundwater resources, endangering aquatic resources; (2) endangering human health; (3) atmospheric pollution; (4) affecting crop production; (5) destructing the natural landscape. Produced water is considered an industrial waste and coal seam gas producers are now required to employ beneficial re-uses or treatment for produced water (Nghiem et al., 2011). Khatib and Verbeek (Khatib and Verbeek) estimate that for 1999, an average of 210 million barrel of water is produced each day worldwide. This volume represents about 77 billion barrel of produced water for the entire year. Recently, approximate 80 million barrels of oil are reported to be produced each day around the world yielding about 250 million barrels of produced water

(Younker et al., 2011). Because huge volumes of produced water are being generated, many countries with oilfields, particularly water-stressed countries, are increasingly focusing on efforts to find efficient and cost-effective treatment methods to clean up produced water as a way to supplement the fresh water resources.

### **2.3.2. Treatment of Produced Water**

Produced water can be treated by physical, chemical, and biological methods. Chemical coagulation is the most widely used treatment technique, where ferric and aluminum salts are the mostly applied agents for destabilization of oil pollutants. Physical methods include heating, centrifugation, and filtration processes such as sand filter and membrane process. In recent years, there has been increasing interest in the use of electrochemical technologies for the treatment of oily wastewaters, including electrocoagulation, electroflotation and electrooxidation. In the following sections, attention will mainly be focused on the techniques that are employed in this dissertation research.

#### *2.3.2.1. Chemical Coagulation*

Chemical oagulation (CC) is widely used in water and wastewater treatments and well known for its capability of destabilizing and aggregating colloids. Coagulation includes all of the reactions and mechanisms involved in the chemical destabilization of particles and in the formation of larger particles through perikinetic flocculation (aggregation of particles in the size range from 0.01 to 1  $\mu\text{m}$ ). Flocculation is used to describe the process whereby the size of particles increases as a result of particle collisions. Coagulation process usually consists of rapid mixing of the coagulant

chemicals with the wastewater followed by flocculation and flotation or settling (Yang, 2007). A coagulant is the chemical that is added to destabilize the colloidal particles in wastewater so that floc formation can result. A flocculant is a chemical, typically organic, added to enhance the flocculation process. Typical coagulants and flocculants include natural and synthetic organic polymers, metal salts such as aluminum sulphate (alum) or ferric sulfate, and prehydrolyzed metal salts such as polyaluminum chloride and polyiron chloride. Flocculants, especially organic polymers, are also used to enhance the performance of granular medium filters and in the dewatering of digested biosolids. In these applications, the flocculant chemicals are often identified as filter aids (Tchobanoglous and Burton, 1991).

There are mainly four mechanisms for colloidal destabilization, including: 1) compression of the double layer by increasing the fluid's ionic strength; 2) adsorption of ions, causing particles charge neutralization; 3) bridging of particles using a polymer; and 4) precipitation of metal salts to produce sweep-floc coagulation (Tchobanoglous and Burton, 1991). In the past decades, coagulation/flocculation has been proven to be effective techniques to destabilize oil emulsions in water. Although this technique involves a number of drawbacks such as the large amount of coagulant dose, corrosion issues with reducing pH and sludge problems produced from the coagulation process, it is still widely applied in the oily wastewater treatment processes.

A new type of coagulant, poly-zinc-silicate-sulfate (PZSS) was synthesized by copolymerization (Zeng and Park, 2009). PZSS exhibits more efficient performance in removing turbidity, SS and COD in the produced wastewater treatment, and a broader range of pH for wastewater than that of polyaluminum chloride (PAC) and polyferric

sulfate (PFS).

The coagulation/flocculation of oil and suspended solids in heavy oil wastewater by PZSS and anion polyacrylamide (A-PAM) was investigated (Zeng et al., 2007). Under the optimum conditions, more than 99% of oil was removed and suspended solid value was less than 5 mg/L, which could satisfy the demands of the pre-treatment process for heavy oil wastewater to be reused or recycled into the injecting well.

It is reported that the efficiencies of the chemical break-up of oil-in-water emulsions with hydrolyzing aluminium salts depended on the total concentration of aluminium and pH (Cañizares et al., 2008). The break-up of the emulsions only took place in the range of pH between 5 and 9, and the amount of aluminium necessary to produce the destabilization of the emulsion was proportional to the oil concentration.

Coagulation of residue oil and suspended solid from palm oil mill effluent using chitosan was explored using a flocculator (Ahmad et al., 2006). The results obtained proved that chitosan was comparatively more efficient and economical to alum and PAC.

The performance of alum in comparison to polyelectrolytes (chitosan and polyacrylamide) as conditioning chemicals for an oil/water emulsion was tested. Polyelectrolyte addition produced the minimum turbidity for the same doses that zero colloidal charge; at higher doses, emulsion was restabilized and became turbid again (Pinotti and Zaritzky, 2001).

#### *2.3.2.2. Adsorption*

Adsorption is one of the most conventional technologies and it offers one means of cleaning produced water as well as meeting environmental standards at minimal cost. The most common sorbents that are applied to treat produced water include: activated carbon,

organoclay, copolymers, and resins, etc.

The technology for removing free and dissolved hydrocarbons from oilfield produced water using organoclay was proposed at early 2000s (Doyle and Brown). Organoclay completely removed free hydrocarbons from wastewaters through adsorption and also removed dissolved hydrocarbons including BTEX. When used in conjunction with a polishing stage of granular activated carbon, organoclay removed free and dissolved hydrocarbons to levels well below current water quality standards.

In a groundwater cleanup project at an air force base, the oily water contained about 1,000 ppm of oil when it entered the settling tank. After letting it settle for several hours, 200 ppm still remained in the water, and the remainder that rose to the surface was skimmed off. One pass through a drum with 250 pounds organoclay lowered it to 5 ppm of oil or less, acceptable for discharge (Alther, 2002).

Powdered bentonite organoclay was used to remove oil from water from production wells at Estevan, Saskatchewan (2005). The concentrations of oil in oily waters varied from 26 to 381 mg/L. Batch studies showed that the equilibrium time for the sorption of oil by organoclay was less than 1 h for all emulsions, indicating that organoclay was an excellent medium for treating oily waters.

A bentonite organoclay/anthracite mixture in the granular form was used in filtration studies in treating four representative oil-in-water emulsions from the Co-operative Oil Refinery, Regina, Saskatchewan. Generally, oil removal efficiencies in a 300 mm organoclay/anthracite bed decreased with an increase in flow rates (Moazed and Viraraghavan, 2001).

The copolymers were used to prepare columns, which were tested as oil remover

from produced water (Carvalho et al., 2002). The results showed that the copolymers with distinct chemical composition could retain different compounds from the produced water. The columns could be re-used after a regeneration process.

A process for the removal of water soluble organic compounds from produced water was provided in one US patent. The process allowed for the removal of water soluble organic compounds by passing the produced water through a column of adsorbing resin which was capable of removing the soluble organic compounds from the water and providing an environmentally acceptable effluent (Means and Braden, 1992).

#### *2.3.2.3. Membrane Filtration*

Membrane separations have been developed greatly over the last 30 years and are becoming a promising technology. A membrane is a selective barrier. At times, it is also an outer covering of cell or cell organelle that allows the passage of certain constituents and retains other constituents found in the liquid. The influent of a membrane is known as the feed stream, the liquid that passes through the membrane is known as the permeate and the liquid containing the retained constituents is the retentate or concentrate.

In the membrane field, the term module is used to describe a complete unit composed of the membranes, the pressure support structure, the feed inlet, the outlet permeate and retentate streams, and an overall support structure. The principal types of membrane modules are tubular, hollow fiber, plate and frame consisting of a series of flat membrane sheets and support plates, and ceramic and polymeric flat sheet membranes and modules.

The degree of selectivity of a membrane depends on the membrane pore size. Depending on the pore size, they can be classified as microfiltration (MF), ultrafiltration

(UF), nanofiltration (NF) and reverse osmosis (RO) membranes. Membranes can also be of various thicknesses, with homogeneous or heterogeneous structure. Membranes can be neutral or charged, and particle transport can be active or passive.

Some key parameters of the membrane process include: membrane permeability ( $k$ ), permeate flux ( $J$ ), transmembrane pressure ( $TMP$ ), rejection percentage ( $R$ ), resistance removal ( $RR$ ) and flux recovery ( $FR$ ). In addition, the fouling and subsequent cleaning of the membrane surface are also essential for the performance of the membrane module. Some parameters are calculated using the following equations:

$$J = \frac{V}{At} \quad (2.1)$$

where  $J$  is the membrane permeate flux;  $A$ ,  $V$  and  $t$  are the membrane area, volumes of collected permeate and filtration time, respectively.

$$k = \frac{J}{TMP} \quad (2.2)$$

where  $k$  is the membrane permeability and  $J$  is the flux rate.  $TMP$  is given by the following equation.

$$TMP = \frac{P_f + P_r}{2} - P_p \quad (2.3)$$

where  $TMP$  is the transmembrane pressure (the operational driving force per unit membrane area);  $P_f$ ,  $P_r$  and  $P_p$  are the pressure of feed, retentate and permeate, respectively.

$$R(\%) = 1 - \frac{C_p}{C_f} \quad (2.4)$$

where  $R$  is the rejection percentage of total dissolved solids, oil-grease content, total suspended solids, or any other feed components.  $C_p$  represents the concentration of a particular component in the permeate, while  $C_f$  is its concentration in the feed.

Fouling and cleaning are quantified via measurements of the resistance before and after cleaning of the membranes. Resistance removal ( $RR$ ) and flux recovery ( $FR$ ) can be used to evaluate membrane fouling and cleaning.

$$FR(\%) = \frac{J_{wc} - J_{ww}}{J_{wi} - J_{ww}} \times 100 \quad (2.5)$$

$$RR(\%) = \frac{R_f - R_c}{R_f} \times 100 \quad (2.6)$$

where  $J_{wi}$ ,  $J_{ww}$  and  $J_{wc}$  are permeate fluxes of the fresh membrane, that of the fouled membrane and that of the chemically cleaned membrane, respectively.  $R_c$  and  $R_f$  are the resistance of the chemically cleaned membrane and that of the fouled membrane, respectively.

Membrane fouling can be defined as the potential deposition and accumulation of constituents in the feed stream on the membrane. Fouling can take place through a number of physicochemical and biological mechanisms which are related to the increasing deposition of solid material onto the membrane surface. The main mechanisms by which fouling can occur, are: 1) Build-up of constituents caused by pore narrowing, pore blocking, or gel/cake layer formation. 2) Formation of chemical precipitates known

as scaling. 3) Colonization of the membrane or biofouling takes place when microorganisms grow on the membrane surface. Developing strategies for fouling control has always been a major challenge in membrane research.

To mitigate membrane fouling, some physical and chemical cleaning techniques can be used. Membrane cleaning is performed when there is a significant drop in permeate flux or salt rejection, or when there is a need to increase the transmembrane pressure significantly to maintain the desired water flux. Back-washing or back-flushing consist of pumping the permeate in the reverse direction through the membrane. Chemical cleaning uses cleaning agents to recovery the membrane permeate flux. Generally, there are five categories of cleaning agents — alkaline solutions, acids, metal chelating agents, surfactants, and enzymes (Ang et al., 2006).

Currently, membranes are widely utilized for the treatment of oily wastewater including oilfield produced water. They have high oil removal efficiency, low energy cost and compact design compared with traditional treatment methods. This technology has several advantages including stable effluent quality, small area requirement, and no chemical addition required (Abadi et al., 2011).

Dimensional analysis of steady state and unsteady state permeation flux was studied for MF of synthetic oily wastewaters using mullite ceramic membranes. Dimensional analysis of unsteady state condition showed that increasing oil content enhanced membrane fouling rapidly and this decreased flux factor. Also, increasing cross flow velocity (CFV) and temperature increased flux factor and decreased membrane fouling (Abbasi et al., 2010b).

An experimental and modeling of separation of oil from industrial oily wastewaters

with mullite ceramic MF membranes were presented (Shokrkar et al., 2011). The aim was to predict the permeation flux as a function of feed temperature, TMP, CFV, oil concentration and filtration time, using a feed-forward neural network. The results showed that the mullite ceramic membrane had a high TOC and COD rejection (94 and 89%, respectively), a low fouling resistance (30%) and a high final permeation flux (75 L/m<sup>2</sup>h).

In another research, an experimental investigation on separation of oil from a real oily wastewater using an UF polymeric membrane are presented (Salahi and Mohammadi, 2011). In order to enhance the performance of UF in API separator effluent treatment and to get higher permeation flux, effects of operating factors on the yield of permeation flux were studied using a Taguchi experimental design.

Wastewater from a household appliance factory containing emulsified oil was treated using a separation method based on an UF membrane (Marchese et al., 2000). By optimizing the process design utilizing this membrane module, it is possible to successfully apply the UF membrane technology to the treatment of industrial emulsified oil waste effluents.

The coal-based MF carbon membrane with low cost for the treatment of oily wastewater was prepared (Song et al., 2006). After treated by coal-based MF carbon membrane, the oil rejection coefficients of oily wastewater were up to 97%, and the oil concentrations of the permeate were less than 10 mg/L, which could meet the National Discharge Standard of China for wastewater.

The possibility of using polyvinylidene fluoride (PVDF) MF membrane to treat the emulsified oily wastewater was investigated (Wang et al., 2009a). Experimental results

showed that MF could effectively treat the laboratory prepared emulsified oily wastewater and the fouled membrane could be recovered by using conventional cleaning methods.

Cross-flow MF processes were studied for treating oily wastewater using a ceramic ( $\alpha$ -Al<sub>2</sub>O<sub>3</sub>) membrane with 50 nm pore size (Hua et al., 2007). A non-steady model of the accumulation volume of permeation was developed. The results showed that the accumulation volume of permeation was significantly affected by the transmembrane pressure, indicating the model was reliable.

An experimental study on separation of oil from actual and synthetic oily wastewaters with mullite and mullite–alumina tubular ceramic membranes was presented (Abbasi et al., 2010a). The results for treatment of emulsions showed that the mullite ceramic membrane has the highest rejection (93.8%) and the lowest fouling resistance (28.97%).

Laboratory-scale studies were carried out to determine the feasibility of the treatment process for Tehran refinery oily wastewater (Salahi et al., 2010). Permeation flux was found to improve with increasing TMP, CFV and temperature at constant feed concentration but rejection decreased slightly. RO was proved to be very suitable for treating and recycling refinery oily wastewater effluents.

A cascaded membrane system consisting of a coalescing backflushed MF membrane used as a pretreatment and an UF membrane were studied for the treatment of oily wastewaters (Peng et al., 2005). The MF/UF hybrid membrane system was found to be very effective in this application, producing permeate with O&G content well below the allowable discharge limit for coastal waters.

The performance and modeling of the separation of oil-in-water emulsions using low-cost ceramic MF membrane was addressed (Nandi et al., 2010). The research confirmed the applicability of the prepared membrane in the treatment of oil-in-water emulsions to yield permeate streams that could meet stricter environmental legislations.

A tubular ceramic MF ( $\alpha$ -Al<sub>2</sub>O<sub>3</sub>) system was employed for treatment of a typical oily wastewater coming from API effluent of Tehran refinery. This system could produce a permeate with O&G content of 4 mg/L that meets the National Discharge Standard and exhibited TOC removal efficiency higher than 95% (Abadi et al., 2011).

Large amounts of co-produced water were generated during natural gas production. The viability and cost effectiveness of ultra-low pressure RO and NF membranes as potential techniques was investigated for beneficial use of produced water by meeting potable and irrigation water quality standards and concentrating iodide in the brine. Findings indicated that these membranes could provide a viable and cost-effective solution for beneficial use of produced water from sandstone aquifers (Xu et al., 2008).

#### 2.3.2.4. *Electrocoagulation*

Electrocoagulation (EC) refers to the *in situ* generation of coagulants by electrolytic oxidation of an appropriate anode material. The generated coagulants then combine small dispersed particles into larger agglomerates which can be easily removed. Compared to chemical coagulation, EC has the advantages of high efficiency in removing light and finely dispersed oil particles without substantial chemical addition and sludge production. In the EC process, operating parameters such as initial oil concentration, pH, current density, coagulation time, electrode distance, and wastewater conductivity might have certain impacts on the treatment efficiencies.

The generation of coagulants is performed by electrically dissolving metal ions from anode electrodes. The electrochemical reactions with aluminum or iron as the anode material are presented as the following equations (2.7) to (2.17) (Xu and Zhu, 2004; El-Naas et al., 2009). The reactions occurring in an electrochemical cell involving aluminum electrodes are:

Anode:



Cathode:



In solution:



Iron upon oxidation in an electrolytic system produces iron hydroxide,  $Fe(OH)_n$ , where n equals to 2 or 3. Two mechanisms have been proposed for the production of  $Fe(OH)_n$  (Xu and Zhu, 2004). The  $Fe(OH)_n$  remains in the aqueous stream as a gelatinous suspension, which can remove the pollutants from wastewater by either complexation or electrostatic attraction, followed by coagulation.

Mechanism 1

Anode:

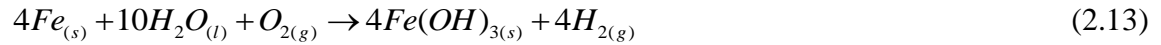




Cathode:



Overall:



Mechanism 2

Anode:



Cathode:



Overall:



The metallic ions can react with the  $OH^-$  ions produced at the cathode during the evolution of  $H_2$  gas, to yield insoluble hydroxides that will adsorb pollutants (oil or suspended solids) out of the solution. Simultaneously, the gas bubble carry the pollutant (especially oil/grease) to the top of the solution where it can be more easily concentrated,

collected and removed. Through neutralizing the electrostatic charges on suspended solids and oil droplets, the sludge produced by electrocoagulation is more compact than that generated from chemical coagulation (Larue et al., 2003).

The removal of COD, turbidity, phenol, hydrocarbon and grease from petrochemical wastewater was experimentally done by using electroflotation (EF) and EC (Dimoglo et al., 2004). The results showed that EC removed the mentioned contaminants more effectively than EF, under different values of residence time, current density, and with iron and aluminium as materials for electrodes.

The separation of finely dispersed oil from oil–water emulsion was carried out in an EF cell which had a set of perforated aluminium electrodes. The effects of operating parameters on the performance of batch cell were examined. It is observed that decrease in salinity and increase in oil content of the effluent enhanced the efficiency of the process (Bande et al., 2008).

The application of EC and electro-oxidation (EO) treatment for the leachate of the oil drilling muds was proposed. EC reduced the processing time, required no addition of chemicals, and was very effective in removing fine colloids. EO was very effective in reducing organic compounds while requiring longer reaction time in the presence of colloids in suspensions (Ighilahriz et al., 2014).

The treatment of oilfield wastewater by EC/EF using sacrificial aluminum electrodes was studied, and the effects of current intensity, electrolysis time, pH and plate spacing on oil removal rate were investigated. The results showed that the treatment effect was influenced by the current intensity and pH distinctly, and the treatment effect under neutral conditions was better than that under acidic and alkaline conditions (Li and

Fu, 2009).

The efficiency of EC process to remove COD, oil and sulfides, from oil petroleum refinery wastewater was evaluated (Mart ínez-Delgado et al., 2010). The iron electrodes had better performance than the aluminum electrodes because it was possible to remove the sulfides from the wastewater. The COD removal rate was the slowest of three parameters and was considered the limiting removal step of the EC process.

Direct and indirect electrochemical oxidation by using boron doped diamond anode, direct electrochemical oxidation by using ruthenium mixed metal oxide electrode, and electrofenton and EC by using iron electrode were investigated for the treatment of petroleum refinery wastewater (Yavuz et al., 2010). Complete phenol and COD removal could be achieved in all electrochemical methods, except EC, provided that electrolysis time was prolonged.

The possibility of using EC to remove phenol from oil refinery waste effluent using a cell with horizontally oriented aluminum cathode and a horizontal aluminum screen anode was explored (Abdelwahab et al., 2009). After 2 h of electrocoagulation, 94.5% of initial phenol concentration was removed from the petroleum refinery wastewater.

Batch EC experiments were carried out to demonstrate the technical feasibility of EC as a possible and reliable technique for the pretreatment of heavily contaminated petroleum refinery wastewater (El-Naas et al., 2009). Although EC was found to be most effective at 25 °C and a pH of 8, the influence of these two parameters on the removal rate was not significant.

EC test runs of oil-in-water emulsions prepared from bio oils and synthetic oils with stainless steel (SS) or aluminum (Al) anode were performed in a batch mode with a

novel bench scale EC apparatus (Karhu et al., 2012). There was no significant difference between treatment results when using a SS or Al anode. However the sludge produced using a SS anode was substantially thicker in structure and thus easier to separate.

#### *2.3.2.5. Combined Treatment*

Every technique has its strength and weakness. Therefore, the integration of certain technologies may overcome the shortcomings and achieve higher contaminant removal from produced water. For example, in combined systems for treating oily wastewater, different physical, chemical, or biological methods are used for pretreatment of membrane units. A combination of these processes appears to be more efficient in terms of satisfying the water discharge limit.

Bench-scale investigation of an integrated adsorption-coagulation-DAF process for produced water treatment was conducted (Younker and Walsh, 2014). The integrated process was evaluated and compared to the individual processes of coagulation-DAF, adsorption-DAF and DAF without pre-treatment for the removal of dispersed oil, naphthalene and phenol from synthetic produced water.

Treatment of oil-in-water emulsions containing n-octane by coagulation and DAF was investigated (Zouboulis and Avranas, 2000). Results indicated that the addition of ferric chloride followed by the application of DAF was found very efficient. More than 95% of the emulsified oil was effectively separated from an initial concentration of 500 mg/L.

Results of a hybrid microfiltration-powdered activated carbon (MF-PAC) system for the treatment of synthetic oily wastewaters with mullite and mullite-alumina ceramic membranes were presented (Abbasi et al., 2011). The experimental results demonstrated

that PAC addition at low concentration (200 ~ 400 ppm) increased permeate flux by 19.6% for mullite and 61% for mullite-alumina MF membranes.

Treatment of oily wastewater produced from post-treatment unit of refinery processes using flocculation and MF membrane was studied (Zhong et al., 2003). The results of filtration tests showed that the membrane fouling decreased and the permeate flux and permeate quality increased with flocculation as pretreatment.

The combined method of demulsification and RO was employed to deal with the filtrate wastewater which was a sort of high-strength and stable oil/water emulsion (Zhang et al., 2008). It was found that the water quality of permeate from the combined treatment process was consistently excellent to meet the 1st grade discharge standard set in the Chinese National Standards for Integrated Wastewater (GB 8978-1996) due to both high removal rate of oil by demulsification and high COD rejection by RO.

The efficacy of a pilot-scale hybrid RO-constructed wetland system for treatment and reuse of produced waters from an oil field was demonstrated (Murray-Gulde et al., 2003a). The pilot-scale RO-constructed wetland system effectively decreased conductivity by 95% and TDS by 94% in the brackish produced water. Following treatment, the produced water was suitable for irrigation or discharge to surface waters.

Although NF membrane satisfied the COD discharge standards, salt concentration was high in permeate. RO membrane could be effectively applied for the treatment of produced water after appropriate pre-treatment (Çakmakce et al., 2008). Results showed that a series of primary sedimentation, oil/water separator, DAF system, 1 µm ceramic or metallic cartridge filter, and 0.2 µm ceramic or metallic MF gave the best pre-treatment option in terms of permeate flux and water quality before RO membrane.

A pilot-scale plant involving aeration tank, air floatation, sand filter and UF was designed and the performance characteristics of the hybrid process were studied for treatment of the oily wastewater in Daqing oilfield, China (Qiao et al., 2008). Operation results showed that this process largely reduced the oil and SS contents in the oily wastewater to less than 0.5 and 1.0 mg/L, respectively, and the concentration levels of other pollutants could also meet the required standard for discharging or injecting water.

In order to treat produced water from polymer flooding, a new treatment method of combining hydrolysis acidification-dynamic membrane bioreactor-coagulation process was developed (Zhang et al., 2010b). The combined process operated continuously for 30 days and the final effluent could meet the class I National Wastewater Discharge Standard of China (GB 8978-1996).

In order to improve the removal efficiencies of phosphate and oils, and to mitigate the membrane fouling, coagulation together with ceramic MF membrane for treating oily wastewater was performed. The results of filtration tests showed that the membrane fouling decreased and the permeate flux and quality increased with coagulation as pretreatment (Zhang et al., 2005).

A synthetic wastewater containing a crude oil emulsion in a brine solution was treated at bench scale using EC and CC in a jar tester with DAF (Younker et al., 2011). The highest COD reduction (62%) was obtained during CC testing at pH 8 at a  $\text{FeCl}_3$  dose of 80 mg/L. The best COD removal with EC (56%) occurred at a dose of 20.6 mg/L of iron at pH 5. CC and EC had comparable performances with respect to COD removal.

The combination and sequence of softening and EC methods to treat hydraulic fracturing flowback and produced water from shale oil and gas operations was addressed

(Esmaeilrad et al., 2015). For TOC, hardness, Ba, Sr, and B removal, application of softening before EC appeared to be the most efficient approach, likely due to the formation of solids before the coagulation process.

A novel three-step process was developed and evaluated for the treatment of highly contaminated refinery wastewater (El-Naas et al., 2014). The process consisted of an EC cell, a spouted bed bioreactor (SBBR), and an adsorption column. The process was found to be highly competitive in comparison with other combined systems used in the treatment of industrial wastewater and can handle highly contaminated refinery or industrial wastewater with relatively wide range of operating conditions.

## **2.4. SORPTION OF ORGANIC COMPOUNDS ON LOW-COST CLAY SORBENTS**

The clays are one type of natural minerals which are generally defined as those minerals that make up the colloid fraction ( $< 2 \mu\text{m}$ ) of soils, sediments, rocks and water and may be mixtures of fine grained clay minerals and clay-sized crystals of other minerals such as quartz, carbonate and metal oxides. Because of their low cost, abundance in most continents of the world, high sorption properties and potential for ion-exchange, clay materials are strong candidates as sorbents (Ahmaruzzaman, 2008). clay is probably the most promising alternative to high-cost sorbents due to their local availability, technical feasibility, easy engineering applications and cost effectiveness (Nayak and Singh, 2007). There are several classes of clays such as smectites (montmorillonite, saponite), mica (illite), kaolinite, serpentine, pyrophyllite (talc), vermiculite and sepiolite (Shichi and Takagi, 2000). The sorption capabilities result from

a net negative charge on the structure of minerals. This negative charge gives clay the capability to sorb positively charged species. Their sorption properties also come from their high-surface-area and high porosity (Crini, 2006). Recently, there are emerging interests in using clay minerals such as montmorillonite, bentonite, kaolin, and diatomite, etc. due to their sorption capacity for not only inorganic ions but also organic compounds. These clay minerals are found widely used in water treatment containing heavy metals (Bailey et al., 1999; Babel and Kurniawan, 2003; Kurniawan et al., 2006), dyes (Crini, 2006; Gupta, 2009; Rafatullah et al., 2010; Yagub et al., 2014), and phenolic compounds (Nayak and Singh, 2007; Ahmaruzzaman, 2008, Gupta et al., 2009).

In addition, clay can be modified to improve its sorption capacity. The common modification methods include modifying the clays with acid, alkaline, microwave, or surfactants. Among all these methods, modification of clays with surfactants is an effective way to increase the sorption for organic contaminants. For example, the modified-sepiolite (with dodecyltrimethylammonium) was reasonably effective sorbent for the removal of organic contaminants such as naphthalene (Gök et al., 2008). The sorption studies of Acid Red 57 onto surfactant-modified sepiolite indicated that this material could be employed as low-cost material for the removal of textile dyes from effluents (Özcan and Özcan, 2005). The feasibility of utilizing inorgano–organo-bentonite, which was bentonite mineral modified with both Fe polycations and cetyltrimethylammonium bromide (CTMAB), was explored to simultaneously remove phosphate and phenanthrene from water (Ma and Zhu, 2006). The selective sorption with organo-bentonite was employed for the removal of PAHs from aqueous surfactant solution as a potential means of recovering surfactant solution after soil washing (Zhou et

al., 2013). Organic clay complex was prepared by associating montmorillonite (MMT) with dissolved organic matter (DOM) extracted from landfill leachate, and the sorption capacity of DOM-MMT complex for phenanthrene was greatly enhanced (Wu et al., 2011b).

Compared to conventional surfactants, modifying clays with gemini surfactants provide clays with higher sorption capacity for organic contaminants. This is supported by the early data that the comparison between sorption of 2-naphthol and 4-chlorophenol onto the clay treated by either the gemini or the conventional surfactants. Results showed that the former were both more efficient at removing the pollutants from the aqueous phase (Li and Rosen, 2000). More recently, the removal of methyl orange by the gemini surfactant modified clay and its monomer modified one was investigated. It is implied that gemini surfactants were more competent than the corresponding monomer in dye wastewater disposal (Wang et al., 2013a). Similarly, one gemini surfactant and its corresponding monomer were prepared and utilized to modify sodium bentonite. The results indicated that the gemini modified bentonite was more effective than the monomer modified bentonite in removing dye from wastewater (Wang et al., 2013c). The removal of phenol and catechol by modified montmorillonite with two novel hydroxyl-containing gemini surfactants, and results indicated that the sorption capacity of catechol was higher than that of phenol in the same experimental conditions (Liu et al., 2014). Montmorillonites were modified by a novel class of gemini surfactants and these modified materials had the potential to treat pollutants such as pesticides, phenol, etc. or being used as antimicrobial materials (Zhou et al., 2009).

This study will focus on the sorption capacity of diatomite and palygorskite. These

two clay minerals and their modified products have been least explored for their potential use in contaminated water remediation (especially organic wastewater). Natural and modified diatomite is a promising sorbent for the removal of hazardous metal ions with high efficiency and low cost because of its unique combination of physical and chemical properties. Until recently, attention has mainly been focused on the removal of heavy metals and dyes from wastewater using diatomite. Literature has extensively reported the sorption of Pb(II) (Sheng et al., 2009), Zinc(II) (Caliskan et al., 2011), Th(IV) (Sheng et al., 2008), Ni(II) (Wang, 2013), Sb(III) (Sari et al., 2010), Uranium (Sprynskyy et al., 2010), and dyes (Al-Ghouti et al., 2005; Zhuang et al., 2013) on natural diatomite and modified diatomite clays. Palygorskite clay is a kind of silicate clay with palygorskite as the main component. Natural and activated palygorskite can be used as the sorbent to remove heavy metals from water (Chen et al., 2007; Chen and Wang, 2007; Wang et al., 2007). After modifying with conventional surfactants, the sorption capacity of palygorskite for hydrophobic contaminants has improved, including herbicides (Xi et al., 2010), pesticides (Sanchez-Martin et al., 2006; Rodríguez-Cruz et al., 2007b), dyes (Huang et al., 2007a; Sarkar et al., 2011), and phenolic compounds (Huang et al., 2007; Chang et al., 2009; Sarkar et al., 2010; Wang et al., 2011a; Sarkar et al., 2012), etc.

## **2.5. SORPTION THEORY**

### **2.5.1. Main Types of Sorption Isotherms**

A general modelling of sorption isotherms, in which four particular cases are now used as the four main shapes of isotherm commonly observed, was proposed by Giles et al. (1960). The sorption isotherms are classified based on their initial slopes and

curvatures, including constant partition C, Langmuir L, high affinity H, and sigmoidal-shaped S isotherm classes. This phenomenological classification is based on pure observation and does not reveal the processes that lead to different isotherm shapes. Generally, C isotherms are defined by a constant sorption affinity, expressing as a straight line. Both H and L isotherms have a convex shape, the slopes of H isotherms reach high values whereas slopes of L isotherms remain constant. This indicates that the sorption affinity of H isotherms increases with decreasing concentration. In addition, S isotherms have a concave shape at low concentrations (Limousin et al., 2007).

C-class isotherms exhibit constant affinity for a wide range of concentrations, implying that “distribution coefficient”  $K$  is constant. At trace concentrations many sorbate–sorbent systems behave this way, especially when the Langmuir equation is an appropriate model for the sorption processes. Many organic substances follow a C isotherm.

The “L” isotherm can be applied when the ratio between the concentration of the compound in the aqueous phase and on the solid decreases as the solute concentration increases, providing a concave curve. It suggests a progressive saturation of the solid. The Langmuir, two-site Langmuir, Toth, and Redlich-Peterson isotherm equations can describe L-type data.

The “H” isotherm is only a special case for the “L” isotherm, where the initial slope of the curve is very high. This case was distinguished from the others because the compound exhibits sometimes such a high affinity for the solid that the initial slope cannot be distinguished from infinity, even if it does not make sense from a thermodynamic point of view (Toth, 1994). Examples of “H” isotherm equation are the

Freundlich, the general Langmuir–Freundlich, and the general Freundlich equations.

The “S” isotherm curve is sigmoidal and thus has an inflection point. Isotherms of the S-class have two causes (Hinz, 2001). First, solute-solute attractive forces at the surface may cause cooperative sorption which leads to the S-shape. Second, the sorption of a solute may be inhibited by a competing reaction within the solution, such as a complexation reaction with a ligand. In many cases the total amount of a solute is measured and not the activity of the different species. The point of inflection illustrates the concentration for which the sorption overcomes the complexation. S-class isotherms can be described by the Freundlich equation with a power greater than one and by the modified Langmuir equation.

Giles et al. (1960) used classification to describe data rather than equations, and they used qualitative criteria lacking mathematical formalism. In the next section, a wide variety of equilibrium isotherm models will be formulated to elucidate sorbate-sorbent interactions through revealing the mathematical correlation between the sorbed amount and the remaining in solution.

The sorption isotherm describes the equilibrium of the sorption of a material at a surface at constant temperature and pH. It represents the amount of material bound at the surface (the sorbate) as a function of the material present in the solution. The analysis of experimental results by equilibrium sorption isotherms are important in developing accurate data that could be used for sorption design purposes. Sorption isotherm is the plot of sorption uptake ( $Q_e$ ) and the equilibrium solute concentration ( $C_e$ ). Modeling of sorption isotherm data is important for predicting and comparing sorption performance. Sorption isotherms are often used as empirical models, and are obtained from measured

data by means of regression analysis. The equation parameters and the underlying thermodynamic assumptions of these equilibrium models often provide some insight into both the sorption mechanism and the surface properties and affinity of the sorbent (Bulut et al., 2008). There are many equations for analyzing experimental sorption equilibrium data. The most frequently used isotherms are the linear isotherm, Freundlich isotherm, and Langmuir isotherm model, etc.

## 2.5.2. Sorption Isotherm Models

### 2.5.2.1. Langmuir Isotherm Model

In 1916, Langmuir (1916) proposed the Langmuir sorption isotherm to originally describe gas–solid–phase sorption onto activated carbon. Nowadays, Langmuir sorption isotherm has been used to quantify and contrast the sorption behavior of various compounds on different sorbents. This empirical model assumes monolayer and homogeneous sorption and has the following hypothesis: all the sorption sites (i) are assumed to be identical, (ii) each site retains one molecule of the given compound and (iii) all sites are energetically and sterically independent of the sorbed quantity (Limousin et al., 2007). The nonlinear and linear forms of Langmuir equation can be represented respectively as:

$$Q_e = \frac{Q_{\max} k_L C_e}{1 + k_L C_e} \quad (2.18)$$

$$\frac{C_e}{Q_e} = \frac{1}{k_L Q_{\max}} + \frac{C_e}{Q_{\max}} \quad (2.19)$$

where  $Q_{max}$  is the maximum sorbate uptake (mg/g) and  $k_L$  the Langmuir equilibrium constant (L/mg).  $C_e$  is the sorbate equilibrium concentration (mg/L). The constant  $k_L$  represents affinity between the sorbent and sorbate. The Langmuir model could estimate the maximum sorbate sorption amount where they might not reach in the experiments.

#### 2.5.2.2. Freundlich Isotherm Model

In 1906, Freundlich (1906) reported the Freundlich sorption isotherm, the earliest known relationship describing the non-ideal and reversible sorption, not restricted to the formation of monolayer. The Freundlich isotherm is originally empirical in nature, but was later interpreted as sorption to heterogeneous surfaces or surfaces with non-uniform distribution of sorption heat and affinity. It is assumed that the stronger binding sites are occupied first and that the sorption energy decreases with the increasing degree of site occupation (Vijayaraghavan et al., 2006). Its non-linearized and linearized equations are listed:

$$Q_e = K_F C_e^{1/n} \quad (2.20)$$

$$\log Q_e = \log K_F + \frac{1}{n} \log C_e \quad (2.21)$$

where  $C_e$  is the equilibrium concentration of sorbate in solution and  $Q_e$  is the corresponding sorbate sorption amount on solids;  $K_F$  and  $1/n$  are the Freundlich constants related to the sorption capacity and the sorption intensity, respectively. The magnitude of the exponent  $1/n$  gives an indication of the favorability of sorption. Generally, if the values of  $1/n$  are in the range of 0.1 ~ 1, it represents favorable sorption. Currently, Freundlich isotherm is widely applied in heterogeneous systems especially for organic

compounds on various sorbents. The slope ranging from 0 and 1 is a measure of sorption intensity or surface heterogeneity. The sorbent surface becomes more heterogeneous as its value getting closer to zero (Foo and Hameed, 2010). The Freundlich sorption isotherm does not envisage the saturation of the solid phase by the sorbate, thus infinite surface coverage is predicted mathematically (Hasany and Chaudhary, 1996).

### 2.5.2.3. Dubinin–Radushkevich Isotherm Model

Dubinin–Radushkevich equation is another popular isotherm model which was initially applied for the sorption of subcritical vapors onto micropore solids following a pore filling mechanism (Dubinin and Radushkevich, 1947). The characteristic sorption curve is reported to estimate the apparent energy of sorption process and is related to the porous structure of the sorbent. The isotherm is as follows:

$$Q_e = (Q_D) \exp(-B_D \varepsilon^2) \quad (2.22)$$

where  $Q_D$  is the Dubinin–Radushkevich model constant (mg/g);  $B_D$  is the Dubinin–Radushkevich isotherm constant ( $\text{mol}^2/\text{kJ}^2$ ) and  $\varepsilon$  is the Polanyi potential.

$$\varepsilon = RT \ln\left(1 + \frac{1}{C_e}\right) \quad (2.23)$$

$R$ ,  $T$  and  $C_e$  represent the universal gas constant (8.314 J/mol K), absolute temperature (K) and sorbate equilibrium concentration (mg/L), respectively.

The constant  $B_D$  is related to the mean energy  $E$  (kJ/mol) of sorption per mole of the sorbate, when  $E$  is transferred to the surface of the sorbent to the infinite distance in the solution (Hasany and Chaudhary, 1996).  $E$  is calculated by the following equation:

$$E = \frac{1}{\sqrt{2B_D}} \quad (2.24)$$

#### 2.5.2.4. Temkin Isotherm Model

It is reported that Temkin isotherm is the early model which is applied into the sorption of hydrogen on platinum electrodes in the acidic solutions. Different from Langmuir equation, Temkin isotherm contains a factor that explicitly takes into account the sorbing species and sorbate interactions (Hosseini et al., 2003). This model has the hypothesis that sorption is characterized by a uniform distribution of binding energies, up to some maximum binding energy (Kim et al., 2004). By ignoring the extremely low and large value of concentrations, the deviation of Temkin isotherm assumes that the decrease of the sorption heat is linear rather than logarithmic (Aharoni and Ungarish, 1977). The sorption heat of all the molecules in the layer would reduce linearly with coverage because of the interactions between sorbate and sorbent. The Temkin isotherm is represented as:

$$Q = \frac{RT}{b_{T_e}} \ln(a_{T_e} C_e) \quad (2.25)$$

where  $R$  is the gas constant (8.314 J/mol · K),  $T$  is the absolute temperature (K),  $b_{T_e}$  is the Temkin constant related to heat of sorption (J/mol), and  $a_{T_e}$  is the Temkin isotherm constant (L/g).

#### 2.5.2.5. Flory-Huggins Isotherm Model

Flory-Huggins isotherm model can be used to elucidate the degree of surface coverage characteristics of sorbate onto sorbent (Vijayaraghavan et al., 2006). The linear form of Flory–Huggins isotherm model is donated as:

$$\log \frac{\theta}{C_0} = \log K_{FH} + n \log(1 - \theta) \quad (2.26)$$

where  $\theta = (1 - C_e/C_0)$  is the degree of surface coverage,  $n$  is the number of sorbate occupying sorption sites,  $K_{FH}$  is the equilibrium constant and  $C_e$  is the equilibrium concentration. Furthermore,  $K_{FH}$  can be used to calculate the Gibbs free energy of spontaneity  $\Delta G^0$  using the following equation:

$$\Delta G^0 = -RT \ln K_{FH} \quad (2.27)$$

Flory-Huggins isotherm model can express the feasibility and spontaneous nature of a sorption process.

#### 2.5.2.6. Redlich and Peterson Isotherm Model

Redlich and Peterson isotherm model combined the features of Langmuir and Freundlich equations into one empirical equation (Redlich and Peterson, 1959). The model can represent sorption equilibria over a wide concentration range, and can be applied either in homogeneous or heterogeneous systems due to its versatility. The isotherm has a linear dependence on concentration in the numerator and an exponential function in the denominator (Gimbert et al., 2008), incorporating three parameters into the following equation:

$$Q = \frac{K_{RP} C_e}{1 + a_{RP} C_e^{\beta_{RP}}} \quad (2.28)$$

where  $K_{RP}$  is the Redlich–Peterson model isotherm constant (L/g);  $a_{RP}$  is the Redlich–Peterson model constant (L/mg); and  $\beta_{RP}$  is the Redlich–Peterson model exponent ranging between 0 and 1. When  $\beta_{RP} \rightarrow 1$ , the isotherm approaches ideal Langmuir

condition; while it becomes more Freundlich, or heterogeneous at high sorbate concentration as  $\beta_{RP} \rightarrow 0$  (Jossens et al., 1978; Ng et al., 2002).

#### 2.5.2.7. Sips Isotherm Model

Sips isotherm incorporates the elements from both Langmuir and Freundlich isotherm and expected to describe heterogeneous surfaces (Sips, 1948). At low sorbate concentrations it reduces to a Freundlich equation, while at high sorbate concentrations it predicts a monolayer sorption capacity characteristic of the Langmuir isotherm (Günay et al., 2007; Pérez-Marín et al., 2007). Sips isotherm has the following form:

$$Q = \frac{K_S C_e^{\beta_S}}{1 + a_S C_e^{\beta_S}} \quad (2.29)$$

where  $K_S$  is the Sips model isotherm constant (L/g);  $a_S$  is the Sips model constant (L/mg); and  $\beta_S$  is the Sips model exponent.

#### 2.5.2.8. Toth Isotherm Model

Toth isotherm, derived from potential theory, has proven applicable in the heterogeneous sorption systems such as phenolic compounds on carbon (Toth, 1971). The model is another empirical equation developed to improve Langmuir isotherm fittings. It assumes an asymmetrical quasi-Gaussian energy distribution with a widened left-hand side, i.e. most sites have a sorption energy less than the peak (maximum) or mean value (Ho et al., 2002). It can be represented by the following equation (Vijayaraghavan et al., 2006):

$$Q = \frac{Q_{\max} b_T C_e}{[1 + (b_T C_e)^{1/n_T}]^{n_T}} \quad (2.30)$$

where  $b_T$  is the Toth model constant and  $n_T$  is the Toth model exponent. Clearly, when  $n_T = 1$ , this isotherm reduces to the Langmuir isotherm model.

## **2.6. SURFACTANT SORPTION MODELING**

### **2.6.1. Mechanisms of Surfactant Sorption at the Solid–Aqueous Interface**

Zhang and Somasundaran (2006) presented a comprehensive summary on the driving forces of surfactants sorption on solids, including:

(1) Electrostatic interactions. In systems where the ionic surfactants and the solid particles are charged, electrostatic interactions play a governing role in the sorption process.

(2) Chemical interactions. Chemical interaction is another important driving force for sorption of surfactants on the solid particles. Compared to other mechanisms, this interaction is specific to certain systems where covalent bonding can occur between the surfactant and the solid.

(3) Hydrophobic lateral interactions. At concentrations above a threshold value, analogous to aggregation in the bulk, surfactant molecules tend to form two-dimensional aggregates at the solid/liquid interface, causing a dramatic increase in the sorption density. These aggregates have been called as “hemimicelles”.

(4) Hydrophobic interaction between the hydrocarbon chains and hydrophobic sites on the solid. The hydrophobic interaction between the alkyl chain of a surfactant and the hydrophobic sites on the solid becomes a significant factor for surfactant sorption on fully or partially hydrophobic surfaces. In this case, the surfactant molecules attach to the hydrophobic sites with the hydrocarbon chains aligning parallel to the surface at low

concentrations and normal to the surface at higher concentrations. Such a sorption process often results in a two-step isotherm.

(5) Hydrogen bonding. Hydrogen bonding between surfactant species and the solid surface species could occur in systems containing hydroxyl, phenolic, carboxylic and amine groups on the surfactant. The sorption of nonionic surfactant often involves hydrogen bonding mechanisms. It should be noted that for sorption due to hydrogen bonding to take place, the bond formed between the surfactant functional groups and mineral surfaces should be stronger than that formed between the mineral and interfacial water molecules.

Depending on the surfactant and solid type, surfactant concentration, electrolyte, pH, temperature, etc., different combinations of the above mechanisms can be involved in different surfactant-solid systems.

### **2.6.2. Modeling Studies of Surfactant Sorption**

The most common approaches for describing the sorption behavior of surfactants on solids are the two-step and four-region sorption isotherms (Atkin et al., 2003c). Literature has reported a wide utilization of two-step isotherm in the surfactant-substrate system (Rupprecht, 1972; Gao et al., 1987; Gu and Huang, 1989; Rupprecht and Gu, 1991). A notable exception is the work of Gao et al. (1987). As shown in Figure 2.3, there are two plateau regions in the sorption isotherm of alkylpyridinium halides to silica. The plateau regions are at low surfactant concentrations (pre critical hemimicelle concentration, CHC) and the saturation level plateau is observed above the CMC. This leads to the proposal of a two-step isotherm for surfactant sorption. The regions

suggested are a low surface excess region (I), a first plateau region (II), a hydrophobic interaction region (III), and a second plateau (IV).

It is suggested that (Gao et al., 1987; Atkin et al., 2003c) in region (I) the surfactant is sorbing via electrostatic interactions with the silica substrate. The surface excess is determined mainly by the surface charge. Sorption is sparse, so interactions between sorbed surfactant molecules are negligible. In region (II), the substrate surface charge has been neutralized. However, the solution activity of the surfactant is not sufficient to lead to any form of aggregation at the interface thus surfactants are still sorbed as monomers. The abrupt increase in sorption at the CHC denotes the onset of region (III). In this region, the solution surfactant concentration is sufficient to lead to hydrophobic interactions between monomers. The monomers electrostatically sorbed in region (II) are thought to act as anchors (or nucleation sites) for the formation of hemimicelles. In this article, a hemimicelle was defined as a spherical structure with surfactant head-groups facing both towards the substrate and into solution. In more recent times this type of structure has been redefined as an admicelle. In region (III) the admicellar structure was not necessarily fully formed, allowing for further sorption. Region (IV) occurred above the CMC, with the formation of fully formed aggregates and saturation levels of surface coverage.

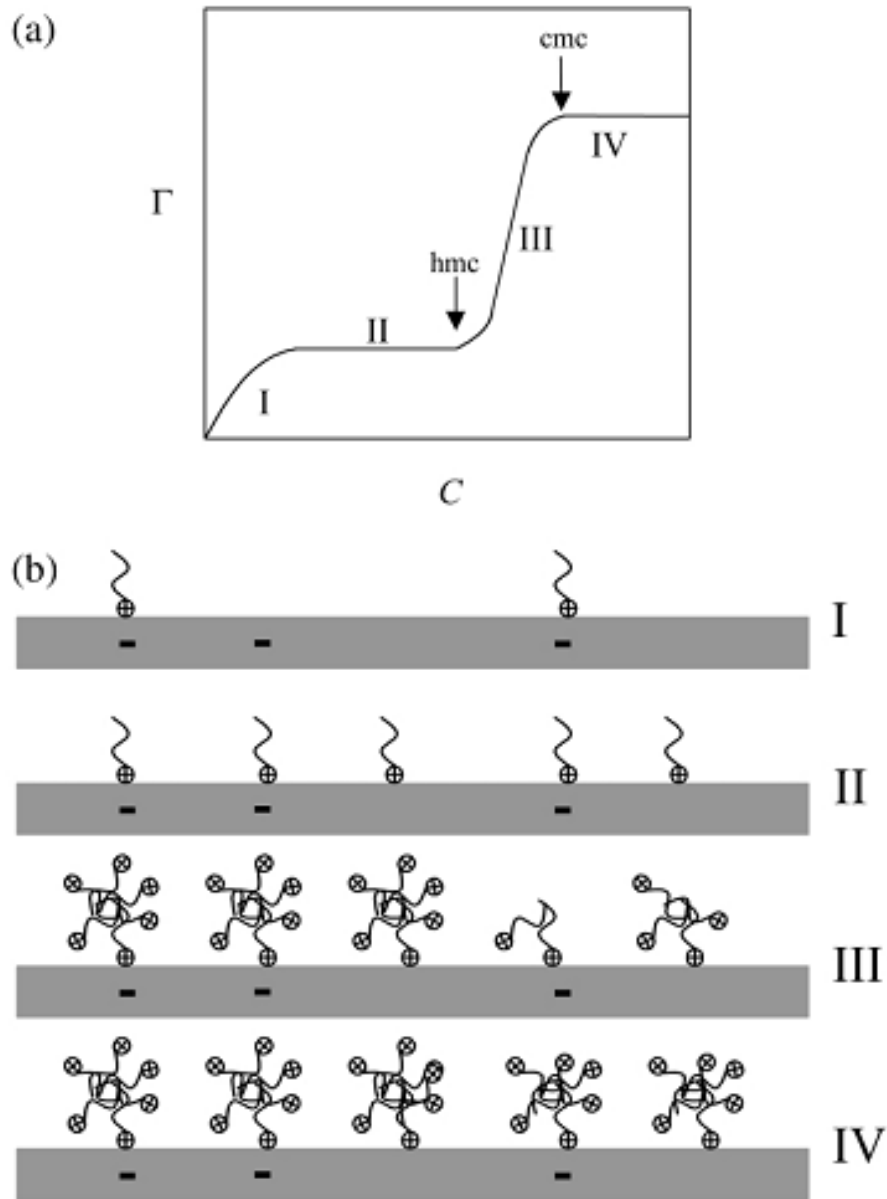


Figure 2.3 The two-step isotherm for cationic surfactants sorbed to silica. (a) The general shape of the sorption isotherm. The  $x$  axis indicates residual surfactant concentration and the  $y$  axis indicates sorption density. (b) The proposed sorption model (Gao et al., 1987).

### 2.6.3. Two-Step Model

The two-step isotherm model was developed later (Zhu and Gu, 1989, 1991; Zhu et al., 1989). It has been widely used to elucidate the sorption behavior of ionic surfactants on various solid surfaces (Lee et al., 2004; Zhou and Somasundaran, 2009; Lo et al., 2010). The basic assumption of the theory is that the sorption of surfactants on solid/liquid interface generally occurs in two steps. In the first step the surface-active species are sorbed as individual ions or molecules (depending on the type of surfactant involved) in the first layer of the solid surface through electrostatic attraction (only present in the case of ionic surfactants, where the surface active ions are sorbed on the oppositely charged solid surface) and/or specific (i.e. van der Waals) attraction. At equilibrium,



In the second step the sorption increases dramatically as hemimicelles form on the sorbent through association or hydrophobic interaction between hydrocarbon chains of the surface active species, and each of the ions or molecules sorbed in the first step provides a possible active center for hemimicellization. In this context the term hemimicelle is used to describe the surface aggregates. At equilibrium,



For the detailed derivation of the formula (Zhu and Gu, 1989, 1991), please refer to the literature . The general surfactant sorption isotherm equation is:

$$Q = \frac{Q_{\max} K_1 C \left( \frac{1}{n} + K_2 C^{n-1} \right)}{1 + K_1 C (1 + K_2 C^{n-1})} \quad (2.33)$$

where  $C$  is the equilibrium concentration of the surfactant, mg/L; and  $Q$  is the sorption amount at concentration  $C$  and  $Q_{\max}$  is the maximum sorption amount at high concentrations, mg/g.  $K_1$  is the equilibrium constant of the first step and  $K_2$  is that of the second step;  $n$  is the hemimicelle aggregation number.

Equation (2.33) has several important limiting cases. If  $K_2 \rightarrow 0$  and  $n \rightarrow 1$ , it can be reduced to Langmuir model:

$$Q = \frac{Q_{\max} K_1 C}{1 + K_1 C} \quad (2.34)$$

If  $n > 1$ , Equation (2.33) has two limiting cases.

When  $K_2 C^{n-1} \ll 1/n$ , Equation (2.33) again is reduced to a Langmuir-type equation, while the monolayer limiting sorption is  $Q_{\max}/n$  instead of  $Q_{\max}$ :

$$Q = \frac{(Q_{\max} / n) K_1 C}{1 + K_1 C} \quad (2.35)$$

When  $K_2 C^{n-1} \gg 1$  or  $K_1 C \ll 1$  and  $K_1 C \ll K_2 C^n$ , Equation (2.33) can be reduced to:

$$Q = \frac{Q_{\max} K_1 K_2 C^n}{1 + K_1 K_2 C^n} \quad (2.36)$$

This is the Sips isotherm model (Foo and Hameed, 2010).

Finally, as the concentration increases, Equation (2.33) reduced to limiting sorption,

$Q_{max}$ , i.e. all the sites are occupied by hemimicelles.

## **2.7. SORPTION BARRIERS AT THE CONTAMINATED SITES FOR GROUNDWATER REMEDIATION**

Many petroleum sites in Canada have suffered from groundwater contamination by complex mixtures of liquid phase hydrocarbons, chlorinated solvents, fuels, metals, and/or radioactive materials. To date, many conventional remediation technologies (e.g., *ex situ* pump and treat systems) have been applied for the cleanup of contaminated groundwater (Mackay and Cherry, 1989). Even after many years of operation, however, it has proven difficult and costly to meet applicable cleanup standards (Mackay and Cherry, 1989). Clearly, more innovative remediation technologies and approaches are needed to mitigate the effects of contaminated subsurface environments.

In recent years, there has been an explosion of activity directed at the development and implementation of permeable reactive barriers (PRB) (Barrier and Table, 1998; Moon et al., 2003), as shown in Figure 2.4. PRBs are an emerging alternative to traditional pump and treat systems for groundwater remediation (Blowes et al., 2000). The barriers constitute *in situ* remediation technologies that utilize media which cause chemical or biochemical reactions to transform or immobilize contaminants. These barriers are installed in the path of flowing groundwater, either as horizontal treatment layers or as vertical treatment walls, to passively remove dissolved constituents through a series of reactions. To be effective as a barrier component, the solid phase must be both sufficiently reactive to result in the desired contaminant change and sufficiently insoluble to remain in place for an economically reasonable length of time. In petroleum sites, the

contaminated soil can be replaced with the reaction mixtures through excavation techniques. An additional advantage of these barriers is that it can be used *in situ*, eliminating the need for extensive operating equipment and surface facilities. There is no need for continuous input of energy, because a natural gradient of groundwater flow would carry contaminants through the reactive zone (Thiruvengkatachari et al., 2008). Extensive data have been reported on utilizing the barriers for groundwater remediation containing heavy metal (Barrier and Table, 1998; Wilkin et al., 2005; Li and Hong, 2009), inorganic anions (Barrier and Table, 1998), and organic compounds (Thiruvengkatachari et al., 2008).

The approach involves placing the barriers in the flow path of a plume of contaminants. As the plume moves through the barriers, the contaminants are transformed to nontoxic or immobile products. *In situ* barriers have proved the efficacy in removing organic contaminants from groundwater flows. For example, the feasibility of using fly ash zeolites to improve the retention properties of the sorptive zone for nonpolar organic molecules and heavy metals was evaluated (Czurda and Haus, 2002). Use of surfactant-modified zeolite as a sorbent in a sub-surface permeable barrier was evaluated (Bowman, 2003). A 15-week pilot test showed that chromate was totally removed from contaminated groundwater while perchloroethylene concentrations were reduced by two orders of magnitude. Significant removal of hexavalent chromium from contaminated groundwater using granular activated carbon as the reactive materials of barriers were achieved and regeneration of carbon by phosphate extraction and acid washing also appeared to be successful (Han et al., 2000). The polyaromatic hydrocarbon removal with barriers using activated carbon and microorganism was evaluated and results showed that

the degradation efficiency of organic material increased when the organic material adsorbed on the carbon (Thiruvengkatachari et al., 2008). Particularly, reports have been found in the application of certain types of soil or clay minerals with surfactants to immobilize organic contaminants (Burriss and Antworth, 1992; Wagner et al., 1994; Juang et al., 2004; Sanchez-Martin et al., 2006; Rodríguez-Cruz et al., 2007a; Rodríguez-Cruz et al., 2007b). Soil/clay with sorbed surfactants can create a hydrophobic organic coating and substantially promote the sorption of hydrocarbons. This has also been demonstrated in the previous literature review. These materials might have the potential to be used as the reactive media in the sorption barriers for petroleum-contaminated groundwater remediation.

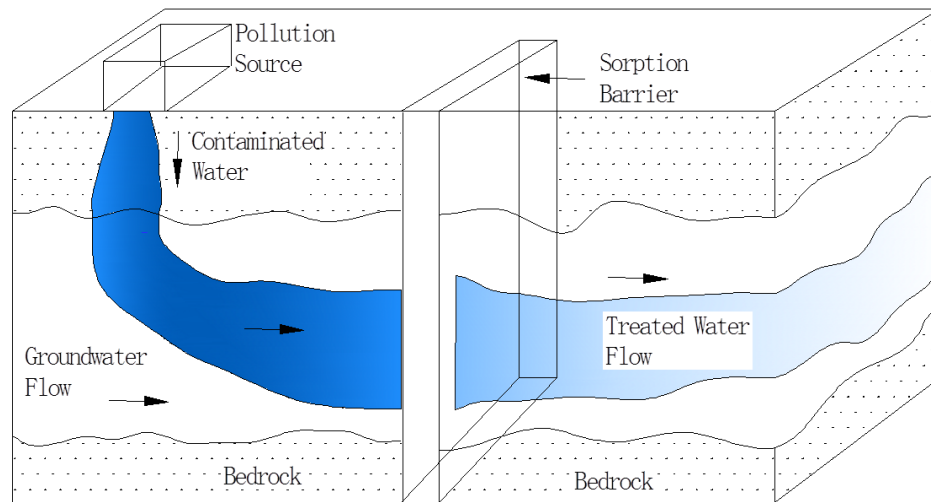


Figure 2.4 *In situ* sorption barriers for groundwater remediation

## **2.8. EXPERIMENTAL DESIGN AND MODELING**

In conventional experimentation, the experiments are conducted keeping all the variables constant except the parameter whose influence is being studied. This type of experiment reveals the effect of the chosen parameters under set conditions, assuming that variables are independent and that the effect will be the same at other values of the remaining variables. However, it does not show what would happen if other variables are changed. Experimental design is an effective strategy to overcome this drawback, which has gained wide application in environmental engineering practice. The combined effect of variables can be predicted and desired optimization can be achieved with the help of the experimental design tool.

### **2.8.1. Factorial Design**

Many experiments involve the study of the effects of two or more factors. In general, factorial designs are most efficient for this type of experiment. It has been widely used in experiments involving several factors where it is necessary to study the joint effects of the factors in a response. By a factorial design, in each complete trial replication of the experiment all possible combinations of the levels of the factors are investigated (Montgomery et al., 1984).

The effect of a factor is defined to be the change in response produced by a change in the level of the factor. This is frequently called a main effect because it refers to the primary factors of interest in the experiment. In some experiments, the difference in response between the levels of one factor is not the same at all levels of the other factors. When this occurs, there is an interaction between the factors. Take a two-factor factorial

experiment in Figure 2.5 for example. Note that  $B^-$  and  $B^+$  lines are approximately parallel in Figure 2.5(a), indicating a lack of interaction between factor A and B. However, Figure 2.5(b) shows that  $B^-$  and  $B^+$  lines are not parallel, indicating an interaction between A and B. Because the effect of A depends on the level selected for factor B, there exists the interactive effects.

Generally, when an interaction is large, the corresponding main effects have little practical meaning. For example in Figure 2.5(b), Factor A has an effect, but it depends on the level of factor B. This is, the AB interaction is more useful than that of main effect. The significant interaction will often mask the significance of main effects. In the presence of significant interaction, the experimenter should always examine the levels of one factor, say A, with levels of the other factors fixed to draw conclusions about the main effect of A.

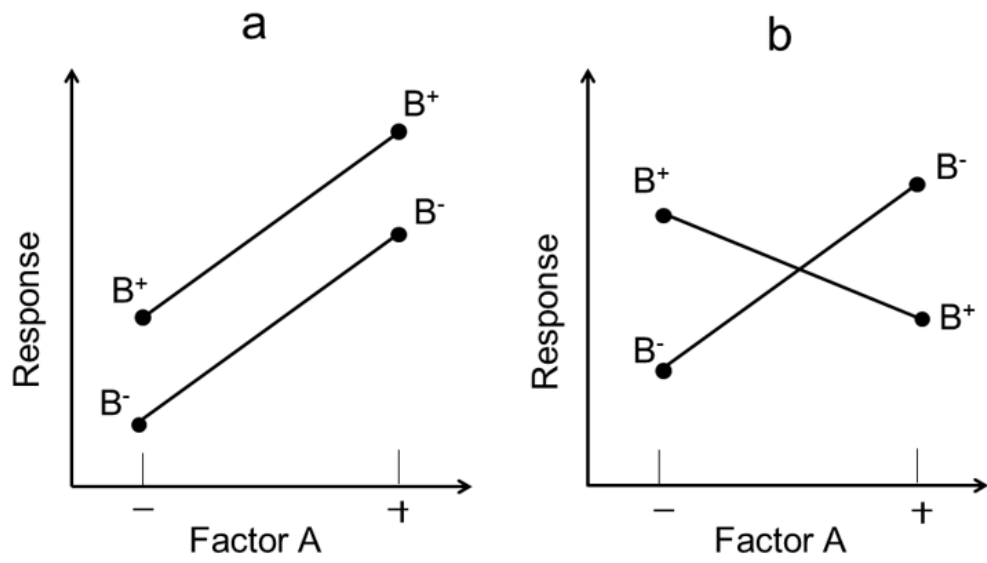


Figure 2.5 A factorial experiment (a) without interaction and (b) with interaction

### 2.8.1.1. The General Factorial Design

There are  $a$  levels of factor A,  $b$  levels of factor B,  $c$  levels of factor C, ..., arranged in a factorial experiment. In general, there will be  $abc\dots n$  total observations if there are  $n$  replicates of the complete experiment. In addition, at least two replicates ( $n \geq 2$ ) are necessary to determine a sum of squares due to error if all possible interactions are included in the model.

If all factors in the experiment are fixed, the test hypotheses about the main effects and interactions can be formulated using ANOVA. For the fixed model, test statistics for each main effect and interaction may be constructed by dividing the corresponding mean square for the effect or interaction by the mean square error. All of these  $F$  test will be upper-tail, one-tail tests. The number of degrees of freedom for any main effect is the number of levels of the factor minus one, and the number of degrees of freedom for an interaction is the product of the number of degrees of freedom associated with the individual components of the interaction.

Assuming A, B, and C are fixed, consider the three-factor analysis of variance model:

$$y_{ijkl} = \mu + \tau_i + \beta_j + \gamma_k + (\tau\beta)_{ij} + (\tau\gamma)_{ik} + (\beta\gamma)_{jk} + (\tau\beta\gamma)_{ijk} + \varepsilon_{ijkl} \quad \begin{cases} i = 1, 2, \dots, a \\ j = 1, 2, \dots, b \\ k = 1, 2, \dots, c \\ l = 1, 2, \dots, n \end{cases} \quad (2.37)$$

The significance of models and their coefficients would be assessed with ANOVA analysis. Usually, ANOVA computations would be done using a statistics software package. The manual computing formulas for the sums of squares are listed in the

following equations. The total sum of squares is found in the usual way as:

$$SS_T = \sum_{i=1}^a \sum_{j=1}^b \sum_{k=1}^c \sum_{l=1}^n y_{ijkl}^2 - \frac{y^2}{abcn} \quad (2.38)$$

The sums of squares for the main effects are calculated as:

$$SS_A = \frac{1}{bcn} \sum_{i=1}^a y_i^2 - \frac{y^2}{abcn} \quad (2.39)$$

$$SS_B = \frac{1}{acn} \sum_{j=1}^b y_j^2 - \frac{y^2}{abcn} \quad (2.40)$$

$$SS_C = \frac{1}{abn} \sum_{k=1}^c y_k^2 - \frac{y^2}{abcn} \quad (2.41)$$

The two-factor interaction sums of squares are represented by following equations:

$$SS_{AB} = \frac{1}{cn} \sum_{i=1}^a \sum_{j=1}^b y_{ij}^2 - \frac{y^2}{abcn} - SS_A - SS_B \quad (2.42)$$

$$SS_{AC} = \frac{1}{bn} \sum_{i=1}^a \sum_{k=1}^c y_{ik}^2 - \frac{y^2}{abcn} - SS_A - SS_C \quad (2.43)$$

$$SS_{BC} = \frac{1}{an} \sum_{j=1}^b \sum_{k=1}^c y_{jk}^2 - \frac{y^2}{abcn} - SS_B - SS_C \quad (2.44)$$

The three-factor interaction sum of squares is computed from:

$$\begin{aligned} SS_{ABC} &= \frac{1}{n} \sum_{i=1}^a \sum_{j=1}^b \sum_{k=1}^c y_{ijk}^2 - \frac{y^2}{abcn} - SS_A - SS_B - SS_C - SS_{AB} - SS_{AC} - SS_{BC} \\ &= SS_{subtotals(ABC)} - SS_A - SS_B - SS_C - SS_{AB} - SS_{AC} - SS_{BC} \end{aligned} \quad (2.45)$$

The error sum of squares may be found by subtracting the sum of squares for each main effect and interaction from the total sum of square:

$$SS_E = SS_T - SS_{subtotals(ABC)} \quad (2.46)$$

Before the conclusions from the ANOVA are adopted, the adequacy of the underlying model should be checked. The primary diagnostic tool is residual analysis (Montgomery et al., 1984).

### 2.8.1.2. Two-Level Factorial Design

The most important factorial design case is of  $k$  factors, each at two levels. The levels of factors can be quantitative or qualitative. A complete replicate of such a design requires  $2 \times 2 \times \dots \times 2 = 2^k$  observations and is called a  $2^k$  factorial design. The  $2^k$  factorial design is particularly useful in the early stages of experimental work when many factors are likely to be investigated. It provides the smallest number of runs with which  $k$  factors can be studied in a complete factorial design. Consequently, these designs are widely used in factor screening experiments.

The statistical model for a  $2^k$  design would include  $k$  main effects,  $\binom{k}{2}$  two-factor interactions,  $\binom{k}{3}$  three-factor interactions, ..., and one  $k$ -factor interaction. That is, the complete model would contain  $2^k - 1$  effects for a  $2^k$  design. For example, a  $2^3$  factorial design with three factors would contain three main effects, three two-factor interactions, and one three-factor interaction.

In a  $2^k$  factorial design, it is easy to express the results of the experiment in terms of a regression model. For the  $2^2$  factorial design, the regression model is:

$$y = \beta_0 + \beta_1x_1 + \beta_2x_2 + \varepsilon \quad (2.47)$$

where  $x_1$  and  $x_2$  are the two experimental factors, and  $\beta_1$  and  $\beta_2$  are the regression coefficients. Note that the relationship between the factor and response variable is linear.

### 2.8.1.3. Multi-Level Factorial Design

The  $3^k$  design provides an opportunity to assess the quadratic relationship between the response and factors. In the  $3^k$  factorial design, there are  $3^k$  treatment combinations, with  $3^k - 1$  degrees of freedom between them. These treatment combinations allow sums of squares to be determined for  $k$  main effects, each with two degrees of freedom;  $\binom{k}{2}$  two-factor interactions, each with four degrees of freedom; ...; and one  $k$ -factor interaction with  $3^k$  degrees of freedom. For example, an  $h$ -factor interaction has  $2^h$  degrees of freedom. If there are  $n$  replicates, there are  $n \times 3^k$  total degrees of freedom and  $3^k \times (n - 1)$  degrees of freedom for error. Each main effect can be represented by a linear and a quadratic component.

In the  $3^k$  system of designs, when the factors are quantitative, the low, intermediate, and high levels are often denoted as -1, 0, and +1, respectively. This facilitates fitting a regression model relating the response to the factor levels. For example, consider the  $3^k$  design and let  $x_1$  represents factor A and  $x_2$  represents factor B. A regression model relating the response  $y$  to  $x_1$  and  $x_2$  that is supported by this design is:

$$y = \beta_0 + \beta_1 x_1 + \beta_2 x_2 + \beta_{12} x_1 x_2 + \beta_{11} x_1^2 + \beta_{22} x_2^2 + \varepsilon \quad (2.48)$$

Clearly the addition of a third factor level allows the relationship between the response and design factors to be modeled as quadratic.

### 2.8.1.4. Applications

Factorial design of experiments especially two-level factorial designs has been

widely applied in sorption studies. For example:

The effects of several factors governing the adsorption process of dye Rhodamine 6G, such as dye concentration, pH, and temperature, on percent of adsorption were investigated using a mixed level factorial design. Results indicated that dye concentration was the most significant factor under the experimental ranges examined (Annadurai et al., 2002).

The biosorption of  $\text{Cr}^{3+}$  and  $\text{Cr}^{6+}$  from water solutions was studied using a  $2^3$  factorial design (Carmona et al., 2005). The most significant effect regarding  $\text{Cr}^{3+}$  uptake was ascribed to interaction between metal concentration and pH. For  $\text{Cr}^{6+}$ , the most significant effect was ascribed to metal concentration.

To evaluate the adsorption of the anionic dye Brilliant Yellow from aqueous solutions on sepiolite, batch adsorption experiments were carried out using a  $2^3$  full factorial design (Bingol et al., 2010). The initial pH of the dispersion exerted the greatest influence on the dye adsorption amount. The factorial experiments demonstrated significant antagonistic interaction between pH and ionic strength.

Batch and continuous experiments were performed for the sorption of distillery spent wash onto fly ash particles (Prasad and Srivastava, 2009). The optimization using  $2^3$  factorial designs of experiments provided optimal removal of color of 93% at dilution (5%), dosage of adsorbent (10 g) and temperature (293 K).

A  $2^4$  factorial design was employed to evaluate the quantitative removal of zinc from aqueous solutions on synthesized hydroxyapatite (Meski et al., 2011). Adsorbent dosage had a positive effect on the removal of zinc, whereas zinc concentration, Ca/P molar ratio and calcination temperature had a negative effect on this process.

A full  $2^3$  factorial design was used to obtain the best conditions of biosorption of  $\text{Fe}^{3+}$  and  $\text{Zn}^{2+}$  from water solutions (Abdel-Ghani et al., 2009). The pH was found to be the most significant factor for the two studied metal ions.

Optimization of the most important factors directly affecting the adsorption of lead onto the biosorbent was carried out by using a  $2(k)$  factorial experiment (Yahiaoui et al., 2011). The results suggested that the most influential factor was the solution pH followed by the initial concentration of lead ions, inactive brewer's yeast dose, and temperature.

A  $2^3$  factorial design was employed to evaluate the quantitative removal of the indigo carmine (IC) dye from aqueous solutions on glutaraldehyde cross-linked chitosan (Cestari et al., 2008). The results indicated that increasing the chitosan mass from 100 to 300 mg decreased the IC adsorption whereas a temperature increase from 25 to 35 degrees elevated it. The factorial experiments demonstrated the existence of a significant antagonistic interaction effect between the chitosan mass and temperature.

A  $3^k$  factorial design was used to determine the interaction effects of carbonization temperature, pH, dosage of adsorbent and type of activating agent on the amount of dye removal (Ozbay and Yargic, 2015). The analysis showed that the adsorption process depended significantly on the type of activating agent used in the preparation of activated carbon.

To identify the operating conditions which influence Remazol Yellow dye sorption from aqueous solutions, the effects of pH, initial dye concentration and contact time were investigated by  $3^3$  full factorial experimental design method (Un et al., 2015). The increasing solution pH and initial dye concentration had negative effect, while increasing contact time had a positive effect on dye removal. The interaction effect between pH and

initial dye concentration was the most influencing interaction.

### **2.8.2. Response Surface Method**

Response surface method, or RSM, is a collection of mathematical and statistical techniques useful for the modeling and analysis of problems in which a response of interest is influenced by several variables and the objective is to optimize the response (Montgomery et al., 1984). The eventual objective of RSM is to determine the optimum operating conditions for the system or to determine a region of the factor space in which the operating parameters are satisfied. RSM is a useful statistical method for evaluating the relationship between the experimental factors and the measured response. It can be performed to evaluate the relative significance of the factors. RSM is suitable for investigating and optimizing the pertinent parameters of an experiment.

In most RSM problems, the form of the relationship between the response and the independent variables is unknown. Therefore, the first step of RSM is to find a suitable approximation for the true functional relationship between  $y$  and the set of independent variables. Usually, a low order polynomial in some region of the independent variables is employed. If the response is well modeled by a linear function of the independent variables, then the approximating function is the first-order model:

$$y = \beta_0 + \beta_1 x_1 + \beta_2 x_2 + \dots + \beta_k x_k + \varepsilon \quad (2.49)$$

If there is curvature in the system, then a polynomial of higher degree must be used, such as the second-order model:

$$y = \beta_0 + \sum_{i=1}^k \beta_1 x_i + \sum_{i=1}^k \beta_{ii} x_i^2 + \sum_{i < j} \beta_{ij} x_i x_j + \varepsilon \quad (2.50)$$

where  $y$  is the response of the system; The coded independent variable, denoted by  $x_1, x_2, \dots, x_k$ , are presumed to be continuous and can be controlled with negligible error.  $\beta_0, \beta_1, \dots, \beta_{ij}$  are regression coefficients for the intercept and linear, quadratic and interaction terms.  $\varepsilon$  is the statistical error.

Almost all RSM problems use one or both of these models. Of course, it is unlikely that a polynomial model will be a reasonable approximation of the true functional relationship over the entire space of the independent variable, but for a relatively small region they usually work quite well.

The least squares method can be used to estimate the parameters in the approximating polynomials. The response surface analysis is then performed using fitted surface. If the fitted surface is an adequate approximation of the true response function, then analysis of the fitted surface will be approximately equivalent to analysis of the actual system. The model parameters can be estimated most effectively if proper experimental designs are used to collect the data.

Fitting and analyzing response surfaces are greatly facilitated by the proper choice of an experimental design. For the first-order model, there is a unique class of designs that minimizes the variance of the regression coefficients. These are the orthogonal first-order designs, including the  $2^k$  factorial designs in which the main effects are not aliased with each other.

The most popular class of designs used for fitting a second-order model is the central composite design or CCD. The CCD is ideal for sequential experimentation and

allows a reasonable amount of information for testing lack of fit while not involving an unusually large number of design points (Montgomery et al., 1984). Another design method that is widely used is the Box-Behnken Design (BBD) method. The BBD is a rotatable second-order design based on three-level incomplete-factorial designs. These designs are usually very efficient in terms of minimum number of required runs. The number of experimental runs and experimental procedure are depending on the detailed experiments. As an effective experimental design technique, RSM has been extensively applied in water treatment fields.

The influences of the temperature and peroxide to 2,4-D initial concentration ratio on degradation of herbicide 2,4-D were investigated and optimized by the application of a three-level factorial experimental design combined with the RSM. It is demonstrated that RSM was a good tool for studying the effects of different variables and their interactions on 2,4-D conversion percentage in the photo-Fenton process (Schenone et al., 2015).

The removal of natural organic matter from surface water by EC was studied (Vepsäläinen et al., 2009). Through the optimization of process variables using RSM, EC could be a suitable method for pretreatment of surface water before deionizing process.

Treatment of textile effluent using an electrochemical technique was designed and analyzed using the Box-Behnken method (Saravanathamizhan et al., 2007). The influence of individual parameters on electro-oxidation of textile effluent was critically examined using RSM, and a quadratic model for COD reduction was developed. It is observed that the predicted values were in good agreement with experimental data with a correlation coefficient of 0.945.

Applying RSM in jar tests as an alternative to the conventional methods was

investigated to find out the optimum operating parameters for coagulation-flocculation process in water treatment plants (Trinh and Kang, 2011). Confirmation of experimental results was found to be close to the prediction derived from the models. This demonstrated the benefits of the approach based on the RSM in achieving good predictions while minimizing the number of required experiments.

The effect of operating conditions including pH value, feed flow and applied pressure on heavy metal removal of a NF membrane for drinking water production was investigated using RSM (Maher et al., 2014). Optimization of operating conditions for maximizing the membrane's heavy metal rejection performance contributed to an elimination of 93% of nickel and 86% of lead ions in the optimum condition.

Statistical experimental design and RSM, were applied to optimize removal of C.I. Acid Black 210 dye from highly concentrated solutions by means of a coagulation/flocculation process (Khayet et al., 2011). The temperature exhibited the strongest effects and high interaction effects existed between the temperature and the concentration of aluminium sulphate. Through using CCD technique, the maximal dye removal obtained under optimal process conditions was confirmed experimentally.

The electrochemical treatment conditions of water-based paint wastewater were optimized using RSM where potential difference, reaction temperature and electrolyte concentration were to be minimized while COD, color and turbidity removal percent and initial COD removal rate were maximized at 100% pollution load (Körbahti et al., 2007).

The decomposition of ibuprofen in synthetic solution and in municipal wastewater effluent was investigated using an electro-sonochemical reactor. A  $2^3$  factorial experimental design demonstrated that the current intensity and treatment time were the

most influent parameters for the sono-electrochemical oxidation of ibuprofen (Tran et al.).

## **2.9. LITERATURE REVIEW SUMMARY**

In the past decades, many research efforts have been made on the various physicochemical treatment methods for the remediation of petroleum-contaminated systems, including chemical coagulation, electrocoagulation, membrane process, sorption, surfactant-enhanced remediation, and sorption barrier techniques. However, improvements in the following areas are still required:

As is indicated in literature studies, synthetic polymers such as PAC, PFS and PAM have been widely used as coagulants or flocculants in wastewater treatment plant. However, chemical coagulants may generate a considerable amount of hazardous sludge which may play side effects to the open water course. Diatomite as a type of natural clay mineral has been aroused emerging interests in wastewater treatment process. Other than normally being used as an adsorbent, diatomite has received little attention as a coagulant aid for the synthetic polymers in the water treatment process. To date, no data has been reported on the coagulation and flocculation characteristics of PAC, PFS and PAM with diatomite to treat produced water in oilfield. Moreover, diatomite as both an adsorbent and a coagulant aid to treat oil suspension has not been extensively investigated.

Conventional methods such as adsorption, coagulation, membrane processes, dissolved air flotation, and various combined processes have been performed to treat produced water from oil fields. However, limited data was reported on the treatment of produced water through EC-RO system. In addition, scaling is a serious problem which might cause the irreversible pore plugging and physical damage of the membrane.

Despite an impressive amount of scientific investigation on contaminant removal through EC, little has been done on the hardness recovery, and none has been conducted to decrease hardness together with COD/turbidity through EC as a RO pretreatment process to reduce fouling and scaling effects. Also, there has been no record related to statistical refinement of hardness removal conditions through EC using response surface method.

In our previous studies, the enhanced solubilization capability of cationic gemini surfactants for PAHs has been demonstrated. It is also reported that the sorption capacity of palygorskite for hydrophobic contaminants has been improved when modified with conventional surfactants. However, there is limited data regarding the modification of palygorskite with a gemini surfactant for the removal of PAHs from aqueous phase. The enriched knowledge regarding the potential applications of gemini modified palygorskite in polluted water treatment and environmental remediation processes is required.

Two-level factorial design techniques have been widely applied in the sorption experiments. All these studies assume that the contaminant sorption capacity is linear over the range of factor levels. However, sorption isotherms generally involve a highly nonlinear relationship between experimental factors and the sorption capacity. The two-level factorial experiment can hardly reveal the curvature. The concept of multi-level factorial designs is able to detect the curvature in sorption isotherms and examine the interactions among factors at multi-levels. However, limited data has been reported on the utilization of multi-level factorial design in elucidating experimental processes. Moreover, fuzzy set theory is a powerful tool to represent the experimenter's subjective judgments on designing experimental factors. However, the multi-level fuzzy-factorial inference approach has never been reported on sorption experiments.

Cationic gemini surfactant, as a series of novel surfactant, has received emerging interest in recent years. However, a number of issues about the characteristic and mechanism of gemini surfactant-induced sorption are poorly understood. The knowledge about corresponding sorption modeling studies is still scarce. A well understanding of the sorption of cationic gemini and nonionic surfactant mixtures on complex soil system is still challenging in many respects. Moreover, the sorption barriers created by cationic-nonionic surfactant mixtures on soil are expected to enhance the retardation of organic contaminants in soil. However, no studies have been reported on the enhanced retention of PAHs by cationic gemini and nonionic surfactant mixtures. The available knowledge of utilizing gemini and its binary surfactant mixtures as the sorption barriers for groundwater remediation is still limited.

# **CHAPTER 3**

## **ENHANCED COAGULATION/FLOCCULATION BY COMBINING DIATOMITE WITH SYNTHETIC POLYMERS FOR PRODUCED WATER TREATMENT**

### **3.1. BACKGROUND**

Produced water comes as a bi-product during recovery of natural gas and crude oil from onshore and offshore production operations. Over the economic life of a producing field, the volume of produced water can be more than 10 times the volume of hydrocarbon produced. Produced water contains a large number of oil droplets, suspended solids, soluble organic compounds, microorganisms, and inorganic salts. These contribute to a high amount of COD and turbidity in the colloidal suspension (Ahmad et al., 2006; Zeng et al., 2007; Yuan et al., 2011). Efficiently treating produced water in order to recycle and/or reuse it can mitigate the cost of water disposal and potentially have a significant impact on sustainable eco-environmental development.

Conventional methods such as adsorption (Ahmad et al., 2004), coagulation (Zeng et al., 2007), membrane processes (Gryta et al., 2001), and biological methods (Nadarajah et al., 2002) have been performed to remove pollutants from oily waters (Xu and Zhu, 2004). Among these, chemical coagulation is still the most widely used treatment technique to destabilize dissolved and colloid impurities and to produce large floc aggregates, which can be removed in subsequent clarification/filtration processes (Gao et al., 2002). Recently, synthetic polymers such as PAC, PFS and PAM have been widely used as coagulants or flocculants in wastewater treatment because of the very low

quantities to produce large shear-stable flocs (Jiang et al., 2004a; Ahmad et al., 2006; Zeng et al., 2007; Seki et al., 2010; Wu et al., 2011a). Considering the overall negative charge of natural colloids, the destabilization by these cationic polymers occurs normally through compression of double layer, adsorption and charge neutralization, inter-particle bridging, and sweep coagulation (Menezes et al., 1996). However, PAC and PFS may generate a considerable amount of hazardous sludge which contains residual aluminum or iron, causing side effects when discharged into the open water course (Shi et al., 2004; Ahmad et al., 2006). PAM is reported to be corrosive and neurotoxic, and it has limited flocculation effects if used alone (Zeng et al., 2007; Seki et al., 2010; Yan et al., 2012). As the conventional coagulation cannot satisfy the requirement for produced water treatment, it is necessary to find other efficient methods.

Adsorption has been proven to be particularly competitive and effective in removing organic and inorganic constituents from the waste effluents (Khraisheh et al., 2004; Wu et al., 2005). Although activated carbon is regarded as one of the most extensively used adsorbents, it involves disadvantages such as costly regeneration and waste disposal (Khraisheh et al., 2004; Erdem et al., 2005; Wang et al., 2005; Wu et al., 2005). As a result, over recent years there has been growing interest in using low-cost natural minerals for wastewater treatment. Among these minerals is diatomite. Diatomite, or diatomaceous earth, consists of about 80% of  $\text{SiO}_2$ , with a relatively small percentage of other oxides such as  $\text{Al}_2\text{O}_3$ ,  $\text{Fe}_2\text{O}_3$ ,  $\text{MgO}$  and others. It is also highly porous, with its structure containing up to 80 ~ 90% voids (Khraisheh et al., 2004). Diatomite is non-toxic, biodegradable, and abundant around the world, thus is available at low cost. Among natural minerals, diatomite is of particular interest due to its unique properties

such as high porosity, high permeability, small particle size, high surface area, low thermal conductivity, and chemical inertness (Danil de Namor et al., 2012). Some literature has already reported that diatomite can be employed to remove heavy metals (Al-Degs et al., 2000; Khraisheh et al., 2004; Danil de Namor et al., 2012), phosphorus (Xiong and Peng, 2008), phenol (Gao et al., 2005), textile dyes (Al-Ghouti et al., 2003; Erdem et al., 2005), algae (Wu et al., 2011a), and microorganisms (Chu et al., 2008; Yang et al., 2010; Chu et al., 2012) from wastewater. It also has a number of industrial applications such as being used as the filtration medium to adsorb inorganic and organic chemicals (Al-Ghouti et al., 2003), as the additive to dynamic membrane reactors to mitigate fouling (Chu et al., 2008, Chu et al., 2012), and as an adsorbent for pet litter and oil spills (Khraisheh et al., 2004).

Other than normally being used as an adsorbent, diatomite has received little attention as a coagulant aid for the synthetic polymers in the water treatment process. As mentioned above, polymeric coagulants (PAC, PFS) can provide positive charges for oil particles and enhance charge neutralization, which results in enlarged flocs and higher removal of supernatant oily matters (Ahmad et al., 2006; Zeng et al., 2007). Due to the high molecular weight and excellent bridging ability, PAM is also an effective alternative for oil removal (Ozkan and Yekeler, 2004; Zeng et al., 2007). It can supply long chain molecules to flocs and colloids, thus enhance the bridging and growing of the flocs. Therefore, the combination of PAC/PFS/PAM with diatomite may produce some optimal properties, and the added diatomite as both an adsorbent and coagulant aid may enhance the coagulation process. Wu et al. (2011a) have investigated the enhanced coagulation process of combining diatomite with PAC to remove algae and natural organic matters.

Cui et al. (2009) have reported that the modification of diatomite by adding conventional coagulants makes electronegative sludge colloid particles lose stabilization and become large and compact flocs, and thus improves the sludge settling and dewatering performance. Similarly, natural clays have also been used as coagulant aids when treating the low particle content water (Nemerow, 1987). It is also reported that natural mineral clays combined with polymeric coagulants (Jiang et al., 2004a) could enhance the adsorption of metal and organic compounds from solutions.

To date, no data has been reported in the literature on the coagulation and flocculation characteristics of PAC, PFS and PAM with diatomite in the produced water treatment. Moreover, diatomite as both an adsorbent and a coagulant aid to treat oil suspension has not been extensively investigated. The objectives of this study are: 1) to evaluate the feasibility of the possible combination of synthetic polymers with diatomite to treat produced water; 2) to explore the mechanisms of synthetic polymers combined with diatomite to promote pollutant removal, using diatomite as an adsorbent and a coagulant aid; and 3) to refine the coagulation/flocculation process by studying the operating variables-chemical dose, initial pH, and settling time.

## **3.2. MATERIALS AND METHODS**

### **3.2.1. Materials**

The produced water was obtained from one oil field located in Saskatchewan, Canada. Samples may vary day to day depending on climate and oil processing conditions. Sediment pre-filters were used to prevent dirt and sediment particles from entering and clogging the laboratory instrument. After the primary separation process of oil from water, the samples were cooled to room temperature and collected for future coagulation experiments. Portions of this suspension were withdrawn and analyzed for their initial residue oil content, COD and other properties. The characteristics of produced water are listed in Table 3.1.

The chemicals used (Sigma-Aldrich, Canada) were of analytical-reagent grade. Solutions were prepared by dissolving chemicals in deionized water during continuous agitation for several hours, followed by a vacuum filtration to eliminate insoluble solids if needed. The initial pH of each run was adjusted to a fixed value if needed using concentrated HCl or NaOH stock solution to minimize the volume change. The pH was measured by the pH Meter (Sartorius PB-10, Sartorius, Germany).

### **3.2.2. Experimental Procedure**

The coagulation experiments were performed in beakers containing 200 mL wastewater, using a series of hot plate magnetic stirrers (C-MAG HS 4, IKA, Germany). The temperature was kept at 25 °C during the experimental process. This experimental setup was simple in operation and time-effective when performing a large number of tests. Each sample was dosed with a predetermined amount of diatomite or PAC/PFS/PAM.

The wastewater-coagulant mixture was then stirred to produce a uniform suspension before the effects of different coagulants on the flocs settling characteristics were observed. Each sample was rapidly mixed for 2 min at 200 rpm to guarantee thorough mixing between the water sample and the coagulant, followed by a slow agitation for 20 min at 50 rpm to allow flocs growth, and at last a quiet sedimentation of 60 min before testing. For combined coagulants, diatomite and PAC/PFS/PAM were added simultaneously when the rapid mixing started. At the end of the settling, the supernatant was taken at 2 ~ 3 cm below the water surface using a 10 mL wide bore pipette. Then the sample was filtered to determine the residual pollutant concentration.

For a single coagulant, chemicals with varied amounts were added into the suspension to find the optimal dosage and maximum pollutant removal efficiency. For combined coagulants, the optimum dosages and maximized removal efficiency were studied following the same procedure as stated earlier. For a specific combination, pH adjustment (5 ~ 10) was done to obtain the best pH condition and lowest pollutant content. The effect of sedimentation time was also analyzed from 0 to 60 min.

Table 3.1 Characteristics of the produced water \*

Parameters	Oil (mg/L)	COD (mg/L)	Turbidity (NTU)	Hardness (as CaCO <sub>3</sub> ) (mg/L)	pH	Electric Conductivity (us/cm)
Values	3000 ± 120	280 ± 12	81 ± 4	300 ± 15	7.6 ± 0.3	3000 ± 150

\* Error limits of parameters are ±5.0%.

### 3.2.3. Analytical Methods

The efficiency of a coagulant to remove oil and grease was evaluated comprehensively by measuring COD (Chemical Oxygen Demand), turbidity and observing flocs settling characteristics. Analysis of the clarified supernatant samples yielded the concentrations of two target constituents - COD and turbidity, based on which the removal efficiency was calculated. In this study, a sample of approximately 50 mL was filtered and then analyzed at the end of each run. COD was measured by the AQUAfast COD Colorimeter (Orion AQ2040, Thermo Scientific, US), and turbidity was determined by the Turbidity Meter (HI-98713-02 ISO, HANNA, US). Batch tests were performed in triplicate for each experimental condition to guarantee the reliability of results. All experiments were carried out at room temperature including blank samples. The removal efficiency was calculated using the following equation:

$$Y(\%) = \frac{y_0 - y}{y_0} \quad (3.1)$$

where  $Y$  is the removal efficiency of COD/turbidity;  $y_0$  and  $y$  are the initial and present concentration in solution, respectively. All data reported were the average of three independent samples and the typical error in the measurement was less than 5%.

### **3.3. RESULTS AND DISCUSSION**

#### **3.3.1. Preliminary Experiments**

There was no published data on the capability of natural diatomite towards oil and COD removal from produced water. Some literature concluded that diatomite itself had no practical use for pollutant removal and it was only used as a coagulant aid to achieve the best contaminant removal. However, we found that diatomite had a better coagulation and adsorption capacity than some polymeric coagulants. Major constituents of produced water were oil and grease, which were measured commonly in terms of COD and turbidity. Parameters used for evaluating the extent of wastewater treatment therefore included the reduction of COD, turbidity and the evaluation of settling characteristics of flocs. Experiments were first conducted using single diatomite, PAC, or PFS respectively to treat the oily waters. The variations in COD removal efficiency and residual turbidity as a function of diatomite, PAC and PFS dosing rate are shown in Figures 3.1 and 3.2.

Diatomite particles were good carriers of fine oil particles and were highly effective in removing COD and turbidity. Diatomite removed over 5.56% of COD from produced water at the initial dosing rate of 250 mg/L. The COD removal was remarkably improved from 11.14% at a dosage of 500 mg/L to 43.33% at a dosage of 1250 mg/L, but no significant increase continued beyond 1250 mg/L. This indicated that a maximum COD recovery by diatomite was achieved around the optimum dosage. The wastewater COD was mainly from two sources - oil and grease as well as dissolved organic compounds; the COD removal was relatively lower due to the fact that coagulation was only effective to remove the oil and grease rather than the dissolved organic compounds (Chen et al., 2000a). A similar pattern was observed for turbidity treated by diatomite, with the

residual turbidity as high as 42.89 NTU at the dosing rate of 250 mg/L and quickly reducing to 14.16 NTU at 1250 mg/L. After that, the removal of turbidity was insignificant. Moreover, the increasing dosage of diatomite had little influence on the solution pH, with a slight increase from the initial pH (7.6) of raw wastewater. Wu et al. (Wu et al., 2005) have reported that the pH increase associated with dosing rates might result from hydroxyl ions, which were produced from lime contributed by the chemical modification of diatomite. Some data stated that diatomite could increase pH and significantly improve pollutant removal as mentioned above (Wu et al., 2005), while others concluded that an increase in pH above 8 might decrease the adsorption of the dissolved carbon onto clay minerals (Jiang and Kim, 2008).

In contrast, only 18.80 and 30.83% of COD was removed by PAC and PFS at the optimum dose of 400 mg/L, and the turbidity reading was 16.16 and 33.58 NTU, respectively. For PFS, the COD removal was superior to PAC, but the residual turbidity was higher at the same dosing rate ranging from 250 to 550 mg/L. This was consistent with the previous work (Wu et al., 2006). However, when increasing the dosage over the optimum dose, there was a slight decrease in the removal rate for turbidity. This was attributed to the fact that the excess addition of polymeric coagulants would result in flocs breakup due to “colloidal restabilization”. As shown in Figures 3.1 and 3.2, turbidity levels tended to increase slightly after the optimum dose of PAC/PFS, indicating that a sufficient degree of over-saturation occurred, producing a rapid precipitation of large quantities of coagulants (Pinotti and Zaritzky, 2001; Ahmad et al., 2006; Zeng et al., 2007). Colloidal particles were packaged by excessive coagulants and soon there would be a repulsive force between them. Thus, the colloids were re-stabilized. Based on the

pollutants removal and the settling performance after optimum dose, it was concluded that PAC or PFS had the relatively lower stability and coagulation capacity compared to diatomite.

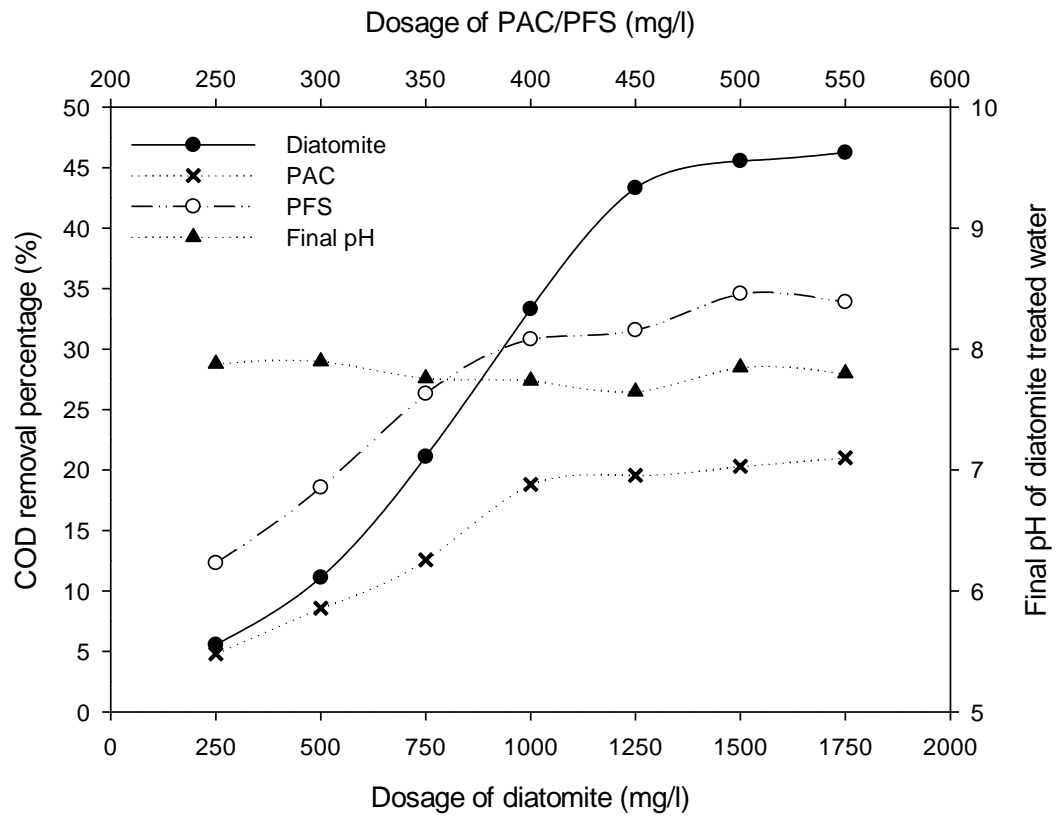


Figure 3.1 Percentage of COD removed at various (mg/L) f diatomite, PAC, and PFS

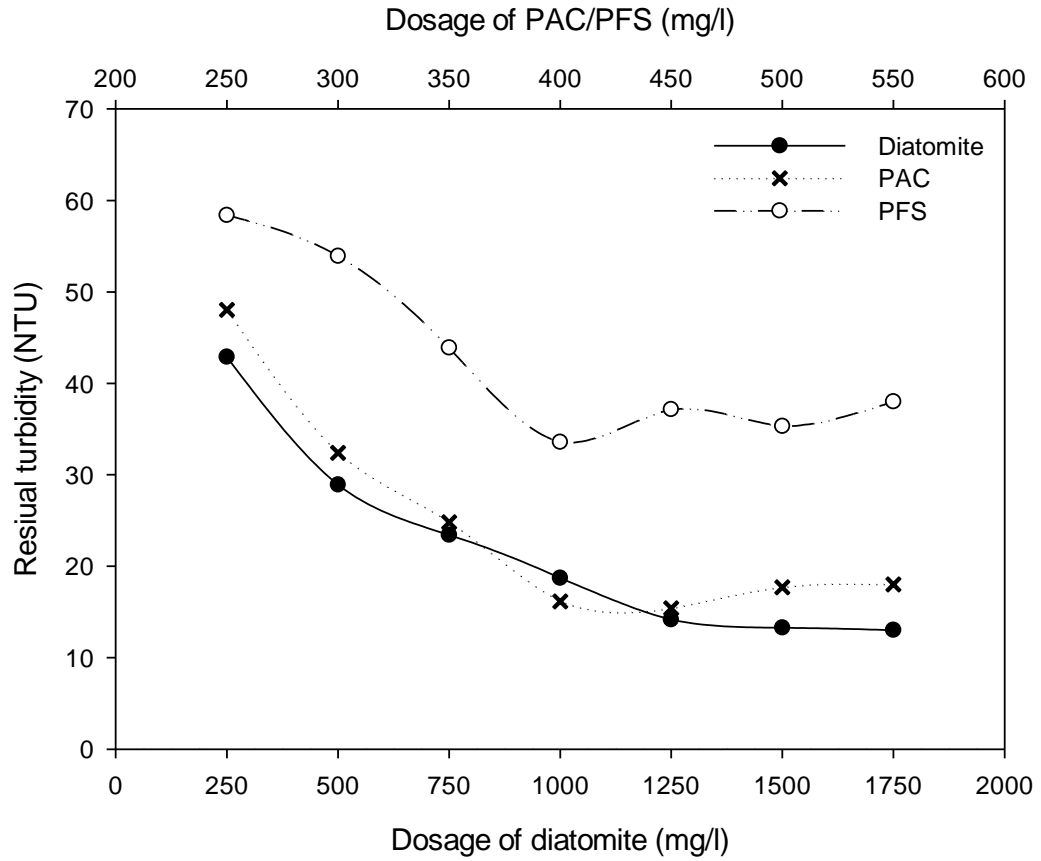


Figure 3.2 Residual turbidity at various dosages of diatomite, PAC, and PFS

In addition, it was observed that the diatomite flocs had a relatively higher settling velocity, and the clarity of supernatant treated with diatomite was much higher than that treated with polymeric coagulants. The flocs size increased while the level of soluble constituents in the aqueous phase decreased, due to the addition of the coagulants (Yang et al., 2010). The diatomite addition was favorable to improve the flocs settleability, reduce the suspended foulants, accelerate the settling rate, and enhance the coagulation process. Diatomite was extremely effective in promoting flocs growth in suspensions while those formed by polymeric coagulants were fairly small with slower settling velocity. Jiang and Kim (2008) studied that flocculation from clay-based coagulants could form larger networking structures, holding the pollutants tightly and catching them effectively. Moreover, the effluent coagulated by diatomite was visually very clear, while some white precipitation existed in PAC treated water, and the PFS samples seemed yellow and turbid. Although the dose of diatomite was comparatively high in comparison with that of PAC and PFS, the abundant availability and low cost, together with non-harmful chemical residuals in the treated water made diatomite an alternative technique to remove oil from produced water.

Diatomite possessed a capacity for adsorption through the formation of chemical bonds between organic molecules and itself; this could be one mechanism for pollutants removal by diatomite (Khraisheh et al., 2004; Wu et al., 2005). It was well known that diatomite was a compound of higher porosity and larger surface area, thus higher adsorption capacity compared to PAC/PFS (de Namor et al., 2012). With the increasing dose, the surface areas for adsorption increased, leading to an enhancement in contaminant removal. When the dosing rate of diatomite increased to 1250 mg/L, the

improvement was negligible due to the limited number of sites on the diatomite surface (Khraisheh et al., 2004). The oil particles might only form one monomolecular layer on the surface at maximum capacity, since adsorption from an aqueous solution usually form one layer rather than multilayers on the adsorbent surface. This agreed with what was reported by Khraisheh et al. (2004), that multilayer formation did not normally occur with metal adsorption. It was also stated that the crystal structure of diatomite contained some ion-exchangeable cations which could be exchanged with organic and inorganic cations (Erdem et al., 2005).

Other than being used as an adsorbent, diatomite was also an excellent coagulant with high coagulation capacity, producing a remarkable aggregation of particles due to its specific surface chemical properties (Wu et al., 2011a). Some dissolved silicic acid generated from silica oxides in the coagulant allowed for the adsorption of impurities onto the surface to form large, heavy flocs (Wang et al., 2005; Wu et al., 2005; Danil de Namor et al., 2012). Diatomite also contained a small percentage of iron oxides and aluminum oxides that were appropriate for producing complex coagulants (Khraisheh et al., 2004; Yang et al., 2010; Danil de Namor et al., 2012). There could be strong interactions between the coagulants and the pollutants, and the resulting complexes could improve the coagulation performance. This assumption was supported by previous research (Jiang et al., 2004a; Jiang et al., 2004b). As a kind of natural mineral clay, diatomite had cation exchange capacity and adsorptive affinity for some organic and inorganic compounds. This feature made it possible for diatomite being used as a coagulant (Jiang et al., 2004b) to treat organic pollutants, and the results achieved were promising. Moreover, diatomite could adsorb and destabilize pollutants, producing flocs

with better settling properties. The destabilization of colloids was mainly due to the individual or interactive effects of charge neutralization, co-precipitation, and bridging, etc. Diatomite particles tended to aggregate together, forming larger colloids and higher density flocs which settled more easily. The flocs recoagulated even after breakage. In this way, the smaller and fine oil particles aggregated and settled easily with the aid of diatomite. Fly ash-based coagulants had the similar coagulation mechanisms with diatomite. The coagulation of fly ash formed alum, and the structure and weight of flocs were greatly improved by the enhanced coagulation process (Yan et al., 2012).

Although there was certain removal of pollutants from produced water using single diatomite, PAC, or PFS, data indicated that the treatment efficiencies were not high (COD removal less than 45% and turbidity less than 85%). To make the treated effluent suitable for reinjection or reuse, some advanced treatment technologies should be investigated.

### **3.3.2. Combining PAC/PFS/PAM with Diatomite**

It was reported that polymeric coagulants combined with natural mineral clays could enhance the adsorption of metal and organic compounds from solutions (Jiang et al., 2004a). In this study, to achieve better pollutant removal efficiencies, polymeric coagulants - PAC, PFS, and PAM were combined with diatomite, respectively - to acquire a large adsorption and coagulation capacity.

#### *3.3.2.1. PAC with Diatomite*

The COD reduction against PAC dose with enhanced coagulation/flocculation combining PAC and diatomite are shown in Figure 3.3. The COD removal with

increasing dose (0 to 87.5 mg/L) of PAC was investigated, while the diatomite dose was kept stable at 1250 mg/L. The diatomite addition significantly improved COD reduction, and the enhancement was remarkably higher (over 50%) than using PAC alone (See Figures 3.1 and 3.3). Results also demonstrated that PAC-diatomite achieved over 73% COD reduction with PAC dose greater than 50 mg/L. However, it should be noted from Figure 3.1 that only 18.80% of COD was separated from the wastewater by 400 mg/L of PAC when no diatomite was added. As for the turbidity removal, when the dosing rate of PAC was 50 mg/L, the added diatomite was found to decrease the residual turbidity from 81 to 6.80 NTU. The visually clear supernatant indicated that greater turbidity reduction was achieved by the enhanced coagulation/flocculation combining PAC and diatomite (See Figures 3.2 and 3.4). High removal efficiencies were achieved by the PAC-diatomite system at the PAC dose of 50 mg/L, and the COD and turbidity removals were 73.62 and 91.60%, respectively. With the assistance of diatomite, the enhanced coagulation/flocculation process also saved more than 85% of the PAC dose. In addition, as the PAC dosing rate rose, the final pH was largely stable with a slight increase notwithstanding occasional turbulence.

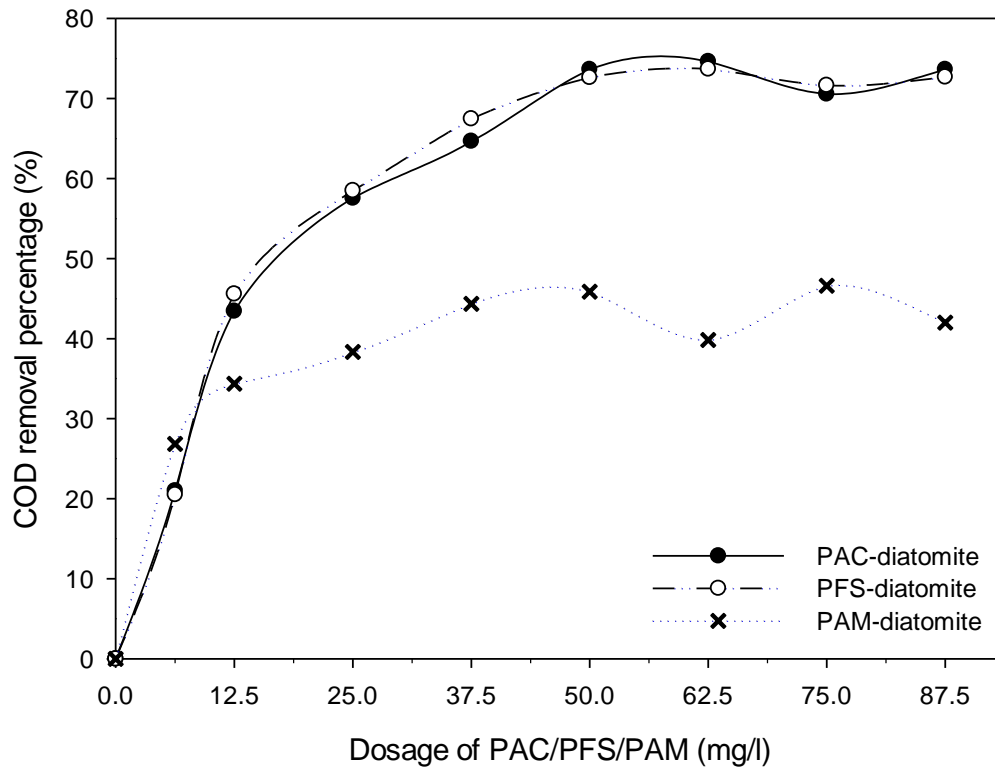


Figure 3.3 Percentage of COD removed at various dosages of PAC, PFS, and PAM when combined with diatomite

The combination of PAC with diatomite might form a new type of coagulant system and produce some optimal properties. Other than the charge neutralization caused by PAC coagulation, the adsorption capacity of the coagulant complexes was substantially enhanced with the increasing surface areas of diatomite. Diatomite caused the netting and bridging of flocs, and enlarged the frame and weight of the network produced by PAC. In this study, diatomite performed as a coagulant aid as well as an adsorbent to enhance the coagulation and adsorption of organic impurities. The added diatomite was embedded in flocs, extended the structure, raised the density, and accelerated the flocs settling (Wu et al., 2011a). Moreover, the residual turbidity in Figure 3.4 indicated that the flocs seldom broke or released into the supernatant even at an excessive dosage. This was totally different from the effluent water treated by PAC in preliminary studies, where the flocs were loose and the residual turbidity was high (See Figure 3.2). It was reported in the early 1970s that natural mineral clays had been used as coagulant aids to treat low particle content water, besides being used as adsorbents (Nemerow, 1987). The content of silica in diatomite offered its structure the credibility as a good adsorbent (Erdem et al., 2005). The silanol group, as a very active group, could react with many polar organic compounds and destabilize them (Khraisheh et al., 2005). In this study, the unique characteristics of high porosity, great specific surface area, and high chemical stability made diatomite applicable for adsorption of oil particles. Wu et al. (2011a) concluded that the enhanced coagulation through the combination of PAC with diatomite, was more effective than traditional coagulation for the economic treatment of slightly polluted algae-containing surface water.

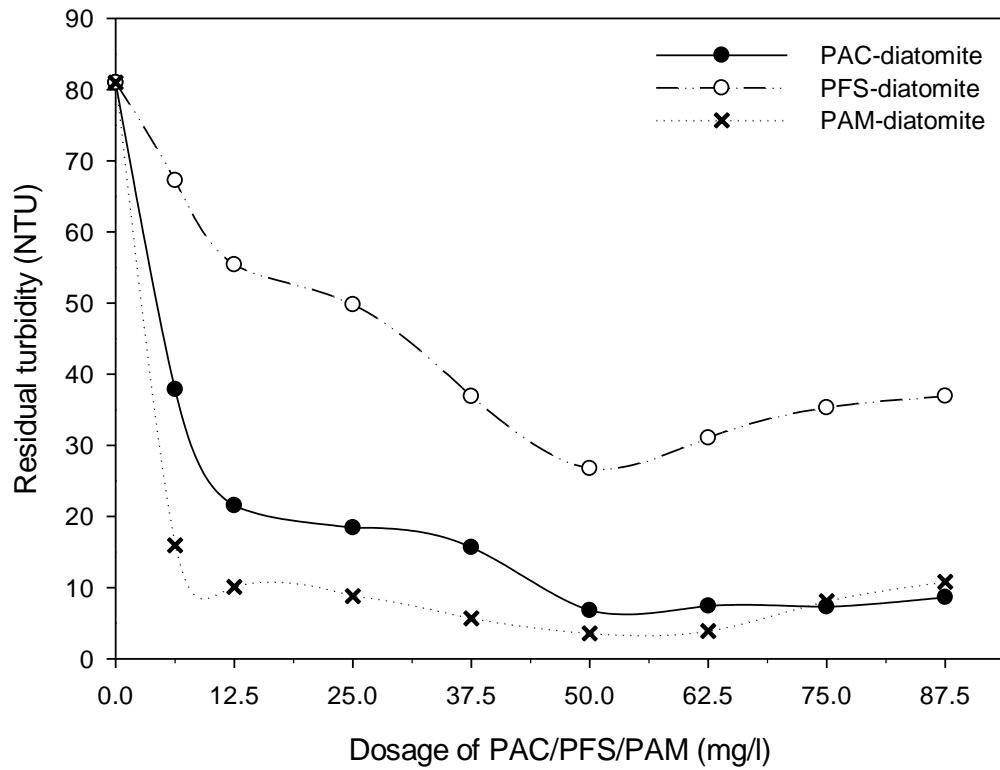


Figure 3.4 Residual turbidity at various dosages of PAC, PFS, and PAM when combined with diatomite

### 3.3.2.2. PFS with Diatomite

Figures 3.3 and 3.4 show the percentage of COD removal and residual turbidity against different PFS dosages from 0 to 87.5 mg/L. The diatomite dose was kept constant at 1250 mg/L. 30.83% COD reduction was achieved by PFS at a dose of 400 mg/L, while 72.63% of COD was removed with PFS-diatomite with merely 50 mg/L of PFS. The percentage was found to be substantially higher than using single PFS. Moreover, to achieve maximum removal, the PFS dosage needed was 87.5% less than using PFS independently. However, the PFS-diatomite system showed a higher turbidity reading. The residual turbidity was 26.73 NTU using the combined coagulant system. The final pH decreased from 7.87 to 7.46 due to the increasing dose of PFS.

PFS supplied positive charges for colloidal and soluble organics and provided flocs with negative charges. This would enhance charge neutralization and flocculation, causing high removal of supernatant organics and enlargement of floc size (Wu and Huang, 2008). Moreover, the extended adsorption areas of the PFS-diatomite mixture made contaminants bind and bridge more easily to form large flocs. In addition, the added diatomite not only agglomerated the residual pollutants but adsorbed them due to diatomite's diverse functional groups. First, the silica oxides contained in diatomite were easy to be adsorbed by oil particles. Second, the iron oxides and aluminum oxides were prone to hydrolysis and forming chain net structures with pollutants. The enlarged cobwebs took the colloids out of stability and bridged them to produce big flocs, which grew faster and sedimentated more easily (See the residual turbidity in Figures 3.2 and 3.4). This proved that the addition of diatomite was a more effective technique to remove pollutants compared to using PFS only. Zheng et al. (2011) developed a diatomite-

supported SPFS flocculant in the treatment of domestic sewage. The composition of  $\text{FeSO}_4 \cdot 7\text{H}_2\text{O}$  with diatomite showed good flocculation performance; the removal of COD was 80.00% and the removal of turbidity was 99.98%. However, in this study, the effluent water appeared slightly yellow and turbid after being treated by PFS combined with diatomite.

### 3.3.2.3. PAM with Diatomite

The effects of PAM dosage on COD removal and residual turbidity were analyzed by varying the PAM dose from 0 to 87.5 mg/L, as shown in Figures 3.3 and 3.4. The selected PAM was the cationic PAM and the added diatomite was still 1250 mg/L for each trial. The experimental results exhibited that C-PAM of high molecular weight performed well, due to the fact that its flocculating properties were primarily influenced by its molecular weight (Ozkan and Yekeler, 2004; Zeng et al., 2007). With the increasing PAM dosage, turbidity removal was facilitated. 95.58% of turbidity was reduced when the PAM dosage was 50 mg/L, as shown in Figure 3.4. After that, the reduction became insignificant. When PAM dose increased to 75 mg/L, the turbidity level rose to 8.1 NTU, indicating the dispersion of flocs. COD removal showed a similar trend as that of turbidity value. The removal percentage with increasing PAM dosage reached a plateau, as shown in Figure 3.3. At a dosage of 50 mg/L, the COD removal increased to 45.86%, and only a slight improvement occurred thereafter. The final pH of the treated water increased slightly higher from 7.98 to 8.15, indicating the pH environment was relatively stable for this system despite the PAM dose.

The PAM-diatomite combination had the best effects on reducing turbidity due to the strong flocculating capability of PAM and the excellent adsorption capacity of

diatomite. On one hand, the very high molecular weight made C-PAM bridge more readily with the negatively-charged impurities and form large net-structure flocs. This was consistent with previous studies that polymers of high molecular weight were extremely effective in promoting flocs growth (Zeng et al., 2007). On the other hand, the added diatomite incited more pollutants to be adsorbed on the flocs surface and destabilized them. Turbidity had its best removal when the PAM dose was 50 mg/L. After that, there was slightest breakage of flocs with the increasing chemical dose. Further increasing the PAM dose might lead to the breakup of flocs and raise the turbidity of sample water. This might be attributed to the fact that an excessive or overdosing of flocculants usually resulted in charge reversal and restabilization of the flocs (Solberg and Wågberg, 2003).

In addition, the COD removal by PAM-diatomite was remarkably lower than that achieved by PAC or PFS combined with diatomite. Moreover, the unit price of PAM was the highest in these three synthetic polymers. Continuously raising the dosage might result in a correspondingly high sludge quantity and capital cost owing to the high PAM consumption. Thus, combining PAM with diatomite may be not practical for the wastewater treatment in oil fields.

Combining polymeric coagulants with diatomite greatly mitigated COD and turbidity in wastewater, and generated flocs with better settling characteristics. Comparisons demonstrated that enhanced coagulation/flocculation by combining PAC with diatomite rendered the best performance for produced water treatment.

### **3.3.3. Operating Refinements by combining PAC with diatomite**

#### *3.3.3.1. Initial pH*

Initial pH was established as an important operating factor influencing the coagulation process (Ahmad et al., 2006; Zeng et al., 2007). The effect of pH was conducted during a range from 5 to 10 using the optimum dosage of chemicals (PAC, 50 mg/L; diatomite, 1250 mg/L). The settling time was 20 min. It was clearly seen from Figure 3.5 that the pollutants removal was maximized when pH was over 7. This indicated that the neutral and alkaline conditions were more favorable to reduce COD and turbidity. COD removal efficiency was over 65% at the broad pH range of 7 ~ 10 while achieving the highest at pH 7 ~ 8. While for PAC, pH needed to be kept around 7 ~ 8 to reach the maximum removal of 20%, which was inferior to the PAC-diatomite system. In addition, the turbidity resulting from PAC-diatomite treatment was less than 6 NTU at the pH range of 7 ~ 10. However, when single PAC was used, it had the lowest level of 14.69 NTU at pH 7 (Figure 3.6).

The added diatomite helped PAC to enhance the adsorption and destabilization of the pollutants in the neutral and alkaline mediums. Voluminous flocs were formed due to the enmeshment of particles by flocs and/or the floc-floc attachment. Around neutral and alkaline pH, the added diatomite made flocs form large and compact particles, possessing the best settling properties and improving settling performance greatly. However, it was reported that at alkaline pH, the flocs produced by PAC settled slowly and dispersed from the dissolution of  $\text{Al}(\text{OH})_4^-$  (Pinotti and Zaritzky, 2001). The breakage of the flocs caused the sample to be turbid again. The above comparison denoted that the enhanced coagulation/flocculation and higher pollutants removal were achieved over a wider pH

range by combining PAC with diatomite.

As shown in Figure 3.5, the initial pH increased when there was an acidic environment for PAC combined with diatomite. However, when the initial pH was higher than 8, the final pH decreased. These results exhibited some pH buffering capacity of the PAC-diatomite system. This newly found advantage was quite meaningful in its application to wastewater treatment. As mentioned earlier, the pH range of raw water was around 7 ~ 8. For this range of influent, the effluent was approximately at neutral pH, as shown in Figure 3.5. Therefore, the effluent could be discharged or reused directly without further pH adjustment. In this study, because of the wide pH adaptability of the PAC-diatomite system, the pH adjustment of raw water was discarded for all experimental trials.

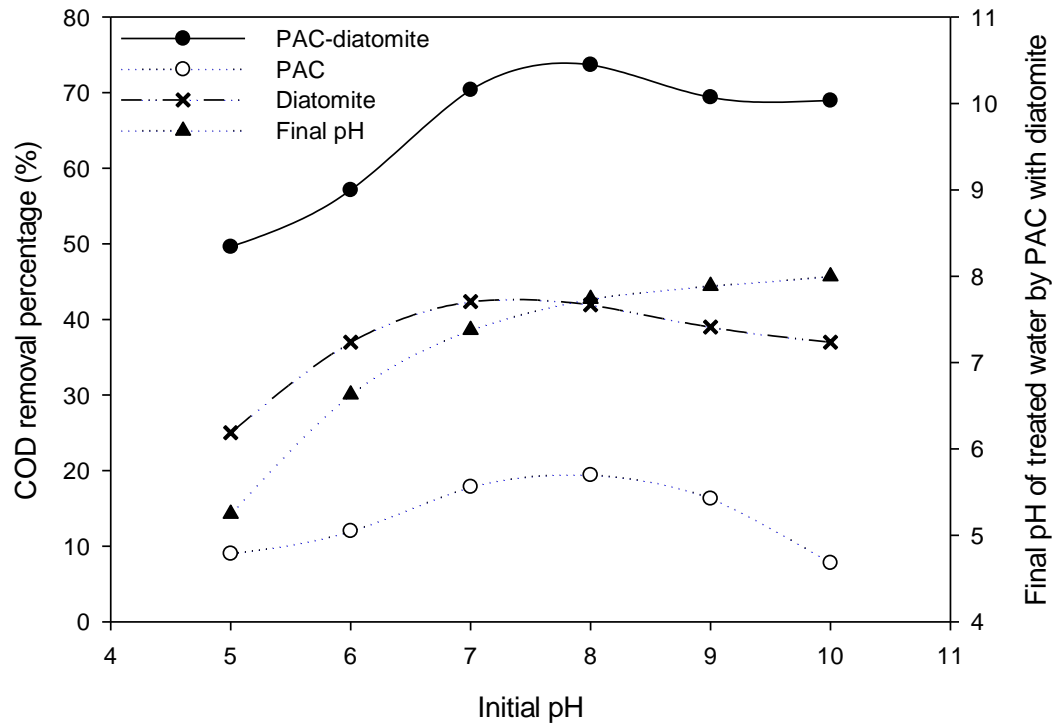


Figure 3.5 Percentage of COD removed at different initial pH by combining PAC with diatomite and by single PAC or diatomite

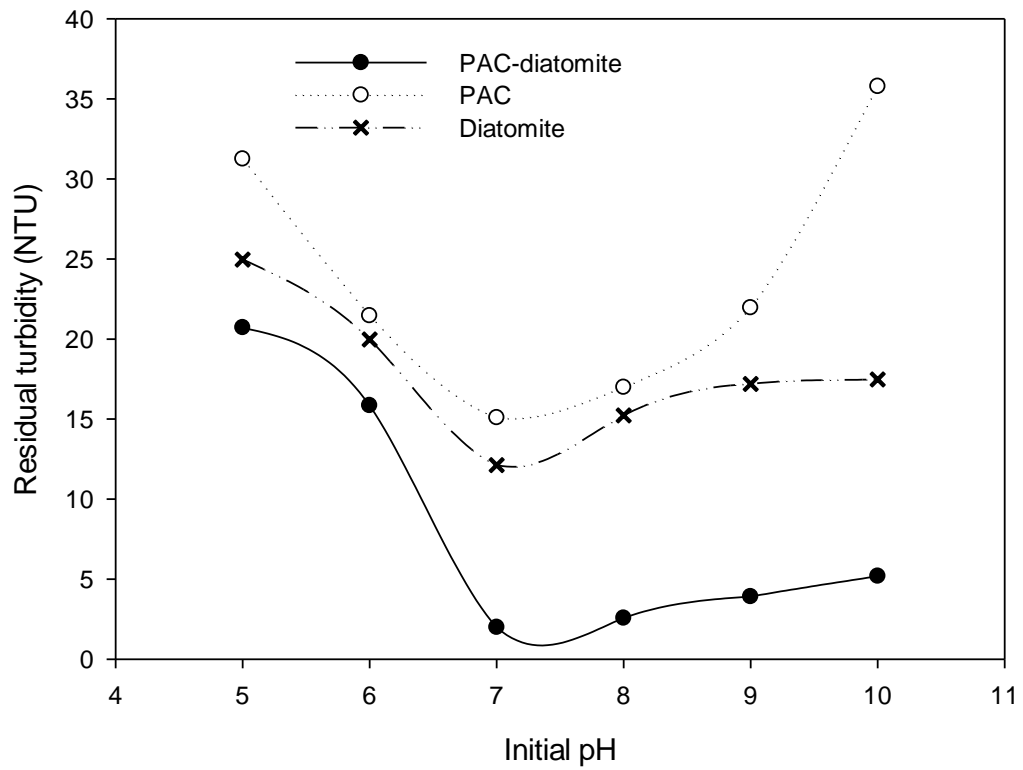


Figure 3.6 Residual turbidity at different initial pH by combining PAC with diatomite and by single PAC or diatomite

### 3.3.3.2. *Settling Time*

The effect of settling time on coagulant performance was analyzed by varying the time from 0 to 60 min at the optimum dose, as shown in Figure 3.7 and 3.8. 20 min was needed to remove 73.98% of COD by PAC combined with diatomite; while for PAC, only 21.47% of COD was reduced even at the sedimentation time of 40 min. The flocs settling rate could be defined as the turbidity that was removed against time. As for the PAC-diatomite system, the settling rate was faster during the first 10 min due to the adsorption capability of diatomite, and the residual turbidity remained below 6 NTU around 60 min. While for PAC the turbidity declined slowly and became stable at 40 min (14.87 NTU). The flocs broke again after 50 min, indicating the restabilization of flocs.

Diatomite as the coagulant aid of PAC promoted the aggregation of the colloids, bridged between the flocs and oil droplets, and incited the particles to form larger coarse flocs, which settled easily. The sample water was clarified immediately once the suspension completely settled within 20 min. However, the flocs produced from using single PAC were loose and showed a tendency to float. The flocs settled slowly during the first 40 min and easily dispersed if the settling time was prolonged.

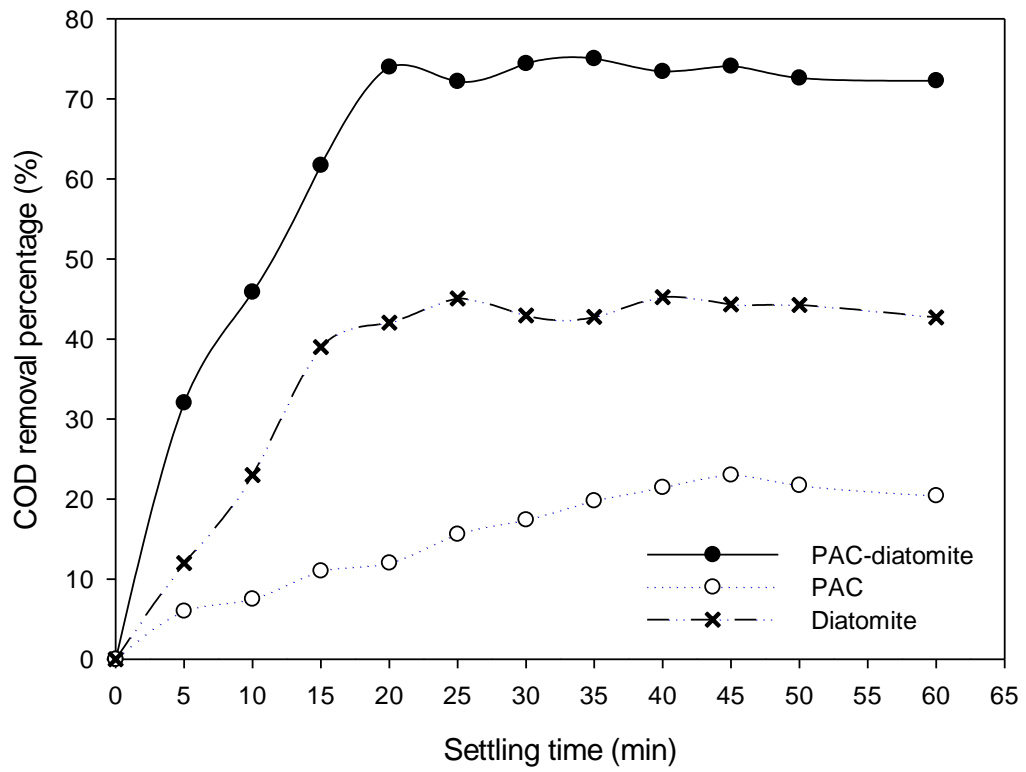


Figure 3.7 Percentage of COD removed against settling time by combining PAC with diatomite and by single PAC or diatomite

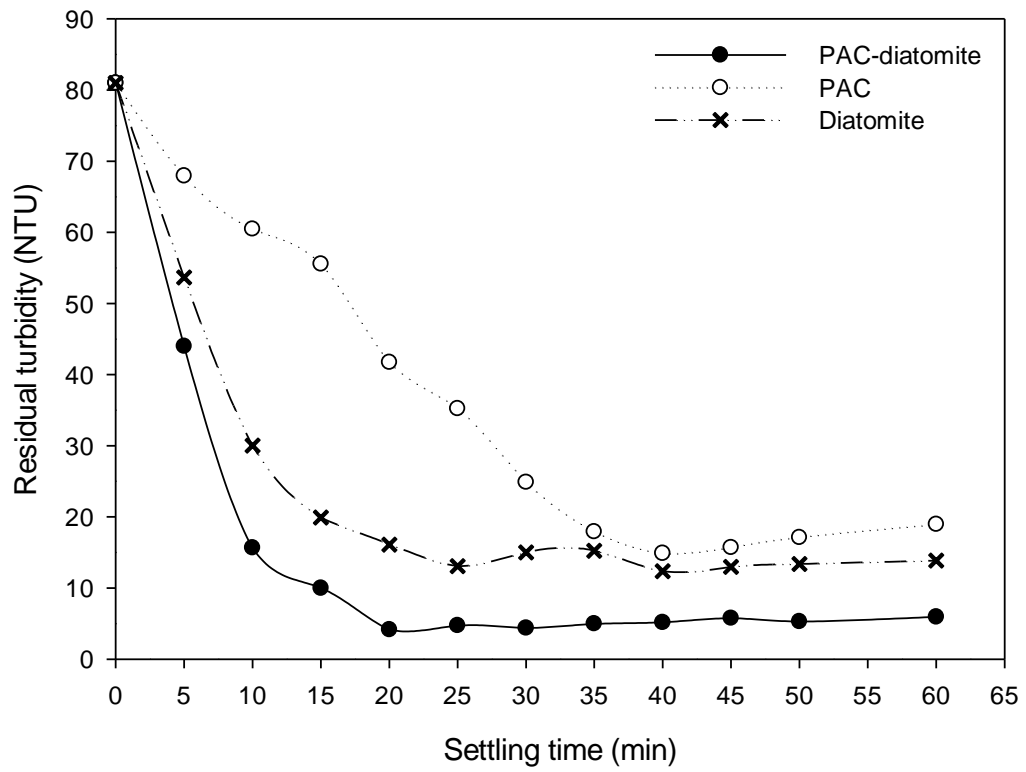


Figure 3.8 Residual turbidity against settling time by combining PAC with diatomite and by single PAC or diatomite

### **3.4. SUMMARY**

In the preliminary experiments, diatomite was favorable to improve the flocs settleability, reduce the suspended foulants, accelerate the settling rate, and enhance the coagulation process.

High removal efficiencies were achieved by the PAC-diatomite system at the PAC dose of 50 mg/L, and the COD and turbidity removals were 73.62 and 91.60%, respectively. The added diatomite saved more than 85% of the PAC dose than using PAC alone. The enhanced coagulation/flocculation by combining PAC and diatomite rendered the best performance for produced water treatment.

The optimum operating conditions of the PAC-diatomite system were: PAC, 50 mg/L; diatomite, 1250 mg/L; initial pH, 7 ~ 10; settling time, 20 min. Over 70% of COD and 90% of turbidity reduction were achieved, and the system exhibited some pH buffering capacity.

Conclusively, the enhanced coagulation/flocculation process by combining PAC with diatomite could be proposed as one alternative to economically treat produced water in oil fields.

**CHAPTER 4**

**HARDNESS, COD AND TURBIDITY REMOVALS FROM  
PRODUCED WATER BY ELECTROCOAGULATION  
PRETREATMENT PRIOR TO REVERSE OSMOSIS  
MEMBRANES**

**4.1. BACKGROUND**

Produced water comes as a byproduct during recovery of natural gas and crude oil from onshore and offshore production operations. Over the economic life of a producing field, the volume of produced water can be more than 10 times the volume of hydrocarbon produced. This volume is expected to increase from maturing conventional oil and gas fields. Produced water is a mixture of organic and inorganic materials (oil and grease, metal ions, sometimes large amounts of hardness, etc.) and it can place serious side effects on environment if the pollutants fail to meet discharge limits. The oil and grease contained in the wastewater aggregates, which foul the sewer system and generate an unpleasant odor (Chen et al., 2000a). Calcium and magnesium chlorides ( $\text{CaCl}_2$  and  $\text{MgCl}_2$ ) are frequently found in the wastewater. Presence of such compounds can cause scaling problems in the API oil separators which are commonly used in many facilities. Efficiently treating produced water for beneficial recycling and/or reuse can reduce the cost of water disposal and mitigate potentially adverse environmental impacts.

Conventional methods such as adsorption, coagulation, membrane processes, dissolved air flotation, and biological processes have been performed to treat produced water from oil fields (Chen et al., 2000a). Among these, Reverse Osmosis (RO) is usually

combined with other pretreatment techniques for the advanced treatment and beneficial reuse of produced water, because it promises high rejection rate of salts and colloids (Murray-Gulde et al., 2003a; Xu et al., 2008; Al-Zoubi et al., 2009; Fakhru'l-Razi et al., 2009). Produced water needs to be pretreated because the pollutants adversely impact RO membranes due to two mechanisms: fouling and scaling. Membrane fouling is primarily caused by the adsorption of oil and other fine organics or the pore-blocking by colloids in the membrane surface (Kumar et al., 2006). The presence of  $\text{Ca}^{2+}$  in the feed solution might cause the deposition of  $\text{CaCO}_3$  and  $\text{CaSO}_4 \cdot 2\text{H}_2\text{O}$ , which are the most common constituents of scale in membrane applications. Scaling tends to impede permeate flow, increase pressure drop, and lead to irreversible pore plugging and physical damage of the membrane (Tzotzi et al., 2007). It is also reported that calcium ions decrease the membrane surface charge and subsequently result in a reduced rejection of solute (Bellona and Drewes, 2005). Therefore, mitigation of scaling is an essential consideration in the operation of most RO processes. To solve these problems, the addition of coagulants prior to membrane filtration has been suggested to improve product water quality and reduce membrane fouling (Zhu et al., 2005). Nevertheless, chemical coagulation involves lots of disadvantages such as space requirement, high chemical consumption, considerable sludge generation, and inadequate removal of light and finely dispersed oil particles (Chen et al., 2000a). In addition, chemical coagulation pretreatment is less effective to deal with the scaling issues during filtration processes (Timmes et al., 2010).

Electrocoagulation (EC) is a feasible alternative prior to RO membranes, for the pretreatment of different types of water, including the brackish water (Den and Wang,

2008), plant feed water (Sadeddin et al., 2011), firefighting water (Baudequin et al., 2011), seawater (Yi et al., 2009), textile wastewater (Bhaskar Raju et al., 2009), and the groundwater (Subramani et al., 2012). In recent years, researchers have started to focus on electrocoagulation owing to its short reaction time, compact size, simple operation, and low capital and operating costs (Chen et al., 2000a). In particular, addition of excessive chemicals and production of unnecessary sludge can be avoided, due to the *in situ* generation of coagulants by electro-oxidation of the sacrificial anode. Dempsey et al. (1984) has reported that the adsorption of humic substances on ‘*in situ*’ formed hydroxides is 100 times greater than that on the pre-precipitated hydroxides (Mollah et al., 2004). Plus EC removes many species that chemical coagulation cannot remove (Khandegar and Saroha, 2013). Particularly, EC has been acknowledged as a promising technology in treating oily wastewater containing light suspended oil particles (Chen et al., 2000a). There are also data available using EC to remove hardness and prevent scale deposition (Malakootian et al., 2010). These probably make EC a more effective RO pretreatment technique than chemical coagulation processes when treating certain types of water. To the best of our knowledge, limited data was reported on the treatment of produced water through EC-RO system.

Despite an impressive amount of scientific investigation on contaminant removal through EC, little has been done on the hardness recovery, and none has been conducted to decrease hardness together with COD/turbidity through EC as a RO pretreatment process to reduce fouling and scaling effects. Also, there has been no record related to statistical refinement of hardness removal conditions through EC.

In this study, the objective is to develop an integrated EC-RO process for

simultaneous removal of hardness, COD, and turbidity, where combined effectiveness of EC for the pretreatment of produced water prior to RO membranes will be highlighted. First, three important operating variables (initial pH, current density, and electrolysis time) will be investigated to assess the recovery of contaminants. Second, the method of Central Composite Design (CCD) will be employed to obtain desired parameters for higher removal efficiency with a limited number of experiments. Third, practical applicability of the EC-RO process will be demonstrated through analysis of permeate flux and effluent quality in treating produced water from one oil field, Canada.

## **4.2. MATERIAL AND METHODS**

### **4.2.1. Materials**

The produced water was obtained from one oil field located in Saskatchewan, Canada. After the primary separation process of oil and water, the produced water was collected for future electrocoagulation experiments. The characteristics of produced water are listed in Table 4.1. The chemicals used (Sigma-Aldrich, US) were of analytical-reagent grade.

### **4.2.2. Experimental Devices**

The pilot-scale EC system (GS-QF-038, DAMING, China) was purchased for research. The volume of the reactor was approximately 80 L (diameter, 0.18 m; height, 0.805 m) and it mainly consisted of four parts: the feed tank; the zone for coagulation, flocculation and sedimentation; the zone for electro-flotation; and the electric control module, as shown in Figure 4.1.

The EC process mainly consisted of four steps (Koby et al., 2003): 1) electrolytic reactions at electrode surfaces; 2) formation of coagulants in the aqueous phase; 3) adsorption of soluble or colloidal pollutants on coagulants; and 4) sedimentation or flotation of aggregates. In the EC process, the water-contaminant mixture separated into the treated water, the floating layer, and the mineral-rich sediment. The electrocoagulation processes for treatment of produced water included the following steps:

(1) Water was pumped upward from the feed tank and was first treated in zone 5 by the coagulants which were generated from the iron electrode. The produced heavy flocs precipitated due to gravitational force at the bottom of the reaction tank, while the light

flocs were lifted by the hydrogen (the cathode product) upward to the electro-flotation zone 6.

(2) Due to the electro-flotation effects, the small fine oil particles floated with the electrolytically generated bubbles upward to the top of the liquid where they were concentrated, collected and removed by skimming. The treated water flowed through outlet 9 and then was recycled to the feed tank for retreatment (through the recirculation pipe 10).

(3) The sedimentation flocs were removed through a drainage valve 11 at the bottom of the EC reaction tank. Some sediment was also gathered at outlet 12 at the bottom of the electro-flotation zone. At the end of the experiment, the clean, treated water was collected at outlet 9 for testing.

In particular, the electrode was made of iron anode and graphite cathode. There were six monopolar electrodes. The three iron anodes were made from plates with dimensions of 15 cm × 12 cm × 0.3 cm, and the graphite cathodes were 15 cm × 12 cm × 1 cm. The electrodes pads were firmly assembled parallel to each other and the spacing between electrodes was 1.5 cm. All the electrodes were physically connected to either the positive or the negative outlet of the electric control module (20 V, 10 A). The current density was maintained constant by the electric control module. Before each run, the residual solids on the electrodes were removed, rinsed and dried. The pH of each run was adjusted to a fixed value using NaOH or H<sub>2</sub>SO<sub>4</sub> measured by a pH Meter (Sartorius PB-10, Sartorius, Germany). All experiments were performed at the room temperature of 25 °C.

Table 4.1 Characteristics of the produced water from one oil site, Saskatchewan, Canada\*

Parameters	Oil (mg/L)	COD (mg/L)	Turbidity (NTU)	Hardness (as CaCO <sub>3</sub> ) (mg/L)	pH	Electric Conductivity (us/cm)
Values	3000	280	135	300	7~8	3000

\*Error limits of parameters are less than  $\pm 10\%$ .

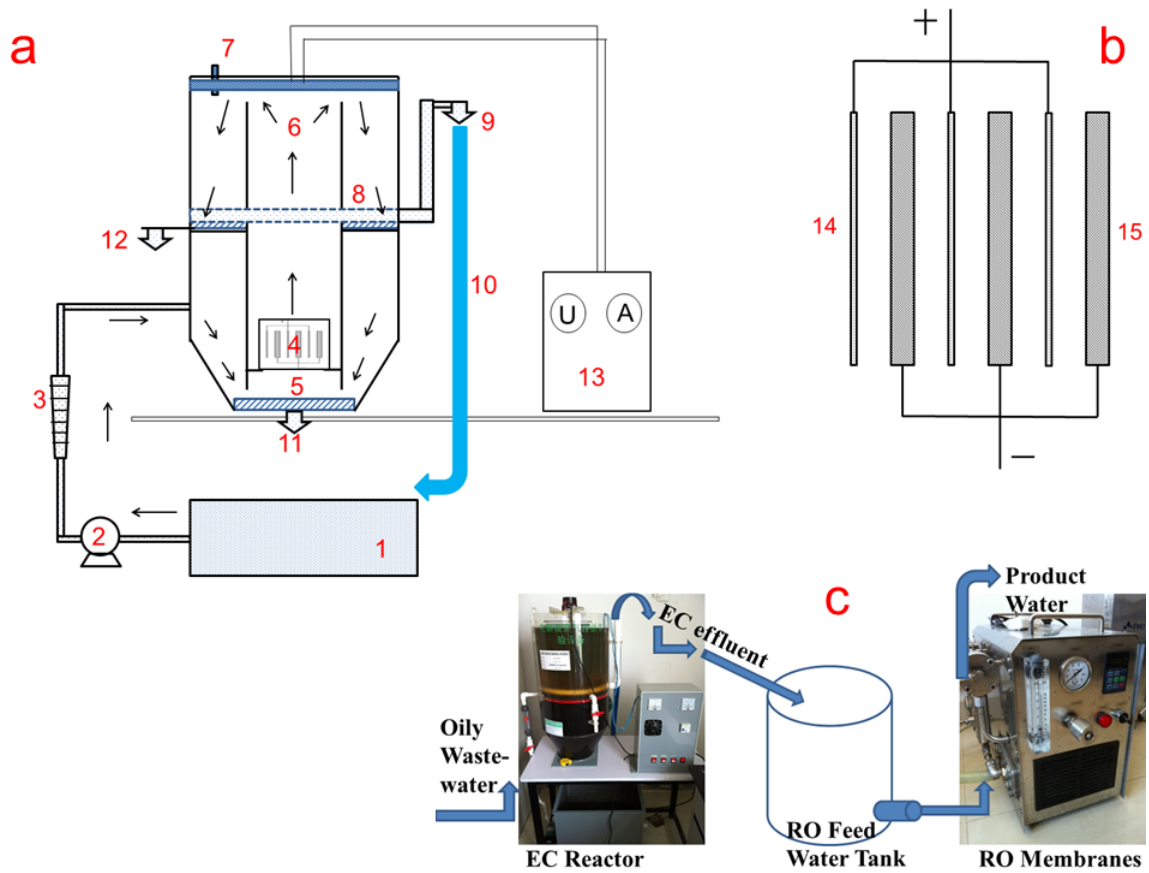


Figure 4.1 Schematic diagram of a) the EC reactor, b) the electrode, and c) the pilot-scale

#### EC-RO process

1. the raw water tank; 2. the recirculation pump; 3. the flow meter; 4. the electrode; 5. the zone for coagulation, flocculation, and sedimentation; 6. the zone for flotation; 7. the skimmer; 8. the perforated outlet pipe; 9. the outlet for treated water; 10. the recirculation pipe; 11. the drainage valve; 12. the drainage valve; 13. the electric control module; 14. the iron anode; 15. the graphite cathode.

The efficiency of EC to remove oil and grease was evaluated by measuring COD and turbidity (Tir and Moulai-Mostefa, 2008; Chavalparit and Ongwandee, 2009). Hardness (as CaCO<sub>3</sub>) removal was for the prevention of scaling issues during membrane processes. At the end of each run, a sample of approximately 250 mL was filtered and analyzed. In this study, COD was measured by the AQUAfast COD Colorimeter (Orion AQ2040, Thermo Scientific, US), turbidity was determined by the Turbidity Meter (HI-98713-02 ISO, HANNA, US), and hardness was tested according to the standard EDTA titration method. The removal efficiency was calculated using the following equation:

$$Y(\%) = \frac{y_0 - y}{y_0} \quad (4.1)$$

where  $Y$  is the removal efficiency of COD/turbidity/hardness;  $y_0$  and  $y$  are the initial and present concentrations of pollutants in solution, respectively. All data reported were the average of three independent samples and the typical error in the measurement was less than  $\pm 10\%$ .

After EC, the pretreated effluent first flowed through a bag filter and then settled for 30 min in the feed water tank, where it was gently and continuously mixed during RO (RNF-0640, Starmem, China). Only the raw water and the EC effluent of refined conditions were selected for the filtration study. The membrane was an aromatic polyamide spring-wound RO membrane (SMR-142, CSM, South Korea) with the minimum salt rejection as 97.5% NaCl. The system was operated in the cross-flow filtration mode at a constant transmembrane pressure of 20 bar and a steady volumetric flow of 0.8 L/min. Filtration experiments were performed without recirculating the

permeate in the feed tank. The permeate flux was measured by transferring the product water to an electronic balance (Sartorius BS 124S, Sartorius, Germany), which recorded the accumulative mass of the permeate as a function of time. Before starting each trail, RO was filtered with ultrapure water in order to remove residues. After experiments, chemical cleaning (1% of self-made detergent consisted of sodium hydroxide (NaOH), sodium tripolyphosphate ( $\text{Na}_5\text{P}_3\text{O}_{10}$ ), and sodium dodecyl sulfate ( $\text{CH}_3(\text{CH}_2)_{11}\text{OSO}_3\text{Na}$ , SDS), etc. in an appropriate proportion) was applied in order to restore most of the membrane's permeability and filtration flux.

#### **4.2.3. Experimental Design**

Conventional refinement of multifactor experiments involves shortcomings such as the requirement for a number of experimental trails and ignorance of combined effects among impact factors. To determine the significance of individual factors and their interactive influences with reduced number of runs, the response surface method (RSM) was utilized previously in many different processes (Tir and Moulai-Mostefa, 2008; Chavalparit and Ongwandee, 2009).

RSM as a statistical technique was utilized in this study to design experiments, build models, evaluate the effects of operating factors, and refine the EC process. The process variables investigated were initial pH ( $X_1$ ), current density ( $X_2$ ) and the electrocoagulation time ( $X_3$ ). Three responses were COD ( $Y_1$ ), turbidity ( $Y_2$ ) and hardness ( $Y_3$ ) removals as mentioned above. In the preliminary experiments, three parameters were studied independently. The data ranges of pH 3 ~ 11, current density 1 ~ 10  $\text{mA}/\text{cm}^2$  and reaction time 10 ~ 50 min were selected to understand how each factor affected the EC

process. Afterwards, CCD was conducted to obtain the refined variables and to achieve the highest removals of COD, turbidity and hardness. The levels of each variable determined by the preliminary experiments are listed in Table 4.2. The values were coded through equation:

$$X_i = \frac{x_i - x_{cp}}{\Delta x_i} \quad (4.2)$$

where  $X_i$  is the coded value of each factor;  $x_{cp}$  is value of the  $x_i$  at the center point obtained from the preliminary experiments; and  $\Delta x_i$  presents the step change.

Table 4.3 shows CCD in the form of a  $2^3$  full factorial design with four additional experimental trials (run numbers 15 to 18) as duplicates of the central point. Eighteen runs were performed sequentially. Each run was performed in triplicate to guarantee the reliability of results (Error limits less than 10%). In addition, a full quadratic model with regression coefficients was selected to fit the experimental data. Other than intercept, linear, and quadratic terms, this model also considers two-way interactions:

$$Y = \beta_0 + \sum_{i=1}^k \beta_i X_i + \sum_{i=1}^k \beta_{ii} X_i^2 + \sum_{i=1}^k \sum_{j=i+1}^k \beta_{ij} X_i X_j + \varepsilon \quad (4.3)$$

where  $Y$  is the removal efficiency of COD/turbidity/hardness;  $\beta_0$ ,  $\beta_i$ ,  $\beta_{ii}$  and  $\beta_{ij}$  are the regression coefficients for intercept, linear, quadratic and interaction terms, respectively, and  $X_i$  and  $X_j$  are the values of independent variables.

As the last step, ANOVA was used through a statistical analysis software (Design Expert 8.0.5b) for graphical analyses of the data to obtain the interaction between the process variables and the responses. The statistical significance was checked by the

Fisher  $F$ -test, and model terms were evaluated by the  $p$ -value (probability) with 95% confidence level. The quality of the fit polynomial model was expressed by the coefficient of determination  $R^2$  and adjusted  $R^2$  in the same program.

Table 4.2 Original and coded variables in the CCD design

Variables	Original Variables	Coded Factors ( $X_i$ )				
		-1.682	-1	0	1	1.682
Initial pH	$x_1$	3.64	5.0	7.0	9.0	10.36
Current Density (mA/cm <sup>2</sup> )	$x_2$	1.82	3.33	5.56	7.78	9.29
Electrolysis Time (min)	$x_3$	13.2	20	30	40	46.8

Table 4.3 A 2<sup>3</sup> full factorial CCD design with its experimental and predicted values

Run	pH (X <sub>1</sub> )	Current Density (X <sub>2</sub> )	Time (X <sub>3</sub> )	% COD removal (Y <sub>1</sub> )		% Turbidity removal (Y <sub>2</sub> )		% Hardness removal (Y <sub>3</sub> )	
				Exp.	Pred.	Exp.	Pred.	Exp.	Pred.
1	-1	-1	-1	48.96	48.82	41.31	42.12	62.54	61.28
2	1	-1	-1	54.79	55.32	55.50	57.86	66.60	66.80
3	-1	1	-1	55.76	56.14	78.27	77.16	75.06	74.08
4	1	1	-1	62.04	62.84	88.82	88.18	83.49	83.88
5	-1	-1	1	50.84	51.32	45.95	48.58	66.64	66.98
6	1	-1	1	56.60	57.50	60.68	64.28	70.80	72.50
7	-1	1	1	58.80	59.56	80.82	80.46	75.99	76.50
8	1	1	1	64.52	65.94	89.73	91.44	84.32	86.30
9	-1.682	0	0	52.76	52.49	57.35	57.26	68.01	69.18
10	1.682	0	0	64.86	63.32	82.81	79.73	84.24	82.06
11	0	-1.682	0	49.75	49.33	39.10	34.58	59.38	59.12
12	0	1.682	0	63.98	62.58	85.54	86.89	82.26	81.49
13	0	0	-1.682	57.04	56.74	76.45	76.68	71.76	73.09
14	0	0	1.682	62.96	61.45	88.27	84.86	82.24	79.91
15	0	0	0	66.58	65.49	90.74	90.53	82.98	84.11
16	0	0	0	64.08	65.49	92.09	90.53	83.16	84.11
17	0	0	0	65.93	65.49	88.99	90.53	85.28	84.11
18	0	0	0	65.07	65.49	89.75	90.53	84.84	84.11

## 4.3. RESULTS AND DISCUSSION

### 4.3.1. Preliminary Experiments

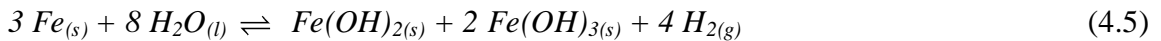
#### 4.3.1.1. Initial pH

Previous studies established that initial pH was an essential factor for the EC process and played an important role in the removal of the contaminants from oily wastewater (Chen et al., 2000a). A pH series from 3 to 11 was studied to determine the effects of initial pH on the removal efficiencies of COD, turbidity and hardness. The reactions for these three conditions were as follows (Gheraout et al., 2008):

Reaction 1 (acid pH):



Reaction 2 (neutral pH):



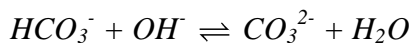
Reaction 3 (alkaline pH):



Different pH conditions accounted for different kinds of flocs. Reaction (4.4) took into consideration the green  $Fe(OH)_{2(s)}$  flocs at acid pH, while Reaction (4.5) reflected green  $Fe(OH)_{2(s)}$  and yellow  $Fe(OH)_{3(s)}$  colloids at neutral pH, and Reaction (4.6) introduced red-brown  $Fe(OH)_{3(s)}$  flocs at alkaline pH. EC efficiency was more effective at alkaline conditions due to the fact that  $Fe(OH)_{2(s)}$  was less efficient than  $Fe(OH)_{3(s)}$  in sweep flocculation or enmeshment (Gheraout et al., 2008).

The current density and electrocoagulation time were kept stable at 5.56 mA/cm<sup>2</sup> and 30 min for all runs. For all contaminants, the removal efficiencies increase as the initial pH increases to the alkaline level, as shown in Figure 4.2. When pH rose from the acidic to neutral level, all pollutants experienced a sharp decrease. However, the reduction slowed down at the alkaline environment. At pH 7, the removals of COD, turbidity and hardness were 64.29, 89.31 and 83.39%, respectively. Afterwards, the increase of pH to 9 and 11 didn't assure a continuous decrease of COD and turbidity, which stayed constant as in the neutral environment. The treated water became visually very clear while the removal of turbidity increased to 91.40% at pH 11. However, the COD reduction was somewhat lower than some previous studies (Tir and Moulai-Mostefa, 2008; Chavalparit and Ongwandee, 2009). According to Chavalparit's research, the residual COD was still high due to less significant removals of glycerol and methanol, which were the two main compositions of organic matter other than oil and grease in the wastewater (Chavalparit and Ongwandee, 2009). Another explanation for the high level of residual COD was that the metal ion (Fe<sup>3+</sup>) dosage was not sufficient to destabilize all colloidal and finely suspended particles when the charge loading was low (Chen et al., 2000).

High pH provoked the precipitation of hardness around the cathode, as indicated in following equations:



The high decline of hardness was also attributed to more sweep flocculation in high pH conditions. According to Reaction (4.6), more  $\text{Fe}(\text{OH})_3$  was formed in alkaline environments, more flocs would be generated and more carbonate salts would be trapped. In this way, hardness was reduced as the precipitation settled down. Malakootian et al. (2010) reported a 95.4% of calcium removal at pH 7.0 and 97.4% at pH 10.0, respectively.

At the cathode, generation of  $\text{H}_2$  and  $\text{OH}^-$  kept a continuous pH increase for all environmental runs, as shown in Figure 4.2. It was the same with the trend of the contaminants-the rise became slower after the neutral pH. This might be attributed to the fact that at alkaline pH, less  $\text{OH}^-$  would be generated because of the high amount of  $\text{OH}^-$  already existing in the solution. According to Reaction (4.6), the reversible reaction was inclined to go leftward at high pH and to act more rightward at low pH. This resulted in a more significant pH increase when initial pH was lower. These phenomena were also stated in (Kobyas et al., 2003; Malakootian et al., 2010), but were different from those in (Cañizares et al., 2007), where the final pH was lower than the initial pH due to a series of complicated reactions of electrodes at alkaline pH. However, all these results revealed that the EC process exhibited some pH buffering capacity, especially in the alkaline pH environment.

In the present study, the pH of the produced water was about 7 to 8, which was basically a neutral pH environment. Contaminants all achieved the maximum removal in this pH condition. Therefore, the following tests were performed using the raw water without pH adjustment. This was the same as some previous studies, where the wastewater was used directly for electrocoagulation experiments (Chen, 2004; Xu and

Zhu, 2004).

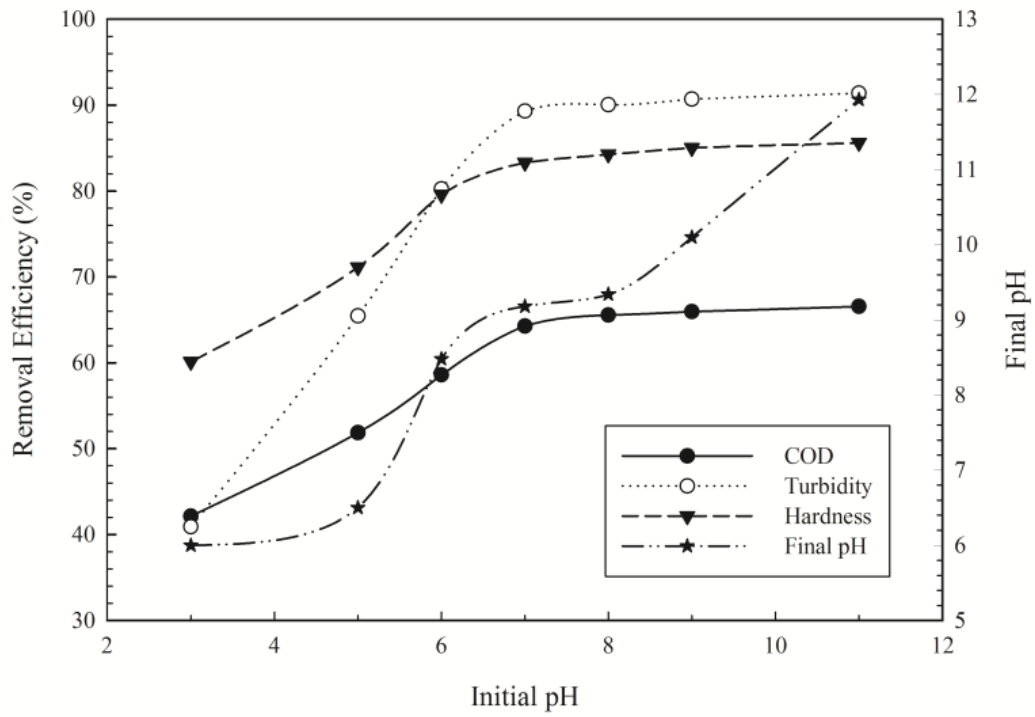


Figure 4.2 Effect of initial pH on COD, turbidity and hardness removals. Current density = 5.56 mA/cm<sup>2</sup>, electrolysis time = 30 min.

#### 4.3.1.2. Current Density

Current density directly determined both coagulant dosage and bubble generation rates, as well as strongly influenced both solution mixing and mass transfer at the electrodes (Nanseu-Njiki et al., 2009). The effects of current density on the removal efficiencies were studied by varying the range from 1 to 10 mA/cm<sup>2</sup>. The electrolysis time was kept stable at 30 min. As shown in Figure 4.3, COD, turbidity and hardness all decline significantly as the current density increases to 5.56 mA/cm<sup>2</sup>. Among these, the reduction of turbidity was the most effective, with a removal efficiency of 90.09%. This was due primarily to an adequate supply of electricity at 5.56 mA/cm<sup>2</sup> to completely destabilize the suspended species in solution. Compared to turbidity, 64.14% of COD and 84.86% of hardness were reduced at 5.56 mA/cm<sup>2</sup>. Beyond this limit, an increase of the current density resulted in a small increase of the removal efficiency where a plateau was reached.

According to Faraday's laws of electrolysis, the coagulant generated from the anode was proportional to the total electric charge passing through, that is, the current density. As the current density increased, huge amounts of Fe(OH)<sub>3</sub> coagulants were produced to destabilize the colloidal particles, together forming more precipitates which would easily settle down (Tir and Moulai-Mostefa, 2008). On the other hand, higher amount of H<sub>2</sub> would be generated from the cathode due to the higher current. Bubble size decreased with the increasing current density, reported by Chen (2004), resulting in the increasing bubble densities and the intense upward flux. Smaller bubbles also provided larger surface area for particle attachment, ensuring high separation efficiency (Chen et al., 2002). Pollutants were taken away through this flotation process with flocs which were

lifted by the large amounts of tiny bubbles. These reasons explained why higher current density created a better reduction for COD, turbidity and hardness.

However, the energy consumption and the operating costs all increased as the current density rose (Kobya et al., 2003). Research implied that the elimination efficiency was controlled by the formation of some complexes and it was not necessary to work with a current density greater than the refined value (Mameri et al., 1998). In this study,  $5.56 \text{ mA/cm}^2$  was selected as the central point in CCD design to obtain sufficient removals with relatively lower costs.

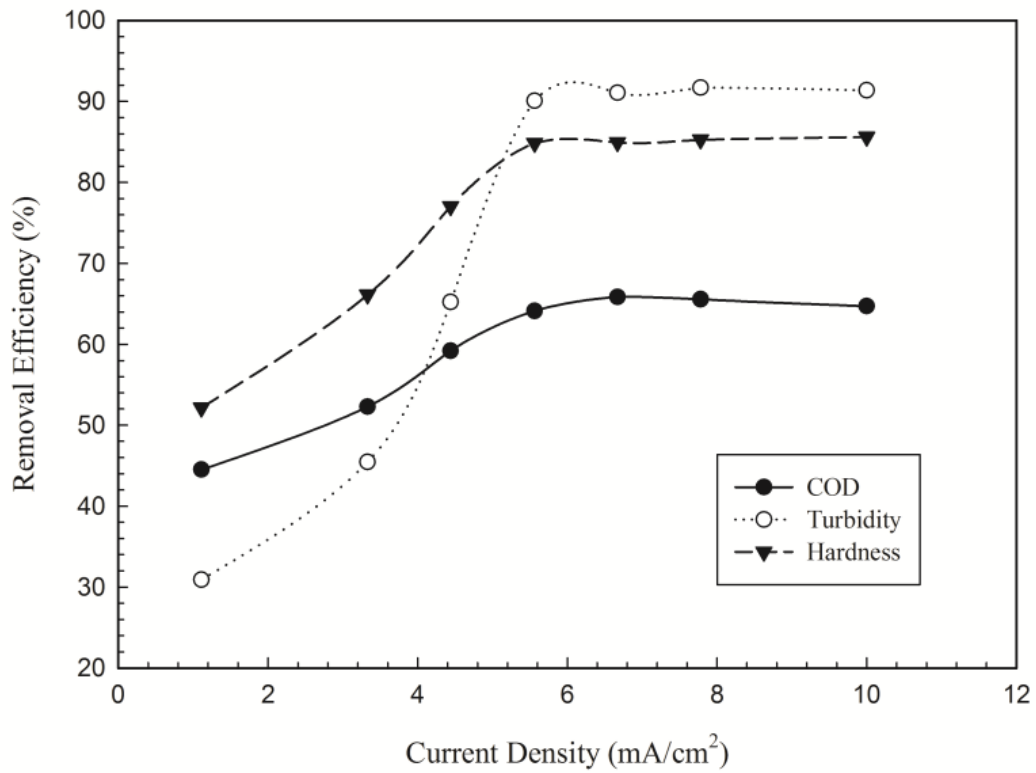


Figure 4.3 Effect of current density on COD, turbidity and hardness removals. Initial pH around 7 ~ 8, electrolysis time = 30 min.

#### 4.3.1.3. *Electrolysis Time*

Electrolysis time was another factor that should be considered in the EC process (Kobyas et al., 2006). The time range from 10 to 50 min was studied to understand how time affected the removal efficiencies. The current density was constantly maintained at  $5.56 \text{ mA/cm}^2$ . As shown in Figure 4.4, an enhanced removal rate results from an increase of the electrolysis time. There was a steep decrease of COD, turbidity and hardness at the beginning of the experiments. When it came to 30 min, 89.64% of turbidity, 65.43% of COD, and 85.51% of hardness were decreased with the flocs. As the amount of dissolved coagulants at the iron electrode increased, there was an increase in the removal efficiency, which might be explained by a sufficient quantity of coagulant dissolving from the iron electrode to effectively reduce the double layer of the suspended metallic hydroxides and to destabilize them (Chou et al., 2009). The released ferric ions and hydroxyl from electrodes formed more hydroxide flocs, which would be adsorbed by more pollutant particles as the time extended (Drouiche et al., 2009). However, further increasing time to 40 and 50 min provided slight reduction of the pollutants, which would not be applied because of the high energy and electrode consumption. Therefore the optimal reaction time was 20 ~ 30 min considering the treatment cost and efficiency, which was also stated in literature (Xu and Zhu, 2004; Kobyas et al., 2006; Malakootian et al., 2010).

Finally, the electrolysis time of 30 min, together with initial pH around 7, and current density of  $5.56 \text{ mA/cm}^2$  was employed in CCD design to find the refined operating parameters for the EC process.

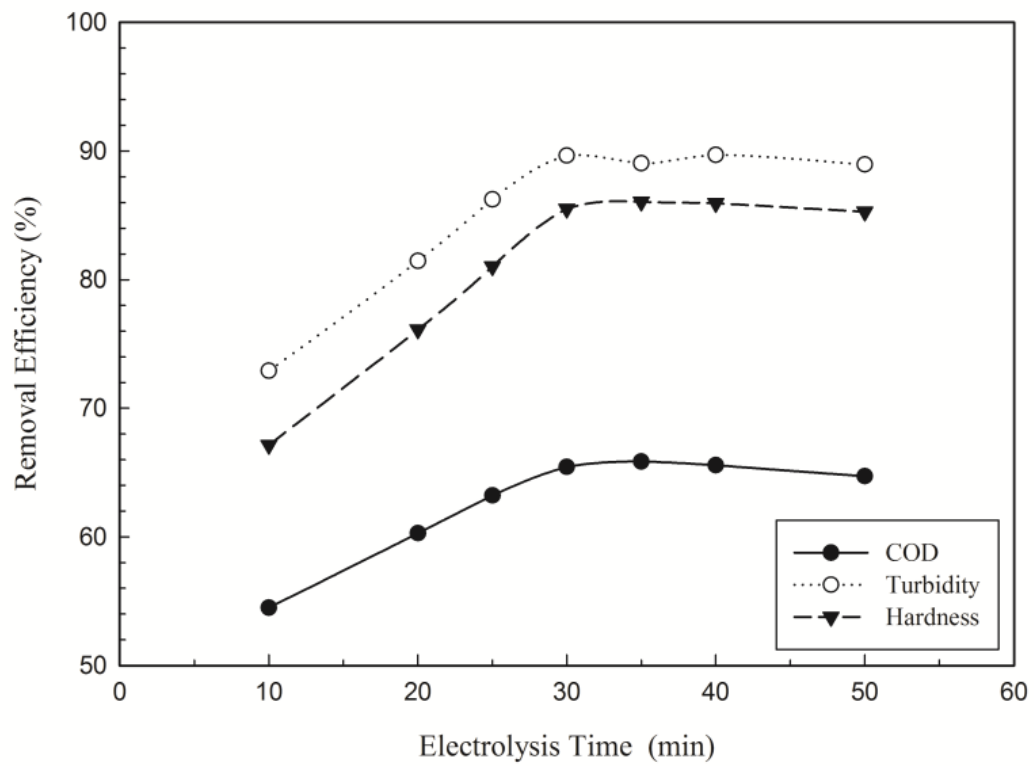


Figure 4.4 Effect of electrolysis time on COD, turbidity and hardness removals. Initial pH around 7 ~ 8, current density = 5.56 mA/cm<sup>2</sup>.

### 4.3.2. CCD Experiments

As discussed in preliminary experiments, the most influential variables which affected the removal efficiency by electrocoagulation were pH, current density and time. CCD experimental design was performed to determine the simple and combined effects of operating parameters on removal efficiency. This process involved three major steps: performing the statistically designed experiments, estimating the coefficients in the proposed model and predicting the response of process, and checking the validity of the model. Experimental data was analyzed using the response surface regression procedure and was fitted to a second-order polynomial model. The following response equations were used to correlate removal efficiencies and independent variables:

$$Y_1 = 65.49 + 3.22 X_1 + 3.94 X_2 + 1.40 X_3 - 2.68 X_1^2 - 3.37 X_2^2 - 2.26 X_3^2 + 0.051 X_1X_2 - 0.079 X_1X_3 + 0.23 X_2X_3 \quad (4.8)$$

$$Y_2 = 90.53 + 6.68 X_1 + 15.55 X_2 + 2.43 X_3 - 7.79 X_1^2 - 10.53 X_2^2 - 3.45 X_3^2 - 1.18 X_1X_2 - 0.14 X_1X_3 - 0.79 X_2X_3 \quad (4.9)$$

$$Y_3 = 84.11 + 3.83 X_1 + 6.65 X_2 + 2.03 X_3 - 3.00 X_1^2 - 4.88 X_2^2 - 2.69 X_3^2 + 1.07 X_1X_2 + 0.000 X_1X_3 - 0.82 X_2X_3 \quad (4.10)$$

The CCD experimental results and predicted values for COD ( $Y_1$ ), turbidity ( $Y_2$ ), and hardness ( $Y_3$ ) removal efficiencies are presented in Table 4.3. Experimental values were the measured response data for a particular run, and the predicted values were evaluated from the model and generated for the same run. As the predicted data were in consistent with the observed values, the obtained second-order regression models were adequate for the prediction of each response. The response model demonstrated a good fit

to the experimental data. Therefore, the models were considered adequate for the predictions and refinement (Khayet et al., 2011).

Furthermore, ANOVA reports are presented in Tables 4.4 to 4.6. The statistical significance of the second-order regression model was determined by  $F$ -value, which was a measurement of variance of data about the mean, based on the ratio of mean square of group variance due to error. If the model presented a good prediction of the experimental data then the calculated  $F$ -value should be greater than the tabulated  $F$ -value (Khayet et al., 2011). In this study,  $F$  values from the ANOVA were 34.97 for COD ( $F$ -tab = 15.49), 65.15 for turbidity ( $F$ -tab = 15.49), and 39.80 for hardness removal ( $F$ -tab = 15.49), indicating that most of the variations in the response could be explained by the regression equations. The associated  $p$ -value was used to estimate whether the  $F$ -statistics were large enough to indicate statistical significance.  $P$ -values in this case were calculated all less than 0.0001 at 95% of probability level, indicating the obtained response models were validated from a statistical standpoint and were good predictors of the experimental data (Tir and Moulai-Mostefa, 2008; Kobya et al., 2011).

The model adequacy was checked by calculating the coefficient of determination  $R^2$ , which provided a measure of how well observed outcomes were replicated by the model, as the proportion of total variation of outcomes explained by the model. The high  $R^2$  value, close to 1, was desirable and the predicted  $R^2$  must be in reasonable agreement with the adjusted  $R^2$  for a significant model (Kobya et al., 2011). A high  $R^2$  coefficient ensured satisfactory adjustment of the second-order regression model to the experimental data. In the present study, the values of  $R^2$  were 0.9752 for COD, 0.9865 for turbidity, and 0.9782 for hardness removal, respectively. This implied that 97.52, 98.65 and 97.82%

of the data deviation could be explained by the independent variables in the model. The adjusted  $R^2$  were 0.9473, 0.9714 and 0.9536 for COD, turbidity, and hardness recovery, indicating the models are significant and adequate to represent the actual relationship between the response and variables (Zaroual et al., 2009). Furthermore, the predicted  $R^2$  values were in agreement with the adjusted statistics  $R^2$ . This meant that significant terms were included in the empirical models.

The Fisher  $F$ -test was used to determine the significance of the regression coefficients of the parameters on COD/turbidity/hardness removals. The regression coefficients values,  $F$  value and associated  $p$ -value are presented in Tables 4 to 6. It should be noted that the initial pH and current density were the two most influential factors, with the associated  $p$ -values less than 0.0001. However, there were no significant interactions among the process parameters-initial pH, current density, and electrocoagulation time-because the values of “Prob  $> F$ ” were all greater than 0.1000, indicating these interaction terms were insignificant. Aleboyeh et al. (2008) refined C.I. Acid Red 14 azo dye removal by EC with RSM and demonstrated that the current density, the time of electrolysis, their interaction, and the quadratic effect of all variables were the most influential factors. The significance of these interactive effects between the variables would have been lost if the experiments were carried out by conventional methods.

Table 4.4 ANOVA report for the RSM model of COD removal

Source	Sum of squares	df	Mean Square	F Value	p-value Prob > F	Remark
Model	596.54	9	66.28	34.97	< 0.0001	Significant
$X_1$ -pH	141.34	1	141.34	74.58	< 0.0001	Significant
$X_2$ -Current Den.	212.39	1	212.39	112.06	< 0.0001	Significant
$X_3$ -Time	26.89	1	26.89	14.19	0.0055	
$X_1X_2$	0.021	1	0.021	0.011	0.9191	
$X_1X_3$	0.050	1	0.050	0.026	0.8751	
$X_2X_3$	0.42	1	0.42	0.22	0.6506	
$X_1^2$	91.06	1	91.06	48.04	0.0001	
$X_2^2$	143.62	1	143.62	75.78	< 0.0001	
$X_3^2$	64.70	1	64.70	34.14	0.0004	
Residual	15.16	8	1.90			
Lack of fit	11.64	5	2.33	1.98	0.3042	Not Significant
Pure Error	3.52	3	1.17			
Cor Total	611.70	17				

Table 4.5 ANOVA report for the RSM model of turbidity removal

Source	Sum of squares	df	Mean Square	<i>F</i> Value	<i>p</i> -value Prob > <i>F</i>	Remark
Model	5823.37	9	647.04	65.15	< 0.0001	Significant
$X_1$ -pH	609.01	1	609.01	61.32	< 0.0001	Significant
$X_2$ -Current Den.	3300.35	1	3300.35	332.33	< 0.0001	Significant
$X_3$ -Time	80.51	1	80.51	8.11	0.0216	
$X_1X_2$	11.19	1	11.19	1.13	0.3195	
$X_1X_3$	0.15	1	0.15	0.015	0.9048	
$X_2X_3$	5.06	1	5.06	0.51	0.4958	
$X_1^2$	767.64	1	767.64	77.30	< 0.0001	
$X_2^2$	1403.55	1	1403.55	141.33	< 0.0001	
$X_3^2$	150.43	1	150.43	15.15	0.0046	
Residual	79.45	8	9.93			
Lack of fit	74.07	5	14.81	8.26	0.0563	Not Significant
Pure Error	5.38	3	1.79			
Cor Total	5902.81	17				

Table 4.6 ANOVA report for the RSM model of hardness removal

Source	Sum of squares	df	Mean Square	<i>F</i> Value	<i>p</i> -value Prob > <i>F</i>	Remark
Model	1250.63	9	138.96	39.80	< 0.0001	Significant
$X_1$ -pH	200.10	1	200.10	57.31	< 0.0001	Significant
$X_2$ -Current Den.	603.16	1	603.16	172.75	< 0.0001	Significant
$X_3$ -Time	56.12	1	56.12	16.07	0.0039	
$X_1X_2$	9.12	1	9.12	2.61	0.1448	
$X_1X_3$	0.000	1	0.000	0.000	1.0000	
$X_2X_3$	5.35	1	5.35	1.53	0.2510	
$X_1^2$	113.95	1	113.95	32.64	0.0004	
$X_2^2$	300.87	1	300.87	86.17	< 0.0001	
$X_3^2$	91.67	1	91.67	26.26	0.0009	
Residual	27.93	8	3.49			
Lack of fit	23.86	5	4.77	3.51	0.1649	Not Significant
Pure Error	4.07	3	1.36			
Cor Total	1278.56	17				

The 3D response surface contour plots to estimate the oil recovery efficiency (through COD and turbidity) and hardness removal over independent variables (pH and current density) are shown in Figures 4.5 to 4.7. The plots showed the individual/combined effects of pH and current density when time was at its zero level. It was obvious that the effects of pH and current density on pollutant removals exhibited the same tendency. The recovery efficiencies increased with increasing pH and current density. There was a gradual increase of the pollutant removal to the maximum with the increase of pH (from 3 to 7) and current density (from 1.82 to 5.56 mA/cm<sup>2</sup>), and then a decrease with further pH and current density enhancements (pH greater than 7, current density greater than 5.56 mA/cm<sup>2</sup>). The plateau reflected the existence of optimal pollutant removal factors.

The refined operating conditions were: pH 7.36, current density 5.90 mA/cm<sup>2</sup>, and electrolysis time 30.94 min. These values were also experimentally validated. Correspondingly, the equivalent coagulant dose was 23.76 mg/L (as Fe<sup>3+</sup>), calculated from the Faraday's law (Zhu et al., 2005). As shown in Table 4.7, the predicted and observed variables are closely related, and the removal efficiencies under refined conditions are maximized as high as 66.64, 93.80 and 85.81% for COD, turbidity, and hardness removals. This was consistent with studies on the optimization of COD and turbidity removal from oily wastewater (Tir and Moulai-Mostefa, 2008; Chavalparit and Ongwandee, 2009). In particular, hardness was statistically refined and reduced by 85.81% simultaneously with COD and turbidity under the same operating conditions. This confirmed that RSM could be effectively used to refine the parameters in complex EC process as the statistical design of experiments.

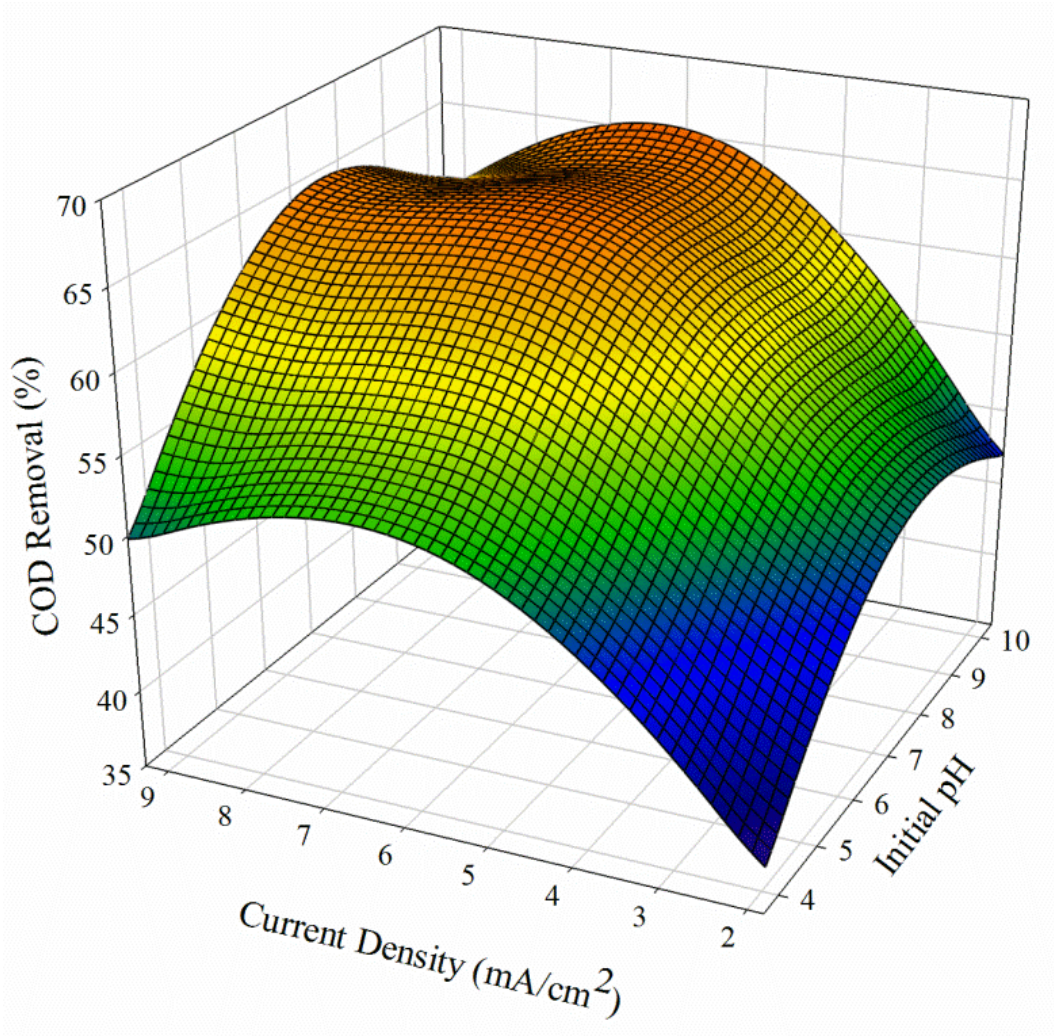


Figure 4.5 Effect of initial pH and current density on COD removal; 3D surface graph and contour plots

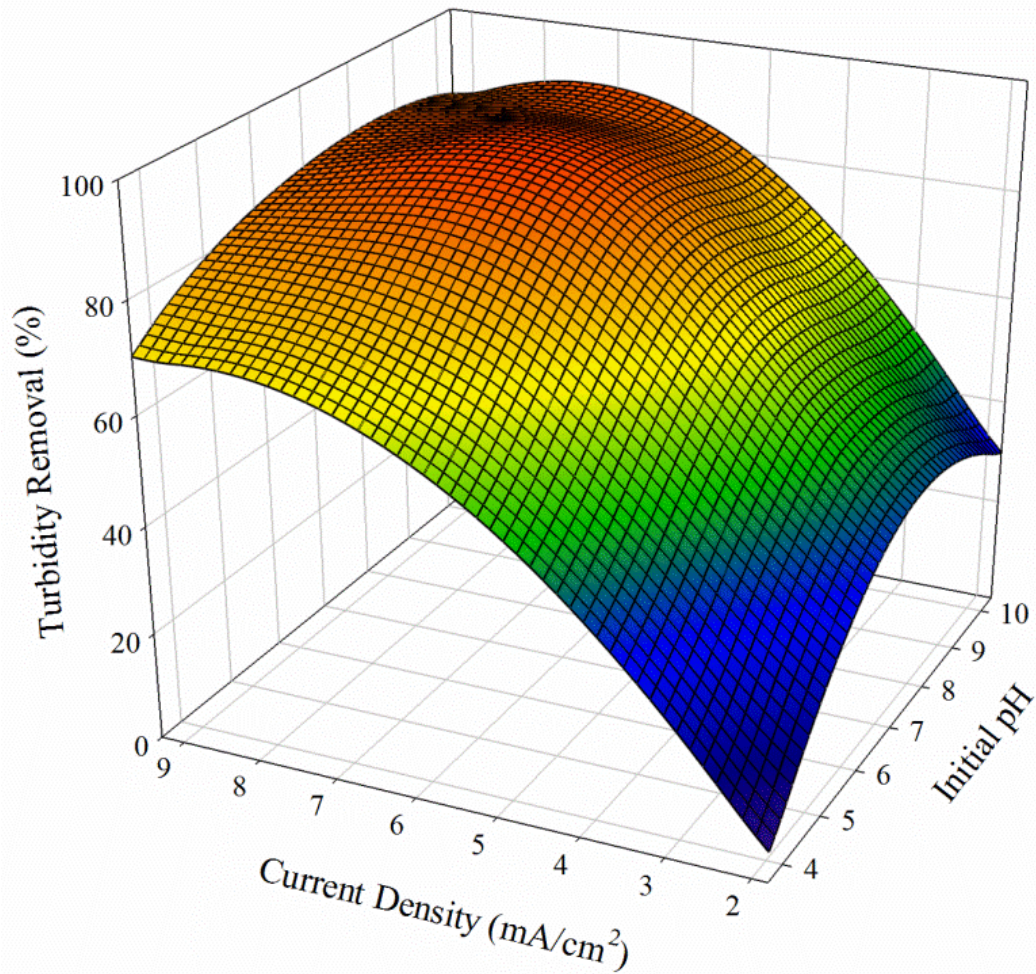


Figure 4.6 Effect of initial pH and current density on turbidity removal; 3D surface graph and contour plots

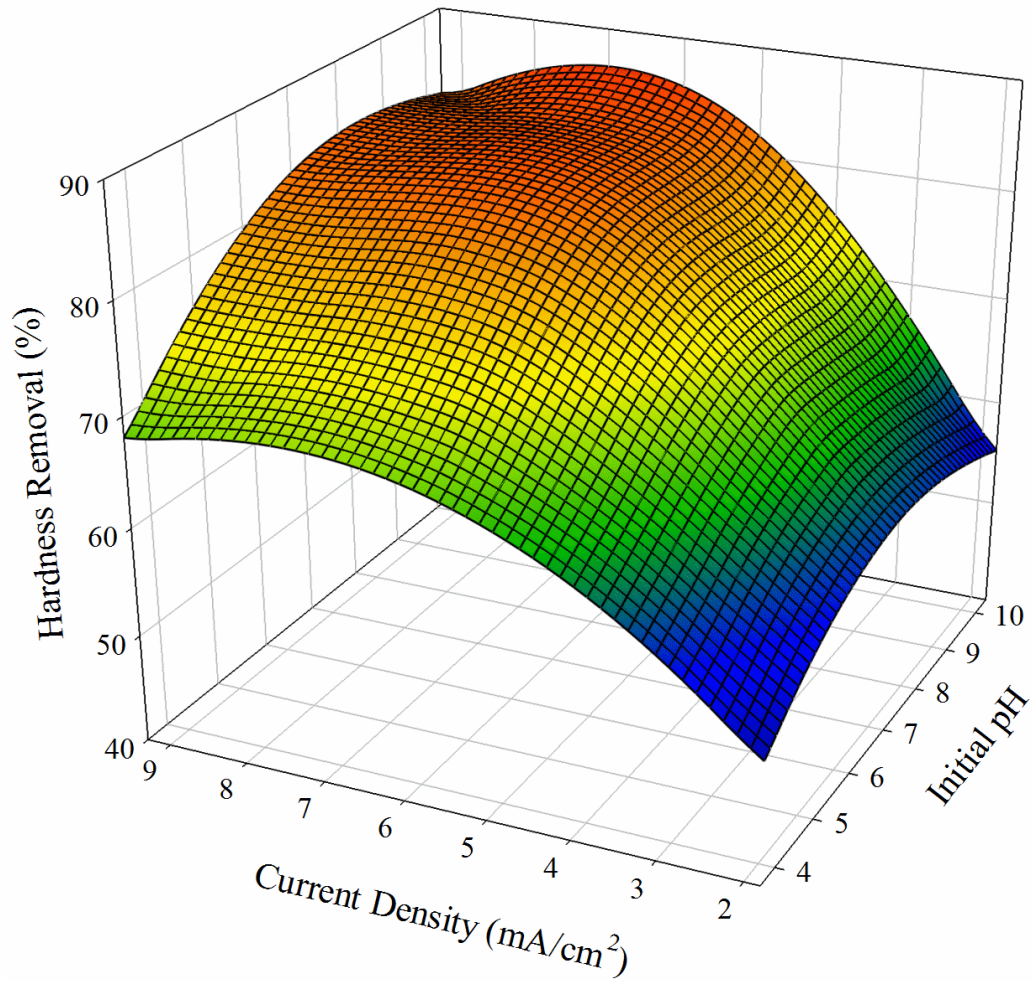


Figure 4.7 Effect of initial pH and current density on hardness removal; 3D surface graph and contour plots

Table 4.7 Validation experiments for the refined operating conditions

Parameter	Refined Value	Experimental Value
COD Removal (%)	66.64	65.97
Turbidity Removal (%)	93.80	92.48
Hardness Removal (%)	85.81	85.36
pH	7.36	7
Current Density (mA/cm <sup>2</sup> )	5.90	5.56
Electrolysis Time (min)	30.94	30

### 4.3.3. Membrane Fouling Studies

To verify the pretreated produced water could successfully prevent or alleviate fouling and scaling associated with oil and calcium precipitation, RO filtration runs were compared between the EC effluent under refined conditions and the raw water sample without EC pretreatment. At the beginning of the filtration, there was a remarkable decrease (Figure 4.8) in the flux of the raw water sample, which was probably due to the high concentration of oil and hardness in the wastewater. There existed a sudden flux decline around 60 min, indicating that the organics and scaling deposition plugged the pores and reduced the membrane permeability (Bani-Melhem and Smith, 2012). Large amounts of white precipitation (probably  $\text{CaSO}_4$  and  $\text{CaCO}_3$ ) also formed in the concentrate at this point. In comparison, the permeate flux for the pretreated water experienced a much lesser extent of initial decline, which was attributed to the effective removal of COD and hardness by previous EC processes. With the minimized influent concentration and steady operating conditions, the permeate flux slightly declined with time. At the end of the experiment, the permeate flux was around  $22 \text{ L}/(\text{m}^2\text{h})$  and the water recovery rate reached 87.83%. The final steady flux indicated that fouling/scaling did not occur significantly for the pretreated water (Salahi and Mohammadi, 2010). As shown in Table 4.8, the EC-membrane equipment demonstrated a more than 95% of removal in oil, COD, turbidity, and hardness. The EC pretreatment strategies successfully reduced RO membranes fouling/scaling and yielded product water suitable for beneficial reuses. It was concluded that under refined conditions, EC pretreatment would improve RO performance both in permeate flux and product water quality.

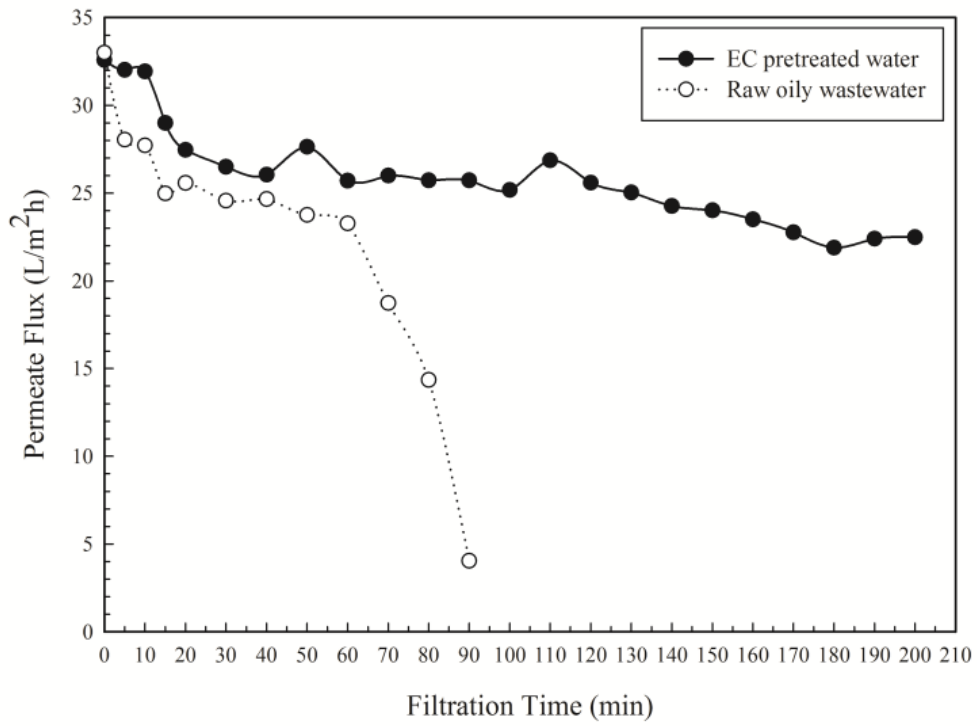


Figure 4.8 Permeate flux trends during RO filtration: Comparison between EC pretreated water and raw produced water

Table 4.8 Characteristics of the product water\*

Parameters	Oil (mg/L)	COD (mg/L)	Turbidity (NTU)	Hardness (as CaCO <sub>3</sub> ) (mg/L)	pH	Electric Conductivity (µs/cm)
Values	0.86	12	1.26	1.37	8.56	556

\*Error limits of parameters are less than  $\pm 5\%$ .

#### 4.4. SUMMARY

For the first time, a pilot-scale electrocoagulation process was developed for simultaneous removal of hardness, COD, and turbidity, with the related experimental design being supported by the RSM. This was critical for mitigating membrane scaling and fouling. A preliminary research was employed to obtain desired operating conditions: initial pH 7, current density 5.56 mA/cm<sup>2</sup> and electrolysis time 30 min. RSM with an eighteen-run CCD design was performed and second-order regression models were generated. ANOVA was conducted to validate the significant consistency between experimental values and predicted ones (Hardness removal:  $R^2$  0.9782,  $F$  value 39.80,  $p$ -value < 0.0001. COD removal:  $R^2$  0.9752,  $F$  value 34.97,  $p$ -value < 0.0001. Turbidity removal:  $R^2$  0.9865,  $F$  value 65.15,  $p$ -value < 0.0001). The pH and current density had the most significant effects on pollutants recovery, while reaction time was least significant. The 3D surface graph and contour plots indicated that the recovery efficiencies would increase with pH and current density. The models derived from the EC process provided optimum operating conditions with the initial pH of 7.36, the current density of 5.90 mA/cm<sup>2</sup>, and the reaction time of 30.94 min. The maximized hardness, COD, and turbidity removal efficiencies were 85.81, 66.64, and 93.80%, respectively. The final steady flux was around 22 L/(m<sup>2</sup> · h) and the water recovery rate reached 87.83%. These indicated that RSM was an effective approach for obtaining desired operating conditions in complex EC pretreatment processes for RO membrane reactors.

# CHAPTER 5

## PHENANTHRENE SORPTION ON PALYGORSKITE MODIFIED WITH GEMINI SURFACTANTS: EFFECTS OF AQUEOUS SOLUTION CHEMISTRY

### 5.1. BACKGROUND

Sorption of organic contaminants to solid phase has a major influence on its fate, transport, and bioavailability in natural aquatic environments. Particularly, clay minerals, such as palygorskite, have received emerging interest as a potential alternative to the conventional sorbents from both the environmental and the economic points of view. Palygorskite is a hydrated magnesium silicate mineral with a fibrous morphology and high surface area, and with a structure consisting of parallel ribbons of 2:1 layers (Chen et al., 2007; Chang et al., 2009). It has moderately high cation exchange capacity because of considerable substitution of  $\text{Al}^{3+}$  by  $\text{Mg}^{2+}$  and  $\text{Fe}^{2+}$  in the octahedral sheet (Sarkar et al., 2010; Sarkar et al., 2012). Due to the intrinsic negative charges of palygorskite, it has been widely used as sorbents for heavy metals (Chen and Wang, 2007; Chen et al., 2007; Thanos et al., 2012). However, being intrinsically hydrophilic, palygorskite minerals show little affinity to hydrophobic organic contaminants. One effective way to modify the surface properties of palygorskite is to replace the natural inorganic exchangeable cations with large organic cations of surfactant molecules (organomodification). Most studies in sorption remediation of organic contaminants by organopalygorskite have concentrated on polar organic compounds. For example, surfactant modified palygorskite has exhibited high potential in remediation of water/soil contaminated by polar pollutants

such as 2,4-D herbicide (Xi et al., 2010), atrazine pesticide (Rodríguez-Cruz et al., 2007b), phenol (Huang et al., 2007) and p-nitrophenol (Chang et al., 2009; Sarkar et al., 2010; Sarkar et al., 2012). However, the removal of nonpolar compounds by organopalygorskite is not well documented.

Partitioning often plays an important role in the sorption of nonpolar contaminants on solid and the sorption amount is considered a function of the organic content in the clay (Lee et al., 1989; Zhu et al., 2003). The organic cations sorbed by clay minerals form a hydrophobic organic phase derived from alkyl hydrocarbon chains. This phase could create an effective organic partition medium for organic contaminants through partitioning or hydrophobic interactions (Lee et al., 1989; Rodríguez-Cruz et al., 2008). In addition, the chemical structure (size and shape) of the organic cation used to modify the clay is another essential factor that influences its sorption capacity (El-Nahhal and Safi, 2004). It is found that organoclays synthesized with long hydrocarbon chains can achieve better organic compounds removal than those synthesized with short hydrocarbon chains. It is also reported that increasing the surfactant chain length and the number of alkyl chains per surfactant molecule can enhance the sorption of organic compounds by organoclays (Zhu et al., 1997; Witthuhn et al., 2005). Containing two hydrophilic heads and two long hydrophobic tails in one surfactant molecule, cationic gemini surfactants have received substantial interest recently. Compared to the single-chain counterparts, gemini surfactants have increasing hydrophobicity and can endow solids with significantly higher organic contents. The sorbed surfactants can act as an effective organic medium for sorbing nonpolar or weakly polar organic pollutants (Zhu et al., 2003).

PAHs are a group of nonpolar hydrophobic contaminants with two or more fused benzene rings from natural as well as anthropogenic sources (Zhu et al., 2003). PAHs can transport and be accumulated in groundwater and surface water for a long period of time, and are difficult to biodegrade. In our previous studies, the enhanced solubilization capability of cationic gemini surfactants for PAHs has been demonstrated (Wei et al., 2011b). The enhancement of phenanthrene sorption on soils with the addition of gemini surfactant has been well established (Zhao et al., 2015). At the low surfactant level, the sorbed surfactant phase acts as a partition medium for phenanthrene and effectively retains PAHs from water. However, to the best of our knowledge, there is limited data regarding the modification of palygorskite with a gemini surfactant for the removal of PAHs from aqueous phase. The sorption behavior of gemini on palygorskite and the related modeling approach has never been studied. The enriched knowledge regarding the potential applications of gemini modified palygorskite in polluted water treatment and environmental remediation processes is required.

Solution chemistry plays an important role in the distribution of organic compounds in solid-liquid system (Ko et al., 1998; Zhang et al., 2010a). Parameters such as pH, ionic strength, temperature, and dissolved organic matter have been identified as essential factors influencing organic contaminants' sorption behaviors at the solid/aqueous interface. For example, a decrease of pH can modify the soil properties (e.g., amount of soil organic matter, extent of surface deprotonation) and affect the interactions of soil with phenanthrene (Zhang et al., 2011). Ko et al. has reported the aqueous chemistry effects (such as pH and ionic strength) on phenanthrene partitioning to sorbed surfactants (Ko et al., 1998). Phenanthrene sorption by soils treated with humic

substances under different pH and temperature has been investigated (Ping et al., 2006). The binding affinity of phenanthrene to fly ash sorbents has been found to increase with the addition of humic acid under different pH conditions (An and Huang, 2012). Despite extensive studies reported in the literature on the factors influencing the sorption process of PAHs, the information regarding the solution chemistry effects on PAHs sorption to palygorskite is still need to be clarified. Therefore, it is of great importance to elucidate the factors controlling the sorption process and explore the corresponding sorption mechanisms.

This study will reveal the effectiveness of the gemini modified palygorskite as a novel remediation material in removing PAHs from aqueous solution. The sorption of gemini surfactants on palygorskite will be studied and a developed Two-step Adsorption and Partition model will be employed to explicate the sorption mechanisms. A fundamental understanding regarding the interactions between PAHs and palygorskite clay will be established. The effects of aqueous chemistry characteristics on PAHs sorption to palygorskite clay will be explored. The results can reveal the distribution of PAHs in a palygorskite–water system and facilitate the potential modification and utilization of palygorskite for enhanced removal of PAHs from contaminated water effluents.

## **5.2. MATERIALS AND METHODS**

### **5.2.1. Chemicals**

Phenanthrene (PHE) was selected as the representative PAH, and was purchased from Sigma Aldrich Chemical Co. (WI, USA) with the purity greater than 99%. Cationic

gemini surfactant (N1-dodecyl-N1,N1,N2,N2-tetramethyl-N2-octylethane-1, 2-diaminium bromide, 12-2-12) was obtained from Chengdu Organic Chemicals Co., Ltd. (Sichuan, China), with a purity of 98%. The molecular structures and properties of PHE and surfactants are given in Table 5.1. Humic acid (HA) was purchased from Sigma (WI, USA). The standard HCl and NaOH solutions of 0.1 M were obtained from Fisher (MA, USA) with the purity greater than 99%.

### **5.2.2. Preparation of Surfactant-Modified Palygorskite**

Palygorskite (PGS) was obtained from Huaiyuan Mining Co. Ltd (Jiangsu, China). Dried PGS (20 g) was mixed with 200 mL of aqueous solution containing 0.4 g of gemini surfactant. The mixture was stirred at 333 K for 3 h. It was then filtrated and washed with deionized water until the liquid was bromide free. After dried at 343 K and activated for 1 h at 378 K, the modified PGS was obtained through mechanically whetted to 100 meshes with a mortar pestle. The sieved solid was homogenized as much as possible and stored in glass containers. Instrumental analyses such as Fourier transform infrared (FT-IR) spectroscopy, BET surface area, and cation exchange capacity (CEC) demonstrated the effective modification of PGS with gemini surfactant. The physical and textural characteristics of PGS and modified PGS are given in Table 5.2.

Table 5.1 The structure and physicochemical properties of the selected surfactants and

PAHs

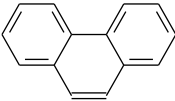
Material	Structure	Molecular Weight (g/mol)	CMC (mM)	Water Solubility (mg/L)	$\log K_{ow}$
12-2-12	$C_{12}H_{25}N^+(CH_3)_2(CH_2)_2-$ $N^+(CH_3)_2C_{12}H_{25} \cdot 2Br^-$	614.67	0.8		
Phenanthrene		178.2		1.06	4.57

Table 5.2 Properties of the original PGS and gemini modified PGS \*

Sorbents	CEC (cmol/kg)	SOM (g/kg)	pH	Surface area (m <sup>2</sup> /g)
PGS	28.5	20.2	7.0	146.149
Modified PGS	28.6	22.3	7.9	148.298

\*Error limits of parameters are less than  $\pm 3\%$ .

### **5.2.3. Sorption Studies**

The batch sorption experiments were conducted in 20 mL glass vials. 20 mg of solid was first added into the glass vial; after that, the appropriate amount of deionized water was added corresponding to different PHE initial concentration. The background solution contained pre-determined volumes of NaCl solution. Then a pre-calculated volume of PHE stock solution was added to each vial, and the initial concentration of PHE was ranging from 0.3 to 1 mg/L. The vials were sealed with Teflon-lined screw caps and were vortexed for 20 s, and then were placed in a reciprocal shaker (SHKE5000, Thermo Scientific, USA) at 283/293/303 K and 200 rpm for 24 h to reach the sorption equilibrium. Preliminary experiments showed that 24 h were sufficient for the sorption process to reach equilibrium and the experimental loss of PHE was negligible. Before testing, the samples were subsequently centrifuged at 5000 rpm (Multifuge X1R, Thermo Scientific, USA) for 30 min and 10000 rpm (Promo Legend Micro 21, Thermo Scientific, USA) for 10 min to separate PGS from solution. An appropriate aliquot of supernatant was then carefully withdrawn with a volumetric pipette to further determine the residual amount of PHE. At the same time, controlled experiments without PHE were conducted and the supernatant of controlled samples were analyzed as the background concentrations for PHE. For detailed procedures, please also refer to previous studies (Yu et al., 2011a; Zhao et al., 2011a; An and Huang, 2012; Wei et al., 2013). The sorption of gemini surfactants was conducted at 293 K using the same procedure.

### **5.2.4. Effect of Aqueous Solution Parameters**

To study the effect of pH on sorption of PHE, the sorption behaviors of PHE were

carried out at 3, 7, and 11. The pH value of suspension was adjusted with standard HCl or NaOH solution, and the ion concentration in the system was kept constant at 0.01 M. The initial concentrations of PHE were ranging from 0.3 to 1 mg/L. Temperature was kept constant at 293 K. Batch sorption experiments were performed in the manner as mentioned in the sorption studies. The effect of HA on the sorption behaviors of PHE was examined in PGS-water system. The sorption experiments were conducted in the presence of HA ranging from 0 to 80 mg organic carbon/L (OC/L). An appropriate volume of PHE stock solution was added and the initial concentrations for PHE varied from 0.3 to 1 mg/L. Temperature was kept constant at 293 K. Batch experiments were performed following the sorption test procedures. To investigate the influence of ionic strength, the sorption tests were conducted. NaCl was added at different concentrations (0.01, 0.1 and 1 M). The initial concentrations of PHE were from 0.3 to 1 mg/L and pH value was 7. The vials were placed on a reciprocal shaker at 293 K and 200 rpm for 24 hours to reach the sorption equilibrium.

#### **5.2.5. Analytical Methods**

PHE was analyzed using HPLC. The HPLC instrument, an Agilent 1260 Infinity LC System (USA), was equipped with vacuum degasser, binary pump, autosampler, thermostated column compartment (set to 303 K), diode array detector (DAD), and ZORBAX Eclipse PAH column (3.5  $\mu$ m particle size, 4.6 mm  $\times$  150 mm ID). A mobile phase consisting of acetonitrile/water (75:25, v/v) was used at a flow rate of 1.0 mL/min. PHE was monitored with DAD at 250 nm. The residual concentration of gemini surfactants was determined by potentiometric titration (G20, Mettler Toledo, Switzerland)

method, using sodium dodecyl sulfonate ( $C_{12}SO_3Na$ , SDS) as the titrant. The titration of blank samples was also carried out. The amounts of PHE/surfactants sorbed to the soil were the difference between the initial amount added and the amount remaining in the solution. The FT-IR spectra of original PGS and gemini modified PGS were recorded on a Bruker FT-IR spectrophotometer (Tensor 27, USA). The specific surface area was determined at 77 K with a TriStar II 3020 (Micromeritics, USA) using BET nitrogen gas sorption method. The pH measurements were conducted through a SevenEasy S20K pH meter (Mettler-Toledo, USA).

#### **5.2.6. Data Analysis**

All of the tests were conducted in duplicate and the typical error in the measurement was less than  $\pm 5\%$ . Sorption equilibrium data were fitted to the corresponding model. The gemini and PHE sorption data were analyzed through nonlinear regression using SigmaPlot 12.0 software (Systat Software Inc., CA, USA). The statistical analyses agreed within 95% confidence demonstrating the accuracy of measurements reported in this manuscript.

### **5.3. RESULTS AND DISCUSSION**

#### **5.3.1. Characterization of the Modified PGS**

First, the FT-IR analysis was performed to explore the interactions between gemini surfactants and PGS. The FT-IR spectra of PGS and modified PGS in the range of  $4000 \sim 400 \text{ cm}^{-1}$  are shown in Figure 5.1. The broad bands at the  $400 \sim 600 \text{ cm}^{-1}$  region are attributed to Si-O and Al-O bending vibrations (Zhao et al., 2015), while the stretching

vibration of Si-O groups is observed at the broad band around  $1000\text{ cm}^{-1}$ . The bands at  $3616\text{ cm}^{-1}$  are assigned to the OH stretching vibration, while the bands at  $1656\text{ cm}^{-1}$  are corresponded to OH bending vibration (Zhou et al., 2009). Compared to the original soil sample, the spectra of the modified soil samples shows two additional peaks at  $2855$  and  $2927\text{ cm}^{-1}$ , which are attributed to the C-H stretching vibration of alkyl chain due to the sorption of gemini surfactant (Liu et al., 2014). The characteristic sorption bands at  $1385$  and  $1468\text{ cm}^{-1}$  are assigned to the bending vibration of the C-H bonds of the gemini cations (Zhou et al., 2009; Liu et al., 2011). The results indicate that gemini surfactants have been successfully intercalated into the PGS layers and/or sorbed on the surface of solid samples (Xue et al., 2013).

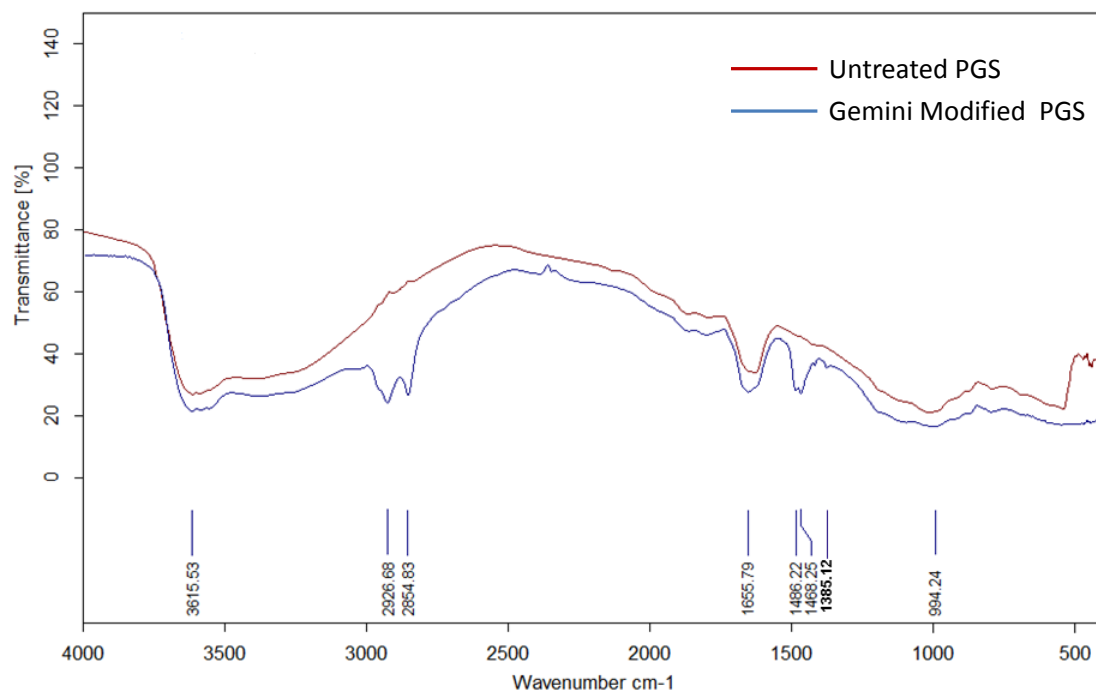


Figure 5.1 FT-IR spectra of untreated PGS and gemini modified PGS

### 5.3.2. Modeling of Gemini Sorption at the PGS/Aqueous Interface

To better understand the modification of PGS by cationic gemini surfactant, the sorption isotherms of gemini on PGS surface were further studied. As indicated in Figure 5.2, it was clear that the amount of the gemini surfactant sorbed on PGS increased sharply at low gemini dose. In the concentration range from 1.5 to 64.6 mg/L, the sorbed gemini amounts increased sharply from 12.1 to 177.9 mg/g. When the gemini concentration was above 70 mg/L, the sorbed amount increase continuously to the plateau value of 288.3 mg/g. The sorption data quantitatively verified that gemini surfactants had been sorbed on PGS.

As discussed in our previous studies (Zhao et al., 2015), electrostatic interaction would be one important mechanism for gemini sorption on natural soil. This mechanism could also contribute to the sorption of gemini surfactants on PGS due to the cation exchange in this process. The hydrophobic bonding between gemini surfactants' long hydrophobic tails also played a major role in the sorption process. In addition, considering the high polarities and large molecular weights, gemini surfactant may partition into PGS organic matter besides adsorbing onto the surface. As shown in Figure 5.2, it is interesting to note the isotherm can be divided into two steps. To gain a deep insight into the related sorption characteristic and mechanism, the sorption process was elucidated through the Two-step Adsorption and Partition Model (TAPM) we developed (Zhao et al., 2015):

$$Q = \frac{Q_{\max} K_1 C (\frac{1}{n} + K_2 C^{n-1})}{1 + K_1 C (1 + K_2 C^{n-1})} + K_p C \quad (5.1)$$

where  $C$  is the equilibrium concentration of the surfactant, mg/L; and  $Q$  is the sorption amount at concentration  $C$  and  $Q_{max}$  is the maximum adsorption amount at high concentrations, mg/g.  $K_1$  is the equilibrium constant of the first step (the predominant mechanism is electrostatic attraction, L/mg) and  $K_2$  is that of the second step (the predominant mechanism is hydrophobic interaction, L/mg);  $n$  is the hemimicelle aggregation number; and  $K_p$  is the partition coefficient due to the partition mechanism, L/g.

The developed TAPM was employed to interpret the isotherms of cationic gemini sorption on PGS surface. The calculated parameters based on experimental data are given in Table 5.3. The results indicated that the developed TAPM fitted well regarding the sorption data, as confirmed by the very high correlation coefficients  $R^2$ . The higher  $R^2$  ensured a satisfactory adjustment of the developed model to the experimental data. Cationic 12-2-12 gemini surfactant can strongly adsorb on the negatively charged PGS surface through electrostatic interaction ( $K_1$ ). The hydrophobic interaction between 12-2-12 gemini surfactants' hydrophobic tails also played a major role in the sorption process ( $K_2$ ). 12-2-12 gemini may partition into PGS organic matter and increase the sorption amount ( $K_p$ ). The  $K$  values corresponding to different forces varied in the sorption process. The  $K$  data exhibited that hydrophobic interaction was the major force in the sorption process due to its highest value.

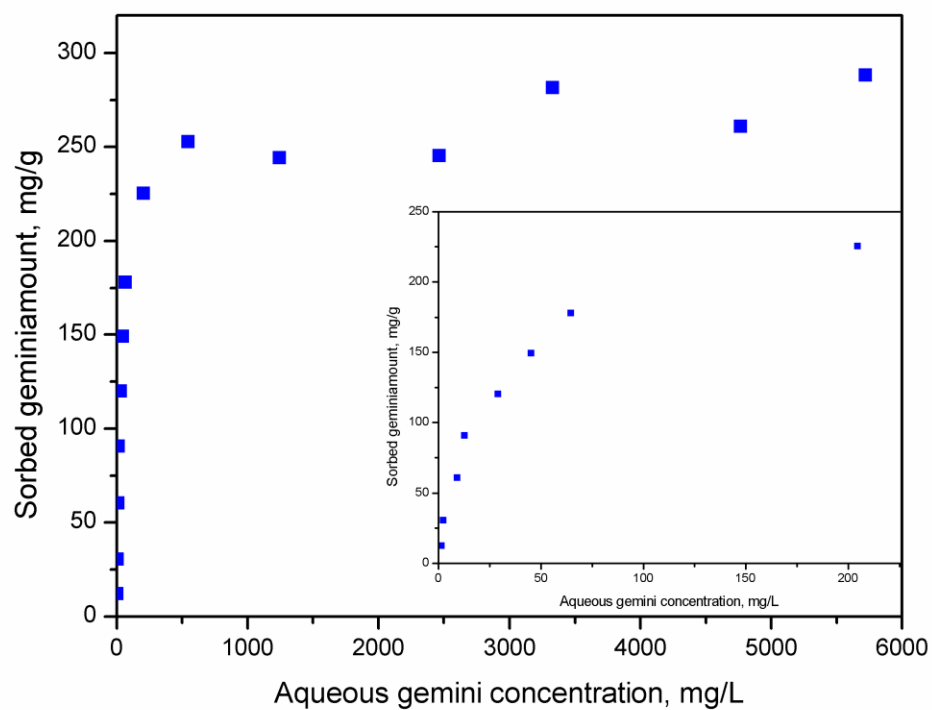


Figure 5.2 The sorption isotherms of 12-2-12 gemini surfactant at PGS/aqueous interface

Table 5.3 Parameters of TAPM for 12-2-12 gemini sorptionon PGS\*

$T$ (K)	$Q_{max}$ (mg/g)	$K_1$ (L/mg)	$K_2$ (L/mg)	$K_p$ (L/g)	$R^2$ (TAPM)
293	252.0	0.00317	12.9	0.00454	0.989

\*Error limits of parameters are less than  $\pm 3\%$ .

### 5.3.3. Effect of Initial pH on PHE Sorption

After the study of modification process, the performance of gemini-modified PGS for the removal of PHE was investigated. The effect of pH on the sorption of PHE onto PGS and modified PGS was studied through batch experiments at pH 3, 7, and 11. Figure 5.3 depicts that pH level can significantly affect the extent of sorption of PHE on PGS and modified PGS. Compared with the original PGS, the modified PGS showed a higher amount of PHE sorption over a narrow concentration interval. It indicates that PHE sorption on the modified PGS was more dependent on pH variation. It was observed that the maximum uptake of the PGS was at pH 11 while that of the modified PGS was at pH 3. Despite the sorption capacity of PHE on original PGS did not vary measurably between pH 3 and 7, an increase in the amount sorbed was observed with elevating pH from 7 to 11. At pH 11, the sorption amount was from 0.10 to 0.33 mg/g for different initial PHE concentration with the untreated PGS. In comparison, with the PGS modified by gemini surfactant, the maximum PHE sorption amount ranged from 0.15 to 0.45 mg/g at pH 3. Then the sorption decreased markedly from pH 3 to 7 at all given concentrations of PHE. Further increase of pH from 7 to 11 had less pronounced influence on the PHE sorption. This trend was consistent with the finding of the previous study in which Sarkar et al. (2012) reported that the sorption capacities of p-nitrophenol with organopalygorskites gradually decreased with the rising pH from 4.5 to 8.5.

The removal of a pollutant from the aqueous medium by sorption was highly dependent on the solution pH, which affected the surface charge of the sorbent and the degree of ionization of the sorbate (Sarkar et al., 2010). The  $\text{pH}_{\text{pzc}}$  of PGS and modified PGS was 7.0 and 7.9, respectively. The mineral surface would be covered with negative

charges when pH was higher than  $\text{pH}_{\text{pzc}}$ , and more negatively charged with the increasing pH value. PGS contained a large number of terminal silicate tetrahedra on the ribbons that were present on its external surface. These broken Si-O-Si bonds usually compensated for their residual charge by accepting a proton or a hydroxyl and thus convert to a Si-OH group (Sarkar et al., 2010). These groups were subjected to protonation at low pH or deprotonation at elevated pH (Zhang et al., 2011). This mechanism would affect the sorption sites for PAHs on sorbent surface.

Previous research on aromatic compound sorption mechanisms mainly focused on 2,4-D herbicide (Xi et al., 2010), atrazine pesticide (Rodríguez-Cruz et al., 2007b), phenol (Huang et al., 2007) and p-nitrophenol (Chang et al., 2009; Sarkar et al., 2010; Sarkar et al., 2012), etc. Three mechanisms applicable to PAHs sorption were proposed: the H-bonding formation, the electron donor-acceptor interaction and the  $\pi$ - $\pi$  interaction (Yuan et al., 2010). According to Fang et al. (2008), because PGS clay contained low amounts of humic substances (Table 5.2), mechanisms such as enhanced dipole interaction between the charged surface (electron acceptors) and PHE with electron-rich  $\pi$  systems (electron donors) might be the major cause of PHE sorption. Schwarzenbach et al. (2005) proposed that partitioning of nonionic organic compounds into the region near mineral surfaces could be one mechanism of PAHs sorption. Two explanations were suggested which were both quite speculative. First, portions of mineral surfaces of intermediate polarity (e.g., siloxane regions,  $-\text{Si}-\text{O}-\text{Si}-$ ) might permit some exchange of polar water and nonpolar organic sorbates. Another possibility was that organic sorbates could partition from the bulk aqueous solution into the “special” water immediately adjacent to solid surfaces or filling the nanometer-sized pores of these solids. Due to

interactions with the solid, water molecules near inorganic surfaces were more organized than corresponding molecules located in the bulk solution. Such surface-ordered water films, called vicinal water, might extend for nanometers away from the solid surface. The volume of this vicinal water per mass of sorbent was related to the intraparticle porosity and surface area.

These mechanisms were to some extent related to solution pH, resulting in a dependence of PAHs sorption on aqueous pH. Experimental data revealed that the amounts of PAHs sorbed by PGS and modified PGS increased and decreased, respectively, when the solution pH was raised from 3 to 11, suggesting the possible involvement of these mechanisms. The completely different trend for PHE sorption between PGS and modified PGS influenced by the solution pH could be attributed to the modification with gemini surfactant. The reduction in the amount sorbed at elevated pH values might be due to the interaction of surfactant molecules with PGS surface (Sarkar et al., 2012). Gemini surfactants might provide some unique surface characteristics to PGS as a new type of remediation material. The different PHE sorption performances at varied pH were influenced by the sorbed gemini surfactant, as well as the solid constitutes and other system conditions. The relative importance of the different mechanisms depended on the physical and chemical properties of the interactive sorbate-sorbent system.

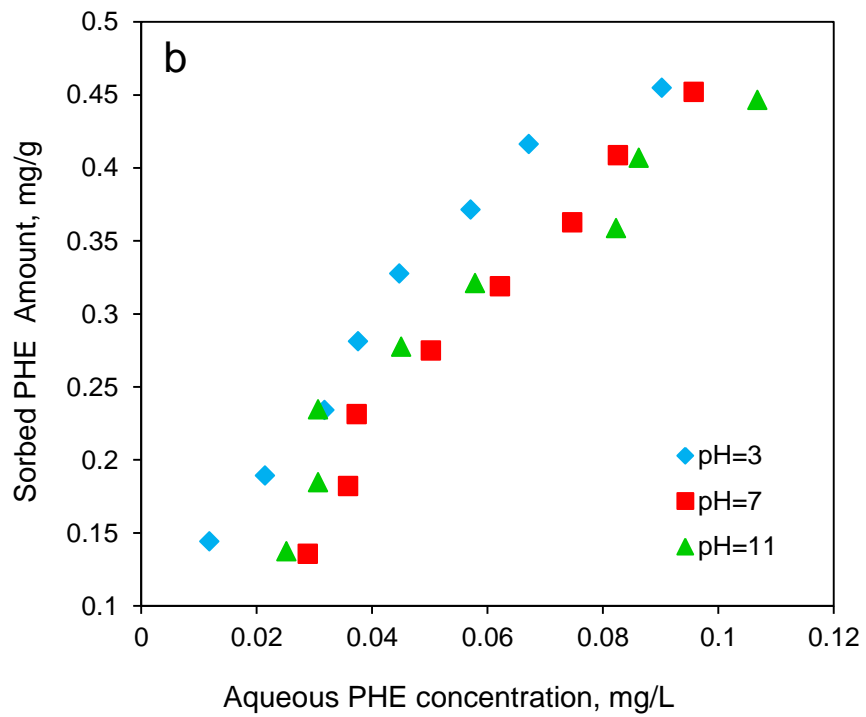
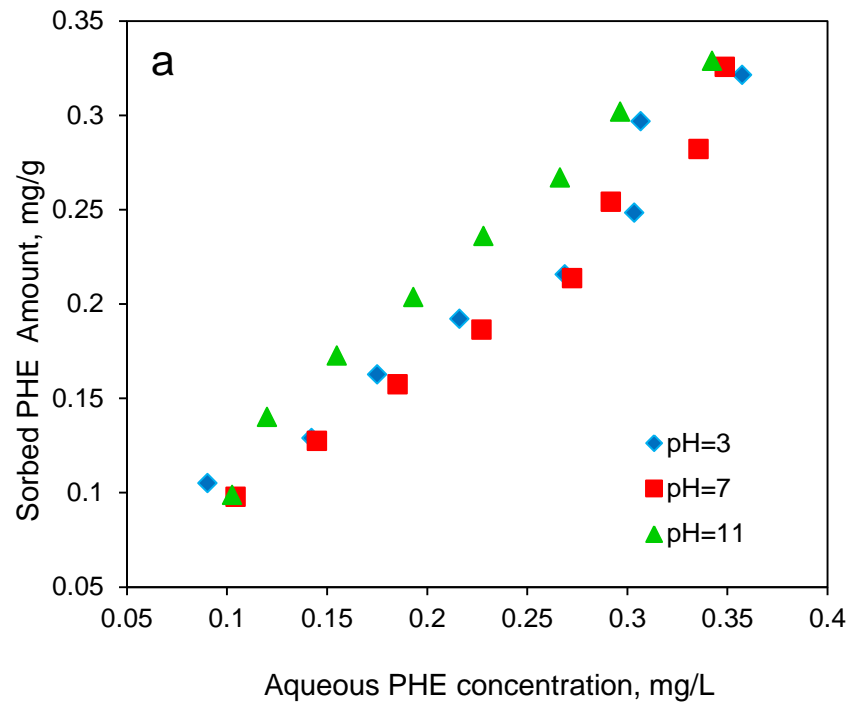


Figure 5.3 The sorption isotherms of PHE on (a) PGS and (b) modified PGS at different pH levels

#### 5.3.4. Effect of Organic Matter on PHE Sorption

Organic matter such as HA are ubiquitous in the aquatic environment and is closely related to the distribution and transport of PHE (An and Huang, 2012). Therefore, the effect of HA on PHE sorption to untreated PGS and gemini modified PGS as a function of HA dose (0 to 80 OC mg/L) was investigated. The initial PHE concentration was 0.5, 0.75, and 1 mg/L, respectively. The results indicated that the PHE sorption onto the sorbents in the presence of HA was significantly different from that in the absence of HA. Compared to untreated PGS, the sorption of PHE was enhanced by the PGS modified with gemini surfactants regardless of the initial concentration of PHE. For the modified PGS, the sorption of PHE increased at the low HA level and then decreased if more HA was added. Specifically, when the added dose of HA was less than 4 mg OC/L, the sorbed PHE amount varied from 0.44 to 0.46 mg/g (Figure 5.4f). However, the binding affinity of PHE to the modified PGS decreased with the further addition of HA. By gradually increasing HA concentration to 80 mg OC/L, the retention of PHE was inhibited from 0.46 to 0.41mg/g. A similar trend was also observed for the sorption of PHE on original PGS, except that the retention of PHE was enhanced again at the high HA dose. As indicated in Figure 5.4, when the initial PHE concentration was 0.5, 0.75, and 1 mg/L, the PHE uptake on PGS increased again with the HA dose of 60, 80, and 50 mg/L, respectively.

At a low HA dose, the initial PHE sorption increase was presumably due to the binding of PHE to HA along with the sorption of HA onto PGS/modified PGS surface, forming the complexation of sorbed HA with PHE (Radian and Mishael, 2012). This complexation improved the PHE sorption by PGS due primarily to the sorption of the

complexed HA to the clay sorbents. The sorption of HA on PGS has been also investigated (Wang et al., 2011b). HA can be sorbed onto clay minerals through mechanisms such as electrostatic interaction, hydrophobicity, van der Waals forces, and hydrogen bonding. In addition, hydrophobic interaction was reported as the main factor responsible for the binding of PAHs to HA (An and Huang, 2012). This process could also be produced by the  $\pi$ - $\pi$  interactions between PHE and humic substance acceptor groups in aqueous solvents (Zhu et al., 2004). The interactions among HA, PHE, and the sorbent provided more preferential binding sites for PHE sorption at the solid/aqueous interface. As a whole, the PHE retention would be enhanced via the HA-PHE complexation with the increasing retention of HA by PGS. The presence of HA at the low concentration contributed to the uptake of PHE due to the cosorption of HA and PHE complex on the sorbent surface. This is in accordance with the known influence of HA on rare earth elements sorption to kaolin at low HA concentration (Wan and Liu, 2006).

At higher HA concentrations, the PHE sorption decreased with increasing HA concentration. Several factors might cause the substantial drop in the sorption of PHE by PGS/modified PGS in the presence of HA. First, with the increasing dose of HA, the sorbent surface would present a higher selectivity towards HA and thus inhibit PHE sorption due to the steric crowding mechanism (Bouras et al., 2010). Wang et al. (2009b) reported that PHE sorption by multiwalled carbon nanotubes would be markedly suppressed in the presence of HA. Instead of cosorption, the HA molecules would hinder PHE retention through competition for limited sites on PGS surface. Second, with the increasing dose of HA, a great number of sorption sites on the sorbent surface may be blocked by the HA molecules due to the large molecular size. It was reported that the

sorption of HA would mask many sorption sites on sorbent surfaces due to surface coverage and pore blockage (Wang et al., 2009b). A portion of large HA molecules would occupy the entrances to pores of sorbents that were large enough to accommodate PHE molecules, thus reducing the accessibility of PHE molecules to sorption sites and reducing the PHE sorption on sorbent surface. This is consistent with an early study, where the decrease of the surface area and pore volume data implied that some micropores were blocked by the sorbed HA and the availability of sorption sites for pentachlorophenol sorption was reduced (Lou et al., 2013). Third, the solute properties (molecular size, hydrophobicity, etc.) played an important role in the interactions among HA, PHE, and the sorbents. The large molecular size of PHE offered HA a relatively strong steric restriction to prevent PHE molecules from approaching and further interacting with the sorbents. The high hydrophobicity of PHE facilitated its solubilization into the hydrophobic HA molecules in solution and hindered the PHE retention on sorbents. Fourth, since the distribution of PHE was closely related to the sorption pattern of HA, the reduction of PHE sorption could be explained by the changes in physicochemical properties of the HA molecules and the sorbent surfaces. The  $\text{pH}_{\text{PZC}}$  values of untreated PGS and modified PGS were 7.0 and 7.9, respectively. Under the test pH, the sorbent surfaces would be negative charged. Similarly, the sorbed HA molecules would have a negative charge owing to the deprotonation of carboxyl groups or phenolic groups along the HA chain (Wang et al., 2011b; An and Huang, 2012; Lou et al., 2013). Therefore, the binding between HA and the sorbent surface would be compromised due to the electrostatic repulsive force. Consequently, the HA sorption on sorbent decreased and more HA molecules would enter the aqueous phase. Because HA is more

hydrophobic than water, HA had a higher sorption affinity to PHE. This would also result in the enhanced PHE solubility in solution and thus reduced PHE sorption from sorbents. This phenomenon revealed that HA was mainly distributed in aqueous phase with similar function to known surfactants, enhancing the solute solubility and suppressing its sorption on solids at certain circumstances.

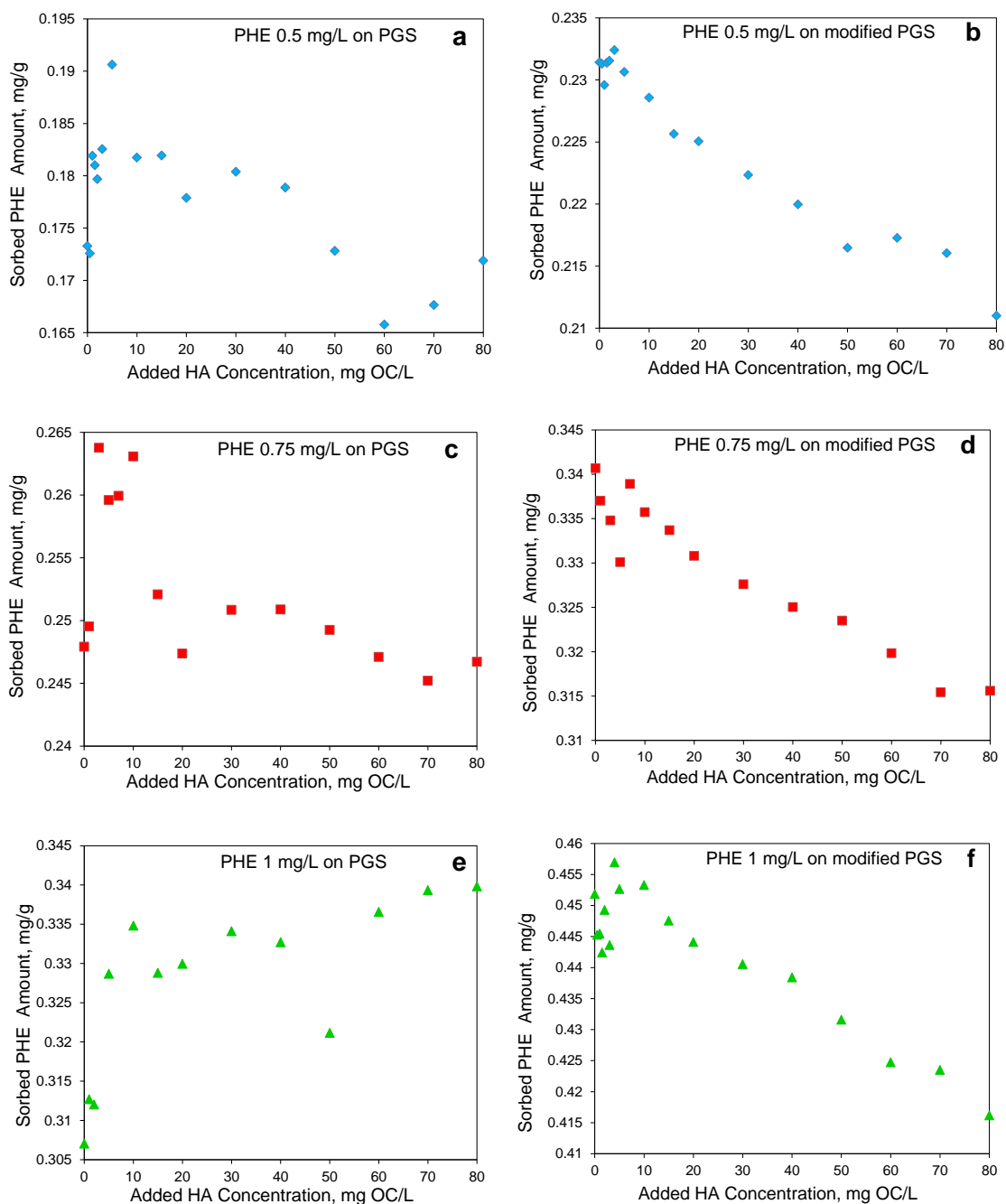


Figure 5.4 The sorption isotherms of PHE on (a) PGS, initial PHE concentration 0.5 mg/L; (b) modified PGS, initial PHE concentration 0.5 mg/L; (c) PGS, initial PHE concentration 0.75 mg/L; (d) modified PGS, initial PHE concentration 0.75 mg/L; (e) PGS, initial PHE concentration 1.0 mg/L; and (f) modified PGS, initial PHE concentration 1.0 mg/L with the addition of HA from 0 to 80 mg/L

### 5.3.5. Effect of Ionic Strength on PHE Sorption

The effect of solution ionic strength on the sorption of PHE on PGS and modified PGS was evaluated at PHE from 0.3 to 1.0 mg/L, ionic strength from 0.01 to 1M, and a constant pH of 7 (Figure 5.5). The modification of PGS by gemini surfactant lowered the PHE equivalent concentration while shifted the sorption isotherms toward higher sorption levels. The PHE sorbed amounts were found to increase significantly with increasing NaCl concentration from 0.01 to 1 M for PGS and modified PGS. It could, to a certain extent, be explained by the “salting-out” effect, which referred to the reduced solubility of organic compounds in aqueous salt solutions (Xie et al., 1997; Ko et al., 1998). PHE is a nonionic compound and the sorption was partially due to hydrophobic interaction mechanisms. This decrease in solubility caused an increase in the sorption capacity of the sorbents due to an increasing hydrophobic interactions induced by the increase of ionic strength (Zhang et al., 2010a). It was reported that a more organized water structure around the cations would be created in the presence of the salt ions, which required more cavity energy for PAHs to dissolve in salt solution than in regular water (Qian et al., 2011). This could cause a decrease of the activity coefficients of PAHs in aqueous phase, and consequently an increase of sorbed amount of PHE.

For PGS, the sorption was enhanced when the ionic strength was increased from 0.01 to 0.1 M. For the modified PGS, the sorption affinities were not influenced by the variance in the ionic strength between 0.01 and 0.1M. Interestingly, the effect of low to medium ionic strength on PHE sorption by sorbents was less prominent in case of gemini modified PGS than in the untreated PGS. This phenomenon could be attributed to the following two reasons: 1) The structure of the surfactant molecules and their orientation

in the clay structure modified the clay properties. The conformation of the gemini surfactant molecules endowed the modified PGS with different surface charge and therefore, the effects of ionic strength on PHE sorption behavior was different (Xi et al., 2007). 2) The increase of ionic strength might also change the aggregation state of modified PGS. For the modified PGS, addition of NaCl from 0.01 to 0.1 M had negligible effect on the sorption of PHE, suggesting that: i) within the ionic strength range of 0.01 ~ 0.1M, the contribution of salting-out effect to PHE was equivalent to that of the squeezing-out effect to modified PGS; or ii) both the salting-out effect and squeezing-out effect were too weak to exert any change in the sorption of PHE on the modified PGS (Zhang et al., 2010a).

Generally, the amount of PHE sorbed by PGS and modified PGS increased with the increasing salt concentrations at a given PHE concentration. The addition of more salt ions, therefore, can enhance the retention of PHE on solid phase. This is of special interest for treatment of PAHs-contaminated water through modified PGS with high salinity level.

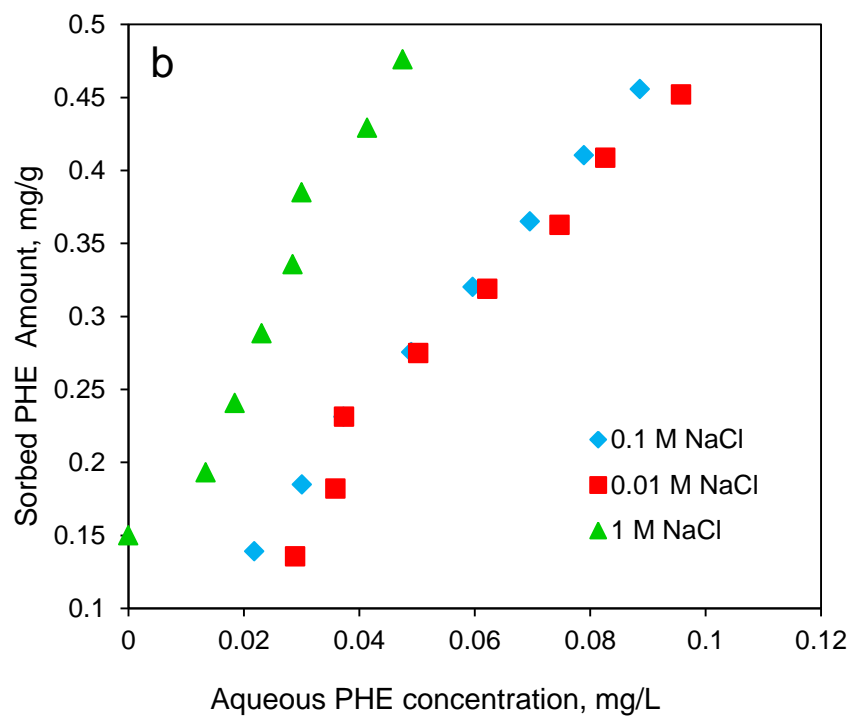
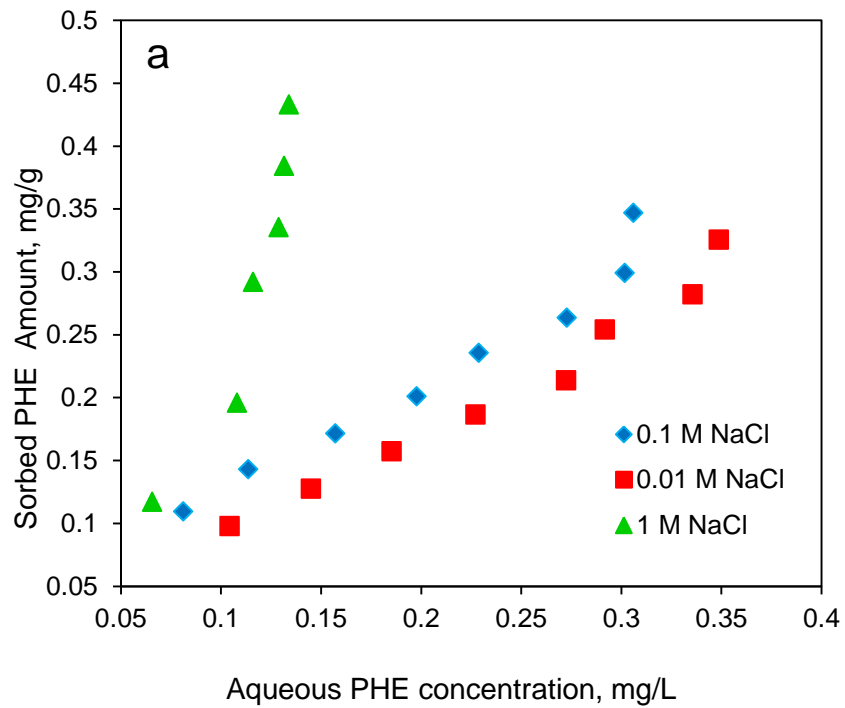


Figure 5.5 The sorption isotherms of PHE on (a) PGS and (b) modified PGS at different ionic strength levels

### 5.3.6. PHE Sorption Isotherms

The developed TAPM model is particularly effective for elucidating the sorption behavior of ionic surfactants, due primarily to the electrostatic interactions between the ionic surfactants and the solid surface. Therefore, TAPM model are not applicable for elaborating the sorption process of PHE because PHE is one type of nonionic compounds. Instead, Freundlich isotherm equation (Equation (5.2)) was employed to investigate the sorption process of PHE on PGS and modified PGS.

$$\log Q_e = \log K_F + \frac{1}{n} \log C_e \quad (5.2)$$

where  $C_e$  is the equilibrium concentration of PHE in solution and  $Q_e$  is the corresponding PHE sorption amount on solids;  $K_F$  and  $1/n$  are the Freundlich constants related to the sorption capacity and the sorption intensity, respectively. The magnitude of the exponent  $1/n$  gives an indication of the favorability of sorption (Huang et al., 2008). Generally, if the values of  $1/n$  are in the range of 0.1 ~ 1, it represents favorable sorption. As indicated in Figure 5.6, the sorption isotherms of PHE at different temperatures were studied. Interestingly, the sorption capacity of PHE on PGS increased with the elevating temperature from 293 to 303 K, while that on modified PGS decreased with the increasing temperature. The selective sorption of tannin from flavonoids by organically modified attapulgite clay at different temperatures exhibited the similar trend (Huang et al., 2008), while the sorption behaviors of p-nitrophenol by anion–cation modified PGS were different (Chang et al., 2009).

The isotherm parameters and the correlation coefficients  $R$  were calculated and listed in Table 5.4. The results indicated that the PGS/modified PGS-PHE sorption

system could be well explained by the Freundlich isotherm with a high degree of fitness. The high value of correlation coefficient indicated a good agreement between the model parameters and the data. It is evident from the  $1/n$  values that the sorption processes of PHE on PGS/modified PGS were favorable. In addition,  $K_F$  values depicted that the sorbents studied had high sorption affinity for PHE. Freundlich isotherm has been widely applied to the sorption process on heterogeneous surface. The well fit of data to Freundlich model might indicate that the sorbents used in the present work were of surface energy heterogeneity. Previous studies also reported the satisfactory fitting of Freundlich equation to the sorption isotherms of organic contaminants on organopalygorskites (Huang et al., 2007; Huang et al., 2008; Sarkar et al., 2010), carbon nanotubes (Zhang et al., 2010a), and soils (Ping et al., 2006), etc.

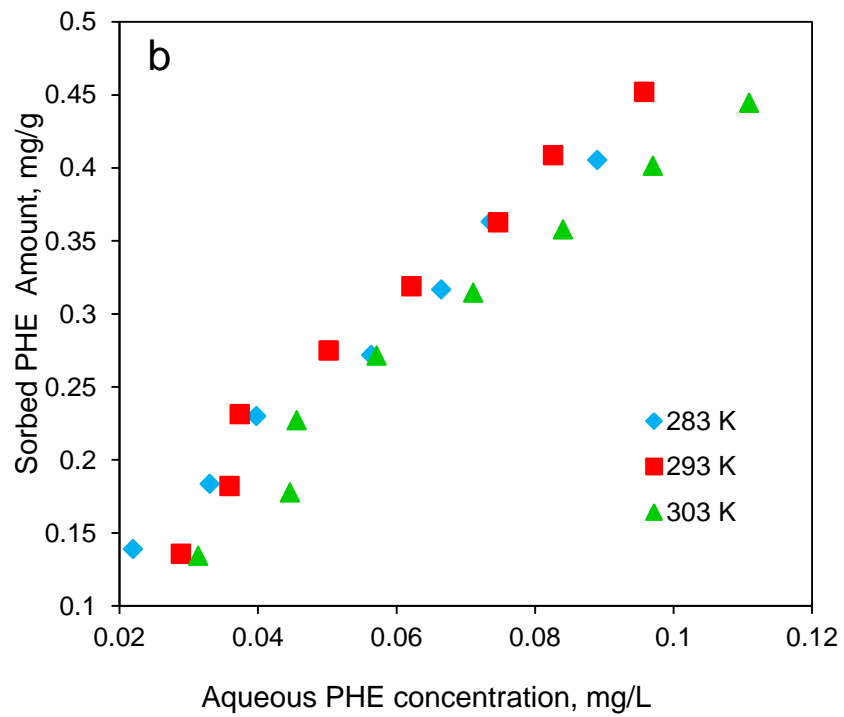
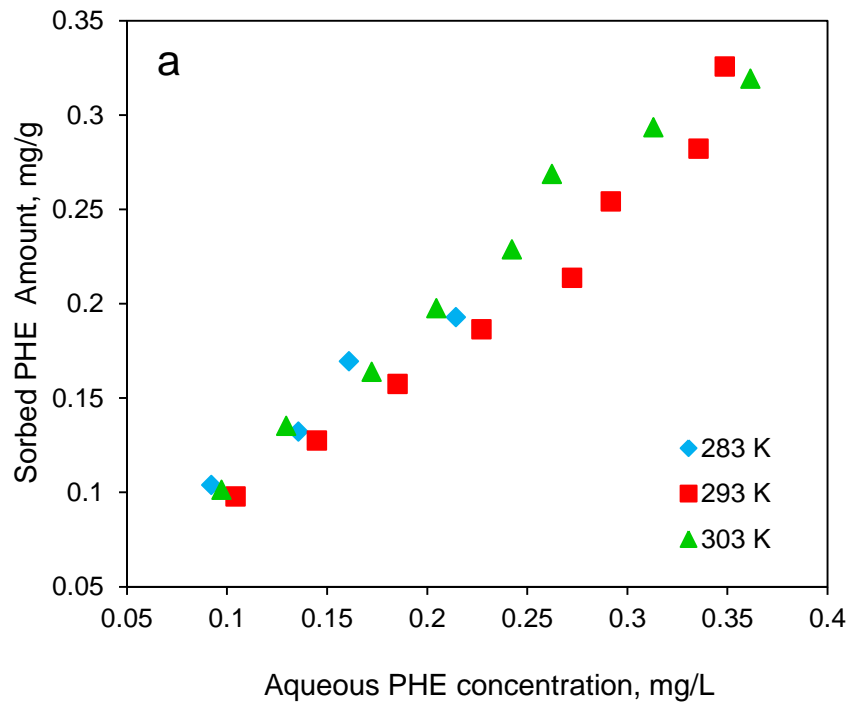


Figure 5.6 The sorption isotherms of PHE on (a) PGS and (b) modified PGS at different temperatures

Table 5.4 Freundlich isotherm parameters for the sorption of PHE on PGS and modified

PGS\*

Sample	$T$ (K)	$K_F$ (mg/g)(L/mg) <sup>1/n</sup>	$n$	$R$
PGS	283	0.622	1.335	0.980
	293	0.909	0.960	0.986
	303	0.804	1.140	0.993
Modified PGS	283	2.653	1.289	0.995
	293	3.505	1.153	0.988
	303	3.106	1.142	0.989

\*Error limits of parameters are less than  $\pm 3\%$ .

### 5.3.7. Thermodynamic Studies of PHE Sorption

The above results showed that temperature is an essential factor in the sorption process. From the thermodynamic point of view, the sorption behavior can be measured by the Gibbs free energy of the sorption process,  $\Delta G$  (KJ/mol) given by the following expression (An and Huang, 2012):

$$\Delta G = -RT \ln K \quad (5.3)$$

where  $R$  and  $T$  are the universal constant of the gases (8.314 J/(mol ·K)) and the absolute temperature (K).  $K$  is the equilibrium constant related to the Freundlich constant  $K_F$  obtained from the sorption isotherms. Equilibrium constants  $K$  are also widely used to calculate thermodynamic parameters such as the enthalpy change ( $\Delta H$ , KJ/mol), and the entropy change ( $\Delta S$ , KJ/(mol ·K)) through the following equations:

$$\ln K = -\frac{\Delta H}{TR} + \frac{\Delta S}{R} \quad (5.4)$$

$$\Delta G = \Delta H - T\Delta S \quad (5.5)$$

The calculated  $\Delta G$ ,  $\Delta H$  and  $\Delta S$  are listed in Table 5.5.  $\Delta H$  and  $\Delta S$  were calculated from values of 293 and 303 K. The negative  $\Delta G$  values indicated the sorption process of PHE on modified PGS was a spontaneous process. However, the sorption of PHE on untreated PGS did rely on gaining energy from an external source due to the positive  $\Delta G$  values (Sarkar et al., 2012). The difference may be due to the modification of PGS with gemini surfactants. The  $\Delta H$  value was negative, indicating the sorption of PHE on modified PGS was an exothermic process when temperature rising from 293 to 303 K.

This is consistent with our previous studies, where the sorption of gemini on soil was an exothermic process when rising the temperature from 283 to 303 K (Zhao et al., 2015). The modification offered PGS with the thermal properties of gemini surfactant. The negative entropy change corresponded to a decrease in the degree of freedom of the sorbed species in the modified PGS-PHE system (Sarkar et al., 2012).

Table 5.5 Thermodynamic parameters for PHE sorption on PGS and modified PGS\*

Sample	$T(K)$	$\Delta G(KJ / mol)$	$\Delta H(KJ / mol)$	$\Delta S(KJ / (mol \cdot K))$
PGS	283	1.117		
	293	0.232	-9.060	-0.032
	303	0.550		
Modified PGS	283	-2.296		
	293	-3.055	-8.920	-0.020
	303	-2.855		

\*Error limits of parameters are less than  $\pm 3\%$ .

## 5.4. SUMMARY

(1) The effectiveness of gemini modified PGS as the novel remediation material in PAHs contaminated water remediation was revealed and examined.

(2) The FT-IR spectra confirmed the sorption of gemini surfactants on PGS surface, and the developed TAPM well simulated the sorption behavior of gemini surfactant on PGS.

(3) The modification of PGS with gemini surfactants provided a favorable partition medium for PHE and enhanced PHE retention in solid particles. The sorption isotherms of PHE on PGS surface at different temperatures well fitted the Freundlich equation.

(4) The chemical structure of the gemini surfactant molecules and their orientation in the clay structure might have modified the clay surface properties. Specifically: (a) The maximum PHE uptake by PGS occurred at high pH level, while that of the modified PGS was at acidic condition. (b) The competitive sorption between PHE and HA was one of the major sorption mechanisms that caused the reduction of PHE sorption on modified PGS in the presence of HA. (c) The sorption of PHE on modified PGS was an exothermic process when temperature increased from 293 to 303 K. (d) Modifying PGS with gemini surfactants mitigated the effects of ionic strength on PHE sorption.

(5) It is revealed that the modification with gemini surfactants probably offered some unique surface characteristics to the clay mineral as a new type of remediation material. This can provide a reference to the potential application of PGS in PAHs contaminated water remediation process.

(6) Future studies will be conducted to explore the role of gemini surfactants in enhancing PHE sorption on PGS. The mechanisms regarding how gemini affects the

surface characteristics of PGS and further the sorption behaviors of PHE will be explored. The combined effects of aqueous solution parameters on the sorption process will be investigated through factorial design techniques.

# **CHAPTER 6**

## **INSIGHT INTO SORPTION MECHANISM OF PHENANTHRENE ONTO GEMINI MODIFIED PALYGORSKITE THROUGH A MULTI-LEVEL FUZZY- FACTORIAL INFERENCE APPROACH**

### **6.1. BACKGROUND**

PAHs are a group of persistent hydrophobic contaminants with two or more fused benzene rings from natural as well as anthropogenic sources (Zhu et al., 2003). It can transport and be accumulated in groundwater and surface water for a long period of time, and are difficult to biodegrade. Sorption of PAHs to solid phase has a major influence on its transport, bioavailability, and fate in natural aquatic environments.

Palygorskite (PGS) has received emerging interest as a potential alternative to the conventional sorbents from both the environmental and the economic points of view. Due to its high surface area and superior structural properties, palygorskite has been used as a promising sorbent for heavy metals (Chen and Wang, 2007; Chen et al., 2007). In addition, the surface charge and cation exchange capacity of palygorskite enables it to be modified by surfactants. The organo-modification can increase the organic matter content in palygorskite and enhance its sorption capacity and affinity for organic pollutants. For example, the sorption capacity of palygorskite for phenol (Huang et al., 2007) and p-nitrophenol (Chang et al., 2009; Sarkar et al., 2012) can be largely enhanced when modifying it with some conventional cationic surfactants. Especially the long-chain organic surfactant can markedly modify the solid surface with increasing hydrophobic

characteristics (Chang et al., 2009). Cationic Gemini surfactants, as a series of relatively novel surfactants type, received substantial interest in academic and industrial fields (Wei et al., 2011b). Containing two hydrophilic heads and two long hydrophobic tails in the molecule, gemini has large molecular weight and can endow solids with significantly higher organic contents. The sorbed surfactants can act as an effective organic medium for for sorbing nonpolar or weakly polar organic pollutants (Zhu et al., 2003). In addition, the enhanced soil retention of PAHs with the addition of gemini surfactants has been demonstrated (Zhao et al., 2015). However, limited data has been reported on the modification of palygorskite with gemini surfactants for the remediation of PAHs in aqueous phase. An improved understanding of the capability of gemini modified palygorskite as specific sorbent for PAHs removal and the mechanisms involved are required.

Aqueous parameters such as initial concentration, pH, ionic strength, temperature, and dissolved organic matter have been identified as essential factors influencing organic contaminants' behaviors at solid/aqueous interface (Ko et al., 1998; Zhang et al., 2010a). These environmental factors are often fuzzy in nature and cannot be determined precisely; their values are decided upon experimenters' experiences or subjective estimates that can be expressed as fuzzy sets. The vertex method proposed by Dong and Shah (1987) is recognized as an effective tool for tackling fuzzy sets based on the  $\alpha$ -cut concept and interval analysis. In addition, during a classical experiment, only one factor can be studied each time with all the other variables being constant. This can hardly reveal the potential interactions among factors on response variables. Factorial design of experiments has been proposed to estimate the overall main factor effects and interactions

of different factors. The most important advantages are that not only the effects of individual parameters but also their relative importance in given process are obtained and that the interaction effects of two or more variables can also be revealed (Seki et al., 2006).

Two-level factorial design techniques have been widely applied in the sorption studies (Kavak, 2009; Zhao et al., 2009). For example, to investigate the biosorption of reactive red RGB from water solution on rice husk treated with nitric acid, factorial design was employed to study the effect of four factors pH, temperature, adsorbent dosage and initial concentration of the dye at low and high levels (Ponnusami et al., 2007). For the process optimization of adsorption of Cr(VI) on activated carbons, the main and interactive effects of four different environmental factors like pH, initial concentration, adsorbent dose, and temperature are investigated through the model equations designed by a two-level full factorial design (Gottipati and Mishra, 2010). To study the adsorption of gallium(III) on bentonite from aqueous solutions, an test was carried out using a  $2^3$  factorial design indicated that pH and mass of bentonite have a positive effect, whereas temperature has negative effect (Chegrouche and Bensmaili, 2002). All these studies took advantage of the two-level factorial design assuming that the contaminant sorption process was linear over the range of factor levels. However, sorption isotherms generally involve a highly nonlinear relationship between experimental factors and the sorption capacity. The two-level factorial experiment can hardly reveal the curvature effects (Wang et al., 2013b; Wang and Huang, 2015). The concept of multi-level factorial designs is thus proposed in this study to detect the curvature in sorption isotherms (Ozbay and Yargic, 2015; Un et al., 2015). Moreover, the

investigated factors are often determined subjectively, with each at fixed levels of interest. Fuzzy set theory is a powerful tool for representing the experimenter's subjective judgments on design factors. Thus, combining the multi-level factorial designs with fuzzy set theory is a sound strategy for not only determining experimental factors effectively, but also detecting the curvature effects of factors and their interactions on response variables.

The objective of this study is to propose a multi-level fuzzy-factorial inference approach for characterizing the curvature effects of environmental factors and their potential interactions, enhancing our understanding of the sorption behavior of phenanthrene on palygorskite modified with a gemini surfactant. Five experimental factors, including initial phenanthrene concentration (factor A), added HA dose (factor B), ionic strength (factor C), temperature (factor D), and pH (factor E) will be studied. Fuzzy vertex analysis will be employed to discretize design factors with triangular membership functions into multiple deterministic levels based on the  $\alpha$ -cut concept and interval analysis. Multi-level factorial ANOVA will be performed to identify the main effects of factors and their interactions on PAHs sorption to modified PGS. Compared to conventional the two-level factorial design technique, the proposed approach can better elucidate the sorption mechanism through detecting the curvature effects of factors and examining their potential interactions in the sorption process.

## **6.2. MATERIALS AND METHODS**

### **6.2.1. Materials**

Phenanthrene (PHE) was selected as the representative PAH, and was purchased

from Sigma Aldrich Chemical Co. (WI, USA) with the purity greater than 99%. Cationic gemini surfactant (N1-dodecyl-N1,N1,N2,N2-tetramethyl-N2-octylethane-1, 2-diaminium bromide, 12-2-12) was obtained from Chengdu Organic Chemicals Co., Ltd. (Sichuan, China), with a purity of 98%. The molecular structures and properties of PHE and surfactants are given in Table 5.1. Humic acid (HA) was purchased from Sigma (WI, USA).

Palygorskite was obtained from Huaiyuan Mining Co. Ltd (Jiangsu, China). Dried palygorskite (20 g) was mixed with 200 mL of aqueous solution containing 0.4 g of gemini surfactant. The mixture was stirred at 333 K for 3 h. It was then filtrated and washed with deionized water until the liquid was bromide free. After dried at 343 K and activated for 1 h at 378 K, gemini modified palygorskite (GPGS) was obtained through mechanically whetted to 100 meshes with a mortar pestle. The sieved solid was homogenized as much as possible and stored in glass containers. The physical and textural characteristics of GPGS are given in Table 5.2.

### **6.2.2. Sorption Studies**

The batch sorption experiments were conducted in 20 mL glass vials with 20 mg GPGS. The appropriate amount of deionized water was added corresponding to different PHE initial concentration. The background solution contained pre-determined volumes of NaCl solution. Then a pre-calculated volume of PHE stock solution was added to each vial. The vials were sealed with Teflon-lined screw caps and were vortexed for 20 s, and then were placed in a reciprocal shaker (SHKE5000, Thermo Scientific, USA) at 283/293/303 K and 200 rpm for 24 h to reach the sorption equilibrium. Preliminary

experiments showed that 24 h were sufficient for the sorption process to reach equilibrium and the experimental loss of PHE was negligible. Before testing, the samples were subsequently centrifuged at 5000 rpm (Multifuge X1R, Thermo Scientific, USA) for 30 min and 10000 rpm (Promo Legend Micro 21, Thermo Scientific, USA) for 10 min to separate GPGS from solution. An appropriate aliquot of supernatant was then carefully withdrawn with a volumetric pipette to further determine the residual amount of PHE. For detailed procedures, please also refer to previous studies (Yu et al., 2011a; Zhao et al., 2011a; An and Huang, 2012; Wei et al., 2013).

PHE was analyzed using HPLC. The HPLC instrument, an Agilent 1260 Infinity LC System (USA), was equipped with vacuum degasser, binary pump, autosampler, thermostated column compartment (set to 303 K), diode array detector (DAD), and ZORBAX Eclipse PAH column (3.5  $\mu\text{m}$  particle size, 4.6 mm  $\times$  150 mm ID). A mobile phase consisting of acetonitrile/water (75:25, v/v) was used at a flow rate of 1.0 mL/min. PHE was monitored with DAD at 250 nm. The amount of PHE sorbed to the sorbent was the difference between the initial amount added and the amount remaining in the solution. The pH measurements were conducted through a SevenEasy S20K pH meter (Mettler-Toledo, USA).

### **6.2.3. Fuzzy Set Theory**

In many engineering systems, there is pervasive fuzzy information, i.e., information which is vague, imprecise, qualitative, linguistic or incomplete. This kind of information plays an important role in decision-making process. When one is conducting sorption experiments, the experimental parameters are often fuzzy in nature, such as the

contaminant initial concentration, aqueous organic content, ionic strength, temperature, pH and so forth. Generally, these parameters can be hardly determined with certainty; instead, they are often decided upon by experimenters' experiences and subjective estimates that can be expressed as fuzzy sets.

Fuzzy set theory is an effective means of expressing experimenters' subjective judgments in practical problems. A fuzzy set  $N$  in  $X$  is characterized by a membership function  $\mu_N$ , where  $X$  represents a space of points (objects), with an element of  $X$  denoted by  $x$ . The  $\mu_N(x)$  represents the membership grade of  $x$  in  $N$ :  $\mu_N(x) \rightarrow [0, 1]$ , where  $\mu_N(x)$  can be viewed as the plausibility degree of  $N$  taking value  $x$ . The closer  $\mu_N(x)$  is to 1, the more likely it is that an element  $x$  belongs to  $N$ ; conversely, the closer  $\mu_N(x)$  is to 0, the less likely it is that  $x$  belongs to  $N$ . Zadeh (1999) defined a possibility distribution associated with  $N$  as numerically equal to  $\mu_N$ . For a linear case, fuzzy subset  $N$  can be defined as the following general format (Cai et al., 2009):

$$\mu_N(x) = \begin{cases} 0, & \text{if } x < \underline{a} \text{ or } x > \bar{a} \\ 1, & \text{if } x = m \\ 1 - \frac{2|m-x|}{\bar{a}-\underline{a}}, & \text{if } \underline{a} \leq x \leq \bar{a} \end{cases} \quad (6.1)$$

where  $[\underline{a}, \bar{a}]$  is an interval imposed by fuzzy set  $N$ .

The well-known vertex method, which is based upon the  $\alpha$ -cut concept and interval analysis, can be used for computing functions of fuzzy variables (Dong and Shah, 1987).  $\alpha$ -cut is a discretization technique on membership value domains of variables instead of on variable domains themselves. By doing so, the abnormality can be avoided compared to the conventional discretization on variable domains. The vertex method greatly

facilitates the implementation of interval calculation and prevents the widening of the function value set due to multi-occurrences of a variable. This method could be applied to many engineering and experimental practice. Moreover, fuzzy sets do not exist independently; instead, they are correlated with each other, and have different effects on response variables. Therefore, factorial analysis can be used to reveal potential interactions among fuzzy variables.

#### **6.2.4. Multi-Level Factorial Analysis**

Multi-level factorial analysis is a powerful statistical technique to study the effects of several independent variables (factors) with multiple levels on a dependent variable (response). It comprises the greater precision in estimating the overall main factor effects and interactions of different factors. Multi-level factorial design is particularly useful when there is a curvilinear relationship between the design factors and the response. In full factorial designs, an experimental run is performed at every combination of factor levels. The sample size is the product of the number of levels of the factors. Specifically, the two-level factorial design has a sample size that is a power of two,  $2^k$ , where  $k$  is the number of factors; the multi-level factorial design with  $s > 2$  has a sample size  $s^k$ , where  $s$  is the number of levels for each factor.

The most important case of the multi-level factorial design is the  $3^k$  factorial design which consists of  $k$  factors with each at three levels. The three levels of factors are represented as low, medium, and high; they are often denoted by  $-1$ ,  $0$ , and  $+1$ , respectively. For example, The  $3^2$  factorial design has two factors with each at three levels, which requires nine treatment combinations. If there are  $n$  replicates,  $n(3^2)$

experiments should be carried out. The total variation of the  $3^2$  design includes the sum of the squares of the A main effect, B main effect, AB interaction and error. Each main effect can be represented by a linear and a curvature component. The  $3^k$  design provides an opportunity to assess the curvilinear relationship between the response and factors (Un et al., 2015).

In real-world problems, nevertheless, the investigated factors may be given as fuzzy sets instead of the standard representation of design factors with fixed levels, resulting in the difficulty addressing such a complexity. It is thus desired to integrate the  $3^k$  factorial design and fuzzy set theory within a general framework, leading to a multi-level fuzzy-factorial inference approach.

In the sorption experiment, the environmental factors largely fell between the following intervals, though they were less likely to reach the boundary values:

$$A = [0, 1.2], B = [0, 80], C = [0, 1], D = [273, 313], E = [0, 14]$$

Figure 6.1 presents the five factors in the format of fuzzy sets with triangular membership functions. Two values were selected for  $\alpha$ , 0.5 and 1.0, respectively. When  $\alpha = 0.5$ ,

$$A_{0.5} = [0.4, 1.0], B_{0.5} = [2, 42], C_{0.5} = [0.05, 0.55], D_{0.5} = [283, 303], E_{0.5} = [3.95, 10.95]$$

Through fuzzy vertex method, the fuzzy sets were discretized into intervals at  $\alpha = 0.5$ . For each parameter, the lower and upper bound were defined as the low level and the high level of the corresponding factors in the multi-level factorial design, respectively.

When  $\alpha = 1.0$ , all intervals degenerated to real numbers:

$$A_{1.0} = 0.8, B_{1.0} = 4, C_{1.0} = 0.10, D_{1.0} = 293, E_{1.0} = 7.90$$

According to the preliminary experiments, these points were mostly concerned and were selected as the midpoints in the factorial design.

Three levels of each parameter were obtained through the fuzzy vertex method, as indicated in Table 6.1.  $3^5 \times 2 = 486$  experiments with all possible combinations of variables were conducted in duplicate. The typical error of the measurement was less than  $\pm 5\%$ . The statistical significance of individual and interaction effects of the experimental factors was checked by the Fisher  $F$ -test, and model terms were evaluated by the  $p$ -value with 95% confidence level. In the next section, a multi-level factorial design will be conducted to elucidate the main effects of factors and their interactions in the sorption process.

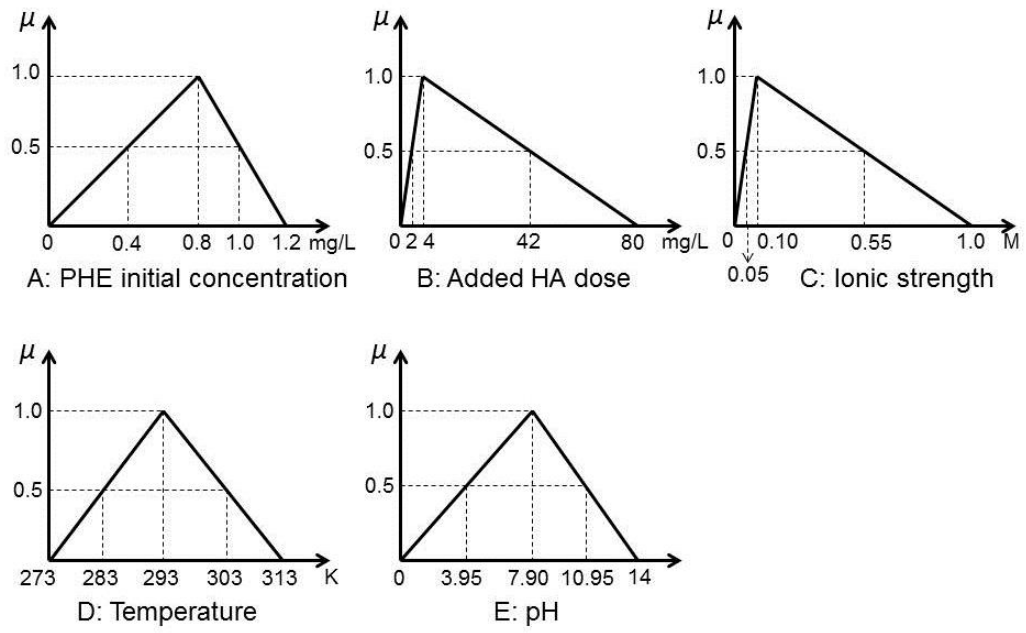


Figure 6.1 Sorption data expressed as fuzzy sets with triangular membership functions

Table 6.1 Experimental factors at low, high, and medium level

Symbol	Factor	Level		
		Low (-1)	Medium (0)	High (+1)
A	Initial PHE concentration, mg/L	0.4	0.8	1.0
B	Added HA dose, mg/L	2	4	42
C	Ionic strength, M	0.05	0.10	0.55
D	Temperature, K	283	293	303
E	pH	3.95	7.90	10.95

## 6.3. RESULTS AND DISCUSSION

### 6.3.1. Multivariate Statistical Analysis

Before the conclusions from the ANOVA were adopted, the adequacy of the underlying model should be checked. Through plotting a normal probability plot of residuals, the normality of the data could be checked. If the data points on the plot fall fairly close to the straight line, then the data are normally distributed (Ponnusami et al., 2007; Gottipati and Mishra, 2010). Figure 6.2(a) shows normal probability plot of residuals for PHE sorption on GPGS. All plotted points fell approximately along the straight line, indicating the experiments came from a normally distributed population.

Plot of residuals versus run number (Figure 6.2(b)) suggested the outliers if there was any. Among the 486 runs, except for five experimental points (run number 8, 301, 347, 406, and 474) all others were found to fall within the range of  $-3$  to  $+3$ . Points corresponding to the five runs were slightly out of this range. Reexamination of data did not reveal any obvious problem and the deviation was not severe enough to have a dramatic impact on the analysis and conclusions. Therefore, all the data were reliable and therefore ANOVA was conducted as indicated in Table 6.2. The estimation of single and interaction effects of experimental factors affecting PHE sorption were determined by performing factorial ANOVA. The effects were statistically significant when  $P$ -value, defined as the smallest level of significance leading to rejection of null hypothesis, was less than 0.05. Therefore, all main effects and two-factor interactions placed significant influences on PHE sorption behavior. By conducting the factorial ANOVA, the statistical significance of factors and their interactions affecting the sorption process was revealed.

Figure 6.3 presents the half-normal plot of effects, which is a plot of the absolute values of effect estimates against their cumulative normal probabilities. The half-normal plot is a graphical technique used to distinguish between important and unimportant effects of factors. Effects that lie along the straight line are deemed to be insignificant, whereas prominent effects lie away from the line (Wang and Huang, 2015). Accordingly, some of the important effects that emerged from this analysis were the main effects of A, C, E, B, and D, as well as the AC, CE, BC, DE, and BE interactions.

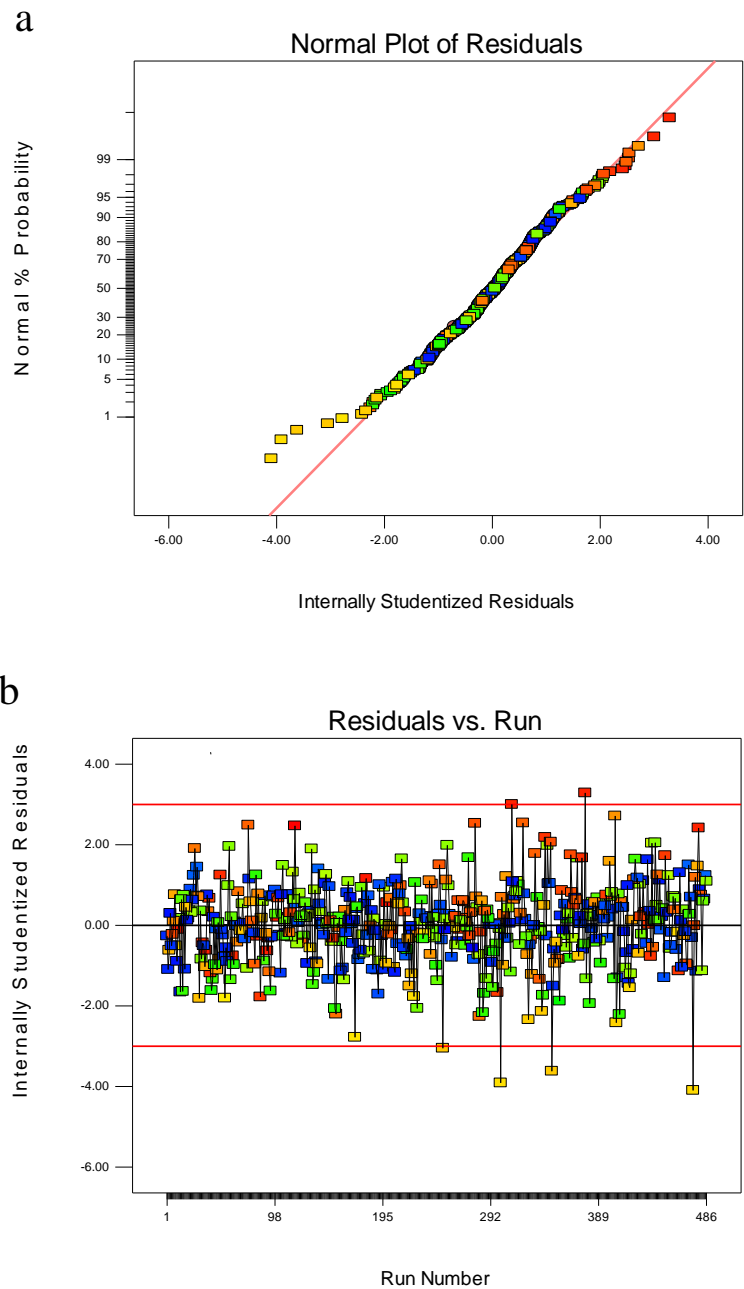


Figure 6.2 (a) Normal probability plot of residuals for PHE sorption data; (b) Residuals versus run number

Table 6.2 Analysis of Variance Table

Source	Sum of Squares	df	Mean Square	<i>F</i> Value	<i>p</i> -value Prob > <i>F</i>	
Model	5.9	130	0.045	3424.1	< 0.0001	Significant
A-Initial concen.	5.8	2	2.9	2.19E+05	< 0.0001	
B-HA	6.80E-03	2	3.40E-03	256.5	< 0.0001	
C-Ionic strength	0.036	2	0.018	1375.9	< 0.0001	
D-Temp.	1.79E-03	2	8.96E-04	67.6	< 0.0001	
E-pH	0.021	2	0.01	789.86	< 0.0001	
AB	8.96E-04	4	2.24E-04	16.9	< 0.0001	
AC	5.97E-03	4	1.49E-03	112.66	< 0.0001	
AD	5.32E-04	4	1.33E-04	10.05	< 0.0001	
AE	1.12E-03	4	2.80E-04	21.16	< 0.0001	
BC	2.99E-03	4	7.47E-04	56.35	< 0.0001	
BD	3.10E-04	4	7.74E-05	5.84	0.0001	
BE	1.48E-03	4	3.69E-04	27.85	< 0.0001	
CD	3.02E-04	4	7.55E-05	5.7	0.0002	
CE	5.77E-03	4	1.44E-03	108.84	< 0.0001	
DE	2.43E-03	4	6.08E-04	45.92	< 0.0001	
ABC	4.07E-04	8	5.09E-05	3.84	0.0002	
ABD	5.60E-05	8	7.00E-06	0.53	0.8349	
ABE	7.17E-04	8	8.96E-05	6.76	< 0.0001	
ACD	1.36E-04	8	1.70E-05	1.28	0.25	
ACE	6.93E-04	8	8.66E-05	6.54	< 0.0001	

ADE	3.05E-04	8	3.81E-05	2.88	0.0041	
BCD	2.17E-04	8	2.71E-05	2.05	0.0403	
BCE	3.34E-03	8	4.18E-04	31.54	< 0.0001	
BDE	1.20E-03	8	1.50E-04	11.29	< 0.0001	
CDE	1.51E-03	8	1.88E-04	14.22	< 0.0001	
Residual	4.70E-03	355	1.33E-05			
Lack of Fit	3.01E-03	112	2.69E-05	3.86	< 0.0001	Signi-ficant
Pure Error	1.69E-03	243	6.97E-06			
Cor Total	5.9	485				

---

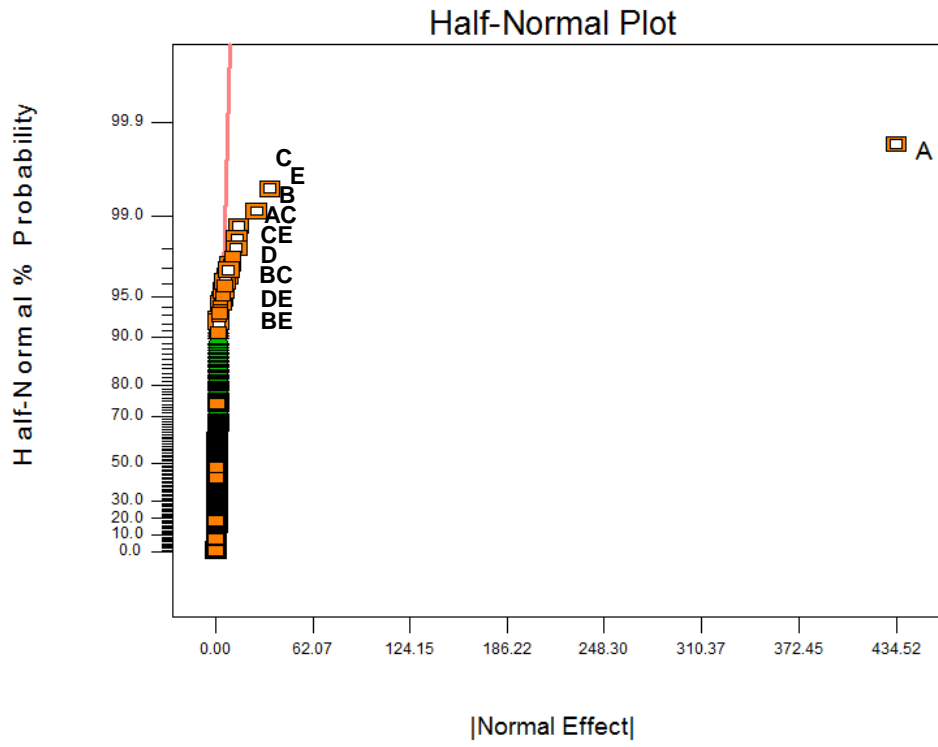


Figure 6.3 Half-normal plot of factor effects

### 6.3.2. Characterization of Linear and Curvature Effects of Factors

In a multi-level factorial design process, the main effects of factors include linear and curvature effects. Linear effects are calculated as the difference between maximum and minimum means of response. The effects of the factor would be positive on response if the linear effects are positive. Reversely, the effects of the factor would be negative on response if the linear effects are negative. The significance of all the factors affecting the sorption capacity is determined according to the linear effects. For example, factor A had the largest value of 0.26, implying that initial concentration had the most significant effect on PHE sorption.

Curvature effects are defined as the difference between the response at medium level and the average of responses at the low and high level. It can reveal the nonlinear relationship between experimental factors and the response variable. On some occasions, the curvature effects even can reveal a completely different influence on the response, compared with the linear effects. For instance, as shown in Table 6.3, the linear effects of factor B is calculated negative, implying that PHE sorption amount would decrease with the increasing HA dose from 2 to 42 mg/L. However, the curvature effects of factor B provided more detailed information. First, clearly the magnitudes of factor effects from low to medium level and from medium to high level were different. Second, the added HA dose from 2 to 4 mg/L placed a positive influence on PHE sorption, while adding HA from 4 to 42 mg/L exerted a negative influence on PHE sorption.

Table 6.3 The main effects of factors

Factors	A Initial concentration	B Added HA dose	C Ionic strength	D Temperature	E pH
Linear effects	0.26	-0.014	0.021	-0.0044	-0.016
Curvature effects	0.045	0.011	-0.0041	0.0017	-0.0041

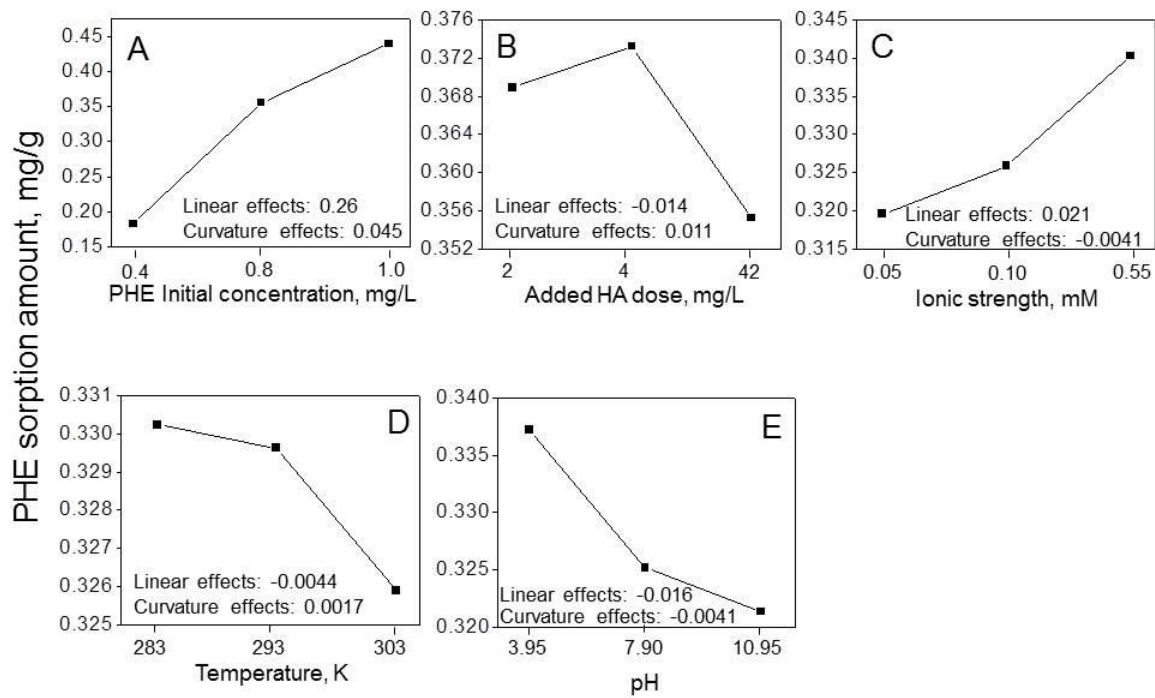


Figure 6.4 Plots for main effects of factors

Figure 6.4 presents the main effects plot for the five factors at three levels, which was helpful in visualizing the magnitudes of main effects of factors. Accordingly, factors A, C, and E were identified as the most dominant factors, while factors B and D were second most dominant factors.

The plots reveal that factor A (the initial concentration) with the most steep slope had the largest positive influence on PHE sorption. The sorption capacity would increase from 0.183 to 0.355 and then to 0.439 mg/g, if the initial concentration of PHE varies from its low level of 0.4 mg/L to its mid-level of 0.8 mg/L and then from its mid-level of 0.8 mg/L to its high level of 1.0 mg/L, respectively. As shown in Table 6.3, the positive linear effects indicated that the initial concentration played a positive effect on PHE sorption. The sorption of PHE was affected by the initial concentration, with a significant sorption increase as the initial concentration increased from 0.4 to 0.8 mg/L and then a slowdown of sorption as the concentration increased from 0.8 to 1.0 mg/L. The initial concentration provided an important driving force to overcome all mass transfer resistance of PHE molecules between the aqueous and solid phases. This phenomenon could be partially explained as follows: there were numerous sorption sites on PGS surface at low PHE concentration. As the quantities of PHE molecules increased, sorption sites were quickly saturated, resulting in a decrease in the sorption efficiency. Therefore, the sorption represented a shape characterized by a strong increase of the capacity between 0.4 and 0.8 mg/L and gradually tailed off thereafter.

PHE sorption increased slowly from 0.320 to 0.325 mg/g when factor C (ionic strength) changed from its low level of 0.05 M to midlevel of 0.10 M; while there was a noticed increase of sorption from 0.325 to 0.340 mg/g when factor C changed from the

midlevel of 0.10 M to its high level of 0.55 M. As shown in Table 6.3, the positive linear effects indicated that the ionic strength played a positive effect on PHE sorption. The increase could be explained by the “salting-out” effect, referring to the reduced solubility of organic compounds in aqueous salt solutions (Ko et al., 1998). Compared to the influence of medium to high level of ionic strength, the effect of low to medium ionic strength on PHE sorption by GPGS was less prominent. This might suggest that: i) within the ionic strength range of 0.05 ~ 0.1M, the contribution of salting-out effect to PHE was equivalent to that of the squeezing-out effect to GPGS; or ii) both the salting-out effect and squeezing-out effect were too weak to exert any change in the sorption of PHE on GPGS with the addition of NaCl from 0.05 to 0.1 M (Zhang et al., 2010a).

The sorption amount would be reduced sharply from 0.337 to 0.325 mg/g and then gradually from 0.325 to 0.321 mg/L, if factor E (pH) varied from its low level of 3.95 to its midlevel of 7.90 and then from its midlevel of 7.90 to its high level of 10.95, respectively. As shown in Table 6.3, the negative linear effects indicated that pH played a negative effect on PHE sorption. Three main mechanisms that may be applicable to PAH adsorption have been proposed: the H-bonding formation, the electron donor–acceptor interaction and the  $\pi$  -  $\pi$  interaction (Yuan et al., 2010). As indicated by Fang et al. (Fang et al., 2008), due to the low amounts of humic substances in GPGS clay, mechanisms such as enhanced dipole interaction between the charged surface (electron acceptors) and PHE with electron-rich  $\pi$  systems (electron donors) might be the major cause of PHE sorption (Zhang et al., 2011). The medium level of pH is the  $\text{pH}_{\text{pzc}}$ , at which point the surface charge of GPGS was zero. Otherwise, the mineral surface would be covered with positive charges when pH was lower than  $\text{pH}_{\text{pzc}}$ , and be covered with negative charges

when pH was higher than  $pH_{pzc}$ . That is, some functional groups on GPGS surface were subjected to protonation at low pH or deprotonation at elevated pH. This might explain an initial distinguished decrease of PHE sorption with pH from 3.95 to 7.90, followed by a reducing sorption of PHE with lower slope at pH from 7.90 to 10.95.

There would be a positive effect on PHE sorption when factor B (added HA dose) varied from its low level of 2 mg/L to its midlevel of 4 mg/L; however, the effect would become negative between its midlevel of 4 mg/L and its high level of 42 mg/L. The curvature effects indicated a favorable sorption from low to medium level of HA dose, while an unfavorable sorption from the medium to high level of HA dose. At a low HA dose below the medium level of 4 mg/L, the slight PHE sorption increase was presumably due to the binding of PHE to HA along with the sorption of HA onto GPGS surface, forming the complexation of sorbed HA with PHE (Radian and Mishael, 2012). The interactions among HA, PHE, and GPGS provided more preferential binding sites for PHE sorption at the solid/aqueous interface. Therefore the PHE sorption was enhanced in the presence of HA from 2 to 4 mg/L. However, at higher HA dose above 4 mg/L, the PHE sorption decreased with increasing HA concentration. Instead of cosorption, the HA molecules would hinder PHE retention through competition for limited sites on GPGS surface. With the increasing dose of HA to 42 mg/L, moreover, a great number of sorption sites on GPGS surface may be blocked by the HA molecules due to the large molecular size (Wang et al., 2009b). The increasing HA concentration also enhanced the solubility of PHE in aqueous phase. Consequently, PHE sorption on GPGS decreased after increasing HA dose above the medium level of 4 mg/L.

There was hardly any decrease of PHE sorption when factor D (temperature) varied

from the low level of 283 K to the midlevel of 293 K. However, reducing sorption from 0.330 to 0.326 mg/g occurred with factor D varying from the midlevel of 293 K to the high level of 303 K. As shown in Table 6.3, the negative linear effects indicated that temperature played a negative effect on PHE sorption. The uptake of PHE was found to decrease with increasing temperature, indicating that PHE sorption on GPGS surface was favored at lower temperatures. The decrease in sorption capacity with increasing temperature from 293 to 303 K indicated an exothermic nature of the sorption process. One explanation was that increased temperature could enhance PHE solubility, and decrease sorption (Ping et al., 2006).

As discussed above, the PHE sorption at the left and right hand side of the midpoint was barely the same due to the curvature effects. This is exactly why the medium level of factors was chosen instead of simply using the two-level factorial design. It indicated different mechanisms of the sorption process from low to midlevel, versus that from medium to high level. Therefore, the multi-level factorial design is capable of detecting the curvature in the factor-response relationship, while it is impossible to reflect such a nonlinear effect with the two-level factorial design due to its assumption of linearity over the range of factor levels.

### **6.3.3. Detection of Interactions among Factors**

#### *6.3.3.1. Interaction between Initial PHE Concentration and Ionic Strength*

The maximum PHE sorption of 0.449 mg/g would be obtained when initial PHE concentration was at its high level and ionic strength was at its high level, as indicated in Figure 6.5(1). It revealed that the change in PHE sorption differed across the three levels

of PHE initial concentration depending on the levels of ionic strength, implying that an interaction between these factors occurred that their effects were dependent upon each other. A variation of initial PHE concentration from its lower level to its midlevel would result in a remarkable increase in PHE sorption no matter what levels ionic strength was at. Comparatively, PHE sorption capacity would be less sensitive to the increase of ionic strength from its low level to its high level at all levels of PHE initial concentration.

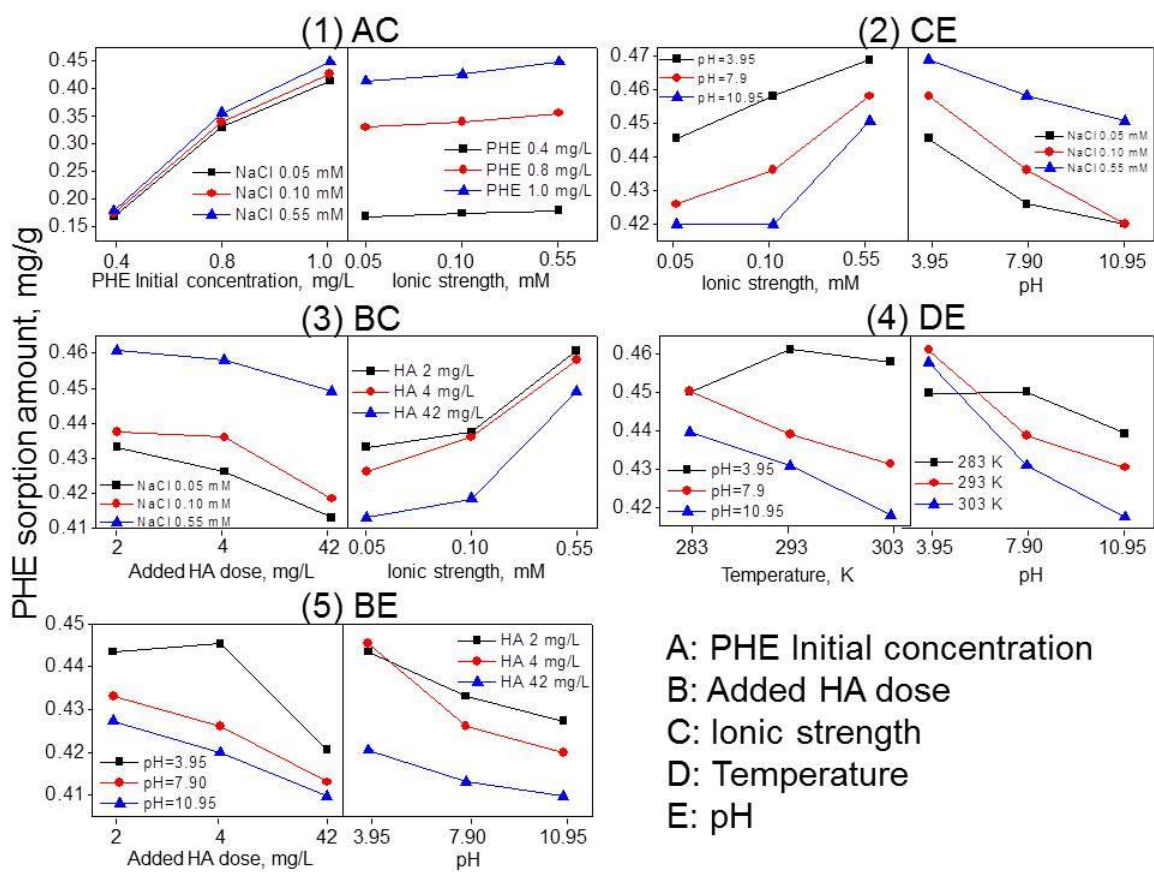


Figure 6.5 Interaction plots for AC, CE, BC, DE, and BE

### 6.3.3.2 Interaction between Ionic Strength and pH

Maximum sorption of 0.461 mg/g occurred when pH was at the low level of 3.95 and ionic strength was at the high level of 0.55 M. Low level of pH and high level of ionic strength favored PHE sorption, no matter what level the other factor was at. Evidently, the increase of ionic strength from low to high elevated PHE sorption at all levels of pH. Adjustment of pH from low to high level reduced PHE sorption at all levels of ionic strength. The increase/decrease rates were different, implying an interaction between this pair of factors. Specifically, at the low level of ionic strength, when pH was increased from 3.95 to 7.90 and then to 10.95, PHE sorption amount increased from 0.420 to 0.426 and to 0.445 mg/g, respectively. At the medium level of ionic strength, PHE sorption amount was 0.420, 0.436 and 0.458 mg/g at pH 3.95, 7.90, and 10.95. At the high level of ionic strength, there was slight increase of PHE sorption capacity from 0.451 to 0.468 mg/g when pH was adjusted from low to high level. It can be seen from Figure 6.5(2) that the sorption of PHE on GPGS at ionic strength 0.10 M was mostly influenced by pH, whereas no drastic difference of PHE sorption was found at ionic strength 0.05 and 0.55 M. Clearly, pH effect on PHE sorption was the highest when ionic strength was at the medium level of 0.10 M; while pH effect was the lowest when ionic strength was at the high level of 0.55 M.

Similarly, ionic strength effect on the PHE sorption was maximized when pH was at the medium level of 7.90. However, its effect on PHE sorption was reduced when ionic strength varied from 0.05 to 0.10 M with pH at the high level of 10.95. When pH increased from 7.90 to 10.95, the sorption of PHE to GPGS declined from 0.436 to 0.420 mg/g at ionic strength of 0.10 M and 0.426 to 0.420 mg/g at ionic strength of 0.05 M. At

the high pH level of 10.95, increasing ionic strength from 0.05 to 0.10 M had no effects on PHE sorption. It can be concluded that pH and ionic strength both placed the highest effects on PHE sorption at the medium level of the two factors. In conventional two-level of factorial design, such curvature effects will not be revealed, and so missed (Cestari et al., 2007; Wang and Huang, 2015).

The interaction between pH and ionic strength was very common in sorption studies. For example, perfluorooctane, an anionic surfactant, its uptake onto goethite was reported increasing at lower pH for any given ionic strength (Tang et al., 2010). Interestingly, the effect of pH was significantly weaker at high background electrolytes concentration, which was consistent with the findings in this study. In another research, curvature effects of pH were also very prominent. The sorption of Cd(II) on GMZ bentonite at pH less than 7.5 was strongly affected by ionic strength, whereas marginal difference of Cd(II) sorption was found at pH higher than 7.5 in different solution concentrations of NaNO<sub>3</sub> (Zhao et al., 2011b).

#### *6.3.3.3. Interaction between Added HA Dose and Ionic Strength*

The highest sorption capacity would be obtained with adding HA from low to medium level (2 to 4 mg/L) and ionic strength at the high level (0.55 M), as shown in Figure 6.5(3). Clearly, the variation of HA dose from the low, to medium and high level resulted in first a slight decrease of PHE sorption and then a continued reduction of the sorption amount (no matter what level of ionic strength was at). The sorption magnitude was the highest for the high ionic strength level of 0.55 M across the low, medium and high level of added HA dose.

In comparison, the increase of ionic strength from its low to medium and high level

placed a positive effect on PHE sorption at all levels of HA dose. The sorption amount at all ionic strength level was the lowest when adding HA dose of 42 mg/L. Slight effects of HA dose on PHE sorption were found at ionic strength of 0.05 M. However, when elevating ionic strength across its low, medium, and high level, the effects were gradually reduced.

#### *6.3.3.4 Interaction between Temperature and pH*

The sorption magnitude (0.461 mg/g) at the low level of pH and medium level of temperature (pH 3.95 and 293 K) for PHE outperformed the sorption at other conditions tested (Figure 6.5(4)). When temperature increased from its low level of 283 K to medium level of 293 K, the sorption magnitude increased from 0.450 to 0.461 mg/g at low pH level of 3.95; while the sorption decreased from 0.450 to 0.439 mg/g, and 0.440 to 0.430 mg/g at medium pH of 7.90 and high pH level of 10.95. However, when increasing temperature from the medium to high level of 303 K, the differences among the sorption rate of three lines were very slight. It indicated that the interaction effects of pH and temperature on the sorption process were more prominent when temperature increased from its low to medium level, compared to that when temperature increased from its medium to high level. The plot (pH at the low level of 3.95) also exposed that, a variation of temperature from its low to its medium and high level would result in first an enhancement of PHE sorption from 0.450 to 0.461 mg/g and then a reduction of PHE sorption from 0.461 to 0.458 mg/g. The highest PHE sorption was achieved at the medium level of temperature 293 K when pH was 3.95. Such curvature effects of factors and interactions in multi-level factorial design were necessary to detect the missing information in the two-level factorial design.

Likewise, there existed strong interactions when pH changed from its low to medium level at 283, 293 and 303 K. However, changing pH from its medium to high level didn't cause much difference among the sorption decrease at 283, 293 and 303 K. The interaction effects of pH and temperature on PHE sorption was diminished above the midlevel of pH for all temperature levels.

#### *6.3.3.5. Interaction between Added HA Dose and pH*

When the HA dose was at its medium level and pH at its low level (HA 4 mg/L, pH 3.95), the sorption of PHE on GPGS reached the maximum value of 0.445 mg/g. It is noticeable that there was slight increase of sorption when HA dose was added from its low level of 2 mg/L to its medium level of 4 mg/L (pH at low level of 3.95). The sorption declined faster when adding HA from the medium level to the high level, compared to the sorption when adding HA from the low to medium level (no matter what level the pH was at). As shown in Figure 6.5(5), the effects of pH on sorption of PHE to GPGS was first amplified and then weakened when HA dose varied from its low, medium, to high level. When adding the HA dose of 2 mg/L, the sorption of PHE to GPGS decreased from 0.443, to 0.433 and 0.427 mg/g with adjusting pH from 3.95 to 7.90 and 10.95. At the medium dose of HA, changing pH from 3.95 to 10.95 placed the most negative influence on PHE sorption by reducing the sorption amount from 0.445 to 0.426 and 0.419 mg/g. At the high dose of HA, there was no apparent decrease of PHE sorption (from 0.420 to 0.410 mg/g) with varying pH from 3.95 to 10.95. Clearly, pH extended its influence on PHE sorption when the added HA dose was at the medium level of 4 mg/L. Such curvature effects and interactions between pH and added HA dose were essential to reveal the mechanisms in the PHE sorption process.

The overall sorption of PHE decreased when increasing pH from its low to high level at all HA doses. The lowest sorption was obtained at the high pH level of 10.95 and at all levels of HA dose. The interaction effects of pH and HA on PHE sorption was obvious when pH varied from the low to medium level. In detail, when HA dose was 2 and 4 mg/L, there was almost no difference of PHE sorption at the low pH level of 3.95. However, change of pH from low to medium level of 7.90 contributed to a faster sorption reduction for HA 4 mg/L than that for HA 2 mg/L. Moreover, the sorption of PHE decreased parallel when increasing pH from its medium to high level, no matter what level the HA dose was at. It indicated that there was no significant interaction between pH and added HA dose when pH varied from the medium to high level. Clearly the curvature effects and interactions provided more elucidation about the effects of aqueous parameters on the sorption behavior of PHE. The interaction plot matrix of the selected experimental factors is shown in Figure 6.6.

The sorption mechanisms of contaminant in presence of HA at different levels of pH were reported in many studies (Sheng et al., 2011). At low pH values, the sorption of the negatively charged HA on the positively charged surfaces of GPGS was easy because of electrostatic attraction. The formed complexation between surface sorbed HA and PHE resulted in the enhancement of PHE sorption to GPGS at low pH values. However, at high pH levels, the sorption of the negatively charged HA on the negatively charged surfaces of GPGS substantially decreased due to the electrostatic repulsion mechanism. The desorbed HA molecules formed soluble complexes of HA-PHE at the aqueous phase, and thereby reduced PHE sorption to GPGS.

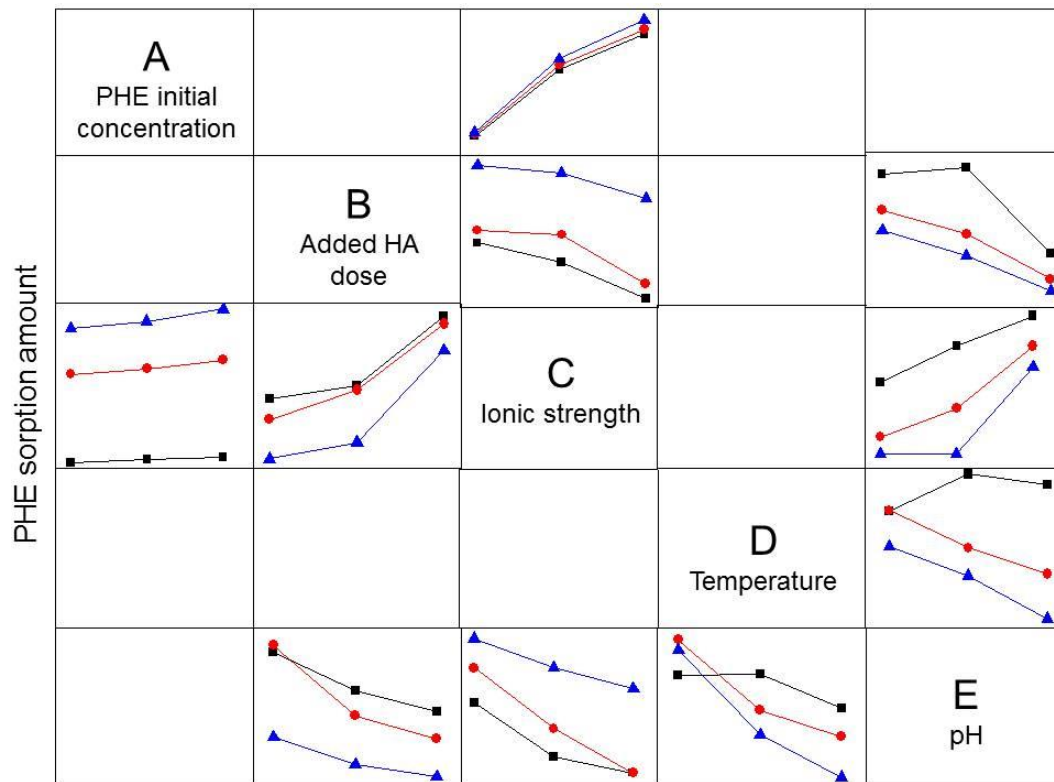


Figure 6.6 The interaction plot matrix of environmental factors at three levels

## 6.4. SUMMARY

The sorption of PHE on GPGS was studied by using a multi-level fuzzy-factorial inference approach. Five experimental factors were discussed, including initial PHE concentration, pH, added HA dose, ionic strength and temperature. Fuzzy vertex analysis was employed to deal with design factors with membership functions based on the  $\alpha$ -cut concept and interval analysis. The factorial ANOVA results indicated the significant factors influencing PHE sorption were: initial PHE concentration, ionic strength, pH, added HA dose, and temperature, sequentially. The calculated curvature effects revealed the nonlinear relationship between experimental factors and the response variable. Curvature effects were revealed explicitly, implying different sorption mechanisms under the influencing factors from low, medium to high levels. For example, pH effect on PHE sorption was the highest when ionic strength was at the medium level of 0.10 M. Ionic strength effect on the PHE sorption was maximized when pH was at the medium level of 7.90. pH extended its influence on PHE sorption when the added HA dose was at the medium level of 4 mg/L. Clearly such curvature effects and interactions were essential to reveal the mechanisms in the PHE sorption process. Compared with two-level factorial design, multi-level factorial experiment can reveal the potential interactions among experimental factors at multiple levels and their curvature effects on the response, as well as the valuable information hidden beneath their interrelationships.

# CHAPTER 7

## ENHANCEMENT OF SOIL RETENTION FOR PHENANTHRENE THROUGH BINARY CATIONIC GEMINI AND NONIONIC SURFACTANT MIXTURES

### 7.1. BACKGROUND

Contamination of soil and groundwater by PAHs has become a global issue. It is reported that PAH concentrations from 1  $\mu\text{g}/\text{kg}$  to over 300  $\text{g}/\text{kg}$  are found in soils and sediments at both contaminated and uncontaminated sites (Yap et al., 2010). PAHs are ubiquitously present and have been identified as carcinogenic, mutagenic, and teratogenic. Sorption of PAHs to soil plays an important role in the fate, transport, and bioavailability of these compounds in natural environment (Zhu et al., 2003; An et al., 2011).

There is an increasing need for developing effective pollution control technology at PAH-contaminated site. Recently, it has been reported that the addition of appropriate surfactant can create a sorption barrier in soil, which can intercept and retard the pollutant plume of organic contaminants. This approach can facilitate the *in situ* soil remediation through the immobilization of PAHs and will be especially useful for fuel burning or waste incineration sites. The addition of organic cationic surfactant, particularly long-chain organic surfactant, can markedly modify the soil surface with increasing hydrophobic characteristic and enhance the sorption capacity of soil for PAHs. Cationic gemini surfactant, as a series of novel surfactant, has received emerging interest in recent years. The sorption of gemini and conventional surfactants onto some soil solids (and clays) for the removal of 2-Naphthol indicated that the former would be more efficient

than the latter in removing pollutants from aqueous media (Li and Rosen, 2000; Rosen and Li, 2001). Liu et al. studied the removal of phenol and catechol by the organo-montmorillonite which was modified with the novel hydroxyl-containing gemini surfactants (Liu et al., 2014). Although these findings are encouraging, a number of issues about the characteristic and mechanism of gemini surfactant-induced sorption are poorly understood. The knowledge about corresponding sorption modeling studies is still scarce.

Compared with single surfactant system, surfactant mixture shows a superior performance, due to the fact that the mixed micelles of surfactant mixture could be more effective for the distribution of organic compounds. Nonionic surfactant has the potential to be used in surfactant mixture to form the sorption barrier because the hydrophobic properties of nonionic surfactant can facilitate their sorption on soils and clays (Lee et al., 2000). One previous study reported the synergistic adsorption of mixtures of cationic gemini and nonionic sugar-based surfactants on silica (Zhou and Somasundaran, 2009). Another research investigated the adsorption characteristics of monomeric/gemini surfactant mixtures at the silica/aqueous interface (Sakai et al., 2010). The previous studies mainly focused on the sorption of surfactant mixture on mineral surface. A well understanding of the sorption of cationic gemini and nonionic surfactant mixtures on complex soil system is still challenging in many respects. Moreover, the sorption of cationic-nonionic surfactant mixtures on soil is expected to enhance the retardation of organic contaminants in soil. However, no studies have been reported on the enhanced retention of PAHs by cationic gemini and nonionic surfactant mixtures and the available knowledge is still limited.

Therefore, a systematical investigation on the efficiency and mechanism of PAHs sorption onto soil in the presence of single gemini and binary surfactant mixtures (cationic gemini and nonionic C<sub>12</sub>E<sub>10</sub>) will be performed. The sorption of individual gemini surfactant at the soil/water interface will be studied and a Two-step Adsorption and Partition model will be developed to elucidate the corresponding sorption mechanism. Thermodynamic investigation will be conducted to further characterize the nature of the sorption process. Moreover, the enhanced soil retention of PAHs through the addition of mixed cationic-nonionic surfactants will be investigated to assess the effectiveness of sorption barrier created by the binary surfactant mixtures. The results obtained from this study will help reveal the interactions among water, soil, surfactant, and contaminant in surfactant-enhanced retardation processes.

## **7.2. MATERIALS AND METHODS**

### **7.2.1. Chemicals**

Phenanthrene (PHE) was selected as the representative PAH, and was purchased from Sigma Aldrich Chemical Co. (WI, USA) with the purity greater than 99%. Cationic gemini surfactant (N1-dodecyl-N1, N1, N2, N2-tetramethyl-N2-octylethane-1, 2-diaminium bromide, 12-2-12) was obtained from Chengdu Organic Chemicals Co., Ltd. (Sichuan, China), with a purity of 98%. Despite some types of cationic gemini surfactants might show poor biodegradability due to the chemical stability, they still have many unique properties that are superior to those of their single-chain counterparts. Nonionic surfactant (Decaethylene glycol monododecyl ether, C<sub>12</sub>E<sub>10</sub>) was also provided by Sigma Aldrich (purity > 98%). The molecular structures and properties of PHE and selected

surfactants are given in Table 7.1. The water solubility of PHE is 1.06 mg/L at 298 K and the octanol-water coefficients ( $\log K_{ow}$ ) is 4.57 (Table 7.1). The stock solution of PHE was made by diluting the desired amount of pure PHE crystals into HPLC-grade methanol solution, and was stored in a dark place at 277 K in an amber borosilicate bottle to minimize photodegradation and volatilization. The stock solutions of surfactants were prepared by dissolving the weighed amounts in deionized water at room temperature. Surfactant solutions with different mole fractions were obtained by mixing pre-calculated volumes of the stock solutions in the appropriate amount of deionized water.

### **7.2.2. Soils**

The soil was derived from Coleville site in Saskatchewan, Canada (51°39'N, 109°13'W). The site map is shown in Figure 7.1. Soil samples were collected at a depth of 3 ~ 5 feet below the ground surface. The soil particles were dried and sieved through a 2-mm sieve. The sieved soil was homogenized as much as possible and stored in glass containers. The physical and textural characteristics of the soil are given in Table 7.2.

### **7.2.3. Sorption Studies**

The batch sorption experiments were conducted in 20 mL glass vials. 0.1 g of soil was first added into the glass vial; after that, the single surfactant or premixed binary mixtures were added into the vial. The background solution contained 0.1 M  $\text{CaCl}_2$  as electrolyte and 0.01 M  $\text{NaN}_3$  as biocide. Then a pre-calculated volume of PHE stock solution was added to each vial, and the initial concentration of PHE was pre-determined for each sample. The vials were sealed with Teflon-lined screw caps and were vortexed

for 20 s, and then were placed in a reciprocal shaker (SHKE5000 Thermo Scientific, USA) at 288/298/308 K and 200 rpm for 24 h to reach the sorption equilibrium. Preliminary experiments showed that 24 h were sufficient for the sorption process to reach equilibrium and the experimental loss of PHE was negligible (An et al., 2011; An and Huang, 2012). Before testing, the samples were subsequently centrifuged (Multifuge X1R, Thermo Scientific, USA) at 5000 rpm for 30 min and 10000 rpm for 10 min to separate soil from solution. An appropriate aliquot of supernatant was then carefully withdrawn with a volumetric pipette to further determine the residual amount of surfactant and PHE. At the same time, three groups of controlled experiments corresponding to three surfactant systems (i.e., 12-2-12 gemini, C<sub>12</sub>E<sub>10</sub> and the binary mixtures) were conducted and the supernatant of controlled samples were analyzed as the background concentrations for surfactant or PHE (Yu et al., 2011b; Zhao et al., 2011a; Wei et al., 2013).

#### **7.2.4. Analytical Methods**

PHE was analyzed using HPLC. The HPLC instrument, an Agilent 1260 Infinity LC System (USA), was equipped with vacuum degasser, binary pump, autosampler, thermostated column compartment (set to 303 K), diode array detector (DAD), and ZORBAX Eclipse PAH column (3.5  $\mu$ m particle size, 4.6 mm  $\times$  150 mm ID). A mobile phase consisting of acetonitrile/water (75:25, v/v) was used at a flow rate of 1.0 mL/min. PHE was monitored with DAD at 250 nm. The residual concentration of gemini surfactants was determined by the potentiometric titration (G20, Mettler Toledo, Switzerland) method, using sodium dodecyl sulfonate (C<sub>12</sub>H<sub>25</sub>OSO<sub>3</sub>Na, SDS) as the

titrant. The titration of blank samples was also carried out. The amounts of PHE/surfactants sorbed to the soil were the difference between the initial amount added and the amount remaining in the solution.

In order to identify the interactions among the soil, PAHs and surfactants, six soil samples were prepared for the instrumental analysis such as FT-IR and the SOM testing. The six soil samples were the original soil sample, the soils with the addition of 12-2-12 cationic gemini surfactant at 0.5, 1, 2, 4, and 12 mM, respectively. The FT-IR spectra were recorded on a Bruker FT-IR spectrophotometer (Tensor 27, USA). To quantify the SOM in the natural soil and the soils with the addition of surfactants, the organic carbon content of each sample was tested by a Costech Elemental Analyzer (ECS 4010, USA). Samples were dried, acidified with 0.3N HCl, rinsed in deionized water, dried again and then packed and combusted in tin capsules.

### 7.2.5. The Apparent Soil-Water Distribution Coefficient

The apparent soil-water distribution coefficient of organic contaminants in presence of surfactant can be evaluated by the following equation (Zhao et al., 2010):

$$K_d^* = \frac{f_{oc} K_{oc} + f_{sf} K_{sf}}{1 + K_{mi} X_{mi} + K_{mc} X_{mc}} \quad (7.1)$$

where  $K_d^*$  (mL/g) is the apparent soil–water distribution coefficient in presence of surfactants, which can also be calculated from the compound concentrations in solid phase ( $C_s^*$ ,  $\mu\text{g/g}$ ) and the equilibrium concentration of compound in aqueous phase ( $C_e^*$ , mg/L) with the equation of  $K_d^* = C_s^*/C_e^*$ .  $f_{oc}$  is the organic carbon content of soil derived from SOM (g/g);  $K_{oc}$  ( $K_{oc} = K_d/f_{oc}$ ) is the  $f_{oc}$  normalized solute distribution coefficient

between SOM and water (mL/g). The distribution coefficient of solute between SOM and water in absence of surfactants,  $K_d$  (mL/g), is calculated from the compound concentrations in solid phase ( $C_s$ ,  $\mu\text{g/g}$ ) and the equilibrium concentration of compound in aqueous phase ( $C_e$ , mg/L) in absence of surfactants with the equation of  $K_d = C_s/C_e \cdot f_{sf}$  is the organic carbon content of soil derived from sorbed surfactants (g/g);  $K_{sf}$  is the  $f_{sf}$  normalized solute distribution coefficient between sorbed surfactants and water (mL/g).  $X_{mn}$  is the concentration of surfactant monomers in water (mg/L);  $X_{mc}$  is the concentration of surfactant micelles in water (mg/L);  $K_{mn}$  is the partition coefficient of a solute between surfactant monomers and water, and  $K_{mc}$  is the solute partition coefficient between the aqueous micellar phase and water.  $f_{oc}K_{oc}$  and  $f_{sf}K_{sf}$  describe the sorption capability of SOM and soil sorbed surfactants respectively for organic contaminants, while  $(1 + K_{mn}X_{mn} + K_{mc}X_{mc})$  describes surfactant solubilization for organic contaminants. Prior to micellization ( $X_{mn} = X$ ,  $X_{mc} = 0$ ),  $K_d^*$  values are seen to increase with increasing surfactant concentrations because the sorbed surfactant is effective medium for partitioning of organic contaminants while the solute partitioning into the surfactant monomers in solution can largely be negligible.

#### 7.2.6. Data Analysis

All of the tests were conducted in duplicate and the typical error in the measurement was less than  $\pm 5\%$ . Sorption equilibrium data were fitted to the developed model. The data were analyzed through nonlinear regression using SigmaPlot 12.0 software (Systat Software Inc., CA, USA). The statistical analyses agreed within 95% confidence demonstrating the accuracy of measurements reported in this manuscript.

Table 7.1 The structure and physicochemical properties of the selected surfactants and PAHs

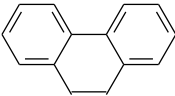
Material	Structure	Molecular Weight (g/mol)	CMC (mM)	Water Solubility (mg/L)	$\log K_{ow}$
12-2-12	$C_{12}H_{25}N^+(CH_3)_2(CH_2)_2-$ $N^+(CH_3)_2C_{12}H_{25} \cdot 2Br^-$	614.67	0.8		
$C_{12}E_{10}$	$C_{12}H_{25}(OCH_2CH_2)_{10}OH$	626.86	0.2		
Phenanthrene		178.2		1.06	4.57

Table 7.2 Properties of the selected soil sample

Sorbents	CEC (cmol/kg)	$f_{oc}$ (%)	pH	Sand (%)	Silt (%)	Clay (%)	Density (g/cm <sup>3</sup> )
soil	15.8	0.76	8.8	40.0	27.3	32.7	2.5

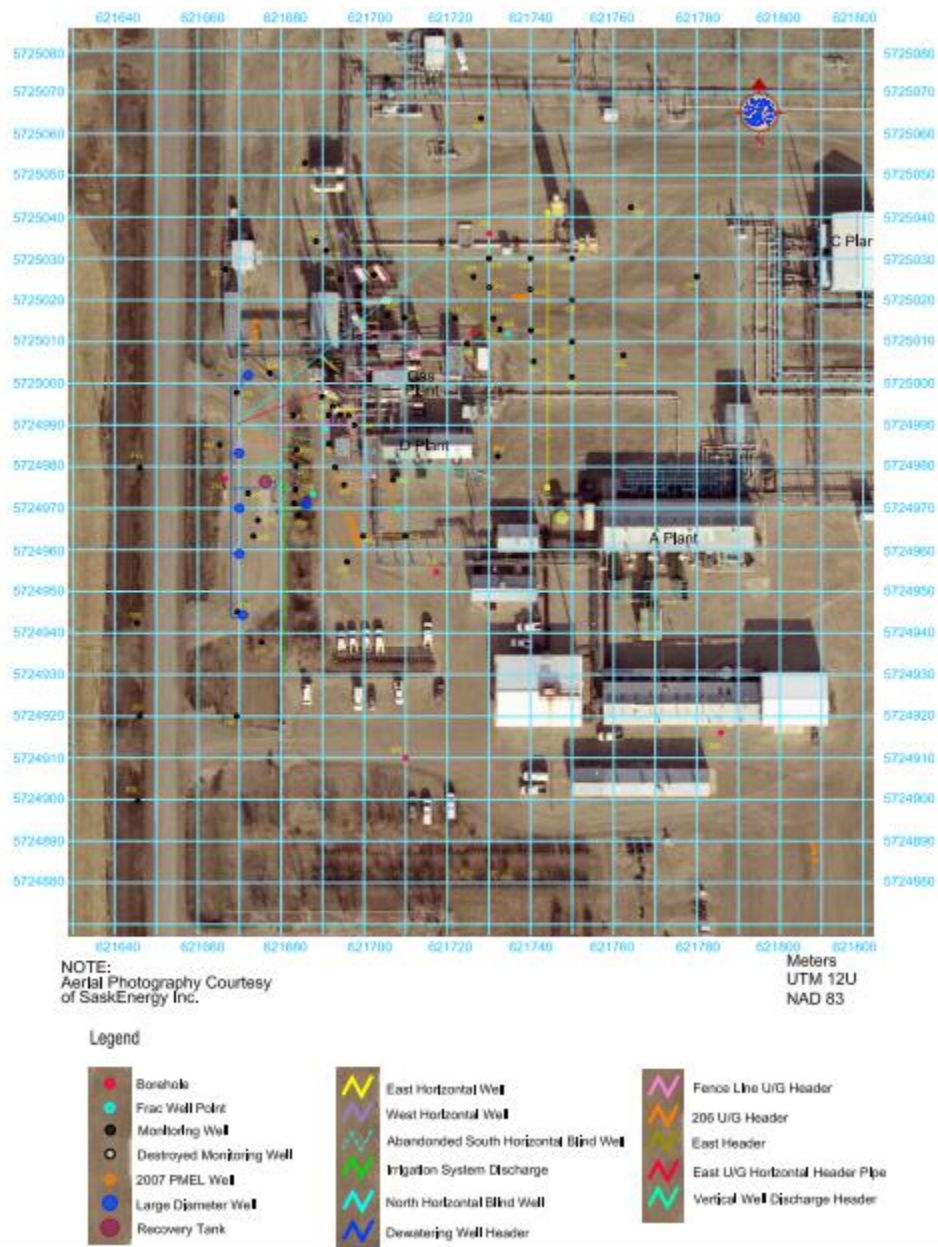


Figure 7.1 Coleville site map

## 7.3. RESULTS AND DISCUSSION

### 7.3.1. Characterization of the Soil Samples

The FT-IR spectra of the pure gemini powder, the natural soil, and the five soil samples (with the addition of gemini surfactants) in the range of  $4000 \sim 500 \text{ cm}^{-1}$  are shown in Figure 7.2. The broad bands at the  $500 \sim 600 \text{ cm}^{-1}$  region were attributed to Si-O and Al-O bending vibrations (Eren et al., 2009), while the stretching vibration of Si-O groups was observed at  $1040 \text{ cm}^{-1}$ . Compared to the original soil sample, much strong vibration occurred around  $1638$  and  $3600 \text{ cm}^{-1}$  for the soil samples with the addition of gemini surfactants. The bands at  $3447 \sim 3625 \text{ cm}^{-1}$  were assigned to the OH stretching vibration, while the bands at  $1638 \text{ cm}^{-1}$  were corresponded to OH bending vibration (Zhou et al., 2009). Compared to the original soil sample, the spectra of the soil samples (with the addition of gemini surfactants) showed two additional peaks at  $2852$  and  $2928 \text{ cm}^{-1}$ , which were attributed to the C-H stretching vibration due to the sorption of gemini surfactants (Liu et al., 2014). The characteristic sorption bands at  $1385 \text{ cm}^{-1}$  were assigned to the bending vibration of the C-H bonds of the gemini cations (Liu et al., 2011). As indicated in Figure 7.2, the intensity of characteristic bands at  $2852$  and  $2928 \text{ cm}^{-1}$  enhanced significantly with the increasing concentration of gemini surfactants from  $0.5$  to  $4 \text{ mM}$ . However, there was no intensity enhancement when the added dose of gemini surfactants increased from  $4$  to  $12 \text{ mM}$ , which might be due to the saturation sorption of gemini surfactants on soil samples. The results indicated that gemini surfactants had been successfully intercalated into the soil layers and/or sorbed on the surface of soil samples (Xue et al., 2013).

In addition, it is reported that the sorption of surfactant could increase the soil

organic matter and enhance the retention of PHE in soils. It is indicated from Table 7.3 that the amount of SOM enhanced substantially with the added surfactants dose. SOM increased from 13.10 to 70.68 g/kg with the increasing concentration of 12-2-12 gemini surfactants from 0 to 4 mM, while there was no enhancement of SOM with the addition of surfactants from 4 to 12 mM. These findings are consistent with the results from the FT-IR analysis. From the instrumental analysis of FT-IR and the elemental analysis, it is convinced that 12-2-12 cationic gemini surfactants can sorb on the soil samples and increase SOM. The analysis of  $K_d^*$  (the measured apparent sorption coefficients of PHE by soil in the presence surfactants) in the manuscript indicates that the surfactant-derived organic matter is a more powerful medium to sorb organic contaminant than natural soil organic matter and to enhance the organic pollutant transfer from water into soil phase.

Table 7.3 Elemental analysis of the original soil and the soil samples with the addition of gemini surfactants

Sample	N, %	$f_{oc}$ , %	C/N	SOM, g/kg
Original soil sample	0.05	0.76	18.97	13.10
Soil with 0.5 mM of gemini	0.17	2.09	14.20	36.03
Soil with 1 mM of gemini	0.28	3.57	15.08	61.55
Soil with 2 mM of gemini	0.32	4.36	15.89	75.17
Soil with 4 mM of gemini	0.37	5.13	16.03	88.44
Soil with 12 mM of gemini	0.29	4.10	16.47	70.68

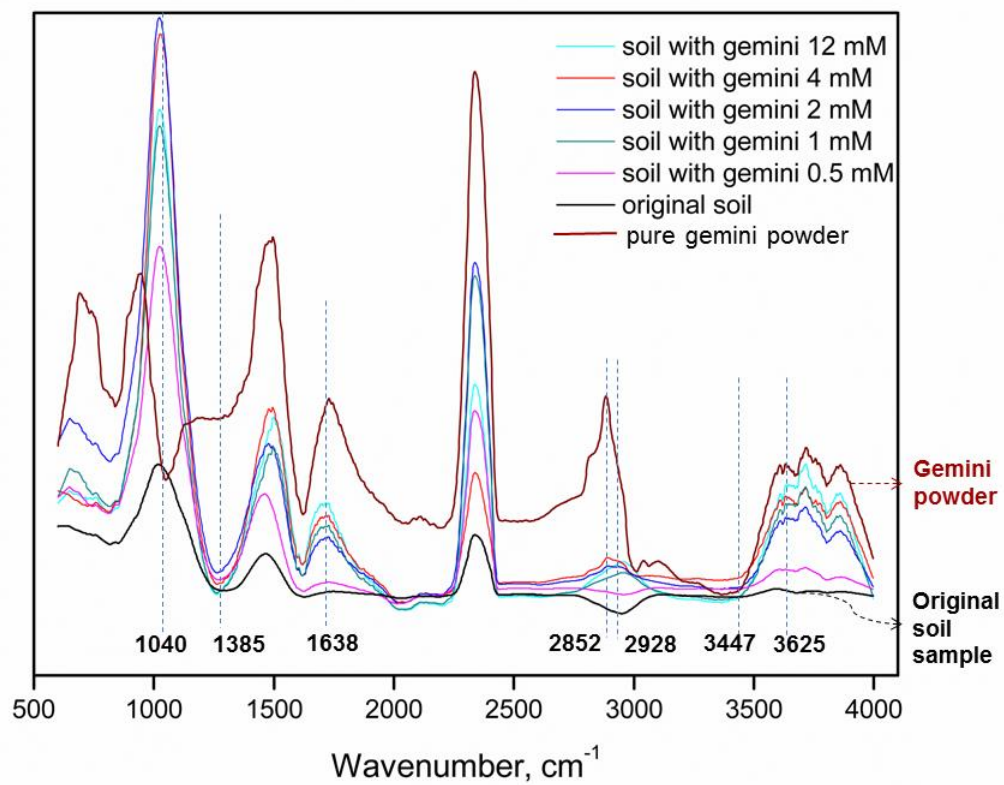


Figure 7.2 FT-IR spectra of the pure gemini powder, the natural soil, and the five soil samples with gemini sorption

### 7.3.2. Sorption of PHE by Soil with the Addition of Single Cationic 12-2-12 Gemini Surfactant

A cationic 12-2-12 gemini surfactant was utilized to retard the mobility of PHE transport. The measured apparent sorption coefficients ( $K_d^*$ ,  $K_d^* = \frac{f_{oc}K_{oc} + f_{sf}K_{sf}}{1 + K_{mn}X_{mn} + K_{mc}X_{mc}}$ , see Equation (7.1)) of PHE by soil in the presence of individual 12-2-12 gemini are shown in Figure 7.3. In the absence of surfactant, the measured apparent sorption coefficient ( $K_d$ ) of 2.3 mL/g was observed. The maximum  $K_d^*$  values with the addition of single 12-2-12 gemini surfactant were two orders of magnitude higher than those without addition of 12-2-12 gemini surfactant, indicating that 12-2-12 gemini could effectively decrease PHE mobility in soil. When the initial concentration of PHE was 1.0 mg/L (Figure 7.4),  $K_d^*$  increased dramatically with the increasing concentration of 12-2-12 gemini, and then reached a plateau at an approximate dose of 1230 mg/L. When the concentration of 12-2-12 gemini surfactant was higher than 1230 mg/L,  $K_d^*$  values decreased steeply because the solubilization of PHE was significantly enhanced. The maximum  $K_d^*$  value for PHE in the presence of single 12-2-12 gemini was approximately 1148.6 mL/g, which was 498 times higher than that of soil without the addition of surfactants (2.3 mL/g). Similar results were obtained when the initial PHE concentrations were 0.5 and 0.75 mg/L. The results suggested that cationic 12-2-12 gemini surfactant could be used to enhance the soil retardation capabilities for PHE. The enhanced sorption of organic contaminants on soil with the added cationic surfactant has been well established (Hernández-Soriano et al., 2007; Yuan et al., 2007). The cationic surfactant at soil surface is more likely to form hemimicelles and admicelles in which contaminants can partition. It can effectively attenuate the mobility of organic contaminants (Lee et al.,

2004). The sharp increase of  $K_d^*$  at the low surfactant level could be attributed to both the 12-2-12 gemini sorption on soil and the partition of PHE into the sorbed-gemini organic content (Figure 7.2 and Table 7.3). With the increasing dose of 12-2-12 gemini above 1230 mg/L, the  $K_d^*$  declined steeply while the sorbed 12-2-12 gemini amount continued to increase to the first and second plateau. When the aqueous concentration of 12-2-12 gemini became higher than CMC (492 mg/L), stable micelles were formed in the aqueous phase. In our previous study, the enhanced solubilization capability of cationic 12-2-12 gemini and nonionic surfactants (Polyethylene glycol dodecyl ether, C<sub>12</sub>E<sub>23</sub>) for PAHs has been demonstrated (Wei et al., 2012). For surfactant-enhanced sorption, the presence of surfactant micelles was undesirable since it could solubilize the sorbed organic pollutants (Hernández-Soriano et al., 2007). At the high surfactant loading, significant partition of PHE into aqueous 12-2-12 gemini micelles might occur, which could retard PHE in surfactant solution and was responsible for the steep decrease in  $K_d^*$  values.

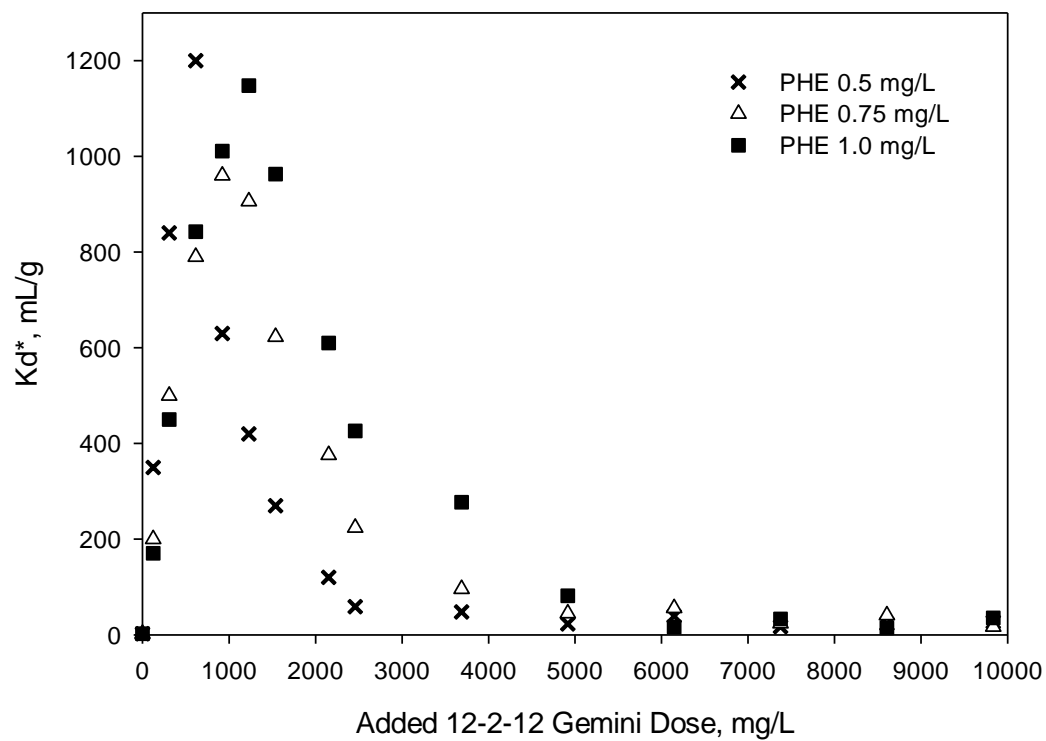


Figure 7.3 The measured apparent sorption coefficients  $K_d^*$  of PHE in presence of single 12-2-12 gemini surfactant (PHE at various initial concentration)

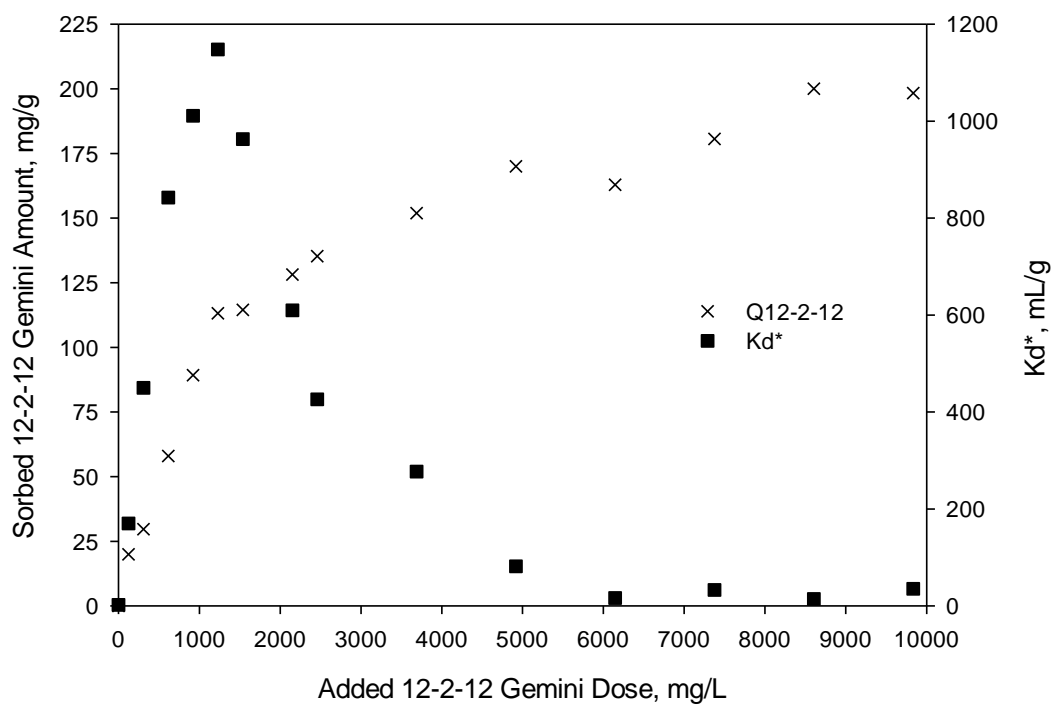


Figure 7.4 The sorbed 12-2-12 gemini amount and measured apparent sorption coefficients  $K_d^*$  of PHE in the presence of single 12-2-12 gemini surfactant (PHE at 1.0 mg/L)

### 7.3.3. Sorption Isotherms of the 12-2-12 Gemini Surfactant at Different Temperatures

The results showed that the retention of PHE was closely related to the sorption of 12-2-12 gemini on soil surface. Therefore the sorption isotherms of 12-2-12 gemini were further studied to better understand the transport of PHE in soil-water system. As shown in Figure 7.5, the sorption capacity of 12-2-12 gemini increased when the temperature ranged from 288 to 298 K, while the sorption capacity decreased above 298 K. For the isotherm of 298 K, it was clear that the amount of sorbed 12-2-12 gemini increased sharply at low 12-2-12 gemini dose. When gemini equilibrium concentration ranged from 10.7 to 97.1 mg/L, the sorbed 12-2-12 gemini amounts increased continually from 29.7 to 113.2 mg/g. After the aqueous concentration over 100 mg/L, the sorbed amount of 12-2-12 gemini increased continuously to the first (170.1 mg/g) and second plateau (200.0 mg/g).

It is generally believed that sorption of cationic surfactants onto soil particles takes place via electrostatic interaction (Boyd et al., 1988; Lee et al., 1989; Sheng et al., 1996; Zhao et al., 2010). According to the soil CEC (15.8 cmol/kg), the sorbed 12-2-12 gemini amounts (i.e., 96 mg/g = 15.6 cmol/kg) at an approximate 12-2-12 gemini dose of 1000 mg/L, could be mainly attributed to the electrostatic attraction between positively charged head-groups of 12-2-12 gemini surfactant and negatively charged soil surface. Additional sorption of 12-2-12 gemini on soil at added dose above 1000 mg/L could be attributed to other mechanisms such as hydrophobic effects (Li and Rosen, 2000; Rosen and Li, 2001; Sakai et al., 2008; Zhou and Somasundaran, 2009; Salako et al., 2013; Liu et al., 2014).

Other than being adsorbed by soil surface through ionic bonding and hydrophobic

interaction, partitioning into soil organic matter was reported as another mechanism for surfactant sorption to soil. Adsorption and partition, associated with other interfacial behaviors, were the main mechanisms for the sorption of organic compound in soil–water system (Lee et al., 2000; Lee et al., 2004). It was observed that nonionic surfactant TX-100 could partition into SOM, the extent being related to the properties of surfactant and SOM (Lee et al., 2000). Considering the high polarities and large molecular weights, cationic surfactant may partition into the SOM besides adsorbing onto certain soil minerals. Gemini surfactant contains two long hydrophobic chains and has a similar molecular weight as TX-100. This may provide gemini surfactant a tendency to partition into SOM other than adsorption on soil surface.

Moreover, only adsorbed surfactant could form a molecular aggregation and the extent may depend on the amount adsorbed and solid surface properties (Rutland and Senden, 1993). The surfactant partitioning into natural SOM was not subject to aggregation and thus had no marked effect on PHE uptake. However, when investigating the surfactant sorption process, partitioning into SOM should be taken into account since it might contribute to large fractions of surfactant distribution in soil.

As shown in Figure 7.5, it is interesting to note the isotherm at 298 K can be divided into two steps. For detailed mechanisms please refer to the Supplementary Material. The proposed sorption schematics for 12-2-12 gemini surfactant at the soil/aqueous interface corresponding to the two-step mechanism are illustrated in Figure 7.6. The schematic process of these two steps is also shown in Figure 7.7. Figure 7.8 represents the schematic diagram of interactions in water, soil, surfactant, and contaminant system.

Step I — The sorbed amount of 12-2-12 gemini increased with the surfactant equilibrium concentration and attained the first inflexion point at 34.4 mg/L. The enhanced sorption was attributed to the strong electrostatic attraction between positively charged head-groups in gemini surfactant and negatively charged soil surface. Since the hydrophobic tails of 12-2-12 gemini are very long (a chain length of 12 carbons), the surfactant chains might lay parallel to the soil surface and block some vacant adsorption sites. At the same time, cationic 12-2-12 gemini can partition into SOM due to the high polarity and large molecular weight.

Step II — With the increasing 12-2-12 gemini dose, the surfactant molecules which lay down at Step I began to stand up and form surface aggregates. At the initial stage of this step, the surfactant monomers were held on the soil surface in the form of hemimicelles. Sorption of surfactant increased dramatically over a narrow concentration interval and the initial concentration was termed as critical hemimicelle concentration (CHC) (Desai and Dixit, 1996). The hydrophobic tails of sorbed 12-2-12 gemini on soil and those in solution could interact with each other. This interaction would be intense since there are two hydrophobic tails included in one surfactant molecule. Once the hemimicelles were formed on soil surface, the 12-2-12 gemini molecules aggregated readily to form admicelles, while a weak partitioning into SOM was still involved at the meantime. The sorption at this stage exhibited a consistent increase and hydrophobic bonding, partition and electrostatic interaction contributed to the sorption of gemini surfactant on soil. Moreover, as the amount of the sorbed surfactant further increased, a hydrophobic surface of soil was obtained. The surfactants that existed as the hemimicelles/admicelles on soil surface could increase the sorbed surfactant-derived

retention for PHE. Afterwards, the sorbed amount of 12-2-12 gemini surfactant increased continuously above CMC and reached the first and second plateau. During the transition from Step I to II, more and more available CEC sites were electrically neutralized by the adsorbed 12-2-12 gemini cations and the natural SOM were gradually saturated with 12-2-12 gemini molecules. At relatively high surfactant concentrations above CMC, therefore, the electrostatic attraction and partition would play a less significant role and sorption took place mainly through hydrophobic interaction with a reduced slope. Two plateaus are shown in isotherms within the surfactant concentration range investigated. The of 12-2-12 gemini on the soil surface exhibited a stepwise pattern. It is conjectured the sorption amount would rise continuously with the increasing surfactant concentration through hydrophobic interaction.

The sorption process was divided into two steps because the predominant mechanisms were different in these two steps. As for the three plateaus in Figure 7.7, the first one represented the sorption behavior of 12-2-12 gemini in Step I resulting from electrostatic attraction and partition mechanisms. The second and the third plateaus represented the stepwise sorption of 12-2-12 gemini on soil surface in Step II. Hydrophobic interaction was the predominant mechanism in this step. Instead of starting a new step, the third plateau in Figure 7.7 was only an extension of the second plateau because their formation both resulted from the same mechanism-hydrophobic interaction. Containing two long hydrophobic tails, the interaction between 12-2-12 gemini molecules would be more intense with the increasing surfactant concentration. There would be more plateaus appearing in Step II and the sorption isotherm would exhibit a stepwise pattern with the increasing surfactant concentration. To gain a deep insight into

the related sorption characteristic and mechanism, it is necessary to further investigate the sorption process with appropriate modeling approach.

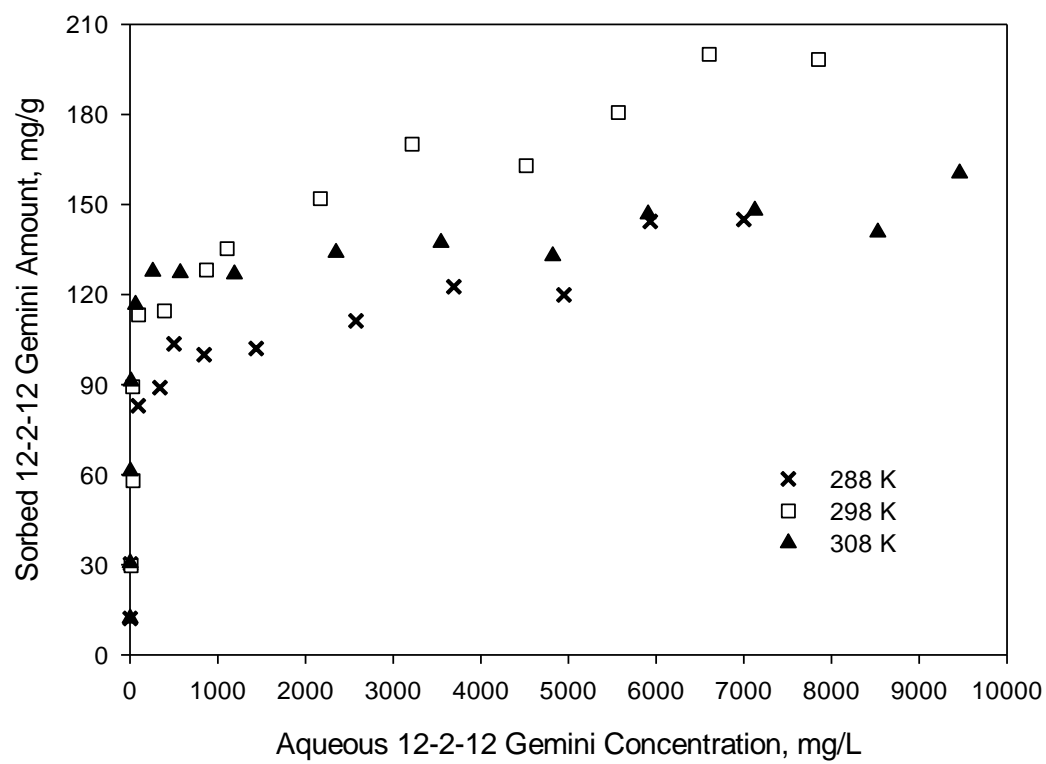
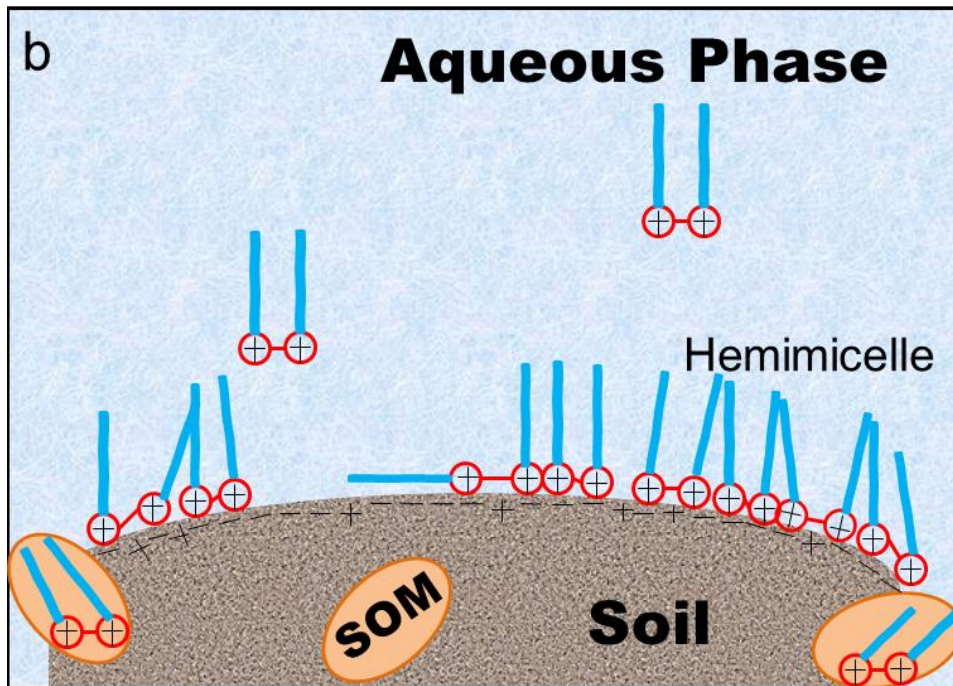
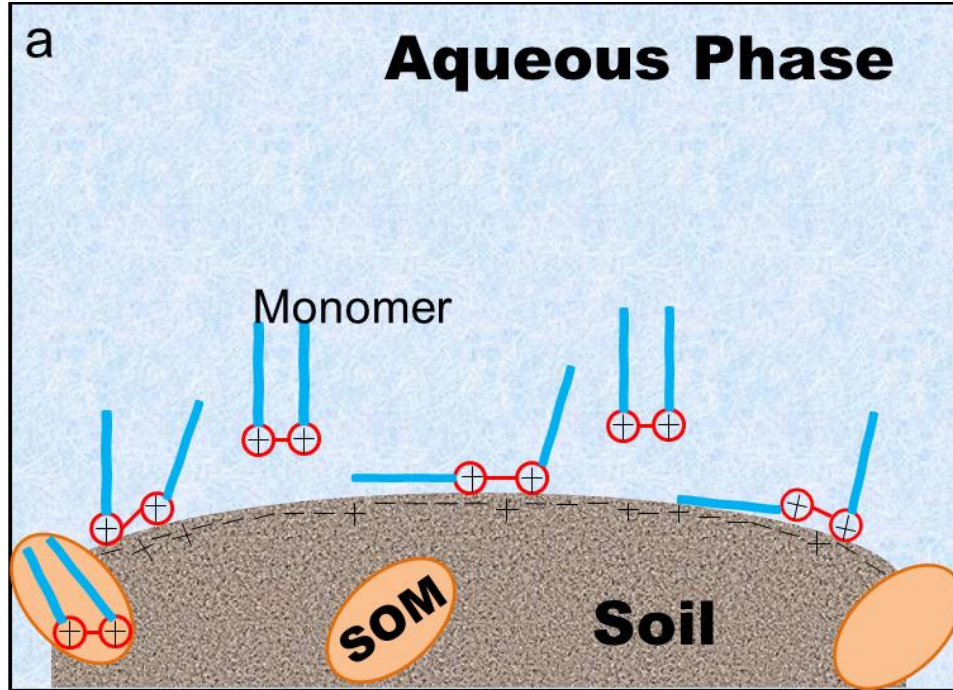


Figure 7.5 The sorption isotherms of 12-2-12 gemini surfactant at different temperatures



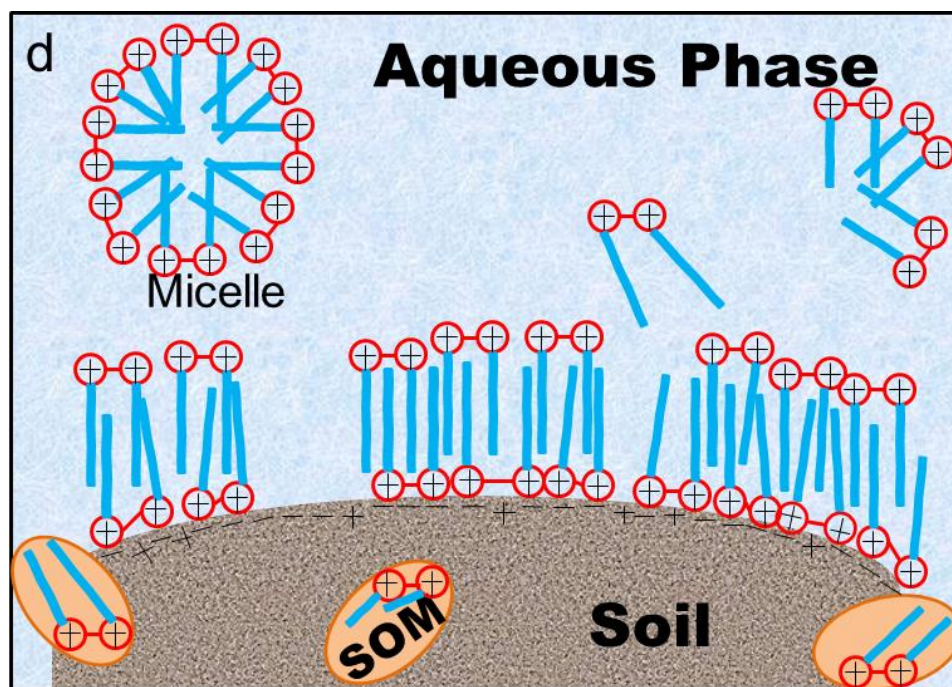
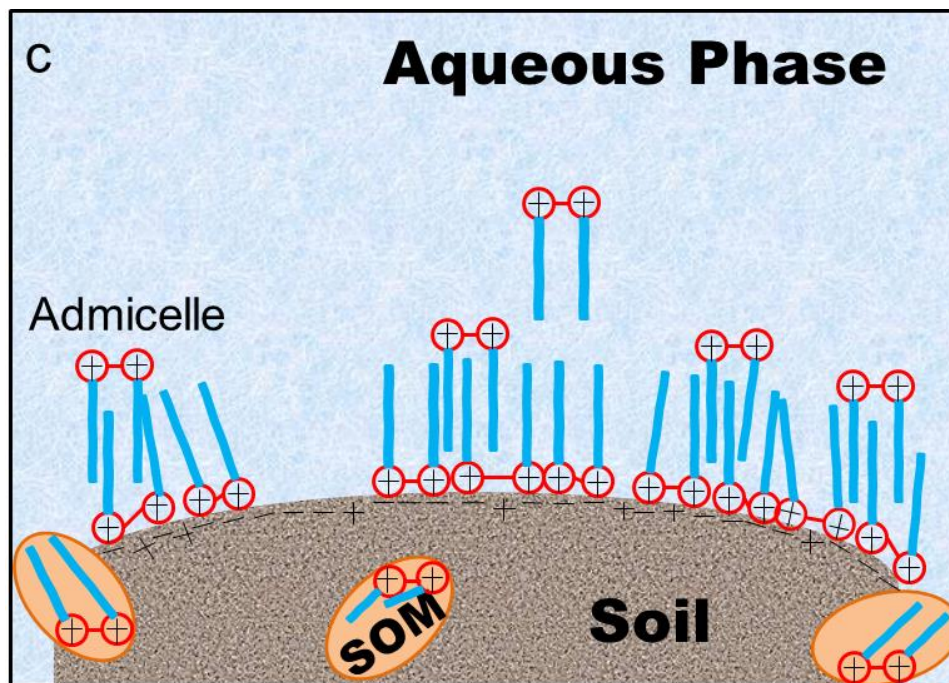


Figure 7.6 The schematic sorption process for 12-2-12 gemini surfactant at the soil/aqueous interface

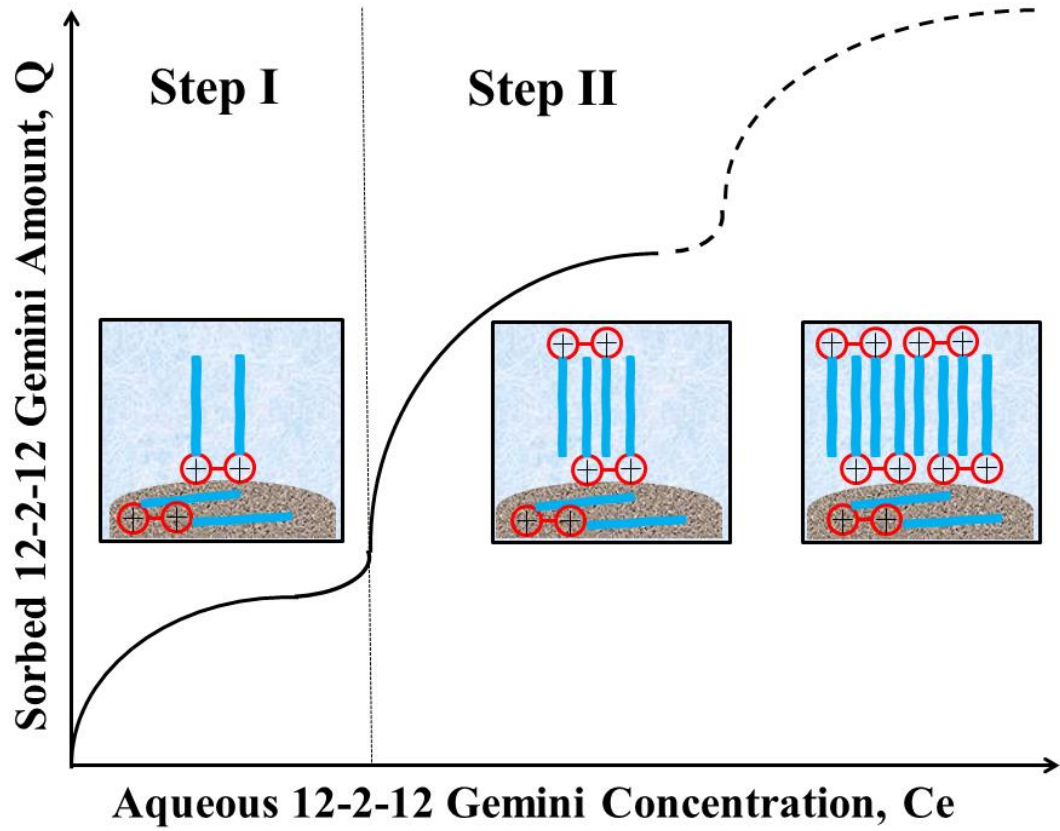


Figure 7.7 The two-step adsorption and partition isotherm of 12-2-12 gemini surfactant at the soil/water interface.

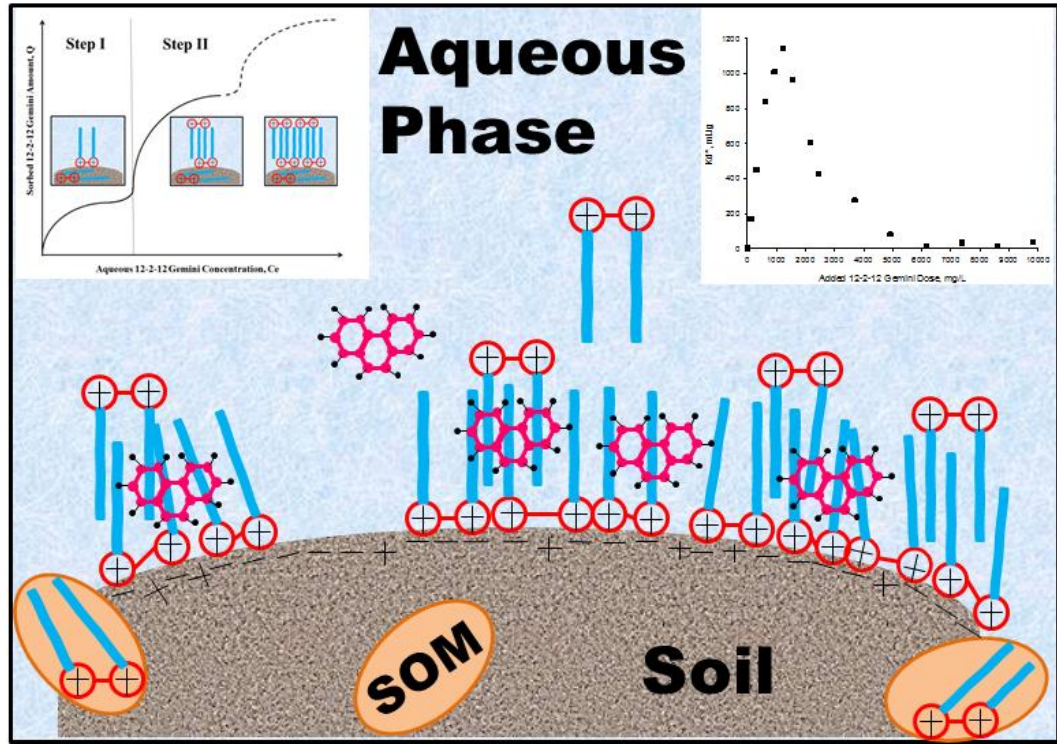


Figure 7.8 Schematic diagram of interactions in water, soil, surfactant, and contaminant system

#### 7.3.4. Modeling of the 12-2-12 Gemini Sorption Process at the Soil/Water Interface

Visual inspection results indicate pronounced nonlinearity in all of the isotherms. However, traditional nonlinear isotherm models cannot well fit the experimental data of 12-2-12 gemini sorption on soil. Much work has been done in this area and various sorption isotherm models including Freundlich and Langmuir models have been applied (Kunjappu and Somasundaran, 1989; Zhang and Somasundaran, 2006; Guo et al., 2009; Liu et al., 2014). Zhu and Gu tried to elucidate the phenomena of surfactant sorption at solid/liquid interfaces (Zhu and Gu, 1989, 1991). They introduced a general Two-step Adsorption Model (TAM) based on the two-step sorption mechanism of surfactants (Zhu and Gu, 1989).

In the first step, the surface-active ionic surfactants were adsorbed on the oppositely charged solid surface through electrostatic attraction and/or other specific forces. At equilibrium,



In the second step, the sorption of surfactants increased steeply because hemimicelles formed on the adsorbent through association or hydrophobic interaction between hydrocarbon chains of the surface-active species. Each of the ions or molecules adsorbed in the first step provided a possible active center for hemimicellization. At equilibrium,



The hemimicelle here was defined as a spherical structure with surfactant head-groups facing both towards the substrate and into the solution. In more recent times, this

type of structure was redefined as an admicelle (Atkin et al., 2003b). This equation has been successfully applied in many previous studies of surfactant sorption at solid/solution interfaces (Zhang and Somasundaran, 2006). However, the sorption of surfactant on soil is a more complex process. According to some previous studies (Lee et al., 2000; Lee et al., 2004), surfactant may partition into the SOM content other than adsorbing on mineral surface. Partition into SOM could be one mechanism for surfactant sorption on soil solids other than electrostatic and hydrophobic effects. Few studies have systematically investigated the related modeling approach. In our study, a Two-step Adsorption and Partition Model (TAPM) can be developed as:

$$Q = \frac{Q_{\max} K_1 C \left( \frac{1}{n} + K_2 C^{n-1} \right)}{1 + K_1 C (1 + K_2 C^{n-1})} + K_p C \quad (7.4)$$

where  $C$  is the equilibrium concentration of the surfactant, mg/L; and  $Q$  is the sorption amount at concentration  $C$  and  $Q_{\max}$  is the maximum adsorption amount at high concentrations, mg/g.  $K_1$  is the equilibrium constant of the first step (the predominant mechanism is electrostatic attraction, L/mg) and  $K_2$  is that of the second step (the predominant mechanism is hydrophobic interaction, L/mg);  $n$  is the hemimicelle aggregation number; and  $K_p$  is the partition coefficient due to the partition mechanism (Xing et al., 1996), L/g.

As described by Zhu and Gu (Zhu and Gu, 1989, 1991), Equation (7.4) (in the manuscript) had some limiting cases. If  $K_2 \rightarrow 0$  and  $n \rightarrow 1$ , it can be reduced to Langmuir dual-mode model (Xing et al., 1996):

$$Q = \frac{Q_{\max} K_1 C}{1 + K_1 C} + K_p C \quad (7.5)$$

The process before the formation of admicelle in Figure 7.4 could be illustrated by this model, since only 12-2-12 gemini monomer formed as the first Langmuir layer in these conditions.

If  $n > 1$ , Equation (7.4) had two limiting cases.

When  $K_2 C^{n-1} \ll 1/n$ , Equation (7.4) again was reduced to a Langmuir-type equation:

$$Q = \frac{(Q_{\max} / n) K_1 C}{1 + K_1 C} + K_p C \quad (7.6)$$

While the sorption peak value was  $Q_{\max}/n$  instead of  $Q_{\max}$ .

When  $K_2 C^{n-1} \gg 1$  or  $K_1 C \ll 1$  and  $K_1 C \ll K_2 C^n$ , Equation (7.4) could be reduced to:

$$Q = \frac{Q_{\max} K_1 K_2 C^n}{1 + K_1 K_2 C^n} + K_p C \quad (7.7)$$

This was the dual-mode model based on Sips isotherm model (Foo and Hameed, 2010).

The developed TAPM was employed to interpret the cationic 12-2-12 gemini sorption isotherms on soil surface. The estimated parameters based on experimental data with the aid of nonlinear regression analysis are given in Table 7.4. The fitting was first done by the TAM and then by TAPM for comparison, as listed in Table 7.4. The results indicated that the developed TAPM fitted better than TAM regarding the sorption data, as confirmed by the very high correlation coefficients  $R^2$ . The higher  $R^2$  ensured a

satisfactory adjustment of the developed model to the experimental data. Cationic 12-2-12 gemini surfactant can strongly adsorb on the negatively charged soil surface through electrostatic interaction ( $K_I$ ). The hydrophobic interaction between 12-2-12 gemini surfactants' hydrophobic tails also played a major role in the sorption process ( $K_2$ ). 12-2-12 gemini may partition into natural SOM and increase the sorption amount ( $K_p$ ). The developed TAPM can well represent the actual relationship between the responses and variables. The developed model involving the partition mechanism has never been reported previously and is very meaningful in the sorption studies of ionic surfactants.

The maximum adsorbed 12-2-12 gemini amount increased by 44.5% as the temperature increased from 288 to 298 K and decreased by 5.5% when the temperature increased from 298 to 308 K. The sorption behaviors of p-nitrophenol by anion-cation modified palygorskite at different temperatures exhibited the similar trend (Chang et al., 2009). The sorption capacity of 12-2-12 gemini is higher than those of conventional monomeric surfactants (Li and Rosen, 2000). The  $K$  values corresponding to different forces varied in the sorption process. The  $K$  data exhibited that hydrophobic interaction was the major force in the sorption process due to its highest value.

Table 7.4 Parameters of TAPM for 12-2-12 gemini sorption on soil\*

$T$ (K)	$Q_{max}$ (mg/g)	$K_1$ (L/mg)	$K_2$ (L/mg)	$K_p$ (L/g)	$R^2$ (TAPM)	$R^2$ (TAM)
288	88.254	0.0614	0.546	0.00716	0.984	0.905
298	127.508	0.0256	0.186	0.00998	0.963	0.876
308	120.532	0.223	0.488	0.00461	0.925	0.875

\*Error limits of parameters are less than  $\pm 3\%$ .

### 7.3.5. Thermodynamic Studies of the 12-2-12 Gemini Sorption at the Soil/Water

#### Interface

The above results showed that temperature played a key role in the sorption process. Despite the small sorption decrease from 298 to 308 K, the sorption amount of 12-2-12 gemini increased greatly with the increasing temperature from 288 to 308 K, indicating the sorption of 12-2-12 gemini onto soil surface might be an exothermic process. From the thermodynamic point of view, all the sorption behavior resulting from electrostatic attraction, hydrophobic interaction, and partition can be measured by the Gibbs free energy of the sorption process,  $\Delta G$  (KJ/mol) given by the following expression (An and Huang, 2012):

$$\Delta G = -RT \ln K \quad (7.8)$$

where  $R$  and  $T$  are the universal constant of the gases (8.314 J/(mol K)) and the absolute temperature (K).  $K$  is the equilibrium constant related to the various coefficients ( $K_f$ ,  $K_2$ , and  $K_p$ ) obtained from the sorption isotherms. Equilibrium constants  $K$  are also widely used to calculate thermodynamic parameters such as the enthalpy change ( $\Delta H$ , kJ/mol), and the entropy change ( $\Delta S$ , KJ/(mol K)) through the following equations:

$$\Delta G = \Delta H - T\Delta S \quad (7.9)$$

$$\ln K = -\frac{\Delta H}{TR} + \frac{\Delta S}{R} \quad (7.10)$$

The calculated  $\Delta G$ ,  $\Delta H$  and  $\Delta S$  are listed in Table 7.5.  $\Delta H$  and  $\Delta S$  are calculated from values of 288 and 308 K. The negative  $\Delta G$  values indicated the corresponding

sorption process was spontaneous and confirmed the high affinity of 12-2-12 gemini on soil. The  $\Delta H$  value was negative, indicating the sorption of 12-2-12 gemini surfactant was an exothermic process when temperature rising from 288 to 308 K. The positive value of  $\Delta S$  reflected the affinity of soil for 12-2-12 gemini and suggested the increasing randomness at solid/liquid interface during the sorption process. Similarly, the thermodynamic studies of SDS surfactant on clean sand particles at different temperatures were studied (Bera et al., 2013).

Table 7.5 Thermodynamic parameters for 12-2-12 gemini sorption on soil\*

$T(K)$	$\Delta G(KJ / mol)$	$\Delta H(KJ / mol)$	$\Delta S(KJ / (mol \cdot K))$
288	-36.5	-27.2	0.0324
298	-41.8		
308	-37.1		

\*Error limits of parameters are less than  $\pm 3\%$ .

### 7.3.6. Sorption of PHE by Soil through the Addition of Single Nonionic C<sub>12</sub>E<sub>10</sub>

#### Surfactant

At the meantime, nonionic surfactants can be partially sorbed on soil surface, producing a hydrophobic environment where PAHs can be immobilized. With the addition of C<sub>12</sub>E<sub>10</sub>,  $K_d^*$  increased sharply to a maximum sorption at the C<sub>12</sub>E<sub>10</sub> dose of 220 mg/L, and then declined steeply if more C<sub>12</sub>E<sub>10</sub> were added (Figure 7.9). The maximum  $K_d^*$  value was 210.0 mL/g, which is 90 times higher than that in absence of surfactants ( $K_d = 2.3$  mL/g). Thus, C<sub>12</sub>E<sub>10</sub> can also be used to enhance the retardation capabilities of soils for PAHs. However, this enhancement generated by C<sub>12</sub>E<sub>10</sub> was lower than that by 12-2-12 gemini (the maximum  $K_d^* = 1148.6$  mL/g), which might be attributed to the significant uptake of PHE by 12-2-12 gemini hemimicelles/admicelles. It was reported that the maximized  $K_d^*$  and sorption amount was obtained at the aqueous nonionic surfactant concentration around CMC (Yang et al., 2006; Hernández-Soriano et al., 2007; Zhang et al., 2012). However, in this study,  $K_d^*$  reached its plateau at two times of the CMC value. With the elevating surfactant concentration, the formation of aqueous C<sub>12</sub>E<sub>10</sub> micelles provided a more favorable medium for PHE partition and thus  $K_d^*$  sharply decreased. In addition, the sorbed amounts of C<sub>12</sub>E<sub>10</sub> on soil increased dramatically through hydrogen bonding to reach a plateau value of 29.3 mg/g at the approximate C<sub>12</sub>E<sub>10</sub> dose of 600 mg/L (Ivanova et al., 1995; Desai and Dixit, 1996). Then the sorption amounts declined sharply to 18.0 mg/g at the C<sub>12</sub>E<sub>10</sub> dosing rate of 880 mg/L. Interestingly, after that, the sorbed amounts of C<sub>12</sub>E<sub>10</sub> rose up again with the increasing C<sub>12</sub>E<sub>10</sub> dosage. The sorbed C<sub>12</sub>E<sub>10</sub> amount kept rising without finally leveling off in the range of concentrations tested in our studies. This is different with some previous

research, in which it was observed that for the sorption of nonionic polyoxyethylene alkyl (or alkylphenyl) ether surfactants onto oxide surfaces, the sorption plateau region appeared at the concentration around the CMC (Sakai et al., 2008). On the other hand, the reducing C<sub>12</sub>E<sub>10</sub> sorption is similar to the results reported in some previous studies (Stellner and Scamehorn, 1989; Paria and Khilar, 2004; Rao and He, 2006). Currently, there is still no settled consensus for this phenomenon (Paria and Khilar, 2004).

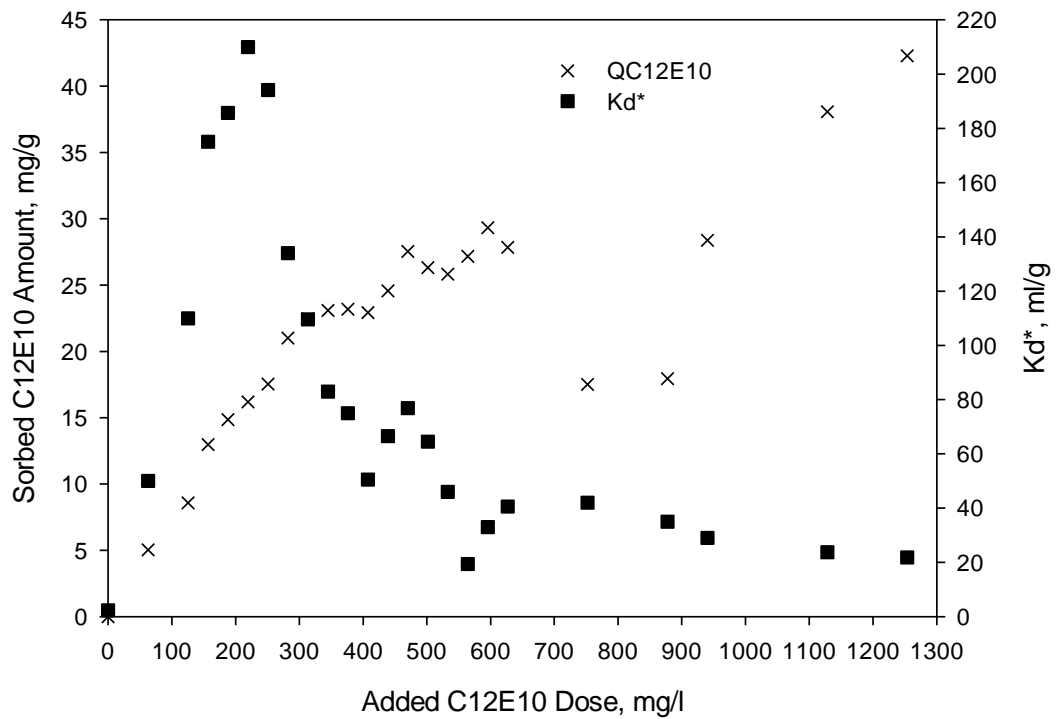


Figure 7.9 The sorbed  $C_{12}E_{10}$  amount and measured apparent sorption coefficients  $K_d^*$  of PHE in presence of individual  $C_{12}E_{10}$  surfactant

### 7.3.7. Sorption of PHE by Soil with the Addition of Binary Mixtures of Cationic 12-2-12 Gemini and Nonionic C<sub>12</sub>E<sub>10</sub> Surfactant

The sorption of PHE on soil in binary mixtures of surfactants was further investigated. The measured apparent sorption coefficients  $K_d^*$  of PHE are shown in Figure 7.10. At certain concentrations of C<sub>12</sub>E<sub>10</sub>,  $K_d^*$  values increased with the added 12-2-12 gemini dose to reach a maximum at 12-2-12 gemini dose of 1230 mg/L and then decreased with the further increase in the concentration of gemini surfactant. For the 12-2-12 gemini dose of 1230 mg/L,  $K_d^*$  increased dramatically at first and decreased subsequently when C<sub>12</sub>E<sub>10</sub> concentration ranged from 60 to 1630 mg/L. When the added 12-2-12 gemini amount was below 1230 mg/L, similar trends were observed except that the variation of  $K_d^*$  at low 12-2-12 gemini concentration was less significant. However, at the 12-2-12 gemini dose above 1230 mg/L, the  $K_d^*$  values declined continuously regardless of the C<sub>12</sub>E<sub>10</sub> dosage. As described in Equation (7.1), the reduction of  $K_d^*$  values can be attributed to the formation of mixed micelles in solution. The maximum  $K_d^*$  value of PHE was 4247.8 mL/g, corresponding to the 12-2-12 gemini and C<sub>12</sub>E<sub>10</sub> dose of 1230 and 220 mg/L, respectively. This peak  $K_d^*$  value was approximately 1846 times higher compared to that of PHE retention in soil without surfactants (2.3 mL/g). Therefore, the binary mixture of 12-2-12 gemini and C<sub>12</sub>E<sub>10</sub> surfactants can be considered as a better alternative than individual 12-2-12 gemini to improve soil retardation capabilities for PHE.

When the gemini surfactant dose was below or equal to 1230 mg/L and C<sub>12</sub>E<sub>10</sub> dose was below certain concentrations, enhanced sorption of PHE can be achieved due to either PHE sorption onto soil-sorbed surfactants or low PHE solubility in surfactant

solution. The results shown in Figure 7.10 are encouraging from the perspective of an enhanced sorption remediation scheme. Partitioning into SOM has been reported as the primary cause of PAHs sorption from water to most soils (Chiou et al., 1979). The sorption amount of PHE may be to a certain degree influenced by the different soil characteristics and surfactant properties (Lee et al., 2004; Yuan et al., 2007; Ahn et al., 2010). Soils with high organic matter serve as large sinks of PAHs, limiting their bioavailability and retarding their mobility effectively (Zhu et al., 2003). It is suggested from Figure 7.10 that the treatment with cationic-nonionic surfactant mixture could endow soil with large organic carbon content, making it favorable for PHE distribution into the sorbed micellar phase.

It is noted that the 12-2-12 gemini concentration may have significant influence on the sorption performance of PHE. (i) When 12-2-12 gemini dose was below 1230 mg/L, it was suggested that the addition of small quantity of C<sub>12</sub>E<sub>10</sub> enhanced the sorption of PHE. Under this condition, more micelle clusters could be formed in the mixed 12-2-12 gemini/C<sub>12</sub>E<sub>10</sub> system compared with that in the presence of 12-2-12 gemini alone. It is concluded that the addition of small amount of nonionic surfactant to cationic surfactant could markedly enhance the retention of pollutants. However, when C<sub>12</sub>E<sub>10</sub> dose was above certain concentrations (e.g., > 220 mg/L at the 12-2-12 gemini dose of 1230 mg/L), mixed surfactants would maintain active concentrations in solution and be more efficient for PHE desorption. Formation of aqueous micelle was essentially responsible for the significant reduction of the PHE retention on soil. (ii) When 12-2-12 gemini dose was above 1230 mg/L, the  $K_d^*$  value decreased with the increasing fraction of C<sub>12</sub>E<sub>10</sub> in the whole concentration range. As shown in Figure 7.10, there were a bunch of curves with

slight differences at the high initial dose of 12-2-12 gemini surfactant. This was due to the formation of large quantity of surfactant micelles in high-surfactant-concentration solution, which contributed to the transfer of PHE from soil to aqueous phase.

The sorption magnitude of binary surfactant mixture (12-2-12 gemini 1230 mg/L and C<sub>12</sub>E<sub>10</sub> 220 mg/L) for PHE outperformed the other mixtures and individual surfactant tested (Figure 7.11). This was attributed to the formation of the most compact arrangement of surfactants in the clusters formed at the solid/liquid interface (Desai and Dixit, 1996). The sorption capabilities of surfactant mixture for PHE were much higher than the summed individual results. The maximum  $K_d^*$  value of PHE was 1148.6 mL/g in the presence of individual 12-2-12 gemini and 210.0 mL/g in the presence of single C<sub>12</sub>E<sub>10</sub> surfactant (Figure 7.9), making the total value of 1358.6 mL/g. However, with the addition of the 12-2-12 gemini/C<sub>12</sub>E<sub>10</sub> binary mixture, the sorption coefficients reached up to 4247.8 mL/g. Such enhancement could be attributed to the synergetic effect of cationic 12-2-12 gemini and nonionic C<sub>12</sub>E<sub>10</sub> surfactant on the retention of PHE. In addition, as indicated in Figure 7.11, the distribution of PHE in soil–water system was significantly affected by the dosage of C<sub>12</sub>E<sub>10</sub> in the binary mixture of 12-2-12 gemini and C<sub>12</sub>E<sub>10</sub> surfactant. Low dosage of C<sub>12</sub>E<sub>10</sub> (< 220 mg/L) could increase the  $K_d^*$  value and hinder the desorption of PHE from soil particles. However, relative high concentration of C<sub>12</sub>E<sub>10</sub> (> 220 mg/L) significantly decreased the  $K_d^*$  value and inhibit the retention of PHE on soil. When increasing C<sub>12</sub>E<sub>10</sub> above 300 mg/L, the  $K_d^*$  value dramatically decreased, suggesting that the presence of excessive C<sub>12</sub>E<sub>10</sub> had negative effect on the distribution of PHE in soil phase.

In order to further investigate how surfactants affect the distribution of PHE in the

soil–water system, the  $K_d^*$  value of PHE as a function of the sorbed 12-2-12 gemini amount at the 12-2-12 gemini dose of 1230 mg/L was explored and the results are shown in Figure 7.12. With the increasing sorption amount of 12-2-12 gemini surfactant,  $K_d^*$  increased at the initial stage.  $K_d^*$  values reached a plateau and then decreased with the further increase of 12-2-12 gemini sorption amount. At low surfactant dose, the sorbed surfactant-derived organic carbon would facilitate the PHE retention in the soil particles. However, at a high dosage of surfactant, the surfactant micelles in solution would contribute to the PHE desorption from soil into aqueous phase.

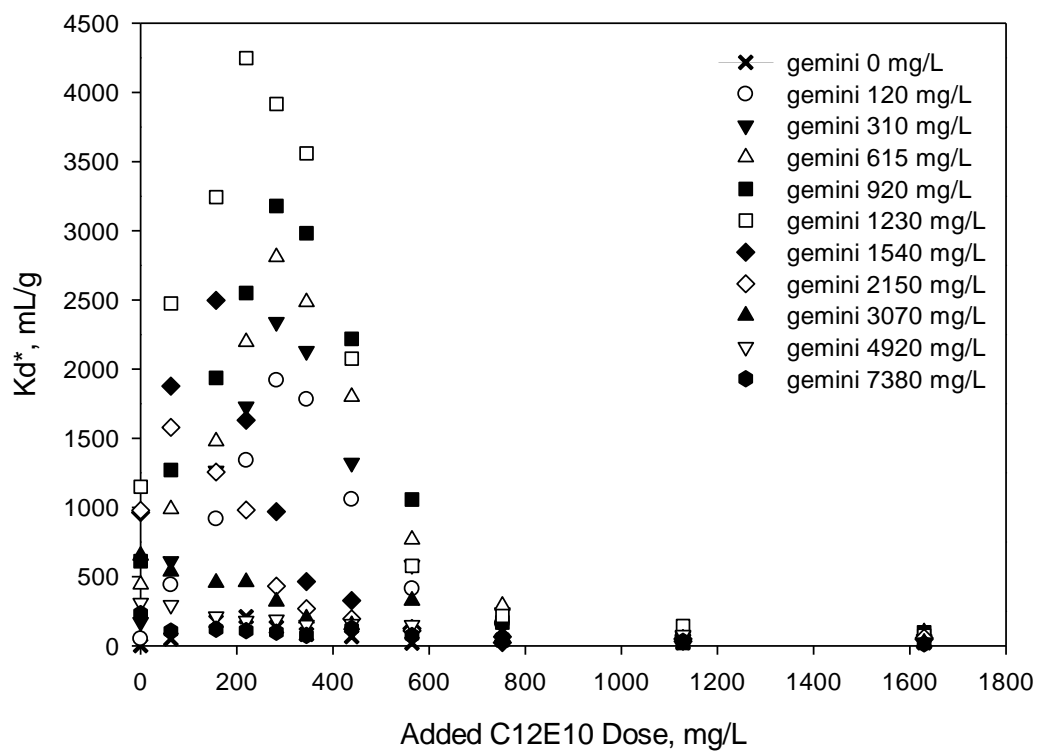


Figure 7.10 The measured apparent sorption coefficients  $K_d^*$  of PHE by soil with the addition of 12-2-12 gemini and  $C_{12}E_{10}$  surfactant mixtures

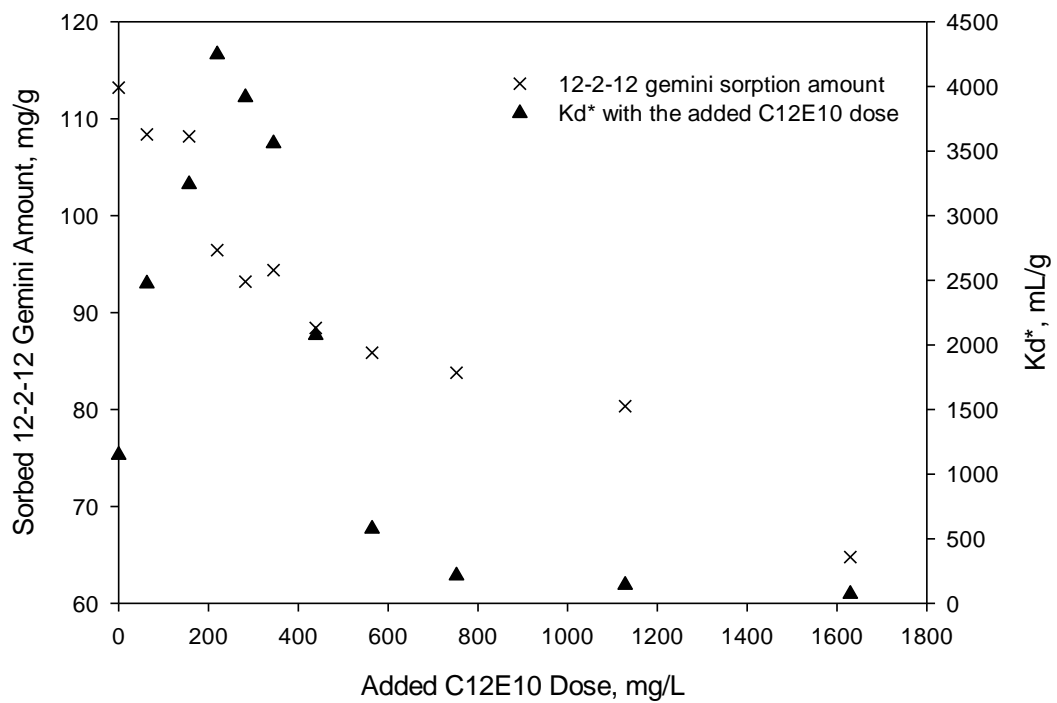


Figure 7.11 The sorbed 12-2-12 gemini amount and measured apparent sorption coefficients  $K_d^*$  of PHE versus the added  $C_{12}E_{10}$  dose at the 12-2-12 gemini dose of 1230 mg/L

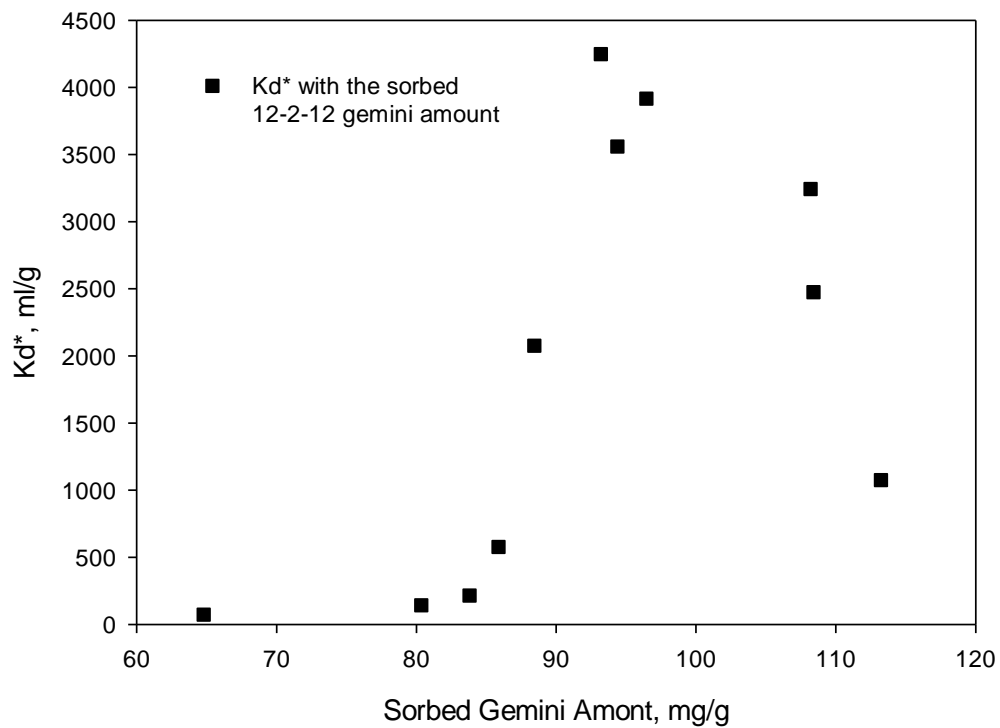


Figure 7.12 The measured  $K_d^*$  value of PHE versus the sorbed 12-2-12 gemini amount at the 12-2-12 gemini dose of 1230 mg/L

### **7.3.8. Sorption of Gemini Surfactant by Soil through the Addition of Binary**

#### **Mixtures of Cationic 12-2-12 Gemini and Nonionic C<sub>12</sub>E<sub>10</sub> Surfactant**

To better understand the role of gemini surfactant, the sorption of gemini surfactant on soil in binary mixtures of 12-2-12 gemini and C<sub>12</sub>E<sub>10</sub> surfactant was investigated and the results are shown in Figure 7.13. There was a consistent decrease in the sorption of 12-2-12 gemini as the C<sub>12</sub>E<sub>10</sub> dose increased to the maximum. Though the sorption of 12-2-12 gemini was reduced by the added C<sub>12</sub>E<sub>10</sub>, the enhancement of the surfactant mixtures on the sorption of PHE still increased sharply at certain range (Figure 7.10). The sorption of 12-2-12 gemini by soil from mixed surfactants was lower than that when 12-2-12 gemini was present alone. It could be inferred that the sorption of 12-2-12 gemini was slightly inhibited in the presence of C<sub>12</sub>E<sub>10</sub> surfactant. Several factors may cause this reduction: (i) At high concentration of C<sub>12</sub>E<sub>10</sub>, some negative sites on soil surface could be blocked by the sorbed oxyethylene chains of C<sub>12</sub>E<sub>10</sub> surfactant, resulting in the decreasing sorption of 12-2-12 gemini surfactant. It has been reported that the competition between cationic and nonionic surfactants for sorption sites could result in the decrease of sorption under saturation conditions (Desai and Dixit, 1996). (ii) In the surfactant mixture, sorption of surfactant was dominated by the fraction of surfactant in the monomeric form, since surfactant molecules could only be sorbed in the monomeric form instead of the micellar state (Gao et al., 1984). However, the interaction between ionic and nonionic surfactants led to a significant decrease in CMC value, which would reduce the monomer concentration of surfactants (Rubingh, 1979). Therefore, the sorption level of ionic surfactant would decrease correspondingly (Xu et al., 1991; Desai and Dixit, 1996). Similarly, the increasing dose of nonionic C<sub>12</sub>E<sub>10</sub> surfactant and the

intense mixed micellization of the binary mixture would result in the reduction in monomer concentration of 12-2-12 gemini surfactant. This process may be also responsible for the decrease in gemini sorption with the addition of the surfactant mixtures. (iii) In a mixture of surfactants, moreover, abundant surfactant sorbed on soil could act as the steric barrier and interfere with the sorption of other surfactants. For example, due to the stronger surface activity of nonionic  $A_{12}E_9$  surfactant (alcohol ethoxylates with 12 carbons and 9 oxyethyl groups) as compared to that of anionic SDBS surfactant (sodium dodecylbenzenesulfonate), large quantities of sorption sites on the second layer would be occupied by  $A_{12}E_9$ . It could result in the decline of SDBS sorption amount at the plateau region within the soil–water system (Rao and He, 2006).  $A_{12}E_9$  and  $C_{12}E_{10}$  have similar chemical structures and properties. It was likely that the decrease of 12-2-12 gemini sorption in the presence of nonionic  $C_{12}E_{10}$  was due to the same mechanism.

It is also interesting to note that the higher initial 12-2-12 gemini dose shows a higher “desorption” rate as indicated by the slope in Figure 7.13. The higher the initial 12-2-12 gemini concentration in solution, the easier it was to form mixed micelles that would not sorb on the soil surface. In that case, the mixed micelles in the aqueous phase were comparatively more stable, and would compete with the hemimicelles on the soil surface for 12-2-12 gemini molecules. Therefore, with the increase of  $C_{12}E_{10}$  concentration, the sorbed cationic 12-2-12 gemini molecules were partially replaced by the nonionic  $C_{12}E_{10}$  molecules at the solid/liquid interface. Particularly, when 12-2-12 gemini dose was 1230 mg/L (see Figure 7.11), clearly the presence of  $C_{12}E_{10}$  played a negative role in the 12-2-12 gemini sorption. The sorption amount of 12-2-12 gemini

decreased linearly with the increasing dose of  $C_{12}E_{10}$ , indicating that 12-2-12 gemini was “washed out” by  $C_{12}E_{10}$ . Similar results were identified in previous studies regarding the competitive sorption (Ivanova et al., 1995; Desai and Dixit, 1996), while others indicated that synergistic interaction was observed during the sorption process of cationic-nonionic surfactant mixtures (Sakai et al., 2008; Zhou and Somasundaran, 2009).

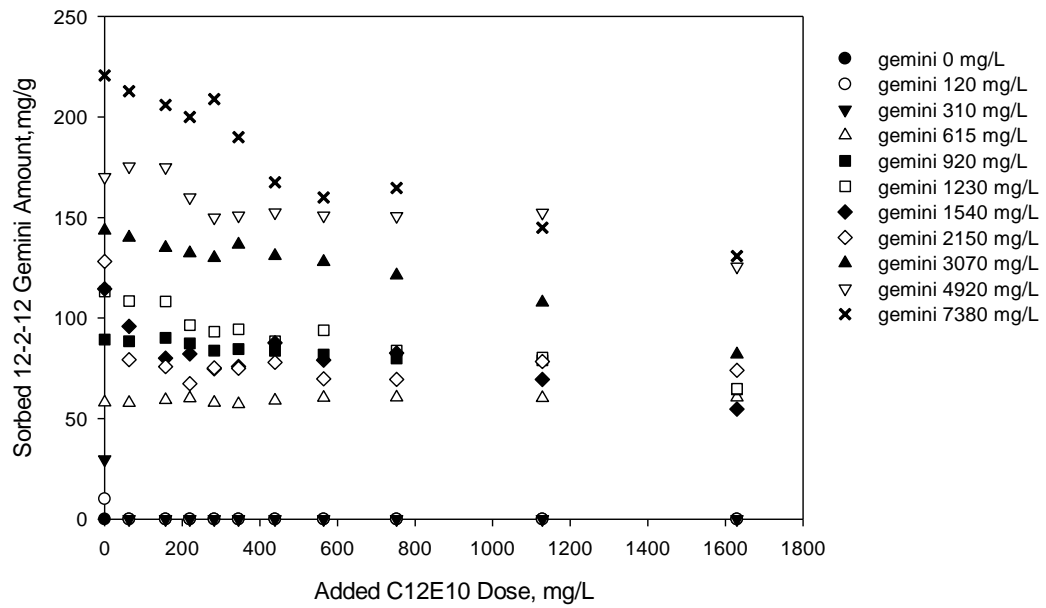


Figure 7.13 The sorbed 12-2-12 gemini amount with the added  $C_{12}E_{10}$  dose in presence of 12-2-12 gemini and  $C_{12}E_{10}$  surfactant mixtures

## 7.4. SUMMARY

In sum, the enhancement of PHE sorption on soil with the added cationic 12-2-12 gemini and the corresponding binary mixtures has been well established. Sorption of 12-2-12 gemini on soil provided a favorable partition medium for PHE and therefore enhanced the PHE retention in soil particles. The 12-2-12 gemini sorption isotherm was divided into two steps and it clearly exhibited a stepwise pattern. The sorption mechanisms mainly included electrostatic attraction, hydrophobic interaction, and partition into the soil organic matter. As an improved method for sorption behavior analysis, the developed TAPM can help well simulate the sorption of gemini surfactant on soil. TAPM can also be applied to other soil-water systems as an alternative to describe the distribution behavior of ionic surfactants. In addition, the gemini surfactant and related surfactant mixtures can be utilized as sorption barriers to facilitate the retention of PAHs. The results of this study have important implications for pollution control at PAH-contaminated sites. Future studies are desired to define the characteristics of gemini surfactant and solution chemistry, as well as their effects to obtain more theoretical foundation for analyzing enhanced PAH retention in soil-water system. The influencing parameters gained from batch tests can be useful for the parameter determination and experimental design of the future column studies and real field applications.

# **CHAPTER 8**

## **CONCLUSIONS**

### **8.1. SUMMARY**

In this dissertation research, several physiochemical processes have been proposed for the produced water treatment and groundwater remediation at petroleum-contaminated sites. A brief summary of this research is given as follow:

(1) The feasibility of treating produced water using synthetic polymers PAC, PFS, and PAM combined with natural diatomite and to refine the operating parameters using diatomite as an adsorbent and a coagulant aid was evaluated. The enhanced coagulation/flocculation by combining PAC with diatomite was investigated through mechanism analysis compared to the combination of PFS/PAM with diatomite, respectively. The effects of coagulant dose, initial pH, and settling time on COD and turbidity were studied using PAC-diatomite in comparison with using PAC only. Diatomite was favorable to improve the flocs settleability, reduce the suspended foulants, accelerate the settling rate, and enhance the coagulation process. The enhanced coagulation/flocculation of diatomite with PAC was better than that with PFS/PAM in terms of COD/turbidity removal and floc settling characteristics, considering costs.

(2) This study enhanced the hardness removal (together with COD and turbidity) from the produced water by a pilot-scale EC system to minimize the scaling and fouling of RO membranes. It also comprehensively evaluated the feasibility of using EC as the pretreatment for RO in oil fields. In preliminary studies, the EC process was experimentally performed and the effects of three main variables (initial pH, current

density and electrolysis time) on pollutants removal were investigated through mechanism analysis. Response surface methodology was employed to evaluate individual/interactive influences of parameters on pollutants recovery and to optimize treatment processes. ANOVA showed a satisfactory agreement of predicted values and experimental data. The 3D surface contour plots were presented to locate optimum regions (points) with the lowest pollutant levels and to characterize the single/combined effects of variables on pollutant removals.

(3) The sorption behavior of gemini surfactants at the PGS/aqueous interface was addressed. The characterizations of gemini modified PGS were investigated using infrared spectroscopy, cation exchange capacity, and surface area analysis. The effects of pH, ionic strength, humic acid, and temperature on sorption of PHE to untreated and modified PGS were systematically studied. Analysis of the equilibrium data indicated that the sorption isotherms of gemini fitted TAPM well. The modification of PGS with gemini surfactants provided a favorable partition medium for PHE and enhanced PHE retention in solid particles. The solution parameters played significant effects on PHE sorption to the modified PGS. The sorption isotherms of PHE on PGS at different temperatures well fitted the Freundlich equation. Thermodynamic calculations confirmed that the sorption process of PHE on modified PGS was spontaneous and exothermic from 293 to 303 K. This can provide a reference to the potential application of PGS in PAHs-contaminated water remediation process.

(4) A multi-level fuzzy-factorial inference approach was proposed to examine the sorption behavior of PHE on PGS modified with a gemini surfactant. Fuzzy set theory was used to determine five experimentally controlled environmental factors with

triangular membership functions, including initial concentration, added humid acid dose, ionic strength, temperature, and pH. The statistical significance of factors and their interactions affecting the sorption process was revealed through a multi-level factorial experiment. Initial concentration, ionic strength, and pH were identified as the most significant factors based on the multi-way ANOVA results. Examination of curvature effects of factors revealed the nonlinear complexity inherent in the sorption process. The potential interactions among experimental factors were detected, which is meaningful for providing a deep insight into the sorption mechanisms under the influences of factors at different levels.

(5) The enhancement of soil retention for PAHs through the addition of a binary mixture of cationic gemini (12-2-12) and nonionic surfactants ( $C_{12}E_{10}$ ) was investigated. The maximum apparent sorption coefficient  $K_d^*$  reached through the addition of mixed 12-2-12 gemini and  $C_{12}E_{10}$  surfactants, which was markedly higher than the summed individual results in the presence of individual 12-2-12 gemini or  $C_{12}E_{10}$  surfactant. However, the sorption of 12-2-12 gemini was inhibited by the increasing  $C_{12}E_{10}$  dose; and a higher initial 12-2-12 gemini dose showed a higher “desorption” rate. The present study also addressed the sorption behavior of the single 12-2-12 gemini surfactant at the soil/aqueous interface. The sorption isotherm was divided into two steps to elucidate the sorption process; and the sorption schematics were proposed to elaborate the growth of surfactant aggregates corresponding to the various steps of the sorption isotherm. Finally, a two-step adsorption and partition model was developed to simulate the sorption process. Analysis of the equilibrium data indicated that the sorption isotherms of 12-2-12 gemini fitted the TAPM model better. Thermodynamic calculations confirmed that the 12-2-12

geminium sorption at the soil/aqueous interface was spontaneous and exothermic from 288 to 308 K.

## **8.2. RESEARCH ACHIEVEMENTS**

(1) The enhanced coagulation/flocculation process by combining PAC with diatomite has been proposed as one alternative to economically treat the wastewater in oil fields. This study has provided an economical and enhanced approach for diatomite utilization in the treatment of produced water, satisfying the demands of reuse or reinjection into the ground.

(2) For the first time, a pilot-scale EC process has been developed for enhanced removal of hardness, COD, and turbidity, with the related experimental design being supported by Response surface method. EC has been proven that it can effectively remove hardness and oil suspensions from treated water and therefore mitigate membrane scaling and fouling. RSM has been demonstrated as an effective approach for obtaining desired operating conditions in complex EC pretreatment processes for RO membrane reactors.

(3) The effectiveness of gemini modified PGS as the novel remediation material in PAHs-contaminated water remediation has been revealed and examined. Clearly the modification with gemini surfactants probably has offered some unique surface characteristics to the clay mineral as a new type of remediation material. The results can reveal the distribution of PAHs in a PGS-water system and facilitate the potential modification and utilization of PGS for enhanced removal of PAHs from contaminated water effluents.

(4) This research is the first attempt to investigate the sorption behavior of PHE on GPGS by using a multi-level fuzzy-factorial inference approach. The proposed method is capable of providing a deep insight into the sorption characteristics of PAHs under environmental factors at different levels. Fuzzy vertex analysis discretized the design factors with triangular membership functions into multiple deterministic levels based on the  $\alpha$ -cut concept and interval analysis. Examination of curvature effects has revealed the nonlinear relationship between experimental factors and the sorption capacity. Compared with the conventional two-level factorial experiment, the multi-level factorial experiment has elucidated sorption mechanisms through revealing the statistical significance of experimental factors and their interactions at multiple levels.

(5) This research is the first attempt to study the enhanced soil retention of PAHs by binary cationic gemini and nonionic surfactant mixtures. The research has addressed the sorption characteristic and mechanism of gemini surfactant in complex soil system, and investigated the sorption process through model development. The Two-step Adsorption and Partition Model involving the partition mechanism has never been reported and provided a deep insight into the sorption characteristics of ionic surfactant. The sorption barrier created by binary surfactant mixtures has substantially enhanced the soil retention capabilities for PHE. The interactions among water, soil, surfactant, and contaminant in groundwater remediation process have been revealed.

### **8.3. RECOMMENDATIONS FOR FUTURE RESEARCH**

Based on the research presented in this dissertation, further studies are desired in the following aspects:

(1) Little data was reported on the flowing EC-RO process for the wastewater treatment. Future research may be conducted on finding the optimum conditions for the flowing EC-RO system to enhance the RO product water quality and improve the water recovery. We will also conduct research to characterize the precipitation salts that are produced during EC process and determine their composition and structures.

(2) Future studies will be conducted to explore the role of gemini surfactants in enhancing PHE sorption on PGS. Mechanisms regarding how gemini affects the surface characteristics of PGS and further the sorption behaviors of PHE will be explored. In addition, mechanism research will be conducted to elucidate the curvature effects of experimental factors on sorption capacity and to explicate the interactions among factors at different levels. This will provide a deep insight into the sorption process when multi-level factors are involved.

(3) Future studies are desired to define the characteristics of gemini surfactant and solution chemistry, as well as their effects to obtain more theoretical foundation for analyzing enhanced PAH retention in soil-water system. The influencing parameters gained from batch tests can be useful for the parameter determination and experimental design of the future column studies and real field applications of sorption barriers created by gemini surfactant mixtures.

## REFERENCES

- Abadi, S. R. H., Sebzari, M. R., Hemati, M., Rekabdar, F. and Mohammadi, T. 2011. Ceramic membrane performance in microfiltration of oily wastewater. *Desalination*, 265(1), 222-228.
- Abbasi, M., Mirfendereski, M., Nikbakht, M., Golshenas, M. and Mohammadi, T. 2010a. Performance study of mullite and mullite–alumina ceramic MF membranes for oily wastewaters treatment. *Desalination*, 259(1), 169-178.
- Abbasi, M., Reza Sebzari, M. and Mohammadi, T. 2011. Enhancement of oily wastewater treatment by ceramic microfiltration membranes using powder activated carbon. *Chemical Engineering & Technology*, 34(8), 1252-1258.
- Abbasi, M., Salahi, A., Mirfendereski, M., Mohammadi, T. and Pak, A. 2010b. Dimensional analysis of permeation flux for microfiltration of oily wastewaters using mullite ceramic membranes. *Desalination*, 252(1), 113-119.
- Abdel-Ghani, N., Hegazy, A. K., El-Chaghaby, G. and Lima, E. C. 2009. Factorial experimental design for biosorption of iron and zinc using *Typha domingensis* phytomass. *Desalination*, 249(1), 343-347.
- Abdelwahab, O., Amin, N. and El-Ashtouky, E. Z. 2009. Electrochemical removal of phenol from oil refinery wastewater. *Journal of Hazardous Materials*, 163(2), 711-716.
- Aharoni, C. and Ungarish, M. 1977. Kinetics of activated chemisorption. Part 2.- Theoretical models. *Journal of the Chemical Society, Faraday Transactions 1: Physical Chemistry in Condensed Phases*, 73(0), 456-464.
- Ahmad, A. L., Sumathi, S. and Hameed, B. H. 2006. Coagulation of residue oil and

- suspended solid in palm oil mill effluent by chitosan, alum and PAC. *Chemical Engineering Journal*, 118(1–2), 99-105.
- Ahmad, Ahmad, A. L., Sumathi, Sumathi, S., Hameed and Hameed, B. H. 2004. Chitosan: A natural biopolymer for the adsorption of residue oil from oily wastewater. *Adsorption Science & Technology*, 22(1), 75-88.
- Ahmaruzzaman, M. 2008. Adsorption of phenolic compounds on low-cost adsorbents: a review. *Advances in colloid and interface science*, 143(1), 48-67.
- Ahn, C. K., Woo, S. H. and Park, J. M. 2010. Surface solubilization of phenanthrene by surfactant sorbed on soils with different organic matter contents. *Journal of Hazardous Materials*, 177(1–3), 799-806.
- Al-Degs, Y. S., Tutunju, M. F. and Shawabkeh, R. A. 2000. The feasibility of using diatomite and Mn–diatomite for remediation of  $Pb^{2+}$ ,  $Cu^{2+}$ , and  $Cd^{2+}$  from water. *Separation Science and Technology*, 35(14), 2299-2310.
- Aleboye, A., Daneshvar, N. and Kasiri, M. B. 2008. Optimization of C.I. Acid Red 14 azo dye removal by electrocoagulation batch process with response surface methodology. *Chemical Engineering and Processing: Process Intensification*, 47(5), 827-832.
- Al-Ghouti, M. A., Khraisheh, M. A. M., Allen, S. J. and Ahmad, M. N. 2003. The removal of dyes from textile wastewater: a study of the physical characteristics and adsorption mechanisms of diatomaceous earth. *Journal of Environmental Management*, 69(3), 229-238.
- Al-Ghouti, M., Khraisheh, M., Ahmad, M. and Allen, S. 2005. Thermodynamic behaviour and the effect of temperature on the removal of dyes from aqueous

- solution using modified diatomite: a kinetic study. *Journal of Colloid and Interface Science*, 287(1), 6-13.
- Alther, G. 2002. Using organoclays to enhance carbon filtration. *Waste Management*, 22(5), 507-513.
- Al-Zoubi, H., Al-Thyabat, S. and Al-Khatib, L. 2009. A hybrid flotation-membrane process for wastewater treatment: an overview. *Desalination and Water Treatment*, 7(1-3), 60-70.
- An, C. and Huang, G. 2012. Stepwise adsorption of phenanthrene at the fly ash–water interface as affected by solution chemistry: experimental and modeling studies. *Environmental Science & Technology*, 46(22), 12742-12750.
- An, C. J., Huang, G. H., Wei, J. and Yu, H. 2011. Effect of short-chain organic acids on the enhanced desorption of phenanthrene by rhamnolipid biosurfactant in soil–water environment. *Water Research*, 45(17), 5501-5510.
- Ang, W. S., Lee, S. and Elimelech, M. 2006. Chemical and physical aspects of cleaning of organic-fouled reverse osmosis membranes. *Journal of Membrane Science*, 272(1-2), 198-210.
- Annadurai, G., Juang, R. S. and Lee, D. J. 2002. Factorial design analysis for adsorption of dye on activated carbon beads incorporated with calcium alginate. *Advances in Environmental Research*, 6(2), 191-198.
- Atkin, R., Craig, V. S. J., Wanless, E. J. and Biggs, S. 2003a. Adsorption of 12-s-12 gemini surfactants at the silica–aqueous solution interface. *The Journal of Physical Chemistry B*, 107(13), 2978-2985.
- Atkin, R., Craig, V. S. J., Wanless, E. J. and Biggs, S. 2003b. Mechanism of cationic

- surfactant adsorption at the solid–aqueous interface. *Advances in Colloid and Interface Science*, 103(3), 219-304.
- Atkin, R., Craig, V., Wanless, E. and Biggs, S. 2003c. Mechanism of cationic surfactant adsorption at the solid–aqueous interface. *Advances in colloid and interface science*, 103(3), 219-304.
- Babel, S. and Kurniawan, T. A. 2003. Low-cost adsorbents for heavy metals uptake from contaminated water: a review. *Journal of Hazardous Materials*, 97(1), 219-243.
- Bailey, S. E., Olin, T. J., Bricka, R. M. and Adrian, D. D. 1999. A review of potentially low-cost sorbents for heavy metals. *Water Research*, 33(11), 2469-2479.
- Bande, R. M., Prasad, B., Mishra, I. and Wasewar, K. L. 2008. Oil field effluent water treatment for safe disposal by electroflotation. *Chemical Engineering Journal*, 137(3), 503-509.
- Bani-Melhem, K. and Smith, E. 2012. Grey water treatment by a continuous process of an electrocoagulation unit and a submerged membrane bioreactor system. *Chemical Engineering Journal*, 198–199(0), 201-210.
- Barrier, P. R. and Table, W. 1998. Permeable reactive barrier technologies for contaminant remediation. 600R98125.
- Baudequin, C., Couallier, E., Rakib, M., Deguerry, I., Severac, R. and Pabon, M. 2011. Purification of firefighting water containing a fluorinated surfactant by reverse osmosis coupled to electrocoagulation–filtration. *Separation and Purification Technology*, 76(3), 275-282.
- Bellona, C. and Drewes, J. E. 2005. The role of membrane surface charge and solute physico-chemical properties in the rejection of organic acids by NF membranes.

- Journal of Membrane Science, 249(1–2), 227-234.
- Bera, A., Kumar, T., Ojha, K. and Mandal, A. 2013. Adsorption of surfactants on sand surface in enhanced oil recovery: Isotherms, kinetics and thermodynamic studies. Applied Surface Science, 284(0), 87-99.
- Bhaskar Raju, G., Thalamadai Karuppiyah, M., Latha, S. S., Latha Priya, D., Parvathy, S. and Prabhakar, S. 2009. Electrochemical pretreatment of textile effluents and effect of electrode materials on the removal of organics. Desalination, 249(1), 167-174.
- Bingol, D., Tekin, N. and Alkan, M. 2010. Brilliant Yellow dye adsorption onto sepiolite using a full factorial design. Applied Clay Science, 50(3), 315-321.
- Blowes, D. W., Ptacek, C. J., Benner, S. G., McRae, C. W., Bennett, T. A. and Puls, R. W. 2000. Treatment of inorganic contaminants using permeable reactive barriers. Journal of Contaminant Hydrology, 45(1), 123-137.
- Bouras, O., Bollinger, J. C. and Baudu, M. 2010. Effect of humic acids on pentachlorophenol sorption to cetyltrimethylammonium-modified, Fe- and Al-pillared montmorillonites. Applied Clay Science, 50(1), 58-63.
- Bowman, R. S. 2003. Applications of surfactant-modified zeolites to environmental remediation. Microporous and Mesoporous Materials, 61(1), 43-56.
- Boyd, S. A., Lee, J. F. and Mortland, M. M. 1988. Attenuating organic contaminant mobility by soil modification. Nature, 333(6171), 345-347.
- Bulut, E., Özacar, M. and Şengil, İ. A. 2008. Adsorption of malachite green onto bentonite: Equilibrium and kinetic studies and process design. Microporous and Mesoporous Materials, 115(3), 234-246.
- Burris, D. R. and Antworth, C. P. 1992. *In situ* modification of an aquifer material by a

- cationic surfactant to enhance retardation of organic contaminants. *Journal of Contaminant Hydrology*, 10(4), 325-337.
- Cai, Y. P., Huang, G. H., Lu, H. W., Yang, Z. F. and Tan, Q. 2009. I-VFRP: An interval-valued fuzzy robust programming approach for municipal waste-management planning under uncertainty. *Engineering Optimization*, 41(5), 399-418.
- Çakmakce, M., Kayaalp, N. and Koyuncu, I. 2008. Desalination of produced water from oil production fields by membrane processes. *Desalination*, 222(1), 176-186.
- Caliskan, N., Kul, A. R., Alkan, S., Sogut, E. G. and Alacabey, İ. 2011. Adsorption of Zinc(II) on diatomite and manganese-oxide-modified diatomite: A kinetic and equilibrium study. *Journal of Hazardous Materials*, 193(0), 27-36.
- Cañizares, P., Martínez, F., Jiménez, C., Sáez, C. and Rodrigo, M. A. 2008. Coagulation and electrocoagulation of oil-in-water emulsions. *Journal of Hazardous Materials*, 151(1), 44-51.
- Cañizares, P., Martínez, F., Lobato, J. and Rodrigo, M. A. 2007. Break-up of oil-in-water emulsions by electrochemical techniques. *Journal of Hazardous Materials*, 145(1-2), 233-240.
- Carmona, M. E. R., da Silva, M. A. P. and Ferreira Leite, S. G. 2005. Biosorption of chromium using factorial experimental design. *Process Biochemistry*, 40(2), 779-788.
- Carvalho, M., Clarisse, M., Lucas, E., Barbosa, C. and Barbosa, L. 2002. Evaluation of the polymeric materials (DVB copolymers) for produced water treatment, Society of Petroleum Engineers.
- Castro, M. J., Kovensky, J. and Fernández Cirelli, A. 2002. New family of nonionic

- gemini surfactants. Determination and analysis of interfacial properties. *Langmuir*, 18(7), 2477-2482.
- CCME report. 2008. Canadian Council of Ministers of the Environment.
- CCME report. 2014. Canadian Council of Ministers of the Environment.
- Cestari, A. R., Vieira, E. F. S., de Oliveira, I. A. and Bruns, R. E. 2007. The removal of Cu(II) and Co(II) from aqueous solutions using cross-linked chitosan-Evaluation by the factorial design methodology. *Journal of Hazardous Materials*, 143(1-2), 8-16.
- Cestari, A. R., Vieira, E. F., Tavares, A. M. and Bruns, R. E. 2008. The removal of the indigo carmine dye from aqueous solutions using cross-linked chitosan-Evaluation of adsorption thermodynamics using a full factorial design. *Journal of Hazardous Materials*, 153(1), 566-574.
- Chang, Y., Lv, X., Zha, F., Wang, Y. and Lei, Z. 2009. Sorption of p-nitrophenol by anion-cation modified palygorskite. *Journal of Hazardous Materials*, 168(2), 826-831.
- Chapelle, F. H. 1999. Bioremediation of petroleum hydrocarbon-contaminated ground water: the perspectives of history and hydrology. *Groundwater*, 37(1), 122-132.
- Chavalparit, O. and Ongwandee, M. 2009. Optimizing electrocoagulation process for the treatment of biodiesel wastewater using response surface methodology. *Journal of Environmental Sciences*, 21(11), 1491-1496.
- Chegrouche, S. and Bensmaili, A. 2002. Removal of Ga(III) from aqueous solution by adsorption on activated bentonite using a factorial design. *Water Research*, 36(11), 2898-2904.
- Chen, G., Chen, X. and Yue, P. 2000. Electrocoagulation and electroflotation of

- restaurant wastewater. *Journal of Environmental Engineering*, 126(9), 858-863.
- Chen, G. 2004. Electrochemical technologies in wastewater treatment. *Separation and Purification Technology*, 38(1), 11-41.
- Chen, H. and Wang, A. 2007. Kinetic and isothermal studies of lead ion adsorption onto palygorskite clay. *Journal of Colloid and Interface Science*, 307(2), 309-316.
- Chen, H., Zhao, Y. and Wang, A. 2007. Removal of Cu(II) from aqueous solution by adsorption onto acid-activated palygorskite. *Journal of Hazardous Materials*, 149(2), 346-354.
- Chen, X., Chen, G. and Yue, P. L. 2000a. Separation of pollutants from restaurant wastewater by electrocoagulation. *Separation and Purification Technology*, 19(1-2), 65-76.
- Chen, X., Chen, G. and Yue, P. L. 2002. Novel electrode system for electroflotation of wastewater. *Environmental Science & Technology*, 36(4), 778-783.
- Chiou, C. T., Peters, L. J. and Freed, V. H. 1979. A physical concept of soil-water equilibria for nonionic organic compounds. *Science*, 206(4420), 831-832.
- Chou, W. L., Wang, C. T. and Huang, K. Y. 2009. Effect of operating parameters on indium(III) ion removal by iron electrocoagulation and evaluation of specific energy consumption. *Journal of Hazardous Materials*, 167(1-3), 467-474.
- Chu, H., Zhang, Y., Dong, B., Zhou, X., Cao, D., Qiang, Z., Yu, Z. and Wang, H. 2012. Pretreatment of micro-polluted surface water with a biologically enhanced PAC-diatomite dynamic membrane reactor to produce drinking water. *Desalination and Water Treatment*, 40(1-3), 84-91.
- Chu, H. Q., Cao, D. W., Jin, W. and Dong, B. Z. 2008. Characteristics of bio-diatomite

- dynamic membrane process for municipal wastewater treatment. *Journal of Membrane Science*, 325(1), 271-276.
- Cline, J. 1998. Treatment and discharge of produced water for deep offshore disposal, pp. 17-18.
- Commission, O. 2005. Report on discharges spills and emissions from offshore oil and gas installations.
- Crini, G. 2006. Non-conventional low-cost adsorbents for dye removal: a review. *Bioresource Technology*, 97(9), 1061-1085.
- Czurda, K. A. and Haus, R. 2002. Reactive barriers with fly ash zeolites for *in situ* groundwater remediation. *Applied Clay Science*, 21(1-2), 13-20.
- de Namor, A. F. D., El Gamouz, A., Frangie, S., Martinez, V., Valiente, L. and Webb, O. A. 2012. Turning the volume down on heavy metals using tuned diatomite. A review of diatomite and modified diatomite for the extraction of heavy metals from water. *Journal of Hazardous Materials*, 241, 14-31.
- Den, W. and Wang, C. J. 2008. Removal of silica from brackish water by electrocoagulation pretreatment to prevent fouling of reverse osmosis membranes. *Separation and Purification Technology*, 59(3), 318-325.
- Desai, T. R. and Dixit, S. G. 1996. Coadsorption of cationic–nonionic surfactant mixtures on polytetra fluoroethylene (PTFE) surface. *Journal of Colloid and Interface Science*, 179(2), 544-551.
- Deshpande, S., Wesson, L., Wade, D., Sabatini, D. and Harwell, J. 2000. Dowfax surfactant components for enhancing contaminant solubilization. *Water Research*, 34(3), 1030-1036.

- Dimoglo, A., Akbulut, H., Cihan, F. and Karpuzcu, M. 2004. Petrochemical wastewater treatment by means of clean electrochemical technologies. *Clean Technologies and Environmental Policy*, 6(4), 288-295.
- Dong, W. and Shah, H. C. 1987. Vertex method for computing functions of fuzzy variables. *Fuzzy Sets and Systems*, 24(1), 65-78.
- Doyle, D. H. and Brown, A. B. 2000. Produced water treatment and hydrocarbon removal with organoclay, Society of Petroleum Engineers.
- Drouiche, N., Aoudj, S., Hecini, M., Ghaffour, N., Lounici, H. and Mameri, N. 2009. Study on the treatment of photovoltaic wastewater using electrocoagulation: Fluoride removal with aluminium electrodes-Characteristics of products. *Journal of Hazardous Materials*, 169(1-3), 65-69.
- Dubinin, M. and Radushkevich, L. 1947. Equation of the characteristic curve of activated charcoal. *Chemistry Central Journal*, 1(1), 875.
- El-Naas, M. H., Alhaija, M. A. and Al-Zuhair, S. 2014. Evaluation of a three-step process for the treatment of petroleum refinery wastewater. *Journal of Environmental Chemical Engineering*, 2(1), 56-62.
- El-Naas, M. H., Al-Zuhair, S., Al-Lobaney, A. and Makhoulf, S. 2009. Assessment of electrocoagulation for the treatment of petroleum refinery wastewater. *Journal of Environmental Management*, 91(1), 180-185.
- El-Nahhal, Y. Z. and Safi, J. M. 2004. Adsorption of phenanthrene on organoclays from distilled and saline water. *Journal of Colloid and Interface Science*, 269(2), 265-273.
- Environment Canada. <https://www.ec.gc.ca/eau-water/default.asp?lang=En&n=6A7FB7>

B2-1

- Erdem, E., Çölgeçen, G. and Donat, R. 2005. The removal of textile dyes by diatomite earth. *Journal of Colloid and Interface Science*, 282(2), 314-319.
- Eren, E., Afsin, B. and Onal, Y. 2009. Removal of lead ions by acid activated and manganese oxide-coated bentonite. *Journal of Hazardous Materials*, 161(2), 677-685.
- Esmailirad, N., Carlson, K. and Omur Ozbek, P. 2015. Influence of softening sequencing on electrocoagulation treatment of produced water. *Journal of Hazardous Materials*, 283(0), 721-729.
- Ezechi, E. H., Isa, M. H., bin Mohamed Kutty, S. R. and Ahmed, Z. 2015. Electrochemical removal of boron from produced water and recovery. *Journal of Environmental Chemical Engineering*, 3(3), 1962-1973.
- Fakhru'l-Razi, A., Pendashteh, A., Abdullah, L. C., Biak, D. R. A., Madaeni, S. S. and Abidin, Z. Z. 2009. Review of technologies for oil and gas produced water treatment. *Journal of Hazardous Materials*, 170(2-3), 530-551.
- Fang, J., Shan, X. Q., Wen, B., Lin, J. M., Lu, X. C., Liu, X. D. and Owens, G. 2008. Sorption and desorption of phenanthrene onto iron, copper, and silicon dioxide nanoparticles. *Langmuir*, 24(19), 10929-10935.
- Foo, K. Y. and Hameed, B. H. 2010. Insights into the modeling of adsorption isotherm systems. *Chemical Engineering Journal*, 156(1), 2-10.
- Freundlich, H. 1906. Over the adsorption in solution. *The Journal of Physical Chemistry*, 57(385), 385-470.
- Gan, S., Lau, E. and Ng, H. 2009. Remediation of soils contaminated with polycyclic

- aromatic hydrocarbons (PAHs). *Journal of Hazardous Materials*, 172(2), 532-549.
- Gao, B. and Sharma, M. M. 2013. A family of alkyl sulfate gemini surfactants. 2. Water-oil interfacial tension reduction. *Journal of Colloid and Interface Science*, 407(0), 375-381.
- Gao, B. Y., Hahn, H. H. and Hoffmann, E. 2002. Evaluation of aluminum-silicate polymer composite as a coagulant for water treatment. *Water Research*, 36(14), 3573-3581.
- Gao, B., Jiang, P., An, F., Zhao, S. and Ge, Z. 2005. Studies on the surface modification of diatomite with polyethyleneimine and trapping effect of the modified diatomite for phenol. *Applied Surface Science*, 250(1-4), 273-279.
- Gao, Y., Yue, C., Lu, S., Gu, W. and Gu, T. 1984. Adsorption from mixed solutions of Triton X-100 and sodium n-alkyl sulfates on silica gel. *Journal of Colloid and Interface Science*, 100(2), 581-583.
- Gao, Y., Du, J. and Gu, T. 1987. Hemimicelle formation of cationic surfactants at the silica gel-water interface. *Journal of the Chemical Society, Faraday Transactions 1: Physical Chemistry in Condensed Phases*, 83(8), 2671-2679.
- Gavaskar, A. R., Gupta, N., Sass, B., Janosy, R. and OSullivan, D. 1998. Permeable barriers for groundwater remediation. Battelle Press, Columbus, OH.
- Ghernaout, D., Badis, A., Kellil, A. and Ghernaout, B. 2008. Application of electrocoagulation in *Escherichia coli* culture and two surface waters. *Desalination*, 219(1-3), 118-125.
- Giles, C. H., MacEwan, T. H., Nakhwa, S. N. and Smith, D. 1960. 786. Studies in adsorption. Part XI. A system of classification of solution adsorption isotherms,

- and its use in diagnosis of adsorption mechanisms and in measurement of specific surface areas of solids. *Journal of the Chemical Society (Resumed)*, (0), 3973-3993.
- Gimbert, F., Morin-Crini, N., Renault, F., Badot, P. M. and Crini, G. 2008. Adsorption isotherm models for dye removal by cationized starch-based material in a single component system: Error analysis. *Journal of Hazardous Materials*, 157(1), 34-46.
- Glickman, A. 1998. Produced water toxicity: steps you can take to ensure permit compliance.
- Gök, Ö., Özcan, A. S. and Özcan, A. 2008. Adsorption kinetics of naphthalene onto organo-sepiolite from aqueous solutions. *Desalination*, 220(1), 96-107.
- Gottipati, R. and Mishra, S. 2010. Process optimization of adsorption of Cr(VI) on activated carbons prepared from plant precursors by a two-level full factorial design. *Chemical Engineering Journal*, 160(1), 99-107.
- Gryta, M., Karakulski, K. and Morawski, A. W. 2001. Purification of oily wastewater by hybrid UF/MD. *Water Research*, 35(15), 3665-3669.
- Gu, T. and Huang, Z. 1989. Thermodynamics of hemimicellization of cetyltrimethylammonium bromide at the silica gel/water interface. *Colloids and surfaces*, 40, 71-76.
- Günay, A., Arslankaya, E. and Tosun, İ. 2007. Lead removal from aqueous solution by natural and pretreated clinoptilolite: Adsorption equilibrium and kinetics. *Journal of Hazardous Materials*, 146(1-2), 362-371.
- Guo, H., Liu, Z., Yang, S. and Sun, C. 2009. The feasibility of enhanced soil washing of p-nitrochlorobenzene (pNCB) with SDBS/Tween80 mixed surfactants. *Journal of Hazardous Materials*, 170(2-3), 1236-1241.

- Gupta, V. 2009. Application of low-cost adsorbents for dye removal - A review. *Journal of Environmental Management*, 90(8), 2313-2342.
- Gupta, V. K., Carrott, P. J. M., Ribeiro Carrott, M. M. L. and Suhas 2009. Low-cost adsorbents: growing approach to wastewater treatment - a review. *Critical Reviews in Environmental Science and Technology*, 39(10), 783-842.
- Hadjar, H., Hamdi, B. and Ania, C. O. 2011. Adsorption of p-cresol on novel diatomite/carbon composites. *Journal of Hazardous Materials*, 188(1-3), 304-310.
- Han, I., Schlautman, M. A. and Batchelor, B. 2000. Removal of hexavalent chromium from groundwater by granular activated carbon. *Water Environment Research*, 72(1), 29-39.
- Haritash, A. and Kaushik, C. 2009. Biodegradation aspects of polycyclic aromatic hydrocarbons (PAHs): a review. *Journal of Hazardous Materials*, 169(1), 1-15.
- Hasany, S. M. and Chaudhary, M. H. 1996. Sorption potential of Haro river sand for the removal of antimony from acidic aqueous solution. *Applied Radiation and Isotopes*, 47(4), 467-471.
- He, L. 2008. Development of integrated simulation and optimization models for petroleum-contaminated groundwater remediation management under various uncertainties. Ph.D., The University of Regina (Canada), Ann Arbor.
- Hernández-Soriano, M. C., Mingorance, M. D. and Peña, A. 2007. Interaction of pesticides with a surfactant-modified soil interface: Effect of soil properties. *Colloids and Surfaces A: Physicochemical and Engineering Aspects*, 306(1-3), 49-55.
- Hinz, C. 2001. Description of sorption data with isotherm equations. *Geoderma*, 99(3-4),

225-243.

- Ho, Y. S., Porter, J. F. and McKay, G. 2002. Equilibrium isotherm studies for the sorption of divalent metal ions onto peat: copper, nickel and lead single component systems. *Water, Air, and Soil Pollution*, 141(1-4), 1-33.
- Hosseini, M., Mertens, S. F. L., Ghorbani, M. and Arshadi, M. R. 2003. Asymmetrical Schiff bases as inhibitors of mild steel corrosion in sulphuric acid media. *Materials Chemistry and Physics*, 78(3), 800-808.
- Hua, F., Tsang, Y., Wang, Y., Chan, S., Chua, H. and Sin, S. 2007. Performance study of ceramic microfiltration membrane for oily wastewater treatment. *Chemical Engineering Journal*, 128(2), 169-175.
- Huang, J., Liu, Y., Jin, Q., Wang, X. and Yang, J. 2007a. Adsorption studies of a water soluble dye, Reactive Red MF-3B, using sonication-surfactant-modified attapulgite clay. *Journal of Hazardous Materials*, 143(1), 541-548.
- Huang, J., Liu, Y. and Wang, X. 2008. Selective adsorption of tannin from flavonoids by organically modified attapulgite clay. *Journal of Hazardous Materials*, 160(2-3), 382-387.
- Huang, J., Wang, X., Jin, Q., Liu, Y. and Wang, Y. 2007. Removal of phenol from aqueous solution by adsorption onto OTMAC-modified attapulgite. *Journal of environmental management*, 84(2), 229-236.
- Ighilahriz, K., Ahmed, M. T., Djelal, H. and Maachi, R. 2014. Electrocoagulation and electro-oxidation treatment for the leachate of oil-drilling mud. *Desalination and Water Treatment*, 52(31-33), 5833-5839.
- Ivanova, N. I., Volchkova, I. L. and Shchukin, E. D. 1995. Adsorption of nonionic and

- cationic surfactants from aqueous binary mixtures onto the solid/liquid interface. *Colloids and Surfaces A: Physicochemical and Engineering Aspects*, 101(2-3), 239-243.
- Jiang, J. Q. and Kim, C. 2008. Comparison of algal removal by coagulation with clays and Al - based coagulants. *Separation Science and Technology*, 43(7), 1677-1686.
- Jiang, J. Q., Zeng, Z. and Pearce, P. 2004a. Evaluation of modified clay coagulant for sewage treatment. *Chemosphere*, 56(2), 181-185.
- Jiang, J. Q., Zeng, Z. and Pearce, P. 2004b. Preparation and use of modified clay coagulants for wastewater treatment. *Water, Air, and Soil Pollution*, 158(1), 53-65.
- Jossens, L., Prausnitz, J. M., Fritz, W., Schlünder, E. U. and Myers, A. L. 1978. Thermodynamics of multi-solute adsorption from dilute aqueous solutions. *Chemical Engineering Science*, 33(8), 1097-1106.
- Juang, R. S., Lin, S. H. and Tsao, K. H. 2004. Sorption of phenols from water in column systems using surfactant-modified montmorillonite. *Journal of Colloid and Interface Science*, 269(1), 46-52.
- Karhu, M., Kuokkanen, V., Kuokkanen, T. and Ränö, J. 2012. Bench scale electrocoagulation studies of bio oil-in-water and synthetic oil-in-water emulsions. *Separation and Purification Technology*, 96(0), 296-305.
- Kaushik, C. and Haritash, A. 2006. Polycyclic aromatic hydrocarbons (PAHs) and environmental health.
- Kavak, D. 2009. Removal of boron from aqueous solutions by batch adsorption on calcined alunite using experimental design. *Journal of Hazardous Materials*, 163(1), 308-314.

- Khan, F. I., Husain, T. and Hejazi, R. 2004. An overview and analysis of site remediation technologies. *Journal of Environmental Management*, 71(2), 95-122.
- Khandegar, V. and Saroha, A. K. 2013. Electrocoagulation for the treatment of textile industry effluent - A review. *Journal of Environmental Management*, 128(0), 949-963.
- Khatib, Z. and Verbeek, P. 2002. *Water to Value - Produced water management for sustainable field development of mature and green fields*, Society of Petroleum Engineers.
- Khayet, M., Zahrim, A. Y. and Hilal, N. 2011. Modelling and optimization of coagulation of highly concentrated industrial grade leather dye by response surface methodology. *Chemical Engineering Journal*, 167(1), 77-83.
- Khraisheh, M. A. M., Al-degs, Y. S. and McMinn, W. A. M. 2004. Remediation of wastewater containing heavy metals using raw and modified diatomite. *Chemical Engineering Journal*, 99(2), 177-184.
- Khraisheh, M. A. M., Al-Ghouti, M. A., Allen, S. J. and Ahmad, M. N. 2005. Effect of OH and silanol groups in the removal of dyes from aqueous solution using diatomite. *Water Research*, 39(5), 922-932.
- Kim, Y., Kim, C., Choi, I., Rengaraj, S. and Yi, J. 2004. Arsenic removal using mesoporous alumina prepared via a templating method. *Environmental Science & Technology*, 38(3), 924-931.
- Ko, S. O., Schlautman, M. A. and Carraway, E. R. 1998. Effects of solution chemistry on the partitioning of phenanthrene to sorbed surfactants. *Environmental Science & Technology*, 32(22), 3542-3548.

- Kobyas, M., Can, O. T. and Bayramoglu, M. 2003. Treatment of textile wastewaters by electrocoagulation using iron and aluminum electrodes. *Journal of Hazardous materials*, 100(1-3), 163-178.
- Kobyas, M., Demirbas, E., Bayramoglu, M. and Sensoy, M. T. 2011. Optimization of electrocoagulation process for the treatment of metal cutting wastewaters with response surface methodology. *Water, Air, & Soil Pollution*, 215(1-4), 399-410.
- Kobyas, M., Hiz, H., Senturk, E., Aydiner, C. and Demirbas, E. 2006. Treatment of potato chips manufacturing wastewater by electrocoagulation. *Desalination*, 190(1-3), 201-211.
- Körbahti, B. K., Aktaş, N. and Tanyolaç, A. 2007. Optimization of electrochemical treatment of industrial paint wastewater with response surface methodology. *Journal of Hazardous Materials*, 148(1-2), 83-90.
- Kumar, M., Adham, S. S. and Pearce, W. R. 2006. Investigation of seawater reverse osmosis fouling and its relationship to pretreatment type. *Environmental Science & Technology*, 40(6), 2037-2044.
- Kunjappu, J. T. and Somasundaran, P. 1989. Comments on "on the structure of aggregates of adsorbed surfactants: the surface charge density at the hemimicelle/admicelle transition". *The Journal of Physical Chemistry*, 93(22), 7744-7745.
- Kurniawan, T. A., Chan, G. Y., Lo, W. H. and Babel, S. 2006. Comparisons of low-cost adsorbents for treating wastewaters laden with heavy metals. *Science of the Total Environment*, 366(2), 409-426.
- Langmuir, I. 1916. The constitution and fundamental properties of solids and liquids. Part

- I. Solids. *Journal of the American Chemical Society*, 38(11), 2221-2295.
- Larue, O., Vorobiev, E., Vu, C. and Durand, B. 2003. Electrocoagulation and coagulation by iron of latex particles in aqueous suspensions. *Separation and Purification Technology*, 31(2), 177-192.
- Lee, J. F., Crum, J. R. and Boyd, S. A. 1989. Enhanced retention of organic contaminants by soils exchanged with organic cations. *Environmental Science & Technology*, 23(11), 1365-1372.
- Lee, J. F., Hsu, M. H., Chao, H. P., Huang, H. C. and Wang, S. P. 2004. The effect of surfactants on the distribution of organic compounds in the soil solid/water system. *Journal of Hazardous Materials*, 114(1), 123-130.
- Lee, J. F., Liao, P. M., Kuo, C. C., Yang, H. T. and Chiou, C. T. 2000. Influence of a nonionic surfactant (Triton X-100) on contaminant distribution between water and several soil solids. *Journal of Colloid and Interface Science*, 229(2), 445-452.
- Li, F. and Rosen, M. J. 2000c. Adsorption of gemini and conventional cationic surfactants onto montmorillonite and the removal of some pollutants by the clay. *Journal of Colloid and Interface Science*, 224(2), 265-271.
- Li, Z. and Hong, H. 2009. Retardation of chromate through packed columns of surfactant-modified zeolite. *Journal of Hazardous Materials*, 162(2), 1487-1493.
- Li, Z. J. and Fu, Z. H. 2009. Study on treatment of oilfield wastewater by electrocoagulation/flotation process. *China Water Wastewater*, 7.
- Limousin, G., Gaudet, J. P., Charlet, L., Szenknect, S., Barthès, V. and Krimissa, M. 2007. Sorption isotherms: A review on physical bases, modeling and measurement. *Applied Geochemistry*, 22(2), 249-275.

- Liu, B., Wang, X., Yang, B. and Sun, R. 2011. Rapid modification of montmorillonite with novel cationic Gemini surfactants and its adsorption for methyl orange. *Materials Chemistry and Physics*, 130(3), 1220-1226.
- Liu, Y., Gao, M., Gu, Z., Luo, Z., Ye, Y. and Lu, L. 2014. Comparison between the removal of phenol and catechol by modified montmorillonite with two novel hydroxyl-containing Gemini surfactants. *Journal of Hazardous Materials*, 267, 71-80.
- Lo, C., Zhang, J., Couzis, A., Somasundaran, P. and Lee, J. 2010. Adsorption of cationic and anionic surfactants on cyclopentane hydrates. *The Journal of Physical Chemistry C*, 114(31), 13385-13389.
- Lou, L., Liu, F., Yue, Q., Chen, F., Yang, Q., Hu, B. and Chen, Y. 2013. Influence of humic acid on the sorption of pentachlorophenol by aged sediment amended with rice-straw biochar. *Applied Geochemistry*, 33(0), 76-83.
- Ma, J. and Zhu, L. 2006. Simultaneous sorption of phosphate and phenanthrene to inorgano-organo-bentonite from water. *Journal of Hazardous Materials*, 136(3), 982-988.
- Mackay, D. M. and Cherry, J. A. 1989. Groundwater contamination: Pump-and-treat remediation. *Environmental Science & Technology*, 23(6), 630-636.
- Maher, A., Sadeghi, M. and Moheb, A. 2014. Heavy metal elimination from drinking water using nanofiltration membrane technology and process optimization using response surface methodology. *Desalination*, 352(0), 166-173.
- Malakootian, M., Mansoorian, H. J. and Moosazadeh, M. 2010. Performance evaluation of electrocoagulation process using iron-rod electrodes for removing hardness from

- drinking water. *Desalination*, 255(1-3), 67-71.
- Mameri, N., Yeddou, A. R., Lounici, H., Belhocine, D., Grib, H. and Bariou, B. 1998. Defluoridation of septentrional Sahara water of North Africa by electrocoagulation process using bipolar aluminium electrodes. *Water Research*, 32(5), 1604-1612.
- Marchese, J., Ochoa, N., Pagliero, C. and Almandoz, C. 2000. Pilot-scale ultrafiltration of an emulsified oil wastewater. *Environmental Science & Technology*, 34(14), 2990-2996.
- Martínez-Delgadillo, S. A., Morales-Mora, M. A. and Barceló-Quintal, I. D. 2010. Electrocoagulation treatment to remove pollutants from petroleum refinery wastewater. *Journal of Environmental Engineering and Management*, 20(4), 227-231.
- Mastral, A. M. and Callen, M. S. 2000. A review on polycyclic aromatic hydrocarbon (PAH) emissions from energy generation. *Environmental Science & Technology*, 34(15), 3051-3057.
- Means, C. M. and Braden, M. L. 1992. Process for removing water soluble organic compounds from produced water, Google Patents.
- Menezes, F. M., Amal, R. and Luketina, D. 1996. Removal of particles using coagulation and flocculation in a dynamic separator. *Powder Technology*, 88(1), 27-31.
- Menger, F. M. and Keiper, J. S. 2000. Gemini Surfactants. *Angewandte Chemie International Edition*, 39(11), 1906-1920.
- Meski, S., Ziani, S., Khireddine, H., Boudboub, S. and Zaidi, S. 2011. Factorial design analysis for sorption of zinc on hydroxyapatite. *Journal of Hazardous Materials*, 186(2), 1007-1017.

- Moazed, H. and Viraraghavan, T. 2001. Organo-clay/anthracite filtration for oil removal. *Journal of Canadian Petroleum Technology*, 40(09), 37-42.
- Moazed, H. and Viraraghavan, T. 2005. Removal of oil from water by bentonite organoclay. *Practice Periodical of Hazardous, Toxic, and Radioactive Waste Management*, 9(2), 130-134.
- Mollah, M. Y. A., Morkovsky, P., Gomes, J. A. G., Kesmez, M., Parga, J. and Cocke, D. L. 2004. Fundamentals, present and future perspectives of electrocoagulation. *Journal of Hazardous Materials*, 114(1-3), 199-210.
- Montgomery, D. C., Montgomery, D. C. and Montgomery, D. C. 1984. Design and analysis of experiments, Wiley New York.
- Moon, J. W., Goltz, M. N., Ahn, K. H. and Park, J. W. 2003. Dissolved organic matter effects on the performance of a barrier to polycyclic aromatic hydrocarbon transport by groundwater. *Journal of Contaminant Hydrology*, 60(3-4), 307-326.
- Mulligan, C., Yong, R. and Gibbs, B. 2001. Surfactant-enhanced remediation of contaminated soil: a review. *Engineering Geology*, 60(1), 371-380.
- Murray-Gulde, C., Heatley, J. E., Karanfil, T., Rodgers, J. H. and Myers, J. E. 2003a. Performance of a hybrid reverse osmosis-constructed wetland treatment system for brackish oil field produced water. *Water Research*, 37(3), 705-713.
- Nadarajah, N., Singh, A. and Ward, O. P. 2002. De-emulsification of petroleum oil emulsion by a mixed bacterial culture. *Process Biochemistry*, 37(10), 1135-1141.
- Nandi, B., Moparthy, A., Uppaluri, R. and Purkait, M. 2010. Treatment of oily wastewater using low cost ceramic membrane: Comparative assessment of pore blocking and artificial neural network models. *Chemical Engineering Research and Design*,

88(7), 881-892.

- Nanseu-Njiki, C. P., Tchamango, S. R., Ngom, P. C., Darchen, A. and Ngameni, E. 2009. Mercury(II) removal from water by electrocoagulation using aluminium and iron electrodes. *Journal of Hazardous Materials*, 168(2-3), 1430-1436.
- Nayak, P. S. and Singh, B. K. 2007. Removal of phenol from aqueous solutions by sorption on low cost clay. *Desalination*, 207(1), 71-79.
- Nemerow, N. L. 1987. *Industrial water pollution: origins, characteristics and treatment*, Krieger.
- Ng, J. C. Y., Cheung, W. H. and McKay, G. 2002. Equilibrium studies of the sorption of Cu(II) ions onto chitosan. *Journal of Colloid and Interface Science*, 255(1), 64-74.
- Nghiem, L. D., Ren, T., Aziz, N., Porter, I. and Regmi, G. 2011. Treatment of coal seam gas produced water for beneficial use in Australia: A review of best practices. *Desalination and Water Treatment*, 32(1-3), 316-323.
- Ozbay, N. and Yargic, A. S. 2015. Factorial experimental design for Remazol Yellow dye sorption using apple pulp/apple pulp carbon–titanium dioxide co-sorbent. *Journal of Cleaner Production*, 100, 333-343.
- Özcan, A. and Özcan, A. S. 2005. Adsorption of Acid Red 57 from aqueous solutions onto surfactant-modified sepiolite. *Journal of Hazardous Materials*, 125(1), 252-259.
- Ozkan, A. and Yekeler, M. 2004. Coagulation and flocculation characteristics of celestite with different inorganic salts and polymers. *Chemical Engineering and Processing: Process Intensification*, 43(7), 873-879.
- Pankow, J. F. and Cherry, J. A. 1996. Dense chlorinated solvents and other DNAPLs in

groundwater: History, behavior, and remediation.

- Paria, S. and Khilar, K. C. 2004. A review on experimental studies of surfactant adsorption at the hydrophilic solid-water interface. *Advances in Colloid and Interface Science*, 110(3), 75-95.
- Peng, H., Tremblay, A. and Veinot, D. 2005. The use of backflushed coalescing microfiltration as a pretreatment for the ultrafiltration of bilge water. *Desalination*, 181(1), 109-120.
- Pérez, L., Torres, J. L., Manresa, A., Solans, C. and Infante, M. R. 1996. Synthesis, aggregation, and biological properties of a new class of gemini cationic amphiphilic compounds from arginine, bis(Arg). *Langmuir*, 12(22), 5296-5301.
- Pérez-Marín, A. B., Zapata, V. M., Ortuño, J. F., Aguilar, M., Sáez, J. and Lloréns, M. 2007. Removal of cadmium from aqueous solutions by adsorption onto orange waste. *Journal of Hazardous Materials*, 139(1), 122-131.
- Pey, C., Maestro, A., Solé I., González, C., Solans, C. and Gutiérrez, J. M. 2006. Optimization of nano-emulsions prepared by low-energy emulsification methods at constant temperature using a factorial design study. *Colloids and Surfaces A: Physicochemical and Engineering Aspects*, 288(1), 144-150.
- Pinazo, A., Wen, X., Pérez, L., Infante, M. R. and Franses, E. I. 1999. Aggregation behavior in water of monomeric and gemini cationic surfactants derived from arginine. *Langmuir*, 15(9), 3134-3142.
- Ping, L., Luo, Y., Wu, L., Qian, W., Song, J. and Christie, P. 2006. Phenanthrene adsorption by soils treated with humic substances under different pH and temperature conditions. *Environmental Geochemistry and Health*, 28(1-2), 189-195.

- Pinotti, A. and Zaritzky, N. 2001. Effect of aluminum sulfate and cationic polyelectrolytes on the destabilization of emulsified wastes. *Waste Management*, 21(6), 535-542.
- Ponnusami, V., Krithika, V., Madhuram, R. and Srivastava, S. N. 2007. Biosorption of reactive dye using acid-treated rice husk: Factorial design analysis. *Journal of Hazardous Materials*, 142(1-2), 397-403.
- Prasad, R. K. and Srivastava, S. 2009. Sorption of distillery spent wash onto fly ash: Kinetics, mechanism, process design and factorial design. *Journal of Hazardous Materials*, 161(2), 1313-1322.
- Qian, Y., Posch, T. and Schmidt, T. C. 2011. Sorption of polycyclic aromatic hydrocarbons (PAHs) on glass surfaces. *Chemosphere*, 82(6), 859-865.
- Qiao, X., Zhang, Z., Yu, J. and Ye, X. 2008. Performance characteristics of a hybrid membrane pilot-scale plant for oilfield-produced wastewater. *Desalination*, 225(1-3), 113-122.
- Radian, A. and Mishael, Y. 2012. Effect of humic acid on pyrene removal from water by polycation-clay mineral composites and activated carbon. *Environmental Science & Technology*, 46(11), 6228-6235.
- Rafatullah, M., Sulaiman, O., Hashim, R. and Ahmad, A. 2010. Adsorption of methylene blue on low-cost adsorbents: a review. *Journal of Hazardous Materials*, 177(1), 70-80.
- Rao, P. and He, M. 2006. Adsorption of anionic and nonionic surfactant mixtures from synthetic detergents on soils. *Chemosphere*, 63(7), 1214-1221.
- Redlich, O. and Peterson, D. L. 1959. A useful adsorption isotherm. *The Journal of*

- Physical Chemistry, 63(6), 1024-1024.
- Riser-Roberts, E. 1998. Remediation of petroleum contaminated soils: biological, physical, and chemical processes, CRC press.
- Rodríguez-Cruz, M. S., Sánchez-Martín, M. J., Andrades, M. S. and Sánchez-Camazano, M. 2007a. Retention of pesticides in soil columns modified *in situ* and *ex situ* with a cationic surfactant. Science of the Total Environment, 378(1-2), 104-108.
- Rodríguez-Cruz, M. S., Sánchez-Martín, M. J., Andrades, M. S. and Sánchez-Camazano, M. 2007b. Modification of clay barriers with a cationic surfactant to improve the retention of pesticides in soils. Journal of Hazardous Materials, 139(2), 363-372.
- Rodríguez-Cruz, M. S., Andrades, M. S. and Sánchez-Martín, M. J. 2008. Significance of the long-chain organic cation structure in the sorption of the penconazole and metalaxyl fungicides by organo clays. Journal of Hazardous Materials, 160(1), 200-207.
- Rosen, M. and Tracy, D. 1998. Gemini surfactants. Journal of Surfactants and Detergents, 1(4), 547-554.
- Rosen, M. J. and Li, F. 2001. The adsorption of gemini and conventional surfactants onto some soil solids and the removal of 2-Naphthol by the soil surfaces. Journal of Colloid and Interface Science, 234(2), 418-424.
- Rubingh, D. (1979) Solution Chemistry of Surfactants. Mittal, K.L. (ed), pp. 337-354, Springer New York.
- Rupprecht, H. and Gu, T. 1991. Structure of adsorption layers of ionic surfactants at the solid/liquid interface. Colloid and Polymer Science, 269(5), 506-522.
- Rupprecht, H. H. 1972. Influence of solvents on adsorption of ionic surfactants on highly

- dispersed silicas. *Journal of Pharmaceutical Sciences*, 61(5), 700-702.
- Rutland, M. W. and Senden, T. J. 1993. Adsorption of the poly(oxyethylene) nonionic surfactant C<sub>12</sub>E<sub>5</sub> to silica: a study using atomic force microscopy. *Langmuir*, 9(2), 412-418.
- Sadeddin, K., Naser, A. and Firas, A. 2011. Removal of turbidity and suspended solids by electro-coagulation to improve feed water quality of reverse osmosis plant. *Desalination*, 268(1-3), 204-207.
- Sakai, K., Matsuhashi, K., Honya, A., Oguchi, T., Sakai, H. and Abe, M. 2010. Adsorption characteristics of monomeric/gemini surfactant mixtures at the silica/aqueous solution interface. *Langmuir*, 26(22), 17119-17125.
- Sakai, K., Tamura, M., Umezawa, S., Takamatsu, Y., Torigoe, K., Yoshimura, T., Esumi, K., Sakai, H. and Abe, M. 2008. Adsorption characteristics of sugar-based monomeric and gemini surfactants at the silica/aqueous solution interface. *Colloids and Surfaces A: Physicochemical and Engineering Aspects*, 328(1-3), 100-106.
- Salahi, A. and Mohammadi, T. 2010. Experimental investigation of oily wastewater treatment using combined membrane systems. *Water Science & Technology*, 62(2), 245-255.
- Salahi, A. and Mohammadi, T. 2011. Oily wastewater treatment by ultrafiltration using Taguchi experimental design. *Water Science & Technology*, 63(7), 1476-1484.
- Salahi, A., Mohammadi, T. and Rekabdar, F. 2010. Reverse osmosis of refinery oily wastewater effluents. *Iranian Journal of Environmental Health Science & Engineering*, 7(5), 413-422.
- Salako, O., Lo, C., Couzis, A., Somasundaran, P. and Lee, J. W. 2013. Adsorption of

- geminic surfactants onto clathrate hydrates. *Journal of Colloid and Interface Science*, 412(0), 1-6.
- Sanchez-Martin, M. J., Rodriguez-Cruz, M. S., Andrades, M. S. and Sanchez-Camazano, M. 2006. Efficiency of different clay minerals modified with a cationic surfactant in the adsorption of pesticides: Influence of clay type and pesticide hydrophobicity. *Applied Clay Science*, 31(3-4), 216-228.
- Saravanathamizhan, R., Mohan, N., Balasubramanian, N., Ramamurthi, V. and Basha, C. A. 2007. Evaluation of electro-oxidation of textile effluent using response surface methods. *CLEAN – Soil, Air, Water*, 35(4), 355-361.
- Sari, A., Çıtak, D. and Tuzen, M. 2010. Equilibrium, thermodynamic and kinetic studies on adsorption of Sb(III) from aqueous solution using low-cost natural diatomite. *Chemical Engineering Journal*, 162(2), 521-527.
- Sarkar, B., Xi, Y., Megharaj, M., Krishnamurti, G. S. and Naidu, R. 2010. Synthesis and characterisation of novel organopalygorskites for removal of p-nitrophenol from aqueous solution: Isothermal studies. *Journal of Colloid and Interface Science*, 350(1), 295-304.
- Sarkar, B., Xi, Y., Megharaj, M. and Naidu, R. 2011. Orange II adsorption on palygorskites modified with alkyl trimethylammonium and dialkyl dimethylammonium bromide—an isothermal and kinetic study. *Applied Clay Science*, 51(3), 370-374.
- Sarkar, B., Megharaj, M., Xi, Y. and Naidu, R. 2012. Surface charge characteristics of organo-palygorskites and adsorption of p-nitrophenol in flow-through reactor system. *Chemical Engineering Journal*, 185, 35-43.

- Schenone, A. V., Conte, L. O., Botta, M. A. and Alfano, O. M. 2015. Modeling and optimization of photo-Fenton degradation of 2, 4-D using ferrioxalate complex and response surface methodology (RSM). *Journal of environmental management*, 155, 177-183.
- Schwarzenbach, R. P., Gschwend, P. M. and Imboden, D. M. (2005) *Environmental Organic Chemistry*, pp. 387-458, John Wiley & Sons, Inc.
- Seki, Y., Seyhan, S. and Yurdakoc, M. 2006. Removal of boron from aqueous solution by adsorption on Al<sub>2</sub>O<sub>3</sub> based materials using full factorial design. *Journal of Hazardous Materials*, 138(1), 60-66.
- Seki, H., Maruyama, H. and Shoji, Y. 2010. Flocculation of diatomite by a soy protein-based bioflocculant. *Biochemical Engineering Journal*, 51(1-2), 14-18.
- Seredyuk, V., Alami, E., NydŹ, M., Holmberg, K., Peresykin, A. V. and Menger, F. M. 2001. Micellization and adsorption properties of novel zwitterionic surfactants. *Langmuir*, 17(17), 5160-5165.
- Sheng, G., Xu, S. and Boyd, S. A. 1996. Mechanism(s) controlling sorption of neutral organic contaminants by surfactant-derived and natural organic matter. *Environmental Science & Technology*, 30(5), 1553-1557.
- Sheng, G., Hu, J. and Wang, X. 2008. Sorption properties of Th(IV) on the raw diatomite—effects of contact time, pH, ionic strength and temperature. *Applied Radiation and Isotopes*, 66(10), 1313-1320.
- Sheng, G., Wang, S., Hu, J., Lu, Y., Li, J., Dong, Y. and Wang, X. 2009. Adsorption of Pb(II) on diatomite as affected via aqueous solution chemistry and temperature. *Colloids and Surfaces A: Physicochemical and Engineering Aspects*, 339(1), 159-

166.

- Sheng, G., Yang, S., Sheng, J., Zhao, D. and Wang, X. 2011. Influence of solution chemistry on the removal of Ni(II) from aqueous solution to titanate nanotubes. *Chemical Engineering Journal*, 168(1), 178-182.
- Sheng, G., Dong, H. and Li, Y. 2012. Characterization of diatomite and its application for the retention of radiocobalt: role of environmental parameters. *Journal of Environmental Radioactivity*, 113(0), 108-115.
- Shi, Y., Fan, M., Brown, R. C., Sung, S. and Van Leeuwen, J. 2004. Comparison of corrosivity of polymeric sulfate ferric and ferric chloride as coagulants in water treatment. *Chemical Engineering and Processing: Process Intensification*, 43(8), 955-964.
- Shichi, T. and Takagi, K. 2000. Clay minerals as photochemical reaction fields. *Journal of Photochemistry and Photobiology C: Photochemistry Reviews*, 1(2), 113-130.
- Shokrkar, H., Salahi, A., Kasiri, N. and Mohammadi, T. 2011. Mullite ceramic membranes for industrial oily wastewater treatment: experimental and neural network modeling. *Water Science & Technology*, 64(3), 670-676.
- Shukla, D. and Tyagi, V. K. 2006. Cationic gemini surfactants: A review. *Journal of Oleo Science*, 55(8), 381-390.
- Sips, R. 1948. On the structure of a catalyst surface. *The Journal of Chemical Physics*, 16(5), 490-495.
- Solberg, D. and Wågberg, L. 2003. Adsorption and flocculation behavior of cationic polyacrylamide and colloidal silica. *Colloids and Surfaces A: Physicochemical and Engineering Aspects*, 219(1-3), 161-172.

- Song, C., Wang, T., Pan, Y. and Qiu, J. 2006. Preparation of coal-based microfiltration carbon membrane and application in oily wastewater treatment. *Separation and purification technology*, 51(1), 80-84.
- Sprynskyy, M., Kovalchuk, I. and Buszewski, B. 2010. The separation of uranium ions by natural and modified diatomite from aqueous solution. *Journal of Hazardous Materials*, 181(1), 700-707.
- Stellner, K. L. and Scamehorn, J. F. 1989. Hardness tolerance of anionic surfactant solutions. 2. Effect of added nonionic surfactant. *Langmuir*, 5(1), 77-84.
- Subramani, A., Cryer, E., Liu, L., Lehman, S., Ning, R. Y. and Jacangelo, J. G. 2012. Impact of intermediate concentrate softening on feed water recovery of reverse osmosis process during treatment of mining contaminated groundwater. *Separation and Purification Technology*, 88(0), 138-145.
- Tang, C. Y., Shiang Fu, Q., Gao, D., Criddle, C. S. and Leckie, J. O. 2010. Effect of solution chemistry on the adsorption of perfluorooctane sulfonate onto mineral surfaces. *Water Research*, 44(8), 2654-2662.
- Tchobanoglous, G. and Burton, F. L. 1991. *Wastewater engineering. Management*, 7, 1-4.
- Tellez, G. T., Nirmalakhandan, N. and Gardea-Torresdey, J. L. 2002. Performance evaluation of an activated sludge system for removing petroleum hydrocarbons from oilfield produced water. *Advances in Environmental Research*, 6(4), 455-470.
- Thanos, A. G., Katsou, E., Malamis, S., Psarras, K., Pavlatou, E. A. and Haralambous, K. J. 2012. Evaluation of modified mineral performance for chromate sorption from aqueous solutions. *Chemical Engineering Journal*, 211-212(0), 77-88.
- Thiruvengkatachari, R., Vigneswaran, S. and Naidu, R. 2008. Permeable reactive barrier

- for groundwater remediation. *Journal of Industrial and Engineering Chemistry*, 14(2), 145-156.
- Timmes, T. C., Kim, H. C. and Dempsey, B. A. 2010. Electrocoagulation pretreatment of seawater prior to ultrafiltration: Pilot-scale applications for military water purification systems. *Desalination*, 250(1), 6-13.
- Tir, M. and Moulai-Mostefa, N. 2008. Optimization of oil removal from oily wastewater by electrocoagulation using response surface method. *Journal of Hazardous Materials*, 158(1), 107-115.
- Toth, J. 1971. State equations of the solid-gas interface layers. *Acta Chimica (Academiae Scientiarum) Hungaricae*, 69(3), 311-328.
- Tóth, J. 1994. Thermodynamical correctness of gas/solid adsorption isotherm equations. *Journal of Colloid and Interface Science*, 163(2), 299-302.
- Tran, N., Drogui, P., Nguyen, L. and Brar, S. K. Optimization of sono-electrochemical oxidation of ibuprofen in wastewater. *Journal of Environmental Chemical Engineering*, doi:10.1016/j.jece.2015.05.001.
- Trinh, T. K. and Kang, L. S. 2011. Response surface methodological approach to optimize the coagulation-flocculation process in drinking water treatment. *Chemical Engineering Research and Design*, 89(7), 1126-1135.
- Turle, R., Nason, T., Malle, H. and Fowlie, P. 2007. Development and implementation of the CCME Reference Method for the Canada-Wide Standard for Petroleum Hydrocarbons (PHC) in soil: a case study. *Analytical and bioanalytical chemistry*, 387(3), 957-964.
- Tzotzi, C., Pahiadaki, T., Yiantsios, S. G., Karabelas, A. J. and Andritsos, N. 2007. A

- study of CaCO<sub>3</sub> scale formation and inhibition in RO and NF membrane processes. *Journal of Membrane Science*, 296(1-2), 171-184.
- Un, U. T., Ates, F., Erginel, N., Ozcan, O. and Oduncu, E. 2015. Adsorption of Disperse Orange 30 dye onto activated carbon derived from Holm Oak (*Quercus Ilex*) acorns: A 3<sup>k</sup> factorial design and analysis. *Journal of environmental management*, 155, 89-96.
- Veil, J. A., Puder, M. G., Elcock, D. and Redweik Jr, R. J. 2004. A white paper describing produced water from production of crude oil, natural gas, and coal bed methane. Argonne National Laboratory, Technical Report.
- Vepsäläinen, M., Ghiasvand, M., Selin, J., Pienimaa, J., Repo, E., Pulliainen, M. and Sillanpää M. 2009. Investigations of the effects of temperature and initial sample pH on natural organic matter (NOM) removal with electrocoagulation using response surface method (RSM). *Separation and Purification Technology*, 69(3), 255-261.
- Vijayaraghavan, K., Padmesh, T. V. N., Palanivelu, K. and Velan, M. 2006. Biosorption of nickel(II) ions onto *Sargassum wightii*: Application of two-parameter and three-parameter isotherm models. *Journal of Hazardous Materials*, 133(1-3), 304-308.
- Wagner, J., Chen, H., Brownawell, B. J. and Westall, J. C. 1994. Use of cationic surfactants to modify soil surfaces to promote sorption and retard migration of hydrophobic organic compounds. *Environmental Science & Technology*, 28(2), 231-237.
- Wan, Y. and Liu, C. 2006. The effect of humic acid on the adsorption of REEs on kaolin. *Colloids and Surfaces A: Physicochemical and Engineering Aspects*, 290(1-3),

112-117.

- Wang, C., Jiang, X., Zhou, L., Xia, G., Chen, Z., Duan, M. and Jiang, X. 2013c. The preparation of organo-bentonite by a new gemini and its monomer surfactants and the application in MO removal: A comparative study. *Chemical Engineering Journal*, 219, 469-477.
- Wang, J., Han, X., Ma, H., Ji, Y. and Bi, L. 2011b. Adsorptive removal of humic acid from aqueous solution on polyaniline/attapulgite composite. *Chemical Engineering Journal*, 173(1), 171-177.
- Wang, S., Boyjoo, Y., Choueib, A. and Zhu, Z. H. 2005. Removal of dyes from aqueous solution using fly ash and red mud. *Water Research*, 39(1), 129-138.
- Wang, S., Huang, G. H., Wei, J. and He, L. 2013b. Simulation-based variance components analysis for characterization of interaction effects of random factors on trichloroethylene vapor transport in unsaturated porous media. *Industrial & Engineering Chemistry Research*, 52(25), 8602-8611.
- Wang, S. and Huang, G. H. 2015. A multi-level Taguchi-factorial two-stage stochastic programming approach for characterization of parameter uncertainties and their interactions: An application to water resources management. *European Journal of Operational Research*, 240(2), 572-581.
- Wang, W., Chen, H. and Wang, A. 2007. Adsorption characteristics of Cd(II) from aqueous solution onto activated palygorskite. *Separation and Purification Technology*, 55(2), 157-164.
- Wang, X. 2013. Interaction of radionickel with diatomite as a function of pH, ionic strength and temperature. *Journal of Radioanalytical and Nuclear Chemistry*,

295(3), 2301-2308.

- Wang, X., Pan, J., Guan, W., Zou, X., Hu, W., Yan, Y. and Li, C. 2011a. Adsorptive removal of 2, 6-dichlorophenol from aqueous solution by surfactant-modified palygorskite sorbents: equilibrium, kinetics and thermodynamics. *Adsorption Science & Technology*, 29(2), 185-196.
- Wang, X., Tao, S. and Xing, B. 2009b. Sorption and competition of aromatic compounds and humic acid on multiwalled carbon nanotubes. *Environmental Science & Technology*, 43(16), 6214-6219.
- Wang, X., Wang, J., Wang, Y., Ye, J., Yan, H. and Thomas, R. K. 2003. Micellization of a series of dissymmetric gemini surfactants in aqueous solution. *The Journal of Physical Chemistry B*, 107(41), 11428-11432.
- Wang, Y., Chen, X., Zhang, J., Yin, J. and Wang, H. 2009a. Investigation of microfiltration for treatment of emulsified oily wastewater from the processing of petroleum products. *Desalination*, 249(3), 1223-1227.
- Wang, Y., Jiang, X., Zhou, L., Wang, C., Liao, Y., Duan, M. and Jiang, X. 2013a. A comparison of new gemini surfactant modified clay with its monomer modified one: characterization and application in methyl orange removal. *Journal of Chemical & Engineering Data*, 58(6), 1760-1771.
- Wei, J., Huang, G., An, C. and Yu, H. 2011a. Investigation on the solubilization of polycyclic aromatic hydrocarbons in the presence of single and mixed gemini surfactants. *Journal of Hazardous Materials*, 190(1), 840-847.
- Wei, J., Huang, G., Yu, H. and An, C. 2011b. Efficiency of single and mixed gemini/conventional micelles on solubilization of phenanthrene. *Chemical*

- Engineering Journal, 168(1), 201-207.
- Wei, J., Huang, G., Zhu, L., Zhao, S., An, C. and Fan, Y. 2012. Enhanced aqueous solubility of naphthalene and pyrene by binary and ternary gemini cationic and conventional nonionic surfactants. *Chemosphere*, 89(11), 1347-1353.
- Wei, J., Huang, G., Wang, S., Zhao, S. and Yao, Y. 2013. Improved solubilities of PAHs by multi-component gemini surfactant systems with different spacer lengths. *Colloids and Surfaces A: Physicochemical and Engineering Aspects*, 423, 50-57.
- Wei, Z. 2007. The development of methods and technologies for the treatment of oil-field produced wastewater. *Environmental Engineering*, 5, 012.
- Wild, S. R. and Jones, K. C. 1995. Polynuclear aromatic hydrocarbons in the United Kingdom environment: a preliminary source inventory and budget. *Environmental pollution*, 88(1), 91-108.
- Wilkin, R. T., Su, C., Ford, R. G. and Paul, C. J. 2005. Chromium-removal processes during groundwater remediation by a zerovalent iron permeable reactive barrier. *Environmental Science & Technology*, 39(12), 4599-4605.
- Witthuhn, B., Pernyeszi, T., Klauth, P., Vereecken, H. and Klumpp, E. 2005. Sorption study of 2,4-dichlorophenol on organoclays constructed for soil bioremediation. *Colloids and Surfaces A: Physicochemical and Engineering Aspects*, 265(1-3), 81-87.
- Wu, C. D., Xu, X. J., Liang, J. L., Wang, Q., Dong, Q. and Liang, W. L. 2011a. Enhanced coagulation for treating slightly polluted algae-containing surface water combining polyaluminum chloride (PAC) with diatomite. *Desalination*, 279(1-3), 140-145.

- Wu, J. and Huang, X. 2008. Effect of dosing polymeric ferric sulfate on fouling characteristics, mixed liquor properties and performance in a long-term running membrane bioreactor. *Separation and Purification Technology*, 63(1), 45-52.
- Wu, J., Chen, F., Huang, X., Geng, W. and Wen, X. 2006. Using inorganic coagulants to control membrane fouling in a submerged membrane bioreactor. *Desalination*, 197(1-3), 124-136.
- Wu, J., Yang, Y. S. and Lin, J. 2005. Advanced tertiary treatment of municipal wastewater using raw and modified diatomite. *Journal of Hazardous Materials*, 127(1-3), 196-203.
- Wu, P., Tang, Y., Wang, W., Zhu, N., Li, P., Wu, J., Dang, Z. and Wang, X. 2011b. Effect of dissolved organic matter from Guangzhou landfill leachate on sorption of phenanthrene by Montmorillonite. *Journal of Colloid and Interface Science*, 361(2), 618-627.
- Xi, Y., Frost, R. L. and He, H. 2007. Modification of the surfaces of Wyoming montmorillonite by the cationic surfactants alkyl trimethyl, dialkyl dimethyl, and trialkyl methyl ammonium bromides. *Journal of Colloid and Interface Science*, 305(1), 150-158.
- Xi, Y., Mallavarapu, M. and Naidu, R. 2010. Adsorption of the herbicide 2, 4-D on organo-palygorskite. *Applied Clay Science*, 49(3), 255-261.
- Xie, W. H., Shiu, W. Y. and Mackay, D. 1997. A review of the effect of salts on the solubility of organic compounds in seawater. *Marine Environmental Research*, 44(4), 429-444.
- Xing, B., Pignatello, J. J. and Gigliotti, B. 1996. Competitive sorption between atrazine

- and other organic compounds in soils and model sorbents. *Environmental Science & Technology*, 30(8), 2432-2440.
- Xiong, W. and Peng, J. 2008. Development and characterization of ferrihydrite-modified diatomite as a phosphorus adsorbent. *Water Research*, 42(19), 4869-4877.
- Xu, P., Drewes, J. E. and Heil, D. 2008. Beneficial use of co-produced water through membrane treatment: technical-economic assessment. *Desalination*, 225(1-3), 139-155.
- Xu, Q., Vasudevan, T. V. and Somasundaran, P. 1991. Adsorption of anionic - nonionic and cationic - nonionic surfactant mixtures on kaolinite. *Journal of Colloid and Interface Science*, 142(2), 528-534.
- Xu, X. and Zhu, X. 2004. Treatment of refractory oily wastewater by electro-coagulation process. *Chemosphere*, 56(10), 889-894.
- Xue, G., Gao, M., Gu, Z., Luo, Z. and Hu, Z. 2013. The removal of p-nitrophenol from aqueous solutions by adsorption using gemini surfactants modified montmorillonites. *Chemical Engineering Journal*, 218, 223-231.
- Yagub, M. T., Sen, T. K., Afroze, S. and Ang, H. M. 2014. Dye and its removal from aqueous solution by adsorption: a review. *Advances in colloid and interface science*, 209, 172-184.
- Yahiaoui, I., Belattaf, A., Aissani-Benissad, F. and Cherif, L. Y. 2011. Full factorial design applied to a biosorption of lead (II) ions from aqueous solution using Brewer's Yeast (*Saccharomyces cerevisiae*). *Journal of Chemical & Engineering Data*, 56(11), 3999-4005.
- Yan, L., Wang, Y., Ma, H., Han, Z., Zhang, Q. and Chen, Y. 2012. Feasibility of fly ash-

- based composite coagulant for coal washing wastewater treatment. *Journal of Hazardous Materials*, 203-204(0), 221-228.
- Yang, C. L. 2007. Electrochemical coagulation for oily water demulsification. *Separation and Purification Technology*, 54(3), 388-395.
- Yang, K., Zhu, L. and Xing, B. 2006. Enhanced soil washing of phenanthrene by mixed solutions of TX100 and SDBS. *Environmental Science & Technology*, 40(13), 4274-4280.
- Yang, X. L., Song, H. L., Lu, J. L., Fu, D. F. and Cheng, B. 2010. Influence of diatomite addition on membrane fouling and performance in a submerged membrane bioreactor. *Bioresource Technology*, 101(23), 9178-9184.
- Yap, C. L., Gan, S. and Ng, H. K. 2010. Application of vegetable oils in the treatment of polycyclic aromatic hydrocarbons-contaminated soils. *Journal of Hazardous Materials*, 177(1-3), 28-41.
- Yavuz, Y., Koparal, A. S. and Ögütveren, Ü. B. 2010. Treatment of petroleum refinery wastewater by electrochemical methods. *Desalination*, 258(1), 201-205.
- Yi, S., Ma, Y., Wang, X. and Jia, Y. 2009. Green chemistry: Pretreatment of seawater by a one-step electrochemical method. *Desalination*, 239(1-3), 247-256.
- Younker, J. M. and Walsh, M. E. 2014. Bench-scale investigation of an integrated adsorption-coagulation-dissolved air flotation process for produced water treatment. *Journal of Environmental Chemical Engineering*, 2(1), 692-697.
- Younker, J., Lee, S., Gagnon, G. and Walsh, M. 2011. Atlantic Canada Offshore R&D: Treatment of oilfield produced water by chemical coagulation and electrocoagulation, Offshore Technology Conference.

- Yu, H. 2010. Combined effects of biosurfactant and porous-medium on the fate and transport of petroleum contaminants. Ph.D., The University of Regina (Canada), Ann Arbor.
- Yu, H., Huang, G. H, Wei, J. and An, C. J. 2011b. Solubilization of mixed polycyclic aromatic hydrocarbons through a rhamnolipid biosurfactant, *Journal of Environmental Quality*, 40(2), 477-483.
- Yu, H., Huang, G. H., An, C. J. and Wei, J. 2011a. Combined effects of DOM extracted from site soil/compost and biosurfactant on the sorption and desorption of PAHs in a soil–water system. *Journal of Hazardous Materials*, 190(1-3), 883-890.
- Yu, L., Han, M. and He, F. A review of treating oily wastewater. *Arabian Journal of Chemistry*, doi:10.1016/j.arabjc.2013.07.020.
- Yuan, M., Tong, S., Zhao, S. and Jia, C. Q. 2010. Adsorption of polycyclic aromatic hydrocarbons from water using petroleum coke-derived porous carbon. *Journal of Hazardous Materials*, 181(1), 1115-1120.
- Yuan, S., Shu, Z., Wan, J. and Lu, X. 2007. Enhanced desorption of hexachlorobenzene from kaolin by single and mixed surfactants. *Journal of Colloid and Interface Science*, 314(1), 167-175.
- Yuan, S., Tong, M. and Wu, G. 2011. Destabilization of emulsions by natural minerals. *Journal of Hazardous Materials*, 192(3), 1882-1885.
- Cui, Y., Liu, L., Guo, Z. and Peng, X. 2009. Modified diatomaceous earth for sludge settlement amelioration, pp. 400-403.
- Zadeh, L. A. 1999. Fuzzy sets as a basis for a theory of possibility. *Fuzzy Sets and Systems*, 100, Supplement 1(0), 9-34.

- Zaroual, Z., Chaair, H., Essadki, A. H., El Ass, K. and Azzi, M. 2009. Optimizing the removal of trivalent chromium by electrocoagulation using experimental design. *Chemical Engineering Journal*, 148(2-3), 488-495.
- Zeng, Y. and Park, J. 2009. Characterization and coagulation performance of a novel inorganic polymer coagulant—Poly-zinc-silicate-sulfate. *Colloids and Surfaces A: Physicochemical and Engineering Aspects*, 334(1), 147-154.
- Zeng, Y., Yang, C., Zhang, J. and Pu, W. 2007. Feasibility investigation of oily wastewater treatment by combination of zinc and PAM in coagulation/flocculation. *Journal of Hazardous Materials*, 147(3), 991-996.
- Zhang, B. 2007. Development of biosurfactant-enhanced methodologies for bioremediation of petroleum-contaminated sites in western Canada. Ph.D., The University of Regina (Canada), Ann Arbor.
- Zhang, H., Fang, S., Ye, C., Wang, M., Cheng, H., Wen, H. and Meng, X. 2008. Treatment of waste filtrate oil/water emulsion by combined demulsification and reverse osmosis. *Separation and Purification Technology*, 63(2), 264-268.
- Zhang, J., Sun, Y., Huang, Z., Liu, X. and Meng, G. 2005. Treatment of phosphate-containing oily wastewater by coagulation and microfiltration. *Journal of Environmental Sciences (China)*, 18(4), 629-633.
- Zhang, R. and Somasundaran, P. 2006. Advances in adsorption of surfactants and their mixtures at solid/solution interfaces. *Advances in Colloid and Interface Science*, 123-126(0), 213-229.
- Zhang, S., Shao, T., Bekaroglu, S. S. K. and Karanfil, T. 2010a. Adsorption of synthetic organic chemicals by carbon nanotubes: Effects of background solution chemistry.

- Water Research, 44(6), 2067-2074.
- Zhang, W., Zhuang, L., Yuan, Y., Tong, L. and Tsang, D. C. 2011. Enhancement of phenanthrene adsorption on a clayey soil and clay minerals by coexisting lead or cadmium. *Chemosphere*, 83(3), 302-310.
- Zhang, Y., Gao, B., Lu, L., Yue, Q., Wang, Q. and Jia, Y. 2010b. Treatment of produced water from polymer flooding in oil production by the combined method of hydrolysis acidification-dynamic membrane bioreactor - coagulation process. *Journal of Petroleum Science and Engineering*, 74(1), 14-19.
- Zhang, Y., Zhao, Y., Zhu, Y., Wu, H., Wang, H. and Lu, W. 2012. Adsorption of mixed cationic-nonionic surfactant and its effect on bentonite structure. *Journal of Environmental Sciences*, 24(8), 1525-1532.
- Zhao, D., Chen, S., Yang, S., Yang, X. and Yang, S. 2011b. Investigation of the sorption behavior of Cd(II) on GMZ bentonite as affected by solution chemistry. *Chemical Engineering Journal*, 166(3), 1010-1016.
- Zhao, Q., Yang, K. and Li, P. 2010. Enhanced soil retention for o-nitroaniline by the addition of a mixture of a cationic surfactant (Cetyl Pyridinium Chloride) and a nonionic surfactant (Polyethylene Glycol Mono-4-nonylphenyl Ether). *Journal of Hazardous Materials*, 182(1-3), 757-762.
- Zhao, S., Huang, G., Fu, H. and Wang, Y. 2014. Enhanced coagulation/flocculation by combining diatomite with synthetic polymers for oily wastewater treatment. *Separation Science and Technology*, 49(7), 999-1007.
- Zhao, S., Huang, G., Cheng, G., Wang, Y. and Fu, H. 2014. Hardness, COD and turbidity removals from produced water by electrocoagulation pretreatment prior to reverse

- osmosis membranes. *Desalination*, 344, 454-462.
- Zhao, S., Huang, G., An, C., Wei, J. and Yao, Y. 2015. Enhancement of soil retention for phenanthrene in binary cationic gemini and nonionic surfactant mixtures: Characterizing two-step adsorption and partition processes through experimental and modeling approaches. *Journal of Hazardous Materials*, 286(0), 144-151.
- Zhao, Y., Han, Y., Ma, T. and Guo, T. 2011a. Simultaneous desulfurization and denitrification from flue gas by Ferrate(VI). *Environmental Science & Technology*, 45(9), 4060-4065.
- Zhao, Y., Wang, J., Luan, Z., Peng, X., Liang, Z. and Shi, L. 2009. Removal of phosphate from aqueous solution by red mud using a factorial design. *Journal of Hazardous Materials*, 165(1-3), 1193-1199.
- Zheng, H. L., Fang, H. L., Jiang, S. J., Yang, C., Ma, J. Y. and Zhang, Z. Q. 2011. Preparation and structural analysis of diatomite-supported SPFS flocculant. *Spectroscopy and Spectral Analysis*, 31(7), 1917-1921.
- Zhong, J., Sun, X. and Wang, C. 2003. Treatment of oily wastewater produced from refinery processes using flocculation and ceramic membrane filtration. *Separation and Purification Technology*, 32(1), 93-98.
- Zhou, L., Chen, H., Jiang, X., Lu, F., Zhou, Y., Yin, W. and Ji, X. 2009. Modification of montmorillonite surfaces using a novel class of cationic gemini surfactants. *Journal of Colloid and Interface Science*, 332(1), 16-21.
- Zhou, Q. and Somasundaran, P. 2009. Synergistic adsorption of mixtures of cationic gemini and nonionic sugar-based surfactant on silica. *Journal of Colloid and Interface Science*, 331(2), 288-294.

- Zhou, W., Wang, X., Chen, C. and Zhu, L. 2013. Removal of polycyclic aromatic hydrocarbons from surfactant solutions by selective sorption with organo-bentonite. *Chemical Engineering Journal*, 233, 251-257.
- Zhu, B., Clifford, D. A. and Chellam, S. 2005. Comparison of electrocoagulation and chemical coagulation pretreatment for enhanced virus removal using microfiltration membranes. *Water Research*, 39(13), 3098-3108.
- Zhu, B. Y. and Gu, T. 1989. General isotherm equation for adsorption of surfactants at solid/liquid interfaces. Part 1. Theoretical. *Journal of the Chemical Society, Faraday Transactions 1: Physical Chemistry in Condensed Phases*, 85(11), 3813-3817.
- Zhu, B. Y., Gu, T. and Zhao, X. 1989. General isotherm equation for adsorption of surfactants at solid/liquid interfaces. Part 2. Applications. *Journal of the Chemical Society, Faraday Transactions 1: Physical Chemistry in Condensed Phases*, 85(11), 3819-3824.
- Zhu, B. Y. and Gu, T. 1991. Surfactant adsorption at solid-liquid interfaces. *Advances in colloid and interface science*, 37(1), 1-32.
- Zhu, D., Hyun, S., Pignatello, J. J. and Lee, L. S. 2004. Evidence for  $\pi$ - $\pi$  electron donor-acceptor interactions between  $\pi$ -donor aromatic compounds and  $\pi$ -acceptor sites in soil organic matter through pH effects on sorption. *Environmental Science & Technology*, 38(16), 4361-4368.
- Zhu, L., Chen, B., Tao, S. and Chiou, C. T. 2003. Interactions of organic contaminants with mineral-adsorbed surfactants. *Environmental Science & Technology*, 37(17), 4001-4006.

- Zhu, L., Li, Y. and Zhang, J. 1997. Sorption of organobentonites to some organic pollutants in water. *Environmental Science & Technology*, 31(5), 1407-1410.
- Zhuang, L., Wang, G., Yu, K. and Yao, C. 2013. Enhanced adsorption of anionic dyes from aqueous solution by gemini cationic surfactant-modified diatomite. *Desalination and Water Treatment*, 51(34-36), 6526-6535.
- Zouboulis, A. I. and Avranas, A. 2000. Treatment of oil-in-water emulsions by coagulation and dissolved-air flotation. *Colloids and Surfaces A: Physicochemical and Engineering Aspects*, 172(1-3), 153-161.